AD NUMBER

ADB264406

NEW LIMITATION CHANGE

TO

Approved for public release, distribution unlimited

FROM

Distribution authorized to U.S. Gov't. agencies only; Critical Tech., Dec 96. Other requests shall be referred to AFRL/MLLN, Wright-Patterson AFB, OH 45433-7817.

AUTHORITY

AFRL ltr, 6 Dec 2002

WL-TR-97-4129

THERMALLY DURABLE GLASS-CERAMIC MATRIX COMPOSITES

D. C. Larsen
K. Chyung
R. L. Stewart
J. M. Torns
S. B. Dawes
H. T. Godard

CORNING INCORPORATED
SCIENCE AND TECHNOLOGY
CORNING NY 14831

NOVEMBER 1997

INTERIM REPORT FOR PERIOD AUGUST 1990 - DECEMBER 1994

MATERIALS & MANUFACTURING DIRECTORATE
AIR FORCE RESEARCH LABORATORY
AIR FORCE MATERIEL COMMAND
WRIGHT-PATTERSON AIR FORCE BASE, OH 45433-7750

REPORT DOCUMENTATION PAGE

1. REPORT DATE (DD-MM-YYYY)	2. REPORT TYPE	3. DATES COVERED (FROM - TO)
14-11-1997	Final Report	01-08-1995 to 01-12-1995

4. TITLE AND SUBTITLE Thermally Durable Glass-Ceramic Matrix Composites Unclassified	**5a. CONTRACT NUMBER** F33615-90-C-5909
	5b. GRANT NUMBER
	5c. PROGRAM ELEMENT NUMBER
6. AUTHOR(S) Larsen, D. C. ; Chyung, K. ; Stewart, R. L. ; Torns, J. M. ; Dawes, S. B. ;	**5d. PROJECT NUMBER**
	5e. TASK NUMBER
	5f. WORK UNIT NUMBER
7. PERFORMING ORGANIZATION NAME AND ADDRESS Cornig Incorporated Science & Technology Corning , NY 14831	**8. PERFORMING ORGANIZATION REPORT NUMBER**
9. SPONSORING/MONITORING AGENCY NAME AND ADDRESS Materials & Manufacturing Directorate Air Force Research Laboratory Air Force Materiel Command Wright-Patterson AFB , OH 45433-7750	**10. SPONSOR/MONITOR'S ACRONYM(S)** AFRL/MLLN
	11. SPONSOR/MONITOR'S REPORT NUMBER(S)

12. DISTRIBUTION/AVAILABILITY STATEMENT
B
Critical Technology
01-12-1996
Materials & Manufacturing Directorate
Air Force Research Laboratory
Air Force Materiel Command
Wright-Patterson AFB , OH 45433-7750

13. SUPPLEMENTARY NOTES

14. ABSTRACT
The thrust of this program was to develop thermally durable ceramic matrix composites (CMCs) with enhanced thermostructural properties.

15. SUBJECT TERMS
ceramic matrix composite; CMC; thermal durability; oxidation embrittlement; BSG-doped MAS; mica interference

16. SECURITY CLASSIFICATION OF:			17. LIMITATION OF ABSTRACT	18. NUMBER OF PAGES	19a. NAME OF RESPONSIBLE PERSON
					Fenster, Lynn lfenster@dtic.mil
a. REPORT Unclassified	b. ABSTRACT Unclassified	c. THIS PAGE Unclassified	Same as Report (SAR)	192	19b. TELEPHONE NUMBER International Area Code Area Code Telephone Number 703 767-9007 DSN 427-9007

NOTICE

WHEN GOVERNMENT DRAWINGS, SPECIFICATIONS, OR OTHER DATA ARE USED FOR ANY PURPOSE OTHER THAN IN CONNECTION WITH A DEFINITELY GOVERNMENT-RELATED PROCUREMENT, THE UNITED STATES GOVERNMENT INCURS NO RESPONSIBILITY OR ANY OBLIGATION WHATSOEVER. THE FACT THAT THE GOVERNMENT MAY HAVE FORMULATED OR IN ANY WAY SUPPLIED THE SAID DRAWINGS, SPECIFICATIONS, OR OTHER DATA, IS NOT TO BE REGARDED BY IMPLICATION OR OTHERWISE IN ANY MANNER CONSTRUED, AS LICENSING THE HOLDER OR ANY OTHER PERSON OR CORPORATION, OR AS CONVEYING ANY RIGHTS OR PERMISSION TO MANUFACTURE, USE, OR SELL ANY PATENTED INVENTION THAT MAY IN ANY WAY BE RELATED THERETO.

THIS TECHNICAL REPORT HAS BEEN REVIEWED AND IS APPROVED FOR PUBLICATION.

ALLAN P. KATZ, Project Engineer
Ceramics Development & Materials
Behavior Branch
Metals, Ceramics & NDE Division

RONALD J. KERANS, Actg Asst Chief
Ceramics Development & Materials
Behavior Branch
Metals, Ceramics & NDE Division

WALTER M. GRIFFITH, Chief
Metals, Ceramics & NDE Division
Materials & Manufacturing Directorate

IF YOUR ADDRESS HAS CHANGED, IF YOU WISH TO BE REMOVED FROM OUR MAILING LIST, OR IF THE ADDRESSEE IS NO LONGER EMPLOYED BY YOUR ORGANIZATION, PLEASE NOTIFY, AFRL/MLLN, WRIGHT-PATTERSON AFB OH 45433-7817 TO HELP US MAINTAIN A CURRENT MAILING LIST.

COPIES OF THIS REPORT SHOULD NOT BE RETURNED UNLESS IT IS REQUIRED BY SECURITY CONSIDERATIONS, CONTRACTUAL OBLIGATIONS, OR NOTICE ON A SPECIFIC DOCUMENT.

REPORT DOCUMENTATION PAGE

Form Approved
OMB No. 074-0188

1. AGENCY USE ONLY (Leave blank)	2. REPORT DATE	3. REPORT TYPE AND DATES COVERED
	14 November 1997	Final Report 08/01/90 - 12/01/94

4. TITLE AND SUBTITLE

Thermally Durable Glass-Ceramic Matrix Composites

5. FUNDING NUMBERS

C: F33615-90-C-5909
PE: 62102F
PR: 2420
TA: 01
WU: AR

6. AUTHOR(S)

D. C. Larsen, K. Chyung, R. L. Stewart, J. M. Torns, S. B. Dawes, H. T. Godard

7. PERFORMING ORGANIZATION NAME(S) AND ADDRESS(ES)

Corning Incorporated
Science & Technology
Corning NY 14831

8. PERFORMING ORGANIZATION REPORT NUMBER

P-97-222-37-TP

9. SPONSORING / MONITORING AGENCY NAME(S) AND ADDRESS(ES)

Materials & Manufacturing Directorate
Air Force Research Laboratory
Air Force Materiel Command
Wright-Patterson AFB OH 45433-7750
POC: Alan P. Katz, AFRL/MLLN, 937-255-1347

10. SPONSORING / MONITORING AGENCY REPORT NUMBER

WL-TR-97-4129

11. SUPPLEMENTARY NOTES

Export Restrictions Apply
Available on CD

12a. DISTRIBUTION / AVAILABILITY STATEMENT

Distribution authorized to US Government agencies only, critical technology, December 1996. Other requests for this document shall be referred to AFRL/MLLN, WPAFB OH 45433-7817.

12b. DISTRIBUTION CODE

13. ABSTRACT ***(Maximum 200 Words)***

The thrust of this program was to develop thermally durable ceramic matrix composites (CMCs) with enhanced thermostructural properties. Two approaches were investigated (1) BSG-doped, SiC whisker toughened MAS CMC's, and (2) Mica-interface CMCs. BSG-MAS CMCs have an MAS cordierite glass-ceramic matrix, and contain a borosilicate glass phase that protect insitu carbon interfaces from oxidation, as well as SiC whisker matrix addition that reduces microcracking upon mechanical loading. These materials were demonstrated in long-term tensile stress rupture to have increased levels of thermal durability, both at high and intermediate temperatures. BSG dopants were dominant at elevated temperatures, boron-modifying the insitu carbon layer and providing a viscous film protection of interfacial carbon layers present with the use of Nicalon fibers. SiC whisker matrix toughening was dominate at intermediate temperatures, reducing matrix microcracking and resulting in reduced pathways for environmental ingress into oxidatively unstable interfacial regions of the composite microstructure. Mica-interface CMCs replace interfacial carbon with an inherently oxidation resistant sheet-silicate mica. These Nicalon MAS glass-ceramic CMCs were shown to be free of oxidation embrittlement at intermediate temperatures. However, the sol-gel mica coatings were nonuniform, and showed evidence of environmental reactivity at elevated temperature.

14. SUBJECT TERMS

Ceramic Matrix Composite, CMC, Thermal Durability, Oxidation Embrittlement, BSG-Doped MAS, Mica Interface

15. NUMBER OF PAGES

192

16. PRICE CODE

17. SECURITY CLASSIFICATION OF REPORT	18. SECURITY CLASSIFICATION OF THIS PAGE	19. SECURITY CLASSIFICATION OF ABSTRACT	20. LIMITATION OF ABSTRACT
UNCLASSIFIED	UNCLASSIFIED	UNCLASSIFIED	SAR

TABLE OF CONTENTS

TABLE OF CONTENTS (continued)

LIST OF FIGURES

LIST OF FIGURES (continued)

LIST OF FIGURES (continued)

LIST OF FIGURES (continued)

LIST OF FIGURES (continued)

LIST OF FIGURES (continued)

LIST OF FIGURES (continued)

LIST OF TABLES

FOREWORD

This is the Final Report on Air Force Contract F33615-90-C-5909, "Thermally Durable Glass-Ceramic Matrix Composites." The overall objective of the program was to develop oxidatively stable CMCs for use at 2000°F and above in thermostructural applications such as advanced aeropropulsion systems. Two material concepts were investigated: (1) BSG-doped MAS cordierite matrix CMCs and their SiC whisker matrix-toughened hybrids, and (2) mica-interface CMCs. Corning acknowledges the support of its subcontractor Pratt & Whitney, particularly Gary D. Linsey of the Composites Group and David S. Murphy of the Mechanical Testing Group. Pratt & Whitney generated the tension, tensile creep, tensile stress rupture, and burner rig data presented in this report. The Air Force Project Engineer was Dr. Allan P. Katz of the Materials and Manufacturing Directorate, Air Force Research Laboratory, W-PAFB, OH.

THERMALLY DURABLE GLASS-CERAMIC MATRIX COMPOSITES

1.0 Introduction And Objective

To enable the innovative design concepts required to achieve a variety of Integrated High Performance Turbine Engine Technology (IHPTET) advanced propulsion goals, advanced materials with proven performance in the harsh thermostructural environment of a gas turbine engine will be required. Materials such as damage-tolerant, high specific strength ceramic composites that could possibly operate uncooled are the key to achieving large increases in propulsion system thrust-to-weight ratio, a measure of operational capability.

The emerging technology of ceramic matrix composites (CMCs) offers several potentially viable materials alternatives to the structural designers of hot-section hardware for advanced turbopropulsion systems. Many current candidates perform well under benign ambient conditions. They are all lightweight, refractory, and generally provide non-catastrophic failure modes leading to flaw- and notch-insensitive, strain-tolerant, and damage tolerant behavior.

However, the full promise of these materials has not yet been realized, since candidate CMCs have lacked the degree of thermal durability necessary for use in the most aggressive applications, that is, in very high temperature oxidative environments. The fundamental problem with these materials is a lack of thermal durability caused by an interfacial environmental instability known as oxidation embrittlement. This phenomenon results in the inability of any of these materials to accumulate localized damage without failure in the in-service thermostructural environment. Thus, oxidation embrittlement is universally accepted as the primary barrier to CMCs gaining design acceptance.

The major objective of this program was to develop material and process technologies suitable for producing oxidation resistant glass-ceramic matrix composites for use in a 2000°F thermostructural environment pertinent to IHPTET gas turbine engine applications. The aim was

to demonstrate novel structural composite materials with greatly enhanced oxidation embrittlement resistance and overall thermal durability.

The thrust of this program was to attempt to develop CMCs that were thermally durable by two approaches: (1) reducing the pathways of oxygen ingress to oxidatively unstable microstructural elements, and (2) replacing oxidatively unstable portions of the microstructure with materials that are inherently oxidation resistant.

2.0 Technical Approach

The weak fiber-matrix interface that is necessary for brittle matrix composites to exhibit good strength and toughness is typically achieved by the presence of carbon or boron nitrite, either applied as a fiber coating, or formed (for carbon) during high temperature processing when using carbon-containing SiC fibers, such as Nicalon or Tyranno.

The oxidation embrittlement degradation mode in CMCs is a multi-step process, first involving the accumulation of damage in the brittle matrix in the form of tensile microcracks. This is true for most CMCs, since the failure strain of ceramic matrices will typically be less than that of the reinforcing fibers. The second step in the embrittlement process is the oxidation of the carbon interface, followed by oxidation and other degradation of the SiC fibers. This weakens the fiber and greatly increases interfacial bonding to a degree that the debonding and frictional sliding that are necessary for pullout toughening do not occur. Instead, the matrix crack propagates directly through the fiber and the composite becomes brittle, exhibiting both low strength and low failure strain. This is a typical phenomenological scenario of events constituting oxygen embrittlement in ceramic matrix composites reinforced with SiC fibers.

The important point to recognize is that the solution to the oxidation embrittlement problem can be approached by both reducing matrix damage accumulation during loading, as well as by providing a sufficiently weak but oxidatively stable interface.

Two concepts for improving the thermal oxidative stability of glass-ceramic matrix composites were identified, and were pursued on this program. Both damage accumulation as well as oxidative stability were addressed. The first involved engineering the matrix of the composite by hybridization (physical additives) as well as chemical doping to protect current carbon-based interphases from oxidation. These in-situ-interface CMCs are known as BSG-doped composites or BSG hybrids, where BSG refers to a borosilicate glass dopant. The second material studied incorporates an inherently oxidation resistant sheet silicate (mica) interface to replace naturally

formed carbon (or BN fiber coatings, which are also oxidatively unstable). This CMC is referred to as a sheet-silicate interface composite.

Glass-ceramic matrices are particularly attractive for achieving thermally durable CMCs since they are fully dense (minimizing one avenue for environmental degradation), inherently oxidation resistant, and are low elastic modulus, which results in the fibers carrying most of the applied load. In addition, the thermal expansion of glass-ceramics is tailorable over a wide range permitting matching to any particular fiber used. But most importantly, glass-ceramics are accommodating to a wide range of chemical dopants and physical additives that can be used advantageously to tailor composite microstructure in an attempt to improve material performance. This attribute of glass-ceramics was investigated in the present program by the use of glass-dopants and physical additives to produce CMC microstructures which exhibit increased interfacial oxidative stability as well as reduced damage (i.e., matrix microcracking) characteristics.

3.0 Program Scope

The technical effort was divided into three principle tasks: (1) Composite Development: identifying, fabricating, and characterizing the constituent phases and optimizing the resultant ceramic composites; (2) Composite Durability Assessment: investigating and identifying the potential critical performance limiting phenomena associated with high temperature oxidative stability of the composites; and (3) Composite Properties Assessment: generating a preliminary materials property data base on selected ceramic matrix composites that are identified for potential use in materials selection and subelement design evaluation studies for IHPTET applications.

The work on BSG-doped CMCs and their matrix-toughened hybrids is described in Section 4. The work on sheet-silicate interface CMCs is contained in Section 5.

4.0 BSG-Doped MAS Composites

With the knowledge that the basic oxidation embrittlement process in CMCs involves the sequential microcacking of the matrix when under load, followed by rapid oxidation of the carbon rich interface that is typically present when using fibers such as Nicalon, an improved composite microstructure was envisioned that entailed modifications of a baseline Nicalon fiber reinforced magnesium aluminosilicate (MAS) cordierite matrix.

Nicalon Si-C-O fibers were chosen as the reinforcement phase, since they were the most mature commercial fiber available, and produced the in situ carbon interfacial layer. MAS cordierite ($2MgO•2Al_2O_3•5SiO_2$) was chosen as the matrix since it exhibits 1250°C refractoriness and has a thermal expansion ($2.2x10^{-6}C^{-1}$) slightly lower than that of the fiber. The modifications planned involved (a) SiC-whisker (SiC_w) addition to the matrix to raise the composite elastic limit to delay matrix microcracking, and (b) BSG addition to form glass matrix pockets to blunt matrix cracks by plastic deformation. Therefore, the concepts investigated involved reducing damage accumulation in the composite, and thus effectively managing the oxidation embrittlement process to an extent that increased thermal durability could be demonstrated. It will be shown that the actual role of the BSG phase was quite different than merely blunting matrix cracks, but nevertheless resulted in significant improvement in overall composite thermal durability.

4.1 Composition And Process Optimization (Task 1)

The objective of Task 1 was to optimize the composition and process for BSG-doped MAS CMCs. This was accomplished by conducting an initial screening evaluation/process window study involving a variety of materials: (a) baseline Nicalon/MAS, (b) Nicalon/BSG-MAS, and (c) Nicalon/BSG-Doped SiC_w-toughened MAS hybrid CMCs. A process window study was conducted with the latter material, with BSG dopant level, SiC whisker level, and process temperature each having a range of three values (i.e., 27 process conditions). Evaluation was made using the following characterization parameters: density, X-ray diffraction (XRD) phase identification, optical microscopy, transmission electron microscope (TEM) replica and thin foil

analysis, scanning Auger elemental analysis, short beam shear strength, transverse thermal expansion, and room-and high-temperature fast fracture flexure strength and failure strain (all conducted at Corning).

4.1.1 Processing

Nine basic compositional modifications consisted of three BSG dopant levels (2.5, 5, 7.5%) and three SiC whisker levels (7.5, 10, 12.5%), selected based on previous work to be ranges within which meaningful optimization could be conducted. Additionally, control composites were investigated containing combinations involving no SiC whisker additive and no BSG dopant.

Batch constituents for the barium-stuffed cordierite (see below) and the dopant glass were co-melted into a homogeneous glass, followed by quenching and ball-milling to the desired particle size. SC-9 SiC whiskers from ACMC (Greer, SC) were blended with the matrix glass powder to produce a whisker-glass mix containing 40 wt.% SiC. After diluting with the glass powder to achieve the desired whisker content, Nicalon SiC fiber tows were impregnated with the whisker-glass powder mixture using Corning's standard slurry-dip, drum-wound prepreg process. Prepreg tapes were stacked and consolidated by uniaxial hot pressing at three maximum temperatures (1200°, 1250°, 1300°C) for each of the nine basic compositions. During hot-pressing, the interfacial carbon layer is formed in situ (Nicalon being the source of carbon), the matrix is densified, and the cordierite crystalline phase is developed.

Note that the basic glass-ceramic matrix employed (i.e., non BSG-doped) is a barium stuffed cordierite. Barium addition accomplishes various things for MAS matrix composites. Ba is a large cation that stabilizes the precursor glass to delay crystallization and promote sintering. Its use thus enhances matrix consolidation prior to crystallization. Furthermore, processing temperatures for in situ carbon layer formation and overall matrix consolidation are significantly lower (which is desirable to minimize fiber degradation) than would be needed for stoichiometric cordierite.

4.1.2 Microstructure

(a) MAS Cordierite Matrix:

The basic matrix under all process conditions is fully dense and high crystalline cordierite, $Mg_2Al_4Si_5O_{18}$. Celsian ($BaAl_2Si_2O_8$) was found by XRD as a minor phase, and $MgAl_2O_4$ spinel was a trace component of the phase assemblage. Figure 1 presents a TEM thin foil bright-field image of the matrix microstructure. The cordierite is observed to consist of fine, equiaxed grains, of nominal size 0.2-0.8 μm. No porosity is detectable in the microstructure. No residual glass is observed in grain boundaries or at multi-grain junctions. Figure 1 shows the presence of small, dark faceted precipitates at grain boundaries, as well as ~10 nm spherical features with dark cores within the cordierite grains (i.e., intragranular). The spherical intragranular precipitates are crystalline (bright-field/ dark-field contrast). The larger dark faceted precipitates were determined by EDS (energy dispersive spectroscopy) to be depleted in Mg and enriched in Ba, Nb, and Fe. Niobium is from the Nb_2O_5 nucleation aid, and iron is a contaminant. These crystalline precipitates are thought to be NbC or barium niobate.

Hybrid versions of the MAS matrix contain addition of SiC whiskers for toughening. Their microstructure is shown in the TEM thin foil micrograph provided in Figure 2. The characteristic stacking faults in the SiC_w phase are clearly seen. Dark faceted Nb- and Ba-rich precipitate also segregate to whisker-cordierite boundaries. Note that the whisker-matrix interface is quite sharp and distinct. This is seen more clearly in the higher magnification micrograph shown in Figure 3. There is no detectable glass phase present at the SiC-MAS boundary or any evidence of reaction at the whisker-matrix interface. This indicates that the SiC whiskers are very compatible with the Ba stuffed cordierite matrix. This will be more definitely demonstrated later in the program in CMCs thermally exposed for greater than 5000 hours.

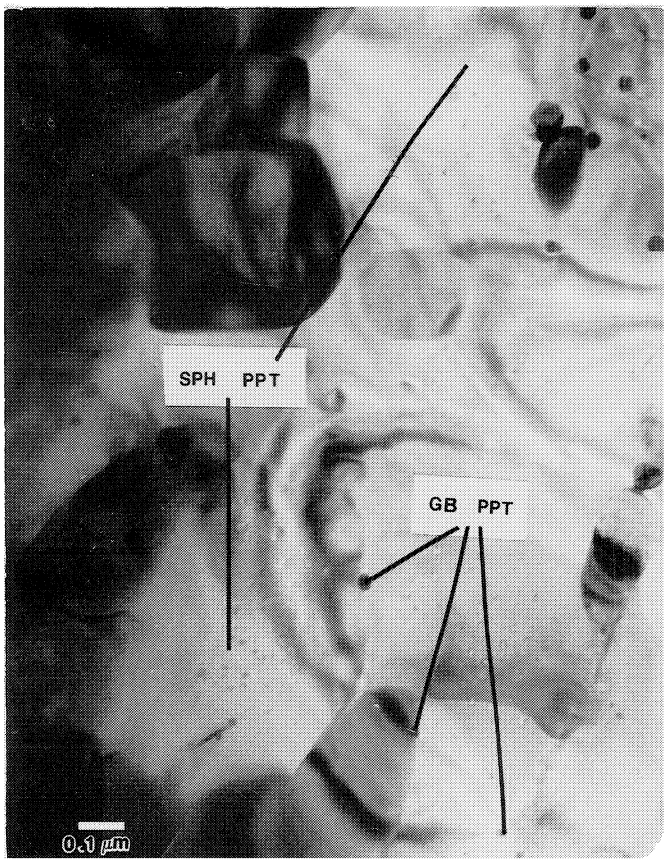

FIGURE 1. **BRIGHTFIELD TEM THIN FOIL IMAGE OF MATRIX MICROSTRUCTURE IN (0/0) Nicalon/Ba-MAS CORDIERITE COMPOSITE**

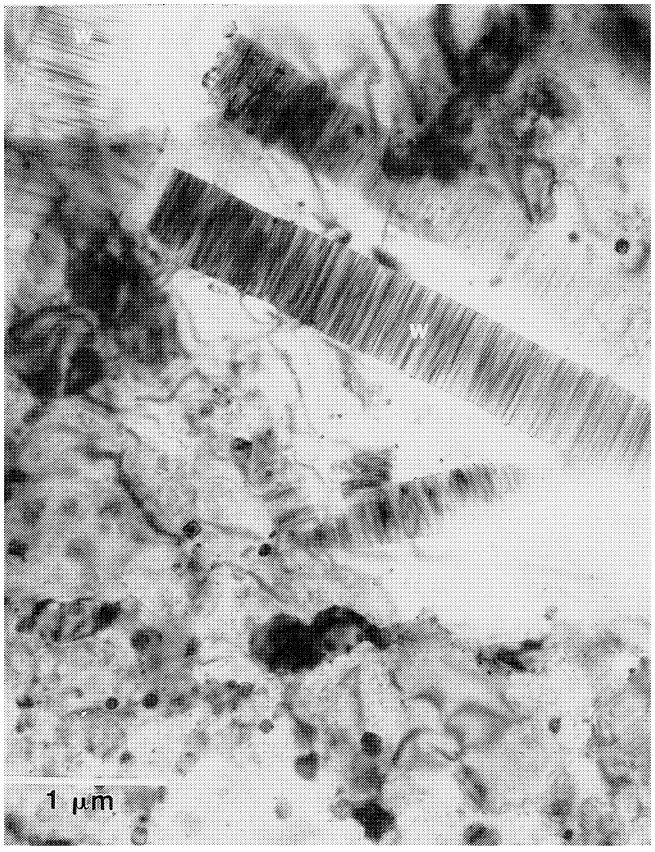

FIGURE 2. **TEM THIN FOIL VIEW OF SiC_w-TOUGHENED MATRIX IN A 2.5% BSG/10% SiC_w MAS HYBRID COMPOSITE**

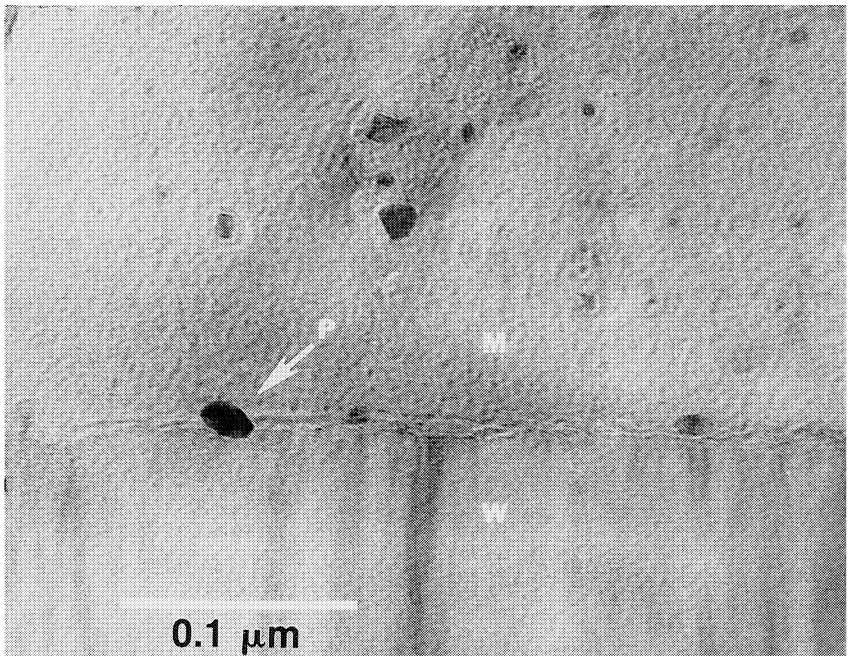

FIGURE 3. **TEM VIEW OF WHISKER-MATRIX INTERFACE IN 2.5% BSG/10% SiC_w MAS CORDIERITE HYBRID COMPOSITE**

(b) BSG-doped MAS Matrices

The large scale microstructure of BSG-doped MAS CMCs was determined by TEM replica examination of polished and etched (hot hydroxide) composites containing varying amount of BSG matrix dopant. The results for a 2.5% BSG MAS (also containing 7.5% SiC whiskers) are shown in Figure 4. In this TEM replica, the easily etched borosilicate glass phase appears in positive relief. The BSG phase is observed to exist in isolated pockets in the microstructure. The size of the glass pockets is roughly 1-3 μm, varies in direct proportion to BSG dopant level, and is relatively uniformly distributed as a discrete phase. Electron diffraction showed the BSG phase to be amorphous. No BSG or other amorphous phases were found in any intergranular locations, even with STM (scanning tunneling microscopy) profiling. Some BSG was found to intersect fiber surfaces. The extent of this is not known. Microstructural studies on thermally exposed CMCs to be presented later would seem to indicate that it is quite prevalent, however.

The grain size and phase assemblage of the MAS cordierite matrix is not affected by BSG doping. The cordierite grain size remains fine (0.5-0.8 μm), and the overall microstructure is highly crystalline and fully dense.

(c) Interface Chemistry and Structure

Baseline Nicalon/MAS CMCs:

Figure 5 illustrates the elemental depth profiles for a non-BSG containing composite, Nicalon/Ba-MAS cordierite processed at 1250°C. These scanning Auger results were obtained with a PHI 670 Nanoprobe, at Physical Electronics, Eden Prairie, MN. Transverse fracture surfaces with exposed fibers and matrix troughs were examined. The interface of non-BSG Ba-MAS composites is seen to consist of a highly pure (~95 at.%) well-developed intrinsic carbon layer, typically 50-80 nm thick [for reference, lithium aluminosilicate (LAS) and calcium aluminosilicate (CAS) matrix composites, processed at somewhat higher temperatures (typically 1300°-1350°C), have intrinsic carbon layers of ~30-100 nm and ~30-50 nm, respectively].

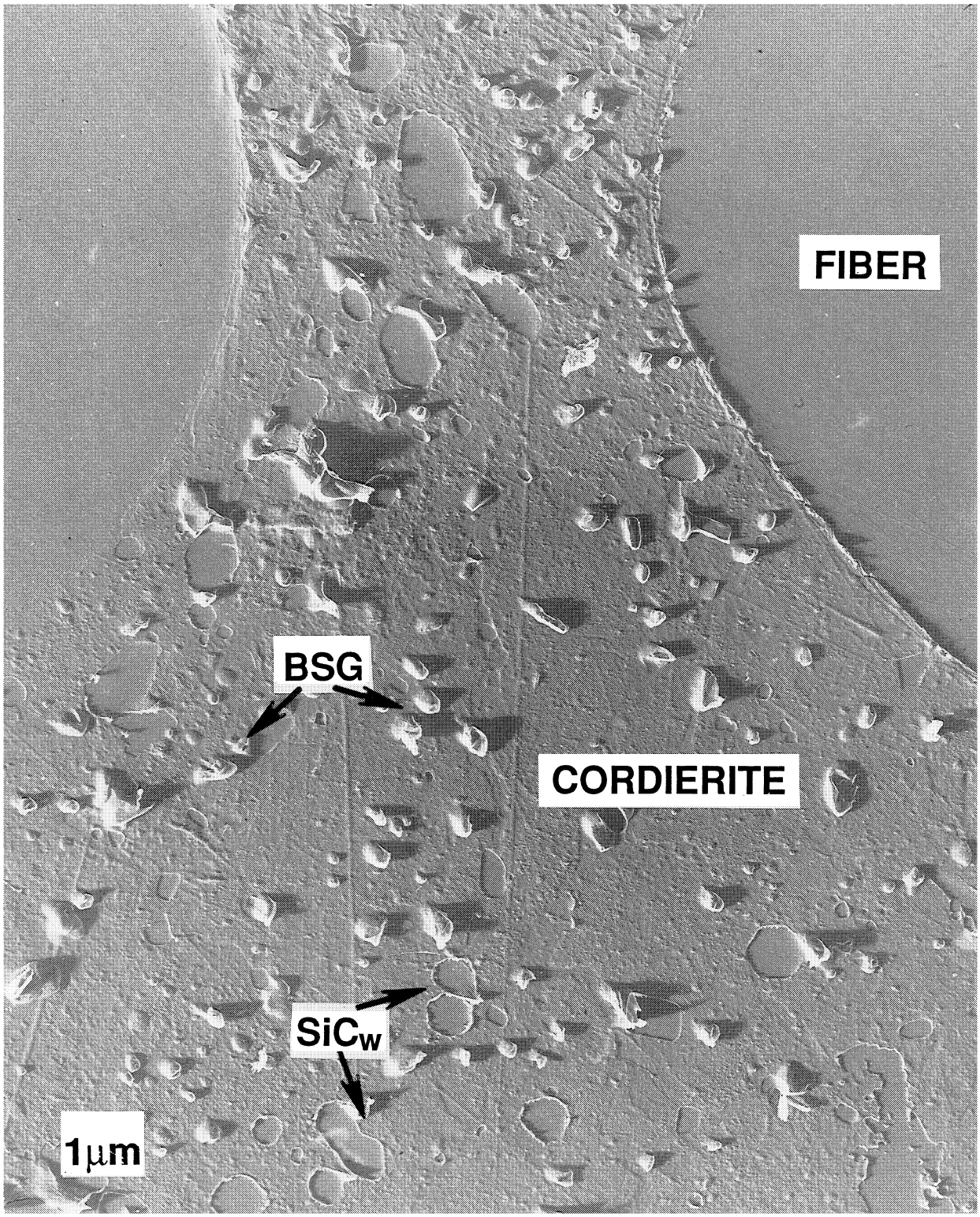

FIGURE 4. **TEM REPLICA MICROGRAPH OF 2.5% BSG/7.5% SiCw MAS HYBRID**

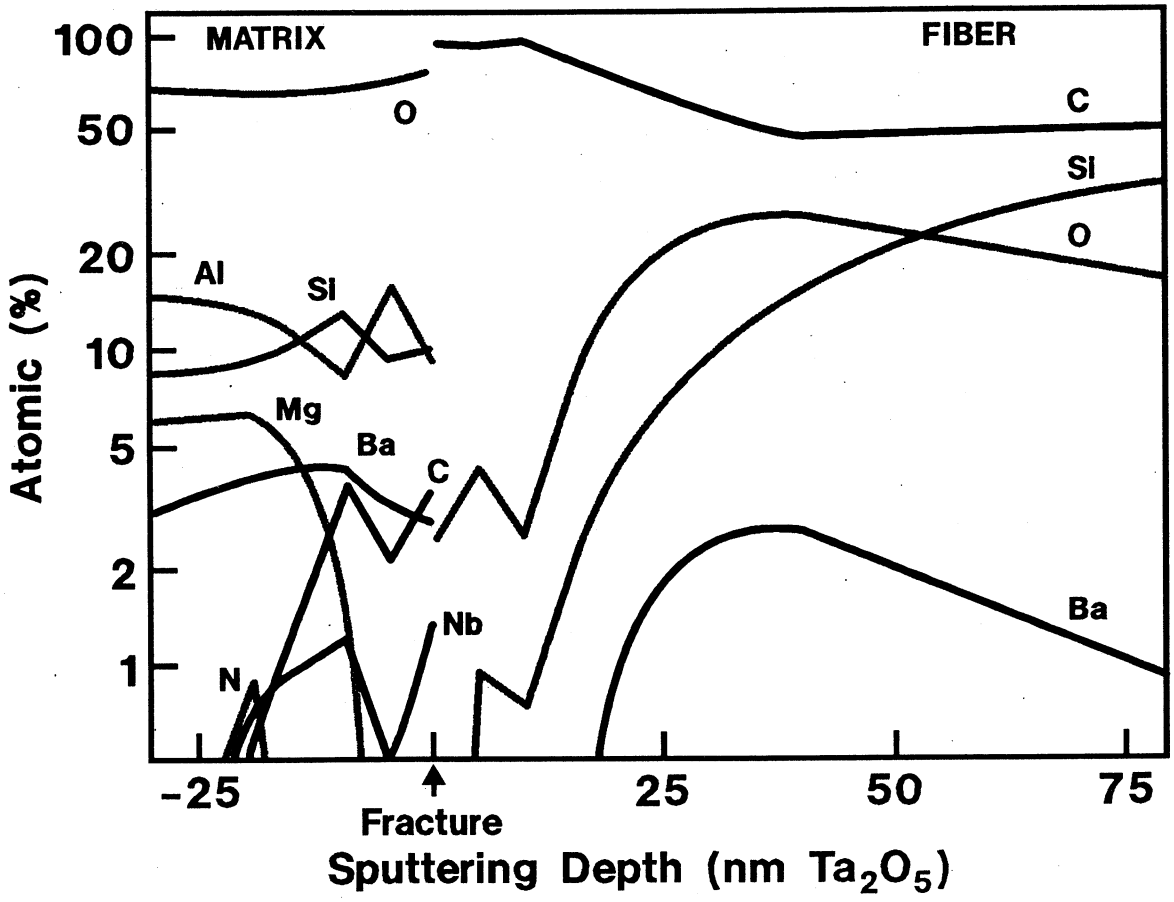

FIGURE 5. **AUGER ELEMENTAL DEPTH PROFILE OF INTERFACE IN NON-BSG CONTAINING Nicalon/Ba-MAS CORDIERITE COMPOSITE**

Fracture for Ba-MAS composites is on the matrix side of the carbon layer. Matrix barium diffuses into the fiber. It is believed that this facilitates the formation of the intrinsic carbon interface at such a low processing temperature as 1250°C. Figure 6 shows a TEM bright-field view of the interfacial region in Nicalon/Ba-MAS cordierite. Note the ~50 nm thick highly crystalline fiber surface adjacent to the pure carbon interface (dark-field imaging of SiC crystallites). This surface structure of the Nicalon reinforcing fiber has been observed in other glass-ceramic matrix composites.

Thus, baseline Nicalon/MAS has a pure carbon interface similar in composition and thickness to that of other conventional glass-ceramic matrix composites, such as those employing LAS and CAS matrices. All of these conventional composites embrittle in oxidizing environments at high temperatures (as will be demonstrated in subsequent sections of this report).

Nicalon/BSG-doped MAS CMCs:

The most interesting aspect of the microstructure of BSG-doped MAS matrix CMCs is the structure and chemistry of the fiber-matrix interface. Figure 7 presents scanning Auger elemental depth profiles of interfacial regions in BSG-doped Ba-MAS matrix composites with 7.5% BSG dopant. Comparison is made to the non-BSG doped baseline CMCs, which were also processed at 1250°C, shown in Figure 5. It is observed that in BSG-doped composites the in situ carbon layer is not pure. It is highly modified chemically, as well as being thinner and less structured in general.

These effects were found to be strongest for the highest BSG dopant level. The interface in the BSG hybrids studied is only ~75-85 at. % carbon, and contains substantial amounts of oxygen and boron that have diffused from the matrix, as well as nitrogen that has diffused from the fiber. Barium, and in some cases aluminum, have diffused into the fiber, indicating some association. Boron, nitrogen, and oxygen are the predominant dopants of the interface. The profiles for boron appear to track with the nitrogen profiles into the fiber, indicating some association. There appears to be relatively little silicon in the interface. Composite fracture occurs between the

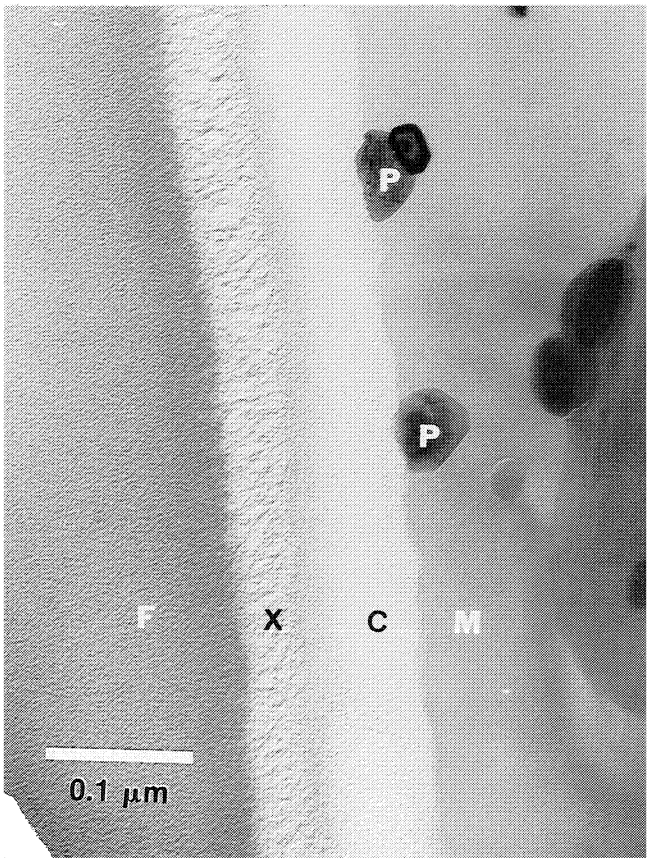

F=fiber
X=crystalline fiber surface
C=carbon interface
M=matrix

FIGURE 6. TEM THIN FOIL BRIGHTFIELD VIEW OF INTERFACIAL REGION IN BASELINE Nicalon/Ba-MAS CORDIERITE

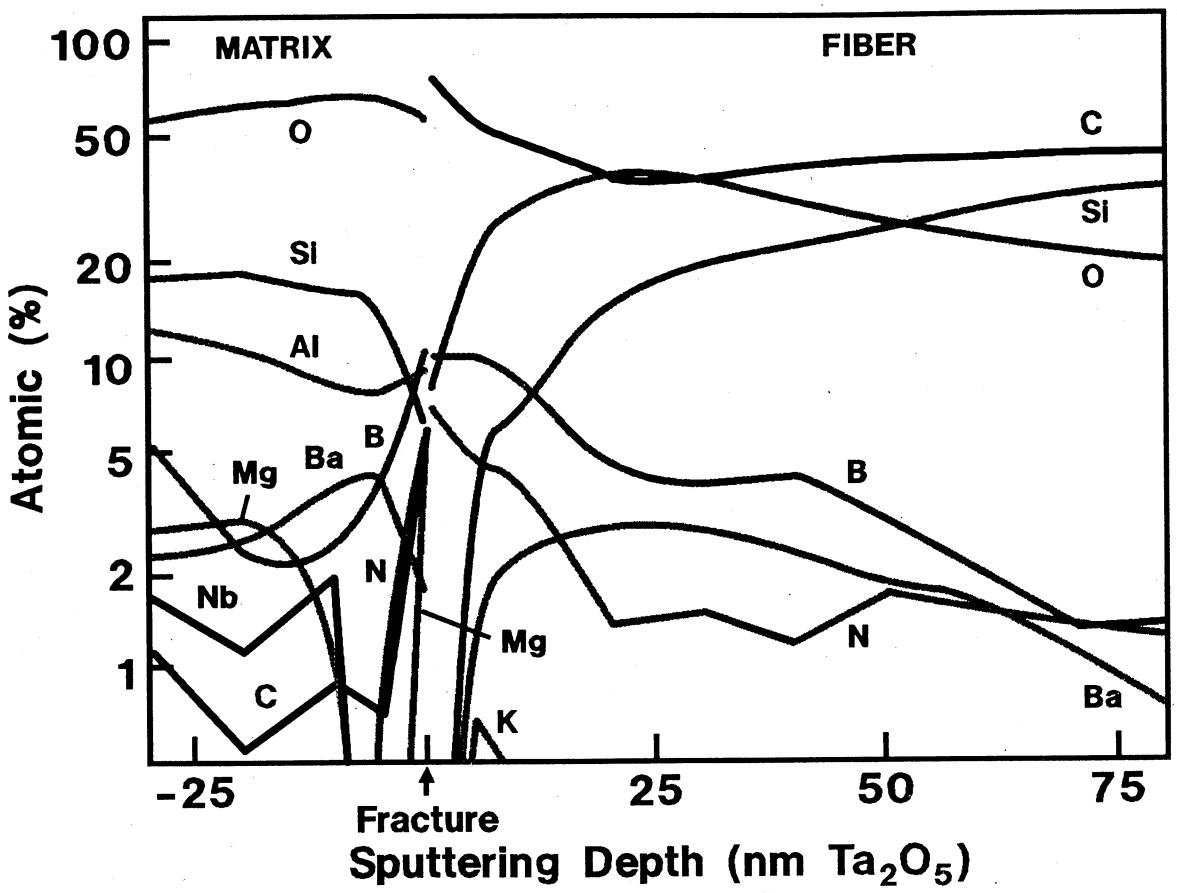

FIGURE 7. AUGER ELEMENTAL DEPTH PROFILE OF INTERFACIAL REGION IN Nicalon/7.5% BSG-DOPED MAS HYBRID COMPOSITE

matrix and the interface, which was also the case for baseline Nicalon/MAS (and generally observed for other Nicalon-reinforced CMCs).

Figure 8 presents a series of TEM thin foil micrographs that show the pronounced changes in interface thickness and structure with increasing BSG content. The interfacial thickness of the baseline (undoped) composite is ~70 nm, and the outer 50 nm of Nicalon is highly crystallized. In the BSG hybrid doped with 5% BSG, the interface thickness decreases to ~40 nm, and less of the outer fiber is crystalline, ~30 nm. At the highest dopant level, 7.5% BSG, Figure 8 shows the presence of a very thin, ~20 nm interface exhibiting the least amount of structure. For this highly doped composite, the fiber structure radially inward appears more uniform, with no apparent crystalline outer layer. The Auger depth profiles of Figures 5 and 7 illustrate that diffusion of matrix cations into the fiber increase substantially as the matrix BSG content is increased from zero to 7.5%. This appears to have a pronounced effect on the structure of the fiber surface.

It is interesting to note in Figure 8 that extremely thin modified carbon interfaces are produced with heavy BSG doping. In fact, one would not ordinarily expect the interface shown in Figure 8 for the 7.5% BSG/10% SiC_w hybrid to be mechanically functional (i.e., to possess a sufficiently low fracture energy to result in strong/tough composite behavior). However, it will be shown later that the composite room temperature strength and toughness actually increase with BSG-dopant level. One possible contributing factor, considering the aforementioned diffusion of cations (e.g., B, Al, Ba) into the fiber (Auger results, Figures 5, 7), and the decrease in crystallinity of the Nicalon fiber surface (TEM results, Figure 8), is that the intrinsic strength and toughness of the Nicalon fiber may be better-preserved during CMC processing for higher BSG dopant levels. This aspect of the structure of BSG hybrids seems plausible. A highly crystalline fiber surface would be quite notch sensitive (the notches would already be present as grain boundaries). The monolithic SiC literature indicates that Al and B in particular have a significant effect on grain growth of silicon carbide. It seems reasonable to expect that the diffusion of such cations into the Nicalcon fiber surface would have an effect on the growth of the SiC microcrystallites that comprise the Nicalon fine scale structure. Preventing such grain growth would decrease process related fiber degradation for Nicalon reinforced composites. This

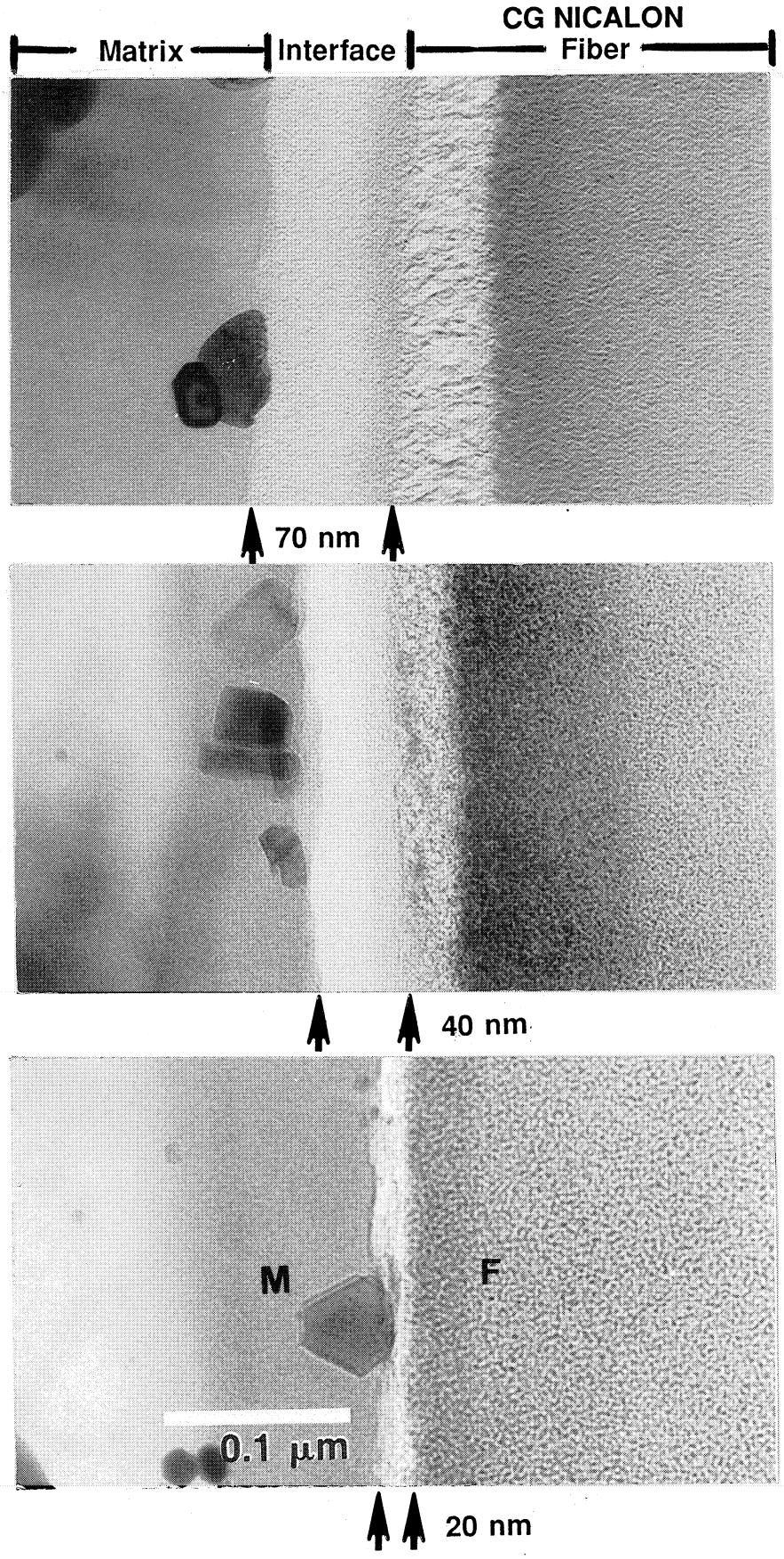

FIGURE 8. **TEM THIN FOIL VIEWS OF INTERFACE IN Nicalon/MAS CORDIERITE COMPOSITES WITH VARYING AMOUNTS OF BSG-DOPING**

may be one of the reasons that BSG-doped MAS hybrids will be demonstrated on this program to have such high strength (as high as 220 ksi in flexure at 25°C) and improved thermal durability.

It thus appears that boron diffusing to the Nicalon fiber has two effects: (1) limiting the formation of the in situ carbon layer, and (2) minimizing fiber crystallization.

The minimization of Nicalon fiber damage notwithstanding, the primary determinant of the resistance to oxidation embrittlement for BSG hybrids (that will be demonstrated below) is the boron modified carbon interface. The portion of the interface that is not carbon will be shown to be responsible for increased thermal durability achieved for BSG-doped composites. Note that the carbon is present, however, in sufficient quantity to result in CMCs with excellent strength and toughness. The presence of the boron containing phase at the interface ensures that such desirable mechanical behavior is maintained at elevated temperature as well. A potential contributing factor is enhanced crack tip plasticity via BSG doping which lessens the severity of matrix microcracking.

Oxidative stability in BSG-doped CMCs must be achieved without attendant loss of refractoriness, and therefore the specific nature of the boron bonding state in the interface is of importance. This was studied with the aid of XPS (X-ray photoelectron spectroscopy, also known as ESCA, electron spectroscopy for chemical analysis) examination of the chemical bonding on the surface of intact fibers bridging a matrix tensile crack. Recall that the fracture is matrix-side of the interface, so bridging fibers will have the intact interface on their surfaces. Using XPS/ESCA, the kinetic energy spectrum of surface-emitted electrons will have characteristics associated with their original bonding state. Energy peaks are compared with standards (e.g. for B_2O_3 and BN) to aid in identification. The results of such analysis of BSG-doped MAS composites is shown in Figure 9. It was found that nitrogen at the interface was bonded entirely to boron. About half the boron atoms are bonded to nitrogen, with the remainder oxygen-bonded. Very little silicon was found at the interface; the oxygen present was bonded to boron. This information indicates that the portion of the interface that is not carbon is BN and

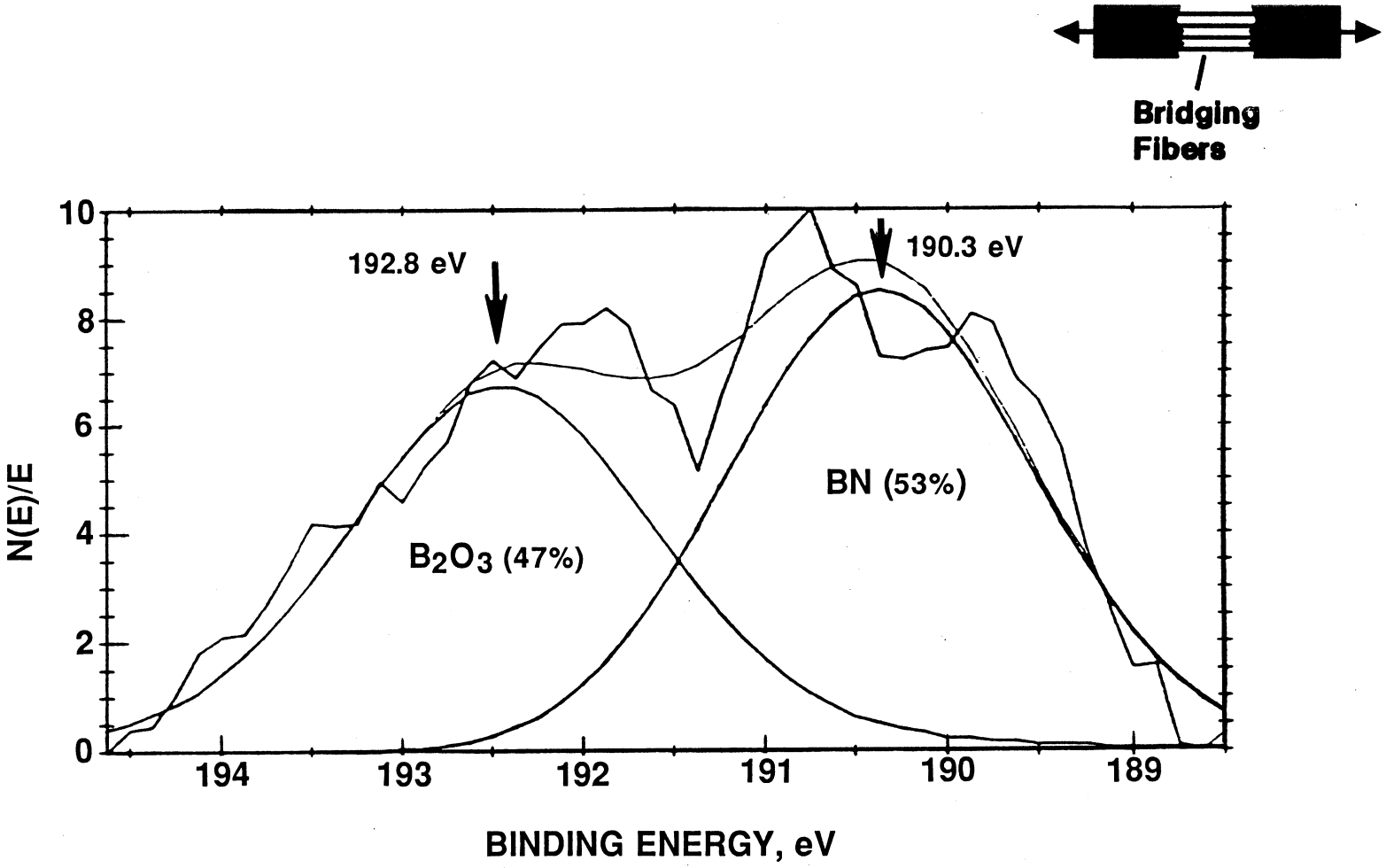

FIGURE 9. **XPS BORON BINDING ENERGY SPECTRUM OF 7.5% BSG-DOPED MAS CORDIERITE CMC SHOWING BONDING STATES OF INTERFACIAL BORON**

B_2O_3. A complex nitrogen-containing borosilicate is not likely, since little or no silicon is present. Such boron containing compounds are known to improve the oxidation resistance of carbon/graphite. Their affect on the thermal durability of BSG hybrid composites will be demonstrated below.

(d) Summary of Microstructural Observations

It is therefore demonstrated that BSG-doped MAS matrix composites have unique interfacial chemistry. The BSG forms as isolated phase-separated regions in the matrix, and provides a source of boron, which diffuses to the interface during composite hot consolidation. This greatly affects the formation of the in situ carbon rich interface (the carbon being an inevitable consequence of using Nicalon fibers). The resultant interface is thin (thinner than for non-BSG-doped CMCs) and contains boron in the form of B_2O_3 and BN. Additionally, there is growing evidence of a BSG glass phase matrix side of the interface. This was not observed in initial microstructural examination, but became more prevalent as thermally exposed samples were evaluated as will be discussed in later sections of this report.

4.1.3 Mechanical Behavior (screening)

The objective of Task 1 screening level mechanical behavioral studies was to (a) characterize the effect of constituent phases, and (b) to optimize the ceramic composite composition and processing conditions. The emphasis was on demonstrating that increased thermal durability could be achieved by BSG-doping and/or SiC whisker matrix additions, and to downselect to the best one or two composites to be more comprehensively studied in Task 2.

Flexure testing was employed (at Corning) to conveniently provide screening data. Testing was performed in a universal test machine in the 4-point configuration, with a span-to-depth ratio of ~30, which is typical of that used in the ceramic composites community to minimize premature shear failures. The elastic beam theory equations were used to calculate the outer fiber tensile stress, commonly called the flexural strength. Strain was estimated by assuming that all crosshead displacement was translated to specimen deflection. Elastic beam theory equations

were used to relate beam deflection to outer fiber tensile strain. In this manner, flexural stress-strain behavior was calculated from load-deflection data.

For more meaningful testing, particularly in assessing the extent of the elastic region of behavior, and the relative influence of BSG-doping vs. SiC-whisker matrix toughening, tensile testing (at 25°C) was performed (at Corning) using Instron hydraulic grips and resistance strain gages.

The results for both zero-condition control compositions as well as a range of BSG-doped, SiC-whisker toughened, MAS cordierite matrix composite compositions is described in the following sections.

4.1.3.1 Composite Baseline and Control Compositions

Various mechanical property tests were performed on control composite compositions, where one of the constituent phases was eliminated and the other maximized. The objective was to demonstrate the individual effect of BSG-doping and SiC_W toughening, compared to the baseline MAS cordierite composite and a CAS anorthite composite, both containing neither additive. These investigations provide insight into the matrix cracking/damage accumulation process in BSG-doped and hybrid (whisker-toughened) composites, as well as their interfacial oxidative stability. Matrix cracking and interfacial oxidative stability combine to determine the overall thermal durability of a ceramic matrix composite.

(a) Matrix Microcracking and Composite Elastic Limit:
Role of BSG-dopant and SiC-whisker Phases

Damage development in the form of matrix microcracking and interfacial oxidation are separate but sequential events that lead to strength and toughness degradation in CMCs subjected to the thermostructural environment. These phenomena are commonly referred to as oxidation embrittlement. The role of matrix microcracking on oxidation embrittlement is well documented

in the literature, in particular the existence of performance limiting damage below the composite elastic limit, i.e., subelastic limit matrix microcracking.

One of the key intended mechanisms of increasing CMC thermal durability through the BSG hybrid approach is to raise the composite elastic limit; that is, to delay matrix cracking to higher levels of composite strain. This is expected to be accomplished by toughening the matrix, raising the matrix phase fracture energy. This is the route to such improvement as predicted by the original ACK theory of matrix strain enhancement[1], or by one of the more recent fracture mechanics based theories. The ACK theory conveniently describes matrix cracking in frictionally-bonded brittle matrix composites in terms of fiber, matrix, and interface constituent properties. The matrix cracking strain (which would define the CMC elastic limit), is given by the relation:

$$\varepsilon_m = \left[\frac{24\tau_o \gamma_m E_f v_f^2}{E_c E_m^2 \phi_f (1-v_f)} \right]^{1/3}$$

where,

τ = interfacial shear strength
γ_m = matrix fracture energy
E_c, E_m = composite and matrix elastic moduli
E_f, ϕ_f = fiber modulus and diameter
v_f = volume fraction fiber

For BSG hybrid composites, our original intention was to increase the matrix fracture energy by the addition of a SiC whisker phase to the MAS cordierite matrix. Gadkaree[2] and Gadkaree and Chyung[3] have demonstrated that glass-ceramics such as MAS cordierite are toughened substantially by the addition of SiC whiskers, as shown in Figure 10. For the fiber-reinforced BSG hybrid CMCs investigated, it was anticipated that such matrix toughening would increase the composite elastic limit, and possibly eliminate subelastic limit cracking (if it is as prevalent in MAS matrix composites as it is in CAS composites). A marked improvement in overall thermal durability would be expected to result. Therefore, room temperature tensile stress-strain

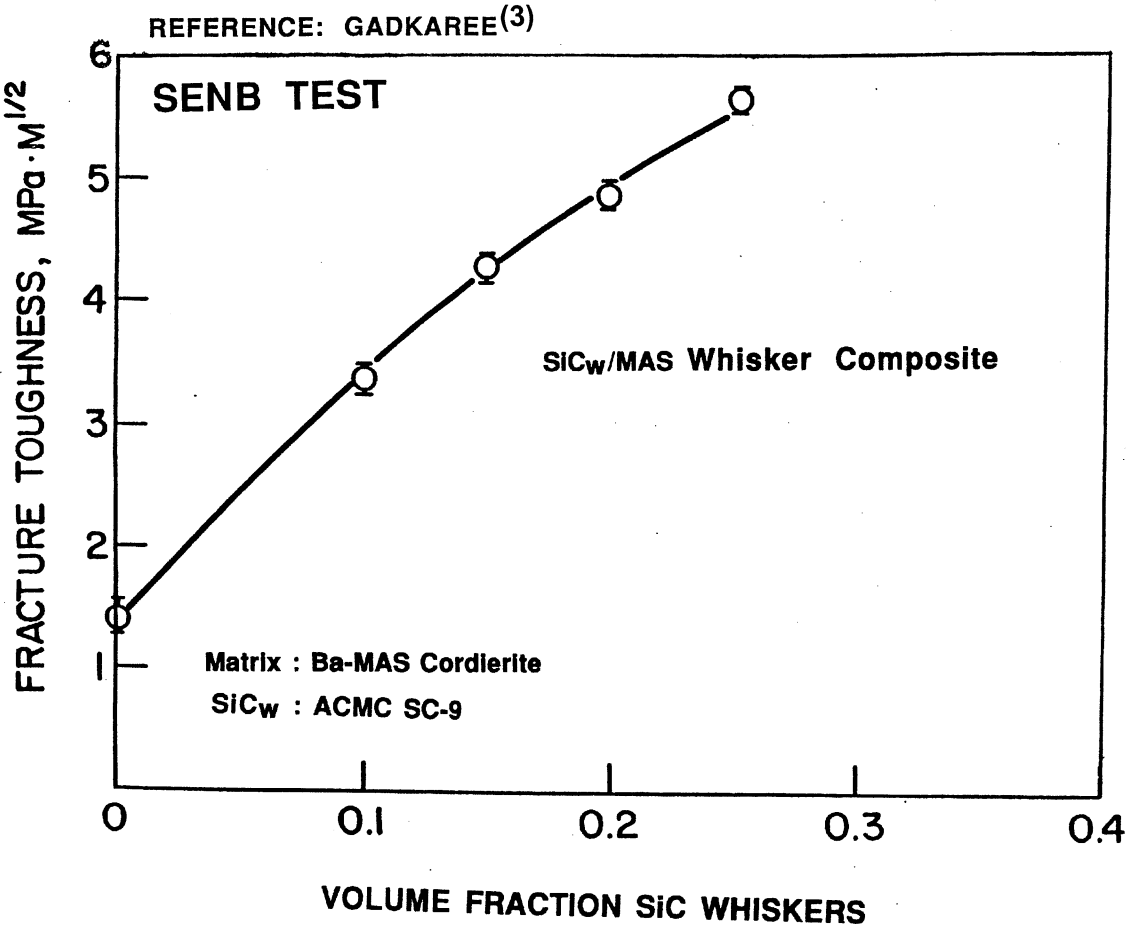

FIGURE 10. FRACTURE THOUGHNESS OF SiC_w/MAS WHISKER-TOUGHENED MATRICES

behavior was measured for a series of (0°) unidirectional baseline and control composites. The objective was to demonstrate the individual effect of BSG-doping and SiC_w toughening, compared to the baseline MAS cordierite composites and a CAS anorthite composite containing neither additive.

Figure 11 presents the tensile stress-strain curves for MAS and CAS baseline composites with in situ carbon interfaces. The MAS matrix thermal expansion (~$2.2x10^{-6}C^{-1}$) is substantially less than that of the SiC fiber (~$4.1x10^{-6}C^{-1}$). Therefore, the MAS matrix has a compressive residual stress axially. The CAS matrix thermal expansion (~$5.1x10^{-6}C^{-1}$) is slightly higher than that of the fiber. Thus, CAS is in axial tension. This most probably contributes to subelastic limit microcracking. However, Figure 11 illustrates that the tensile stress-strain curves are qualitatively similar for the two materials (although the MAS composite has less of a damage accumulation plateau than the CAS composite). This tends to indicate that the difference in matrix expansion for these two composites is not expected to be a major behavioral factor, at least in comparison to the primary influence of BSG and SiC whisker additives (as will be shown below). Both baseline CAS and MAS composites exhibited the substantial amount of fiber pullout that is associated with good composite toughness.

Tensile stress-strain curves are presented in Figure 12 for control composites containing only BSG dopant (7.5/0) or only SiC_w additives (0/10), in comparison to the baseline Nicalon/MAS composite (0/0). It is apparent that both the elastic limit stress as well as the elastic limit strain are greatly improved at room temperature by either adding just SiC whiskers to the matrix, or by adding just BSG to the matrix. Note that a ~2X increase in elastic limit is accomplished by either matrix additive. Both BSG doping and SiC whisker matrix toughening significantly alter the manner in which damage accumulates in the composite matrix. The fracture surface of the BSG-doped (7.5/0) composite generally exhibited less fiber pullout than the baseline MAS CMC. Good crack bridging and fiber pullout was observed for the SiC_w whisker matrix-toughened CMC, as well.

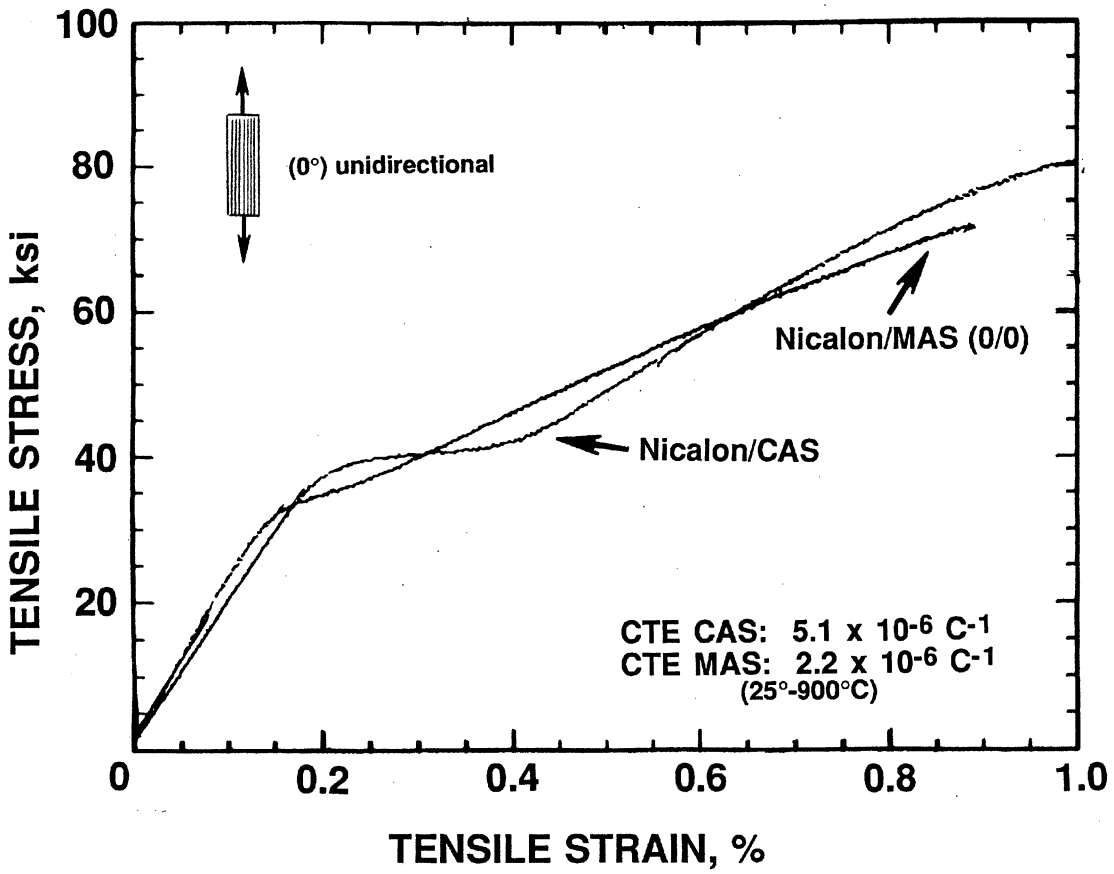

FIGURE 11. TENSILE STRESS-STRAIN BEHAVIOR OF BASELINE MAS CORDIERITE AND CAS ANORTHITE COMPOSITES

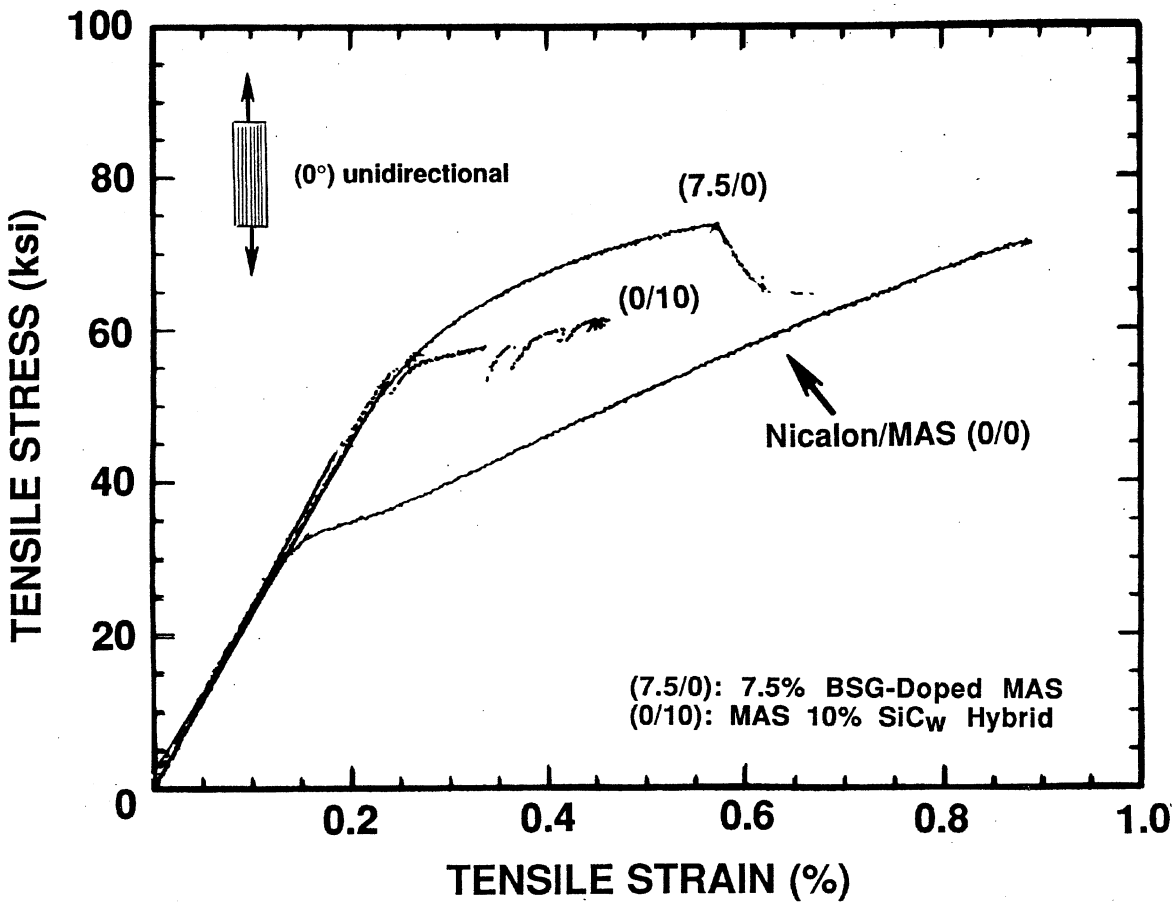

FIGURE 12. **TENSILE STRESS-STRAIN BEHAVIOR OF BASELINE AND CONTROL BSG-DOPED MAS HYBRID COMPOSITES**

Two distinctly different mechanisms of increasing the elastic limit appear to be operable in these composites. The results for the (0/10) material (no BSG/10% SiC_w) shown in Figure 12 demonstrate that increasing the matrix fracture energy (γ_m) by whisker toughening increases the composite elastic limit as predicted by Equation 1. The results for the 7.5/0 material (7.5% BSG/no SiC_w) demonstrate that the composite elastic limit can be increased to an equivalent or greater extent at RT by BSG doping the matrix. Recalling that TEM and SAM (Scanning Auger microprobe) microscopy indicated that BSG doping modifies the fiber-matrix interface to a great extent, consideration of Equation 1 leads to the conclusion that BSG doping increases the interfacial shear resistance (τ_o). This seems plausible, knowing that the interface in BSG hybrids is thinner, and is not pure carbon, but also contains $BN+B_2O_3$ as discussed in section 4.1.2 above. Stronger interfacial bonding due to higher interfacial shear resistance would be expected. Such increase in τ_o would increase the composite elastic limit as predicted by Equation 1.

(b) Effect of BSG-Doping and SiC_w-Toughening at Elevated Temperatures

The high temperature behavior of control compositions (either SiC_w or BSG added singly) and baseline CMCs (CAS and MAS with neither additive) was determined by flexure testing in air atmosphere.

The composite elastic limit, as measured by the first deviation from linearity on a flexural stress-strain curve, is plotted as a function of temperature for the baseline and control composites in Figures 13 and 14 (elastic limit stress and strain, respectively). It is noted that BSG doping appears to have the stronger influence on elastic limit at 25°C. However, the benefits of both BSG doping and SiC_w matrix toughening are apparently lost at elevated temperature. The low proportional limits at high temperature, however, are most probably due to increased deformation in the (matrix-dominated) flexure test, and not to a matrix tensile microcracking event that would adversely affect thermal durability. This is possibly an indication that the benefits of SiC whisker hybridization and BSG-doping would be more effective at elevated temperature with a matrix more refractory than MAS cordierite.

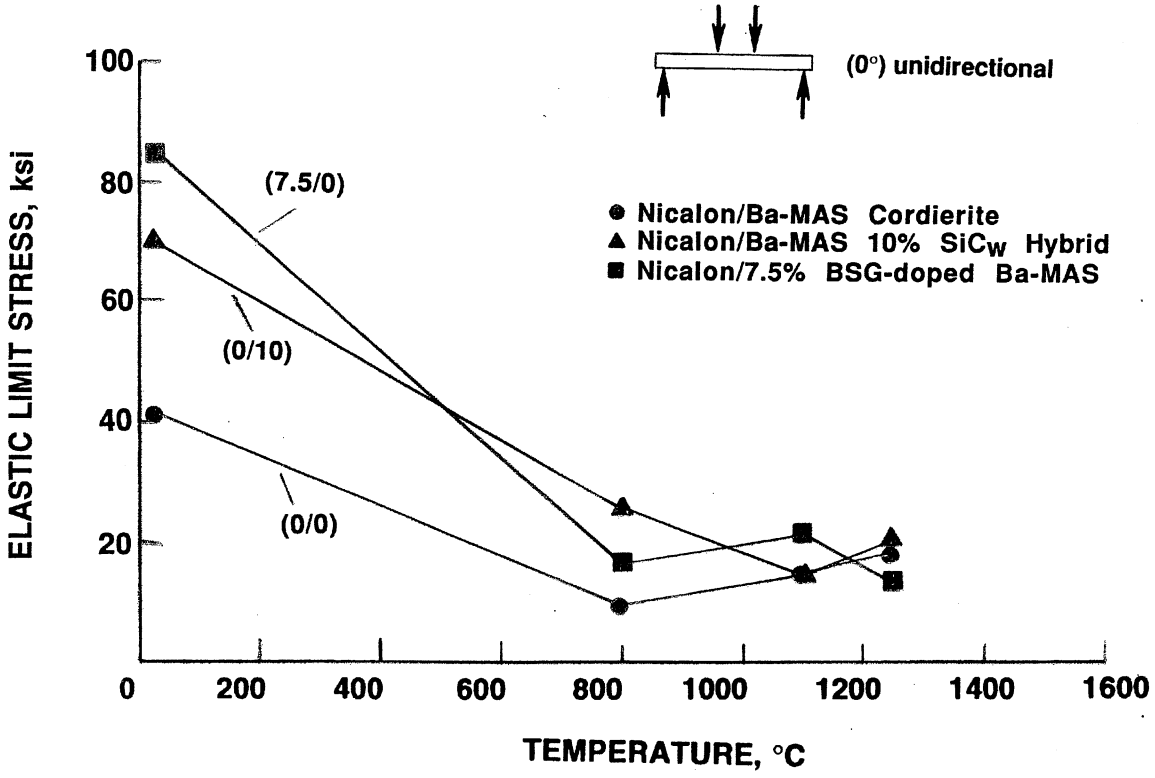

FIGURE 13. ELASTIC LIMIT STRESS FOR BASELINE, WHISKER-TOUGHENED, AND BSG-DOPED MAS CORDIERITE COMPOSITES

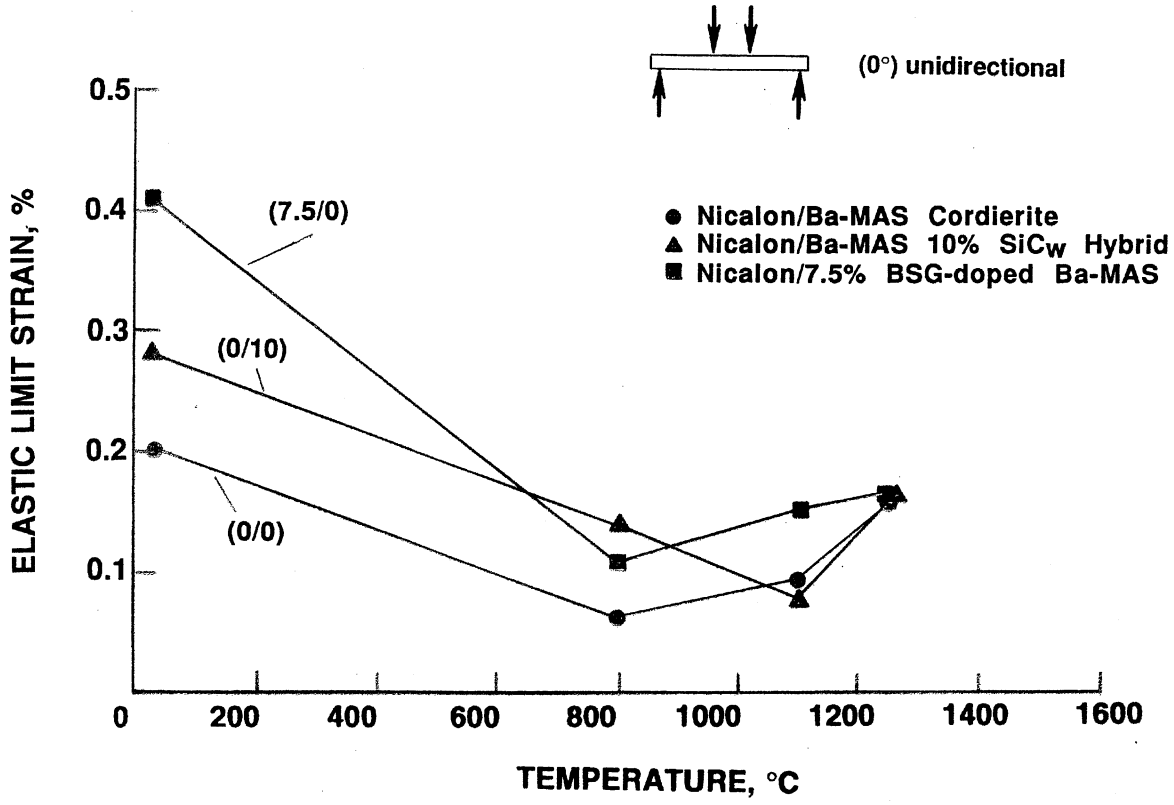

FIGURE 14. **ELASTIC LIMIT STRAIN FOR BASELINE, WHISKER-TOUGHENED, AND BSG-DOPED MAS CORDIERITE COMPOSITES**

The ultimate properties (i.e., flexure strength and strain at ultimate load) for the baseline and control CMC compositions are shown in Figures 15 and 16, respectively. The BSG dopant has the most pronounced affect on mechanical behavior as seen for both strength and ultimate strain. Up to and including 1100°C (2000°F) the 7.5% BSG-dopant results in composites with vastly improved strength and ultimate strain as shown in Figures 15 and 16. Comparing the 25°C and 1100°C fracture surfaces for these CMCs [i.e., the (0/0), (0/10) and (7.5/0) materials shown in Figures 17-19, respectively] reveals that the reason for this is that the (0/0) and the (0/10) composites severely embrittled at 1100°C, whereas the (7.5/0) CMC did not. Figure 19b illustrates that the (7.5/0) composite failed mainly by extensive shearing. Note in Figure 19b that the shear/delamination failure mode was accompanied by noticeable permanent deformation. The flexure test is matrix dominated and this result indicates refractory limitations of the BSG-doping approach to achieving CMC thermal durability. The (7.5/0) composite has good strength and failure strain at 1100°C due to the increased resistance to embrittlement that BSG-doping provides. At 1250°C this material does not exhibit such high values of strength because of loss of refractoriness. The large failure strain, massive shear and interlaminar failure, and permanent deformation occurring at a relatively low stress so indicate. Any comparative increases in refractoriness for the non-BSG doped CMCs (i.e., (0/0), (0/10)) cannot be tested and observed due to their premature brittle failures.

(c) Summary of Baseline/Control Compositions

Testing of control CMC compositions, where one or both of the BSG and SiC_W composition variables was set at zero, indicated that the BSG dopant was dominant and controlled the mechanical performance of the CMCs. BSG-doping results in more superior thermal durability than obtained for conventional CMCs.

With respect to matrix microcracking and the damage accumulation process, both BSG-doping and SiC whisker toughening were shown to raise the composite elastic limit at 25°C by inhibiting matrix cracking. BSG-doping has the stronger influence, and appears to affect τ_o, the interfacial shear resistance, which is related to the interfacial toughness and its control of

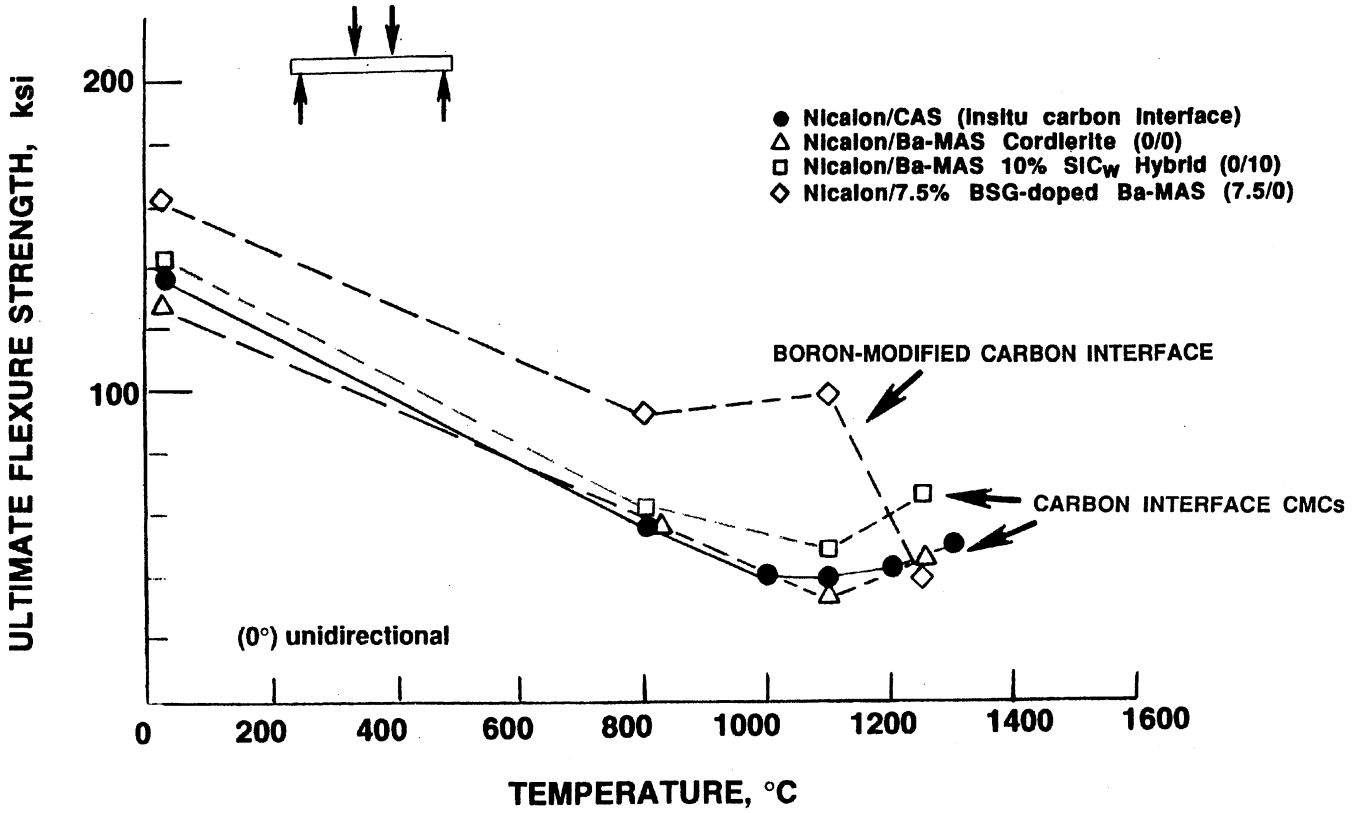

FIGURE 15. ULTIMATE STRENGTH OF BASELINE CAS AND MAS CORDIERITE COMPOSITES

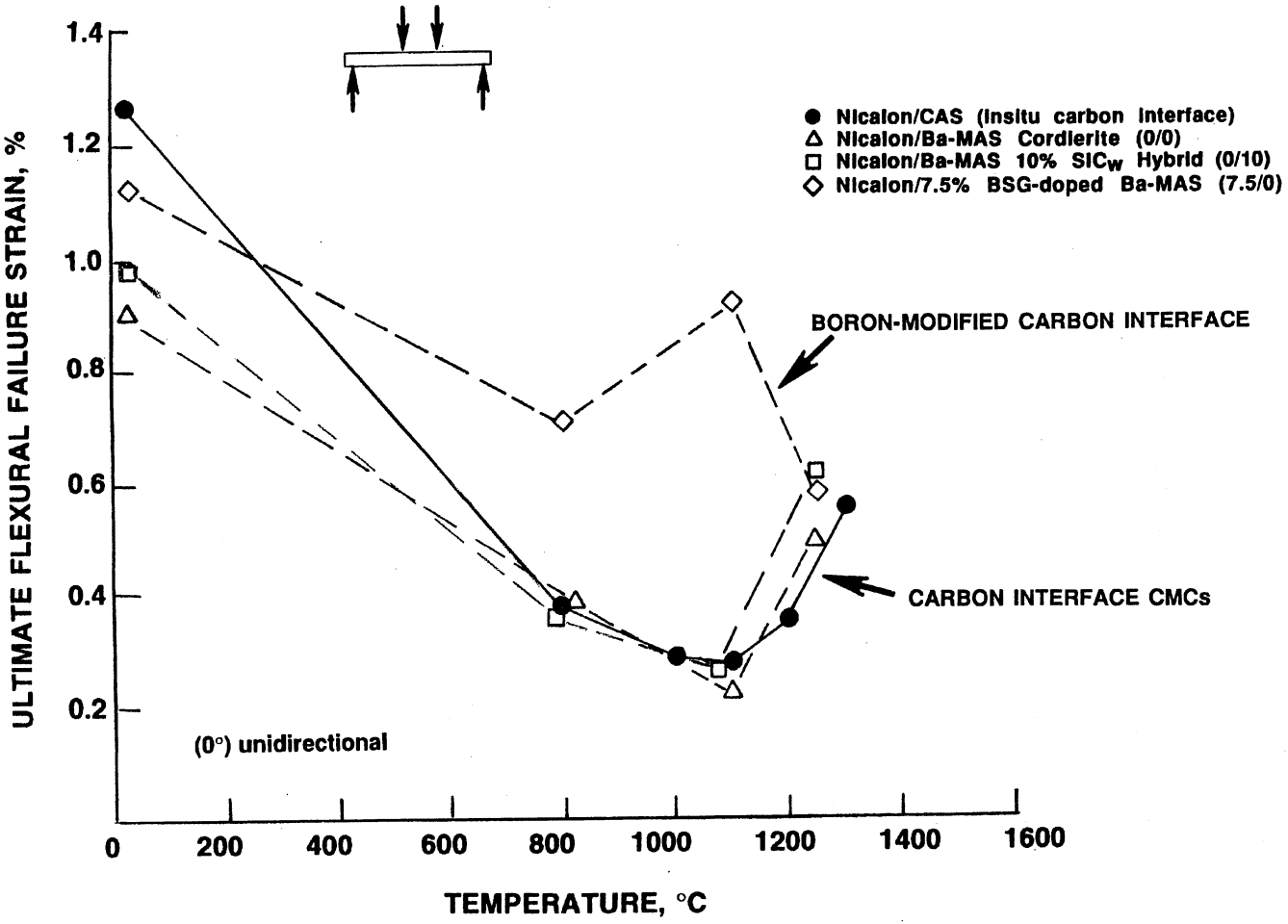

FIGURE 16. ULTIMATE FAILURE STRAIN OF BASELINE CAS AND MAS CORDIERITE COMPOSITES

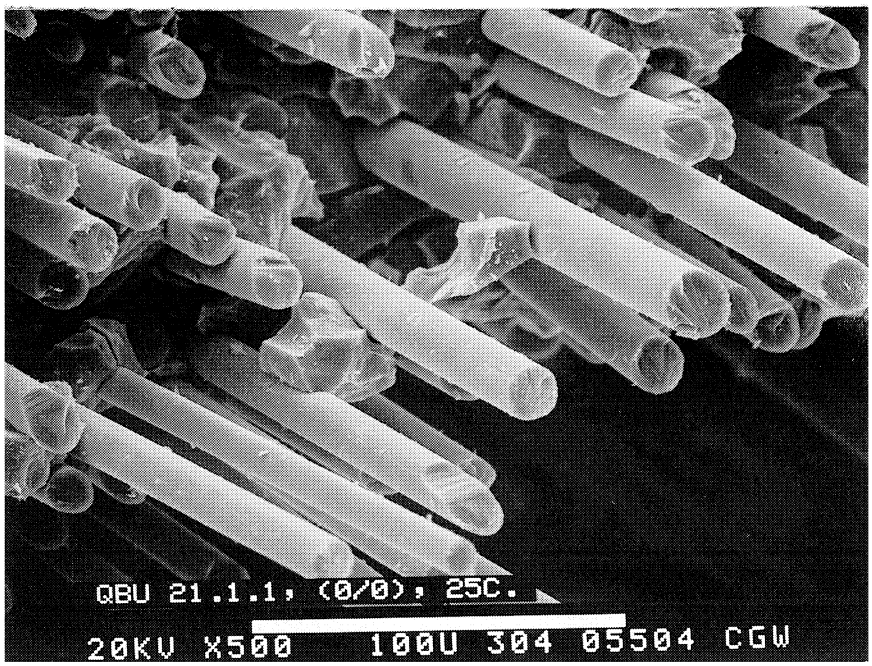

(A) 25°C FRACTURE SURFACE SHOWING FIBER PULLOUT

(B) 1100°C FRACTURE SURFACE SHOWING EXTREME EMBRITTLEMENT

FIGURE 17. SEM VIEWS OF THE FRACTURE SURFACE OF Nicalon/Ba-MAS CORDIERITE (BASELINE (0/0) CMC)

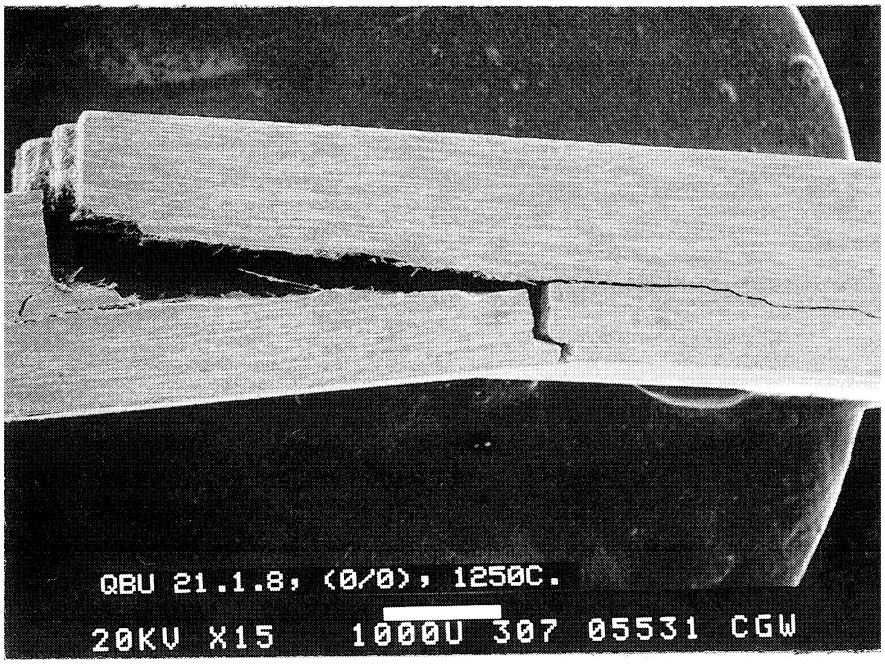

(C) 1250°C: NO DETECTABLE PERMANENT DEFORMATION

FIGURE 17. CONCLUDED (BASELINE (0/0) CMC)

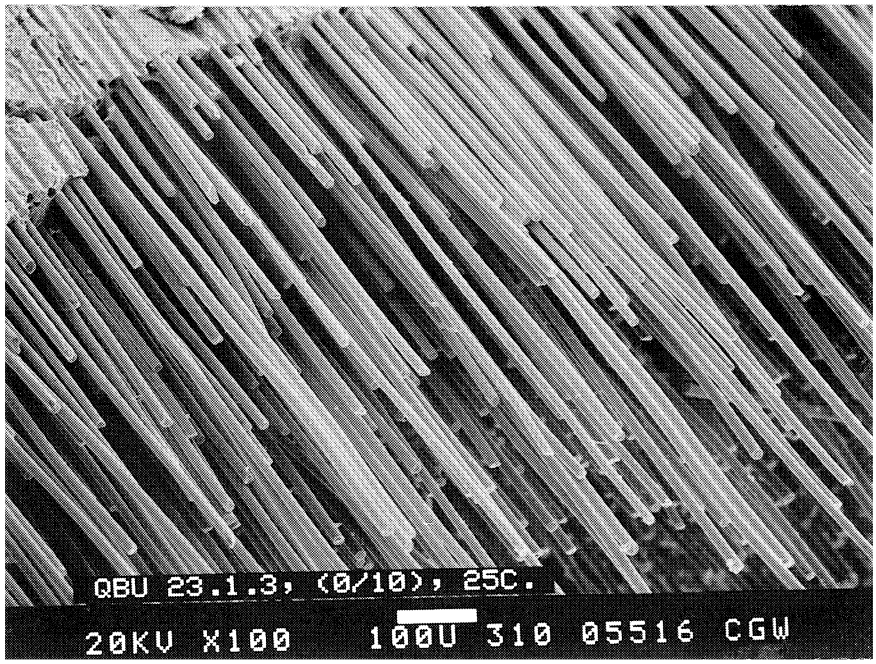

(A) 25°C FRACTURE SURFACE SHOWING GOOD FIBER PULLOUT

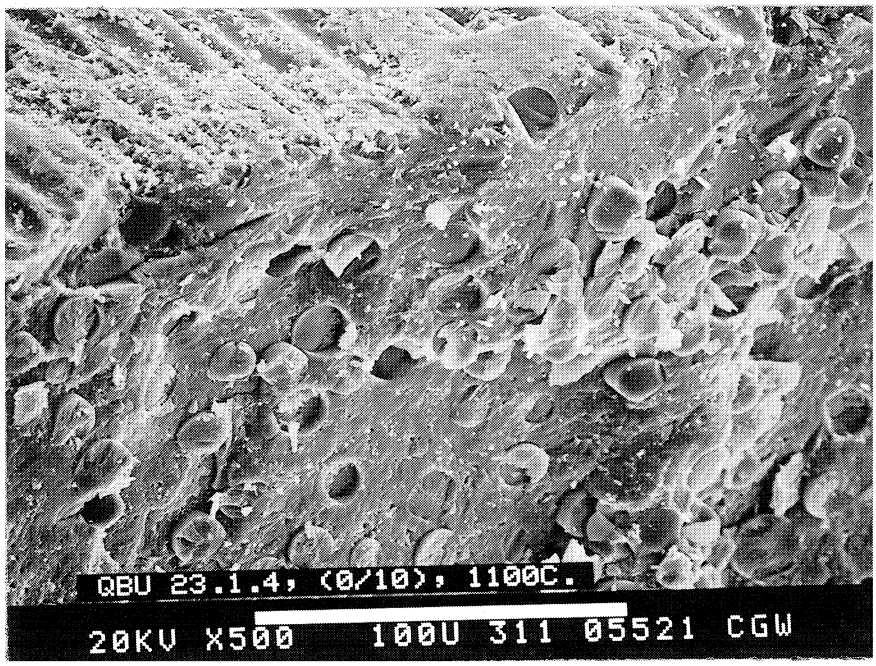

(B) 1100°C FRACTURE SURFACE SHOWING EXTREME EMBRITTLEMENT

FIGURE 18. SEM VIEWS OF THE FRACTURE SURFACE OF MATRIX-TOUGHENED Nicalon/MAS 10% SiC_w-HYBRID CMC (CONTROL (0/10) COMPOSITE)

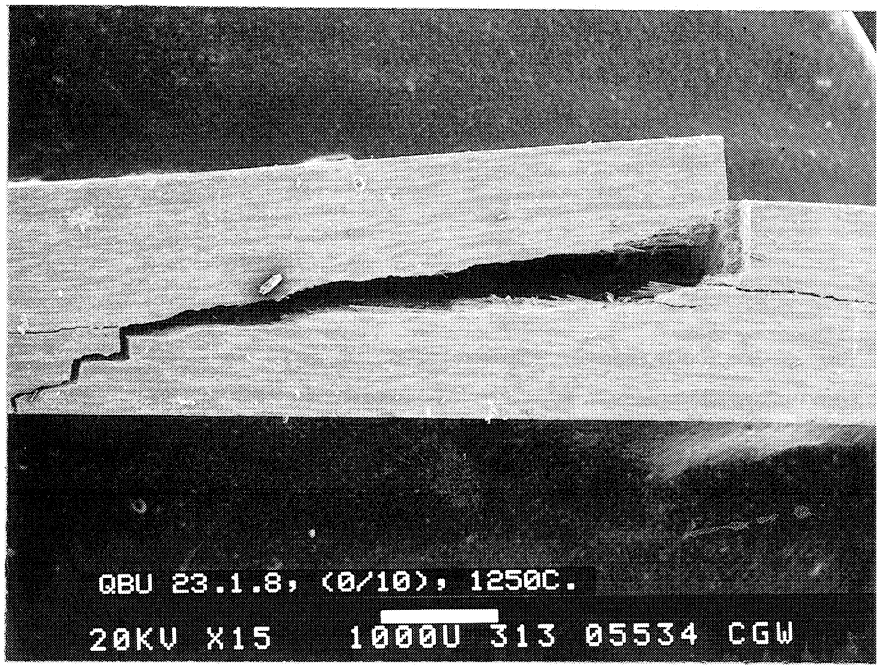

(C) 1250°C: NO PERMANENT DEFORMATION

FIGURE 18. CONCLUDED (CONTROL (0/10) CMC)

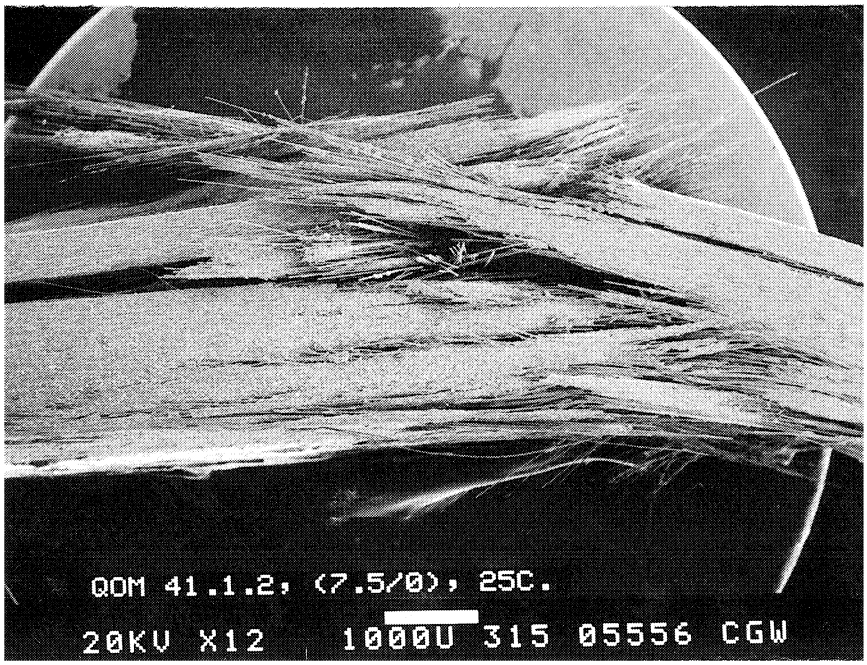

(A) VERY SPLINTERY FRACTURE AT 25°C

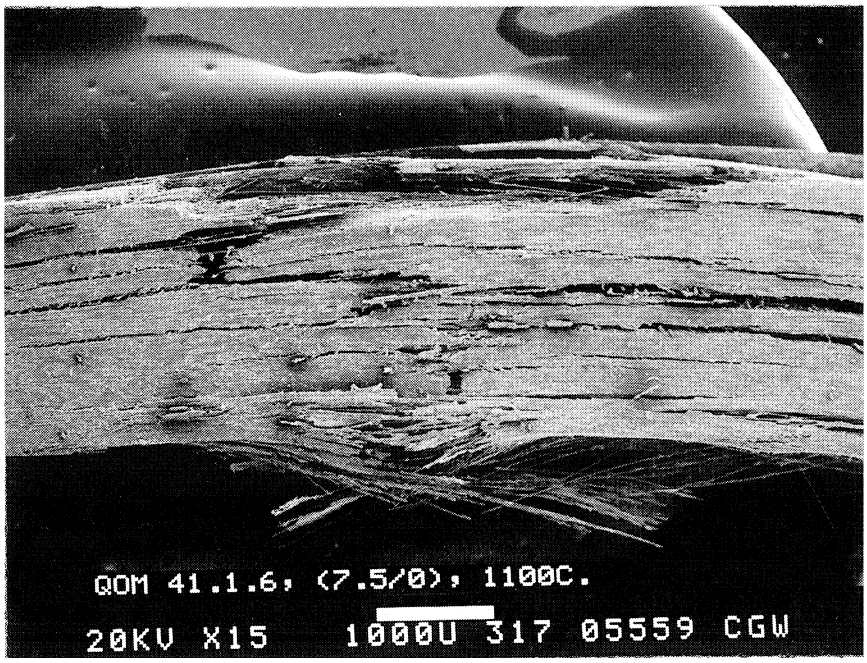

(B) 1100°C EXTENSIVE SHEAR DEFORMATION OF BEAM WITH LITTLE TENSILE PROPAGATION. NOTE COMPRESSIVE FAILURE AND SLIGHT PERMANENT DEFORMATION

FIGURE 19. SEM VIEWS OF THE MODE OF FRACTURE IN A 7.5% BSG-DOPED MAS CORDIERITE COMPOSITE (CONTROL (7.5/0) CMC)

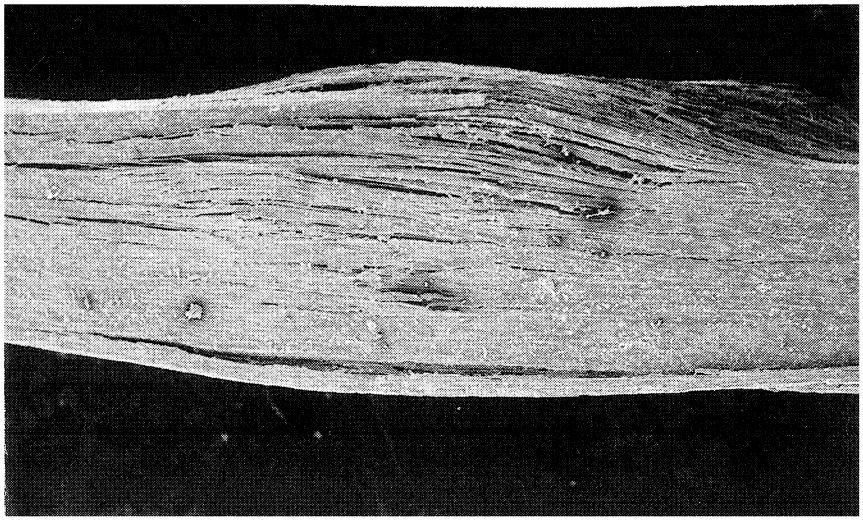

(C) 1250°C, SHOWING EXTENSIVE COMPRESSIVE FAILURE

FIGURE 19. CONCLUDED (7.5/0)

debonding and frictional sliding at the interface. SiC-whisker toughening of the CMC matrix is less effective in raising the composite elastic limit.

However, neither additive was shown to be effectual in increasing the composite elastic limit at high temperature. It is speculated that a more refractory matrix and higher SiC_w additive levels would be more successful in inhibiting high temperature matrix cracking in these CMCs, if they could be successfully fabricated (i.e., consolidated to full density).

The BSG dopant had a profound effect in reducing oxidation embrittlement by creating a more oxidatively stable/mechanically functional interface. The BSG-modified carbon interface is responsible for the increased thermal durability exhibited by BSG hybrids. However, there is a refractoriness loss associated with the use of the BSG-dopant. Thus a trade-off exists between embrittlement resistance and refractoriness.

These results for baseline and control CMCs provide insight into the interpretation of the mechanical behavior of BSG Hybrid CMCs, where BSG doping and SiC whisker matrix toughening are employed simultaneously. These materials are discussed in the following section.

4.1.3.2 BSG-doped MAS-SiC_w Hybrid CMCs

A variety of screening-level room and high temperature tests were conducted on a wide range of BSG Hybrid compositions containing both BSG doping as well as SiC-whisker matrix toughening. The full compliment of variables consisted of three SiC_w levels, three BSG levels, and three hot-press temperatures. Various aspects of the mechanical performance of BSG hybrids were studied, including: (a) matrix microcracking and the composite elastic limit, (b) the effects of SiC_w and BSG on composite ultimate properties, and (c) various aspects of the refractoriness of BSG hybrid CMCs.

(a) Process-Window Study

Hot consolidation was accomplished by hot-pressing at 1200°, 1250°, and 1300°C. All composites fabricated were fully dense and of the desired matrix phase assemblage (highly crystalline cordierite) as described in Section 4.1.2. Optical microscopy revealed that the microstructure of all processed CMCs was uniform.

There were no clearly apparent major trends in the room temperature flexure results: all hot-press conditions resulted in good composites, with ultimate strengths ranging from 100-180 ksi, and ultimate strains ranging from 0.5 to 1.2%. The elastic limit varied from roughly 50-80 ksi, 0.22-0.4% strain. High whisker loading tended to give the lowest ultimate failure strains, but not always the highest elastic limit properties. High BSG loading tended to yield the best composite properties. The results were similar for all process temperatures, thereby demonstrating the wide process window for BSG hybrids.

(b) Thermal Durability/High Temperature Behavior

It was discussed above that BSG doping as well as SiC-whisker matrix toughening was effective in raising the composite elastic limit, with BSG-doping apparently being dominant. The control of the composite elastic limit is important since it is typically defined by a matrix microcracking event that leads to embrittlement at high temperature in oxidizing environment. The existence of subelastic limit cracking makes the use of CMCs more problematic since only a very small portion of a CMC's stress-strain behavior will be usable under in-service conditions. Hence, our interest in damage accumulation phenomena on this program.

To illustrate the benefit of combining BSG-doping with SiC_w matrix toughening , consider the stress-strain behavior of various composite compositions. The 25°C tensile stress-strain behavior for BSG hybrid, control, and baseline composites is provided in Figure 20. It is evident that both BSG doping as well as SiC-whisker toughening alter the manner in which damage in the form of matrix microcracking accumulates in the composite. The elastic region of the BSG hybrid (5/10)

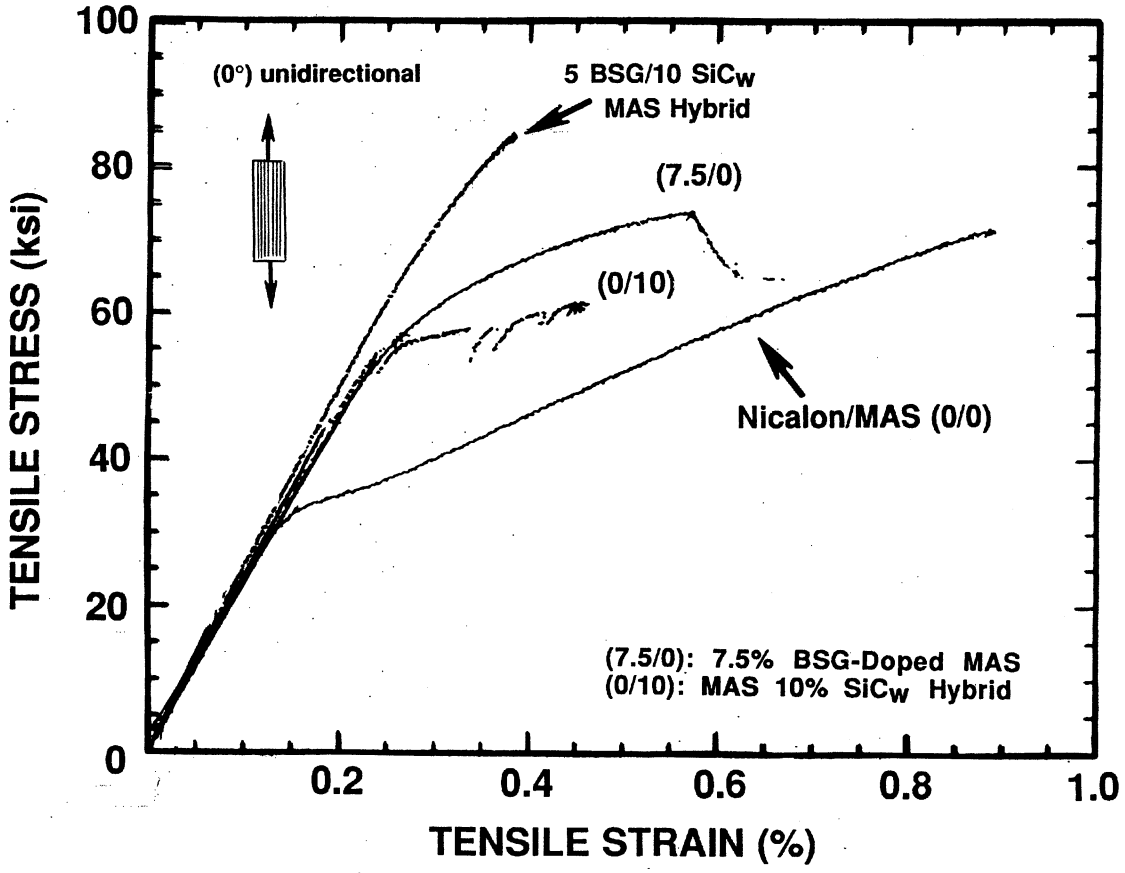

FIGURE 20. TENSILE STRESS-STRAIN BEHAVIOR OF BASELINE AND CONTROL BSG-DOPED MAS HYBRID COMPOSITES

composite is seen to extend to a stress/strain level twice that of the baseline composite. Such damage accumulation phenomena are thought to be directly related to thermal durability, since the BSG-MAS hybrid accumulates damage in the form of tensile microcracks much differently than the baseline CMC. Figure 20 indicates that the hybrid either (1) does not microcrack appreciably prior to ultimate failure, or (2) does not experience extensive pullout and crack extension after micro-cracking. The BSG-MAS hybrid fails at nominally the same stress as the nonhybrid, since the ultimate stress is determined by fiber fracture in both materials. However, the hybrid fails at a much lower total strain. The net result of BSG-doping and SiC_w hybridization is apparently the more gradual development of damage and more elastic behavior to failure.

Since improving the thermal durability of CMCs by (a) altering the manner in which damage accumulates in the matrix, and (b) providing an oxidatively stable yet mechanically functional interface, is the objective and thrust of this program, extensive testing of candidate compositions was then performed at elevated temperature. Unidirectional (0°) composites were investigated in Task I, since embrittlement effects are most apparent in that ply orientation. Evaluation was conducted in flexure, with testing performed at Corning. While not ideal for CMCs, this method was an efficient way to judge the 27 CMCs (3 BSG x 3 SiC_w x 3 H-PT) at room and several elevated temperatures in Task I. The major areas investigated at high temperature were (a) elastic limit properties, (b) effects of SiC-whisker matrix toughening, and (c) effects of temperature on strength, ultimate strain, and fracture mode, and in particular, (d) the role of the BSG dopant on oxidative stability.

Elastic Properties:

It was shown above that taken individually, both BSG-doping and SiC_w matrix additives were ineffectual in increasing the composite proportional limit at elevated temperatures, at least over the ranges of additive content investigated (i.e., 2.5-7.5% BSG; 7.5-12.5% SiC_w). Since it was also shown above that there is an apparent room temperature performance benefit to combining

these two mechanisms, it was of interest to determine if this extended to high temperatures as well.

The result of simultaneous whisker hybridization and BSG doping on composite elastic limit stress and strain is shown in Figures 21 and 22, where the flexural elastic limit properties for the 5%BSG/10% SiC_w BSG hybrid are plotted as a function of temperature, in comparison to the baseline in situ carbon interface Nicalon/MAS material. There appears to be a synergistic effect of combining BSG doping with SiC_w toughening at high temperature. This is observed in Figures 21 and 22, in comparison to the high temperature behavior shown in Figures 13 and 14, where the matrix additives were incorporated individually. When both BSG and SiC_w additives are present, the composite elastic limit properties appear to be improved to 1100°C (2000°F).

Ultimate Properties:

The majority of the remaining screening study entailed a high temperature investigation of a wide range of BSG dopant levels in an attempt to determine the optimum BSG content that will provide both enhanced oxidation embrittlement resistance and minimally reduced refractoriness in BSG hybrid CMCs, i.e., those that also contain the matrix-toughened SiC-whisker addition..

The ultimate strength and failure strain versus temperature for 7.5% SiC_w-containing CMCs with BSG-doping level varying from 2.5% to 7.5% are shown in Figures 23 and 24. The effect of BSG dopent level is illustrated.

The variation of flexure strength with temperature (Figure 23) for the highly doped 7.5/7.5 hybrid follows the same trends as observed in other glass-ceramic matrix composites. Namely, a double inflection that is phenomenologically described by four regions of behavior: (1) an initial low temperature region of temperature independence (not investigated on this program), (2) property decrease at intermediate temperatures, followed by (3) strength increase at higher temperature caused by plasticity, crack blunting, and stress redistribution in the deforming flexure bar, and (4) precipitous strength decrease at the highest test temperatures where the

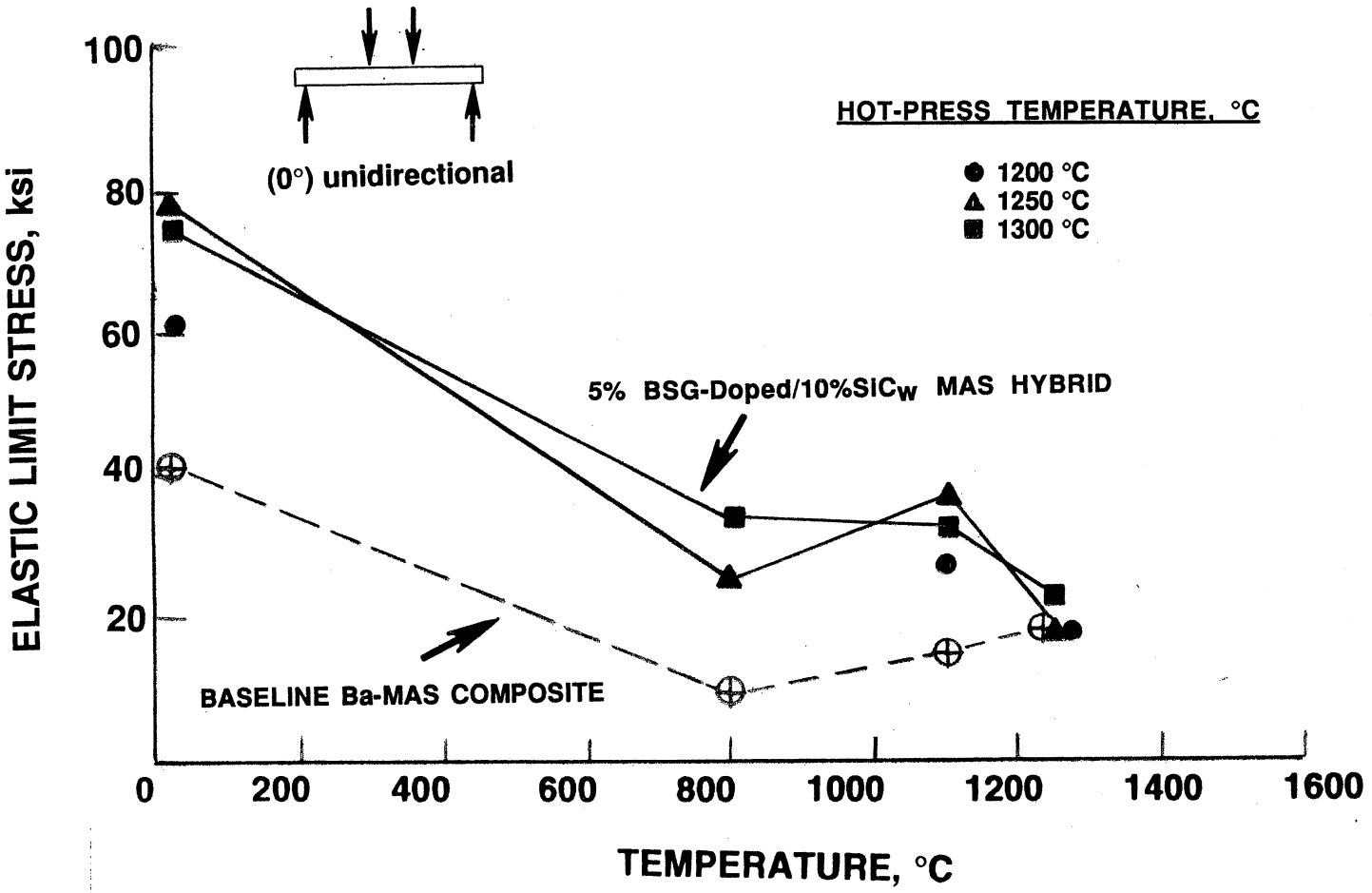

FIGURE 21. ELASTIC LIMIT STRESS FOR BSG HYBRID AND BASELINE MAS COMPOSITES

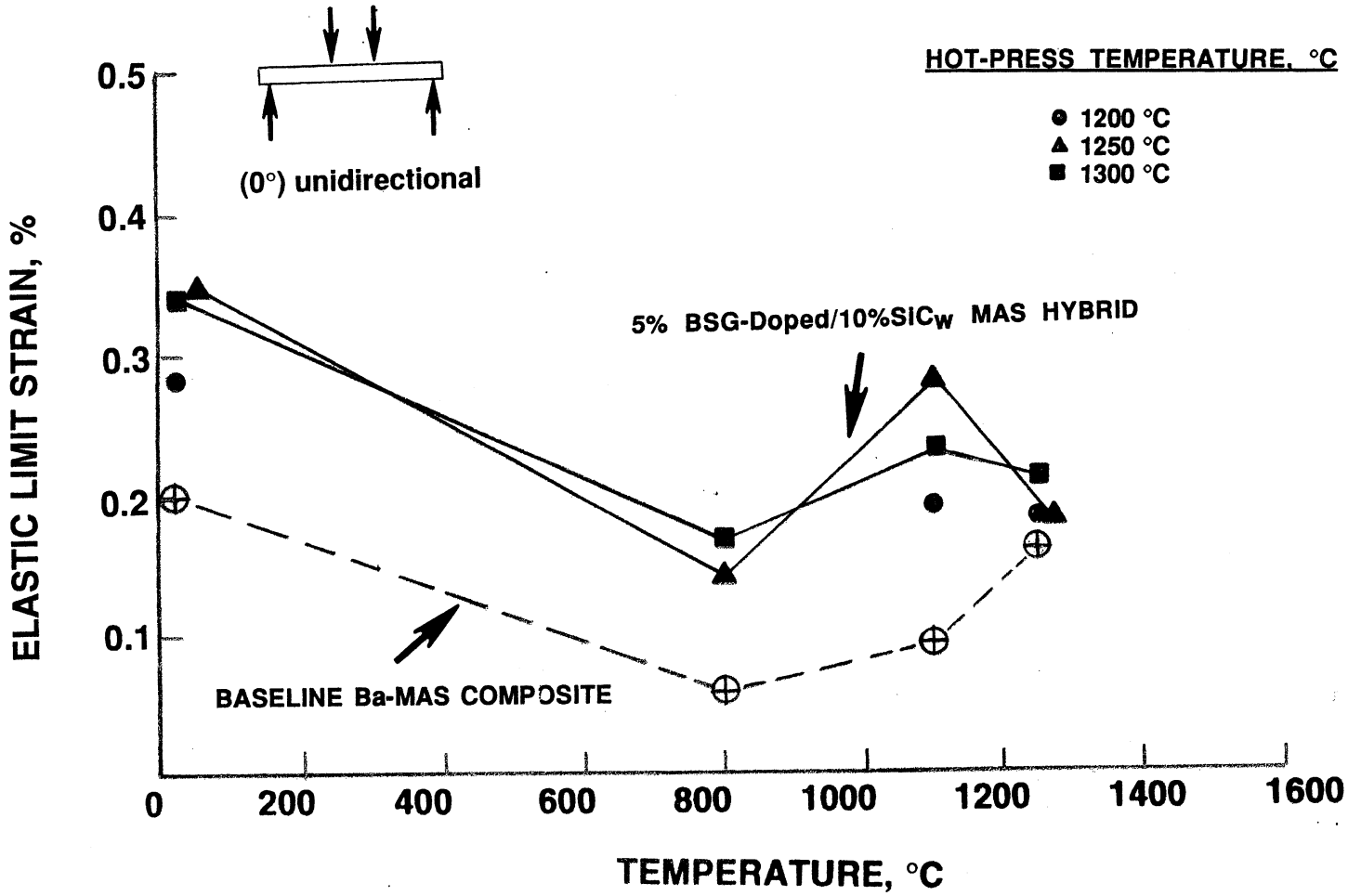

FIGURE 22. ELASTIC LIMIT STRAIN FOR BSG HYBRIDS AND BASELINE MAS COMPOSITES

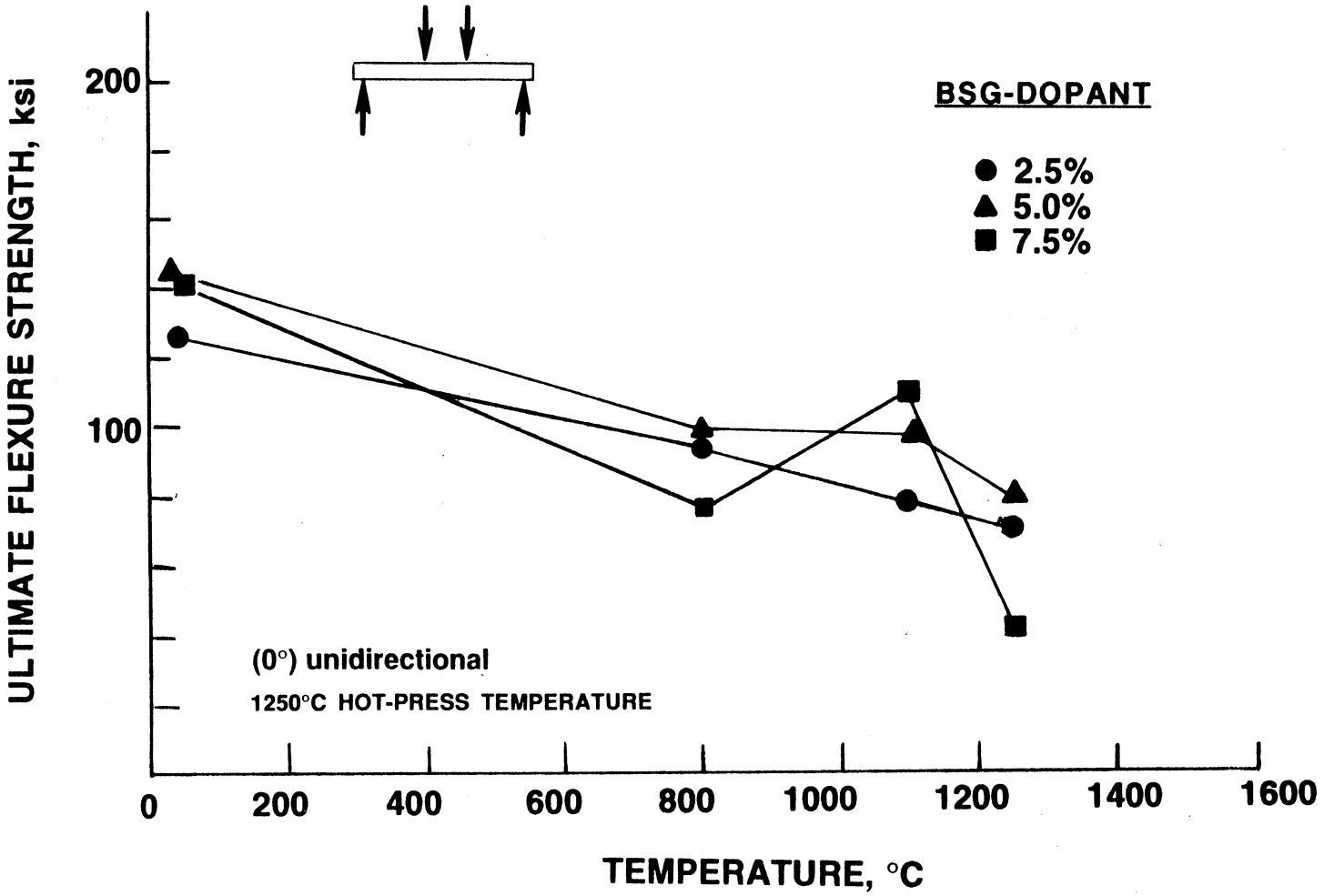

FIGURE 23. ULTIMATE STRENGTH OF BSG-DOPED MAS COMPOSITES CONTAINING 7.5% SiC WHISKERS

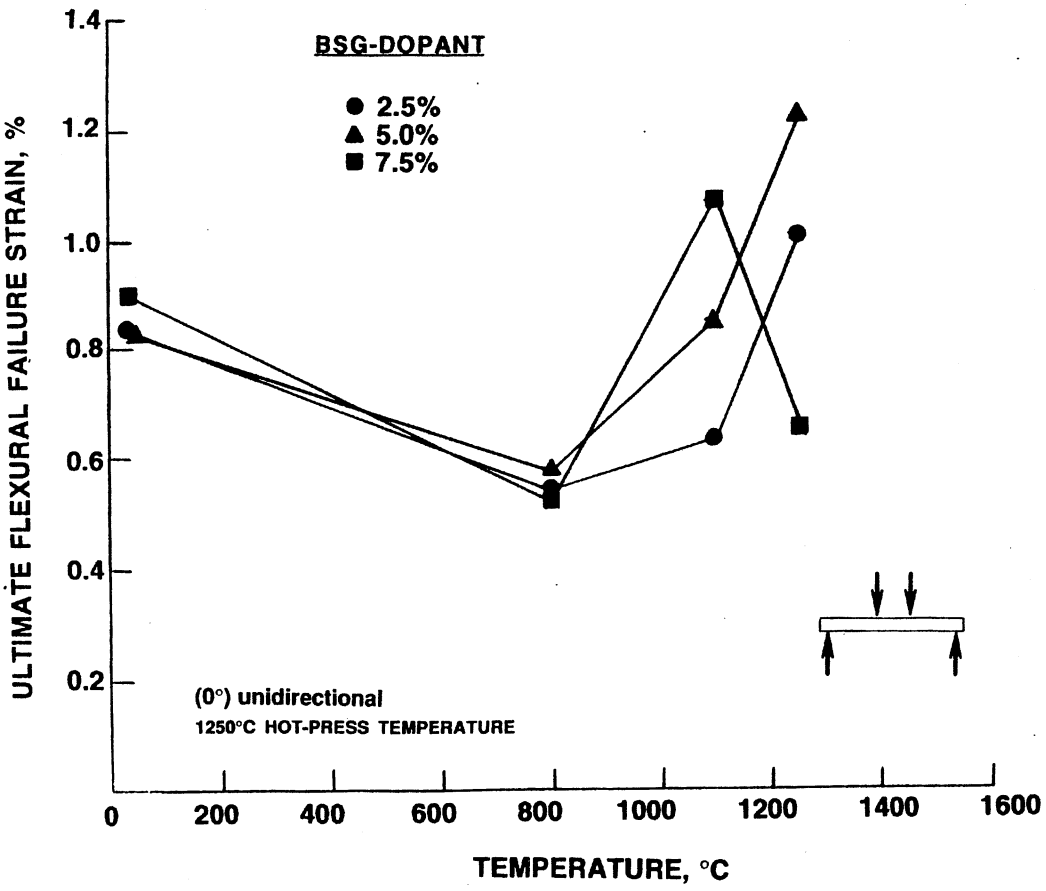

FIGURE 24. ULTIMATE FAILURE STRAIN OF BSG-DOPED MAS COMPOSITES CONTAINING 7.5% SiC WHISKERS

matrix loses load bearing capacity. The major cause of this type of flexure behavior is thought to be loss of refractoriness of the composite matrix. Therefore, a dopant level of 7.5% BSG is too high. The data of Figure 23 show that the 2.5% and 5% BSG doped hybrids do not exhibit such a double inflection in strength as a function of temperature, and in fact only decrease slightly in strength throughout the 25°-1250°C temperature range. The implications are that the BSG level is (1) high enough to provide for significant oxidation embrittlement resistance, and (2) low enough to have only minimal influence on matrix load bearing capability up to 1250°C (2300°F). At intermediate temperature, 1100°C, the failure strain date provided in Figure 24 indicate a pronounced direct benefit of BSG-doping with failure strain increasing from 0.6 to > 1% as the BSG level is increased from 2.5% to 7.5%. It is concluded that at 1100°C (2000°F) the mechanical behavior appears to be controlled by the enhanced embrittlement resistance provided by the BSG dopant, and not adversely affected to any great extent by the resultant loss of refractoriness that BSG use promotes. Therefore a dopant level of 5% BSG would appear to be optional.

SiC-whisker additions to the glass-ceramic matrix have not been shown on this program to be a major determinant of high temperature composite behavior. This is evident in the ultimate flexure strength and failure strain of whisker-toughened 5% BSG-doped CMCs shown in Figures 25-26. Similar mechanical behavior is observed for all SiC_w levels tested. However, there are other potential benefits of the use of SiC-whisker additions to the glass-ceramic matrix. Other materials properties would be expected to be altered significantly by their use; for instance: (a) higher thermal conductivity for reduced thermal stress, (b) increased erosion and abrasion resistance, (c) increased hardness for impact resistance, (d) possible increases in composite off-axis properties and interlaminar properties, and (e) to provide more structural and electrical tailorability in the composite structure. Investigation of these aspects of material performance, however, were beyond the scope of this program. However, the potential of significantly improving such properties as these illustrates the compositional flexibility of the glass-ceramic matrix approach. The component designer therefore has more flexibility in choice of materials for application-specific designs.

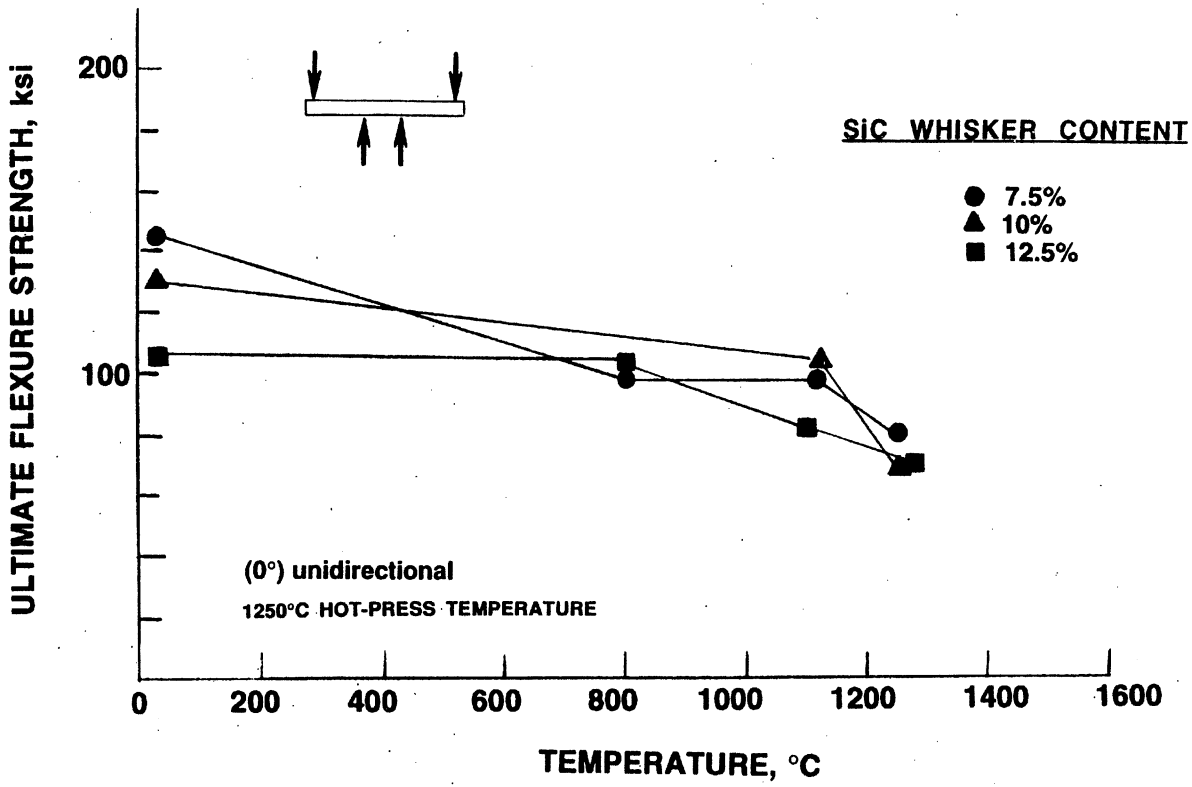

FIGURE 25. ULTIMATE STRENGTH OF 5% BSG-DOPED MAS HYBRID COMPOSITES

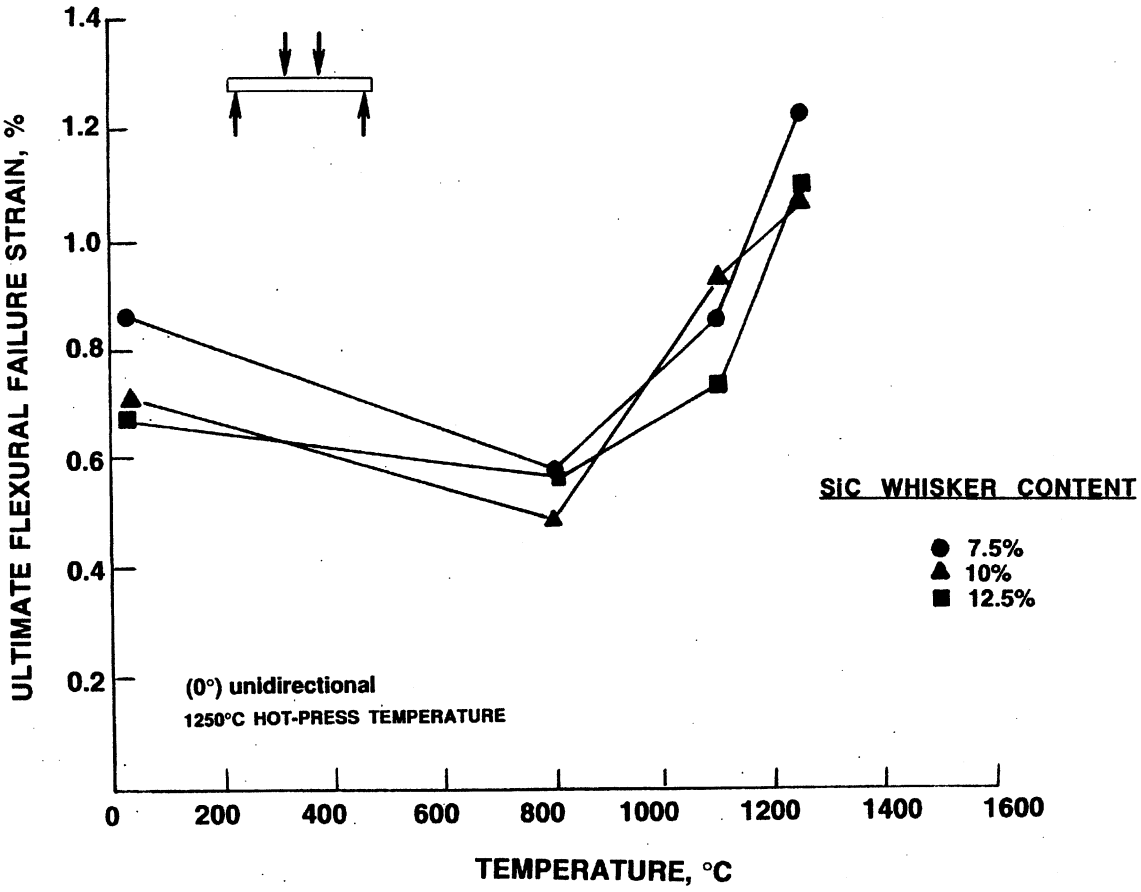

FIGURE 26. ULTIMATE FAILURE STRAIN OF 5% BSG-DOPED MAS HYBRID COMPOSITES

4.1.3.3 Summary of Screening Studies

BSG-doped MAS hybrid composites derive their demonstrated improved thermal durability from (1) delayed microcracking of the cordierite matrix, and (2) the existence of an oxidation resistant/mechanically functional interface that is formed in situ during CMC processing. BSG (borosilicate glass) doping of the barium-stuffed cordierite matrix results in (a) the formation of isolated pockets of BSG within the fine-grained cordierite microstructure, rather than being located in grain boundaries or in multigrain junctions, and (b) the diffusion of boron to the interface, which combines with oxygen and nitrogen (from the fiber) to form an oxidation resistant carbon layer apparently containing detectable BN and B_2O_3. The highly boron-modified carbon-rich interface exhibits the oxidation resistance of boron-inhibited carbon, without losing the mechanical functionality of a carbon interface. The SiC-whisker matrix additive is chemically compatible with the MAS matrix. However, the BSG additions to the matrix are primarily responsible for improved thermal durability through thermochemical and structural modification of the interfacial carbonaceous layer.

The ultimate flexural strength and the strain at ultimate load of various BSG hybrid CMCs are compared to baseline MAS cordierite and CAS anorthite CMCs in Figures 27 and 28, respectively. The ability of the BSG-doped hybrids to maintain mechanical integrity to high temperatures is evident. This is especially evident when comparing the apparent work of fracture (WOF) for the various materials, as provided in Figure 29. The WOF as used herein is calculated from the area under the flexural load-deflection curve, and therefore represents a combined measure of strength and toughness as a function of test temperature.

Note in Figures 27-29 that there is a distinct loss of CMC refractoriness at the highest BSG levels (7.5%). Shear-dominated failure became more prevalent at high temperature as the BSG content increased. Loss of matrix shear strength is suspected. Therefore, the benefits in thermal durability resulting from BSG-doping are offset by loss of usable high temperature strength.

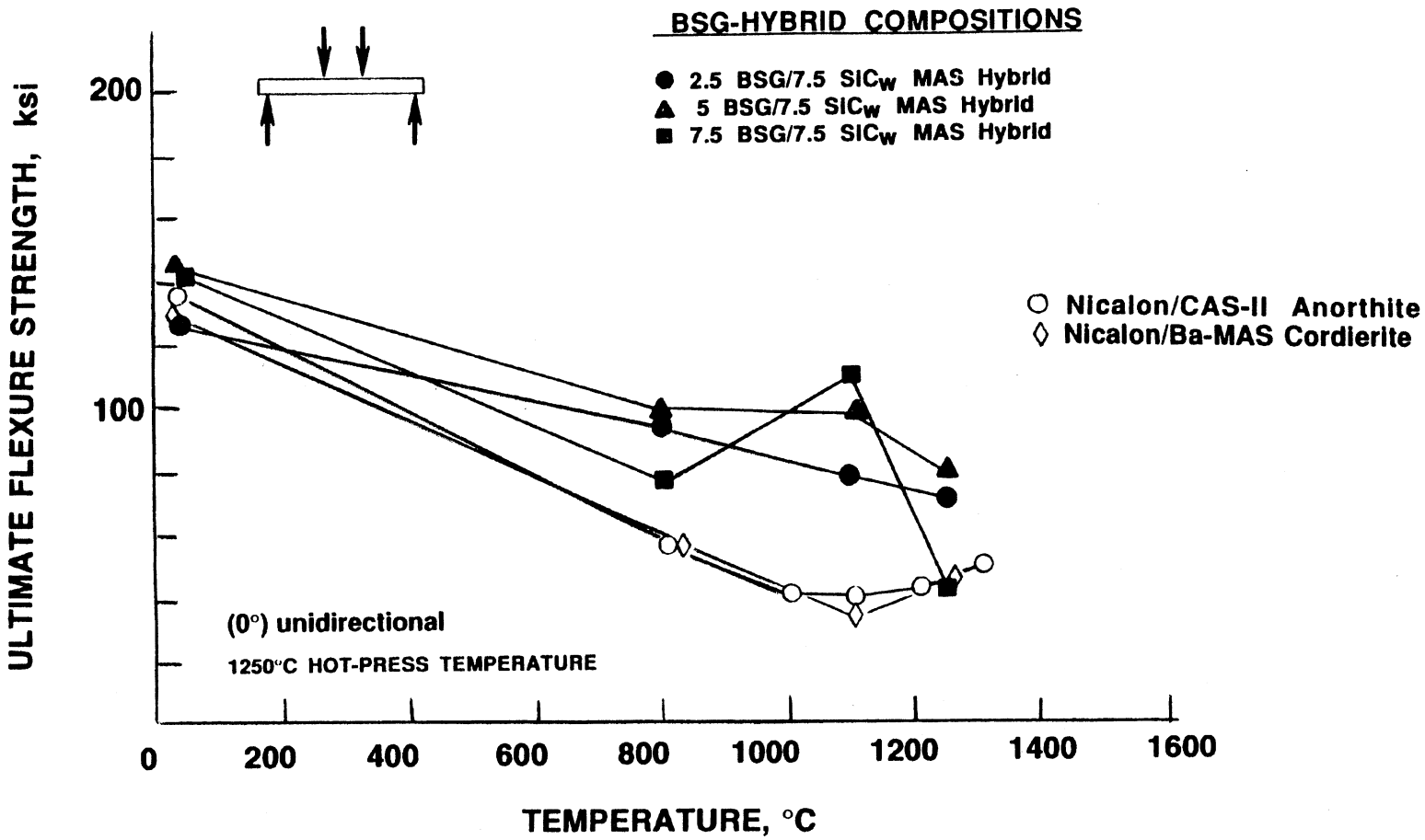

FIGURE 27. ULTIMATE STRENGTH OF BASELINE AND BSG-HYBRID COMPOSITES

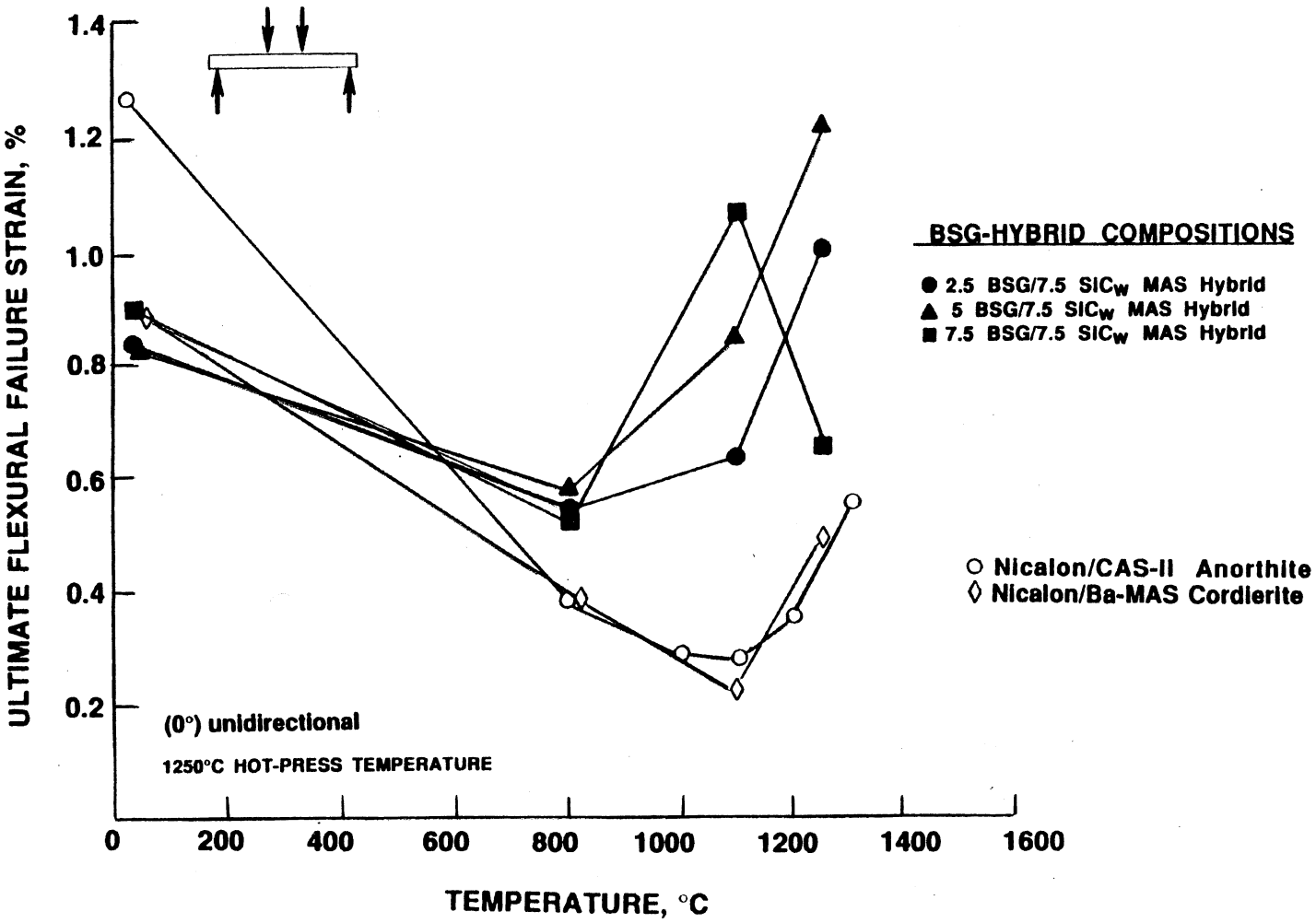

FIGURE 28. FAILURE STRAIN OF BASELINE AND BSG-HYBRID COMPOSITES

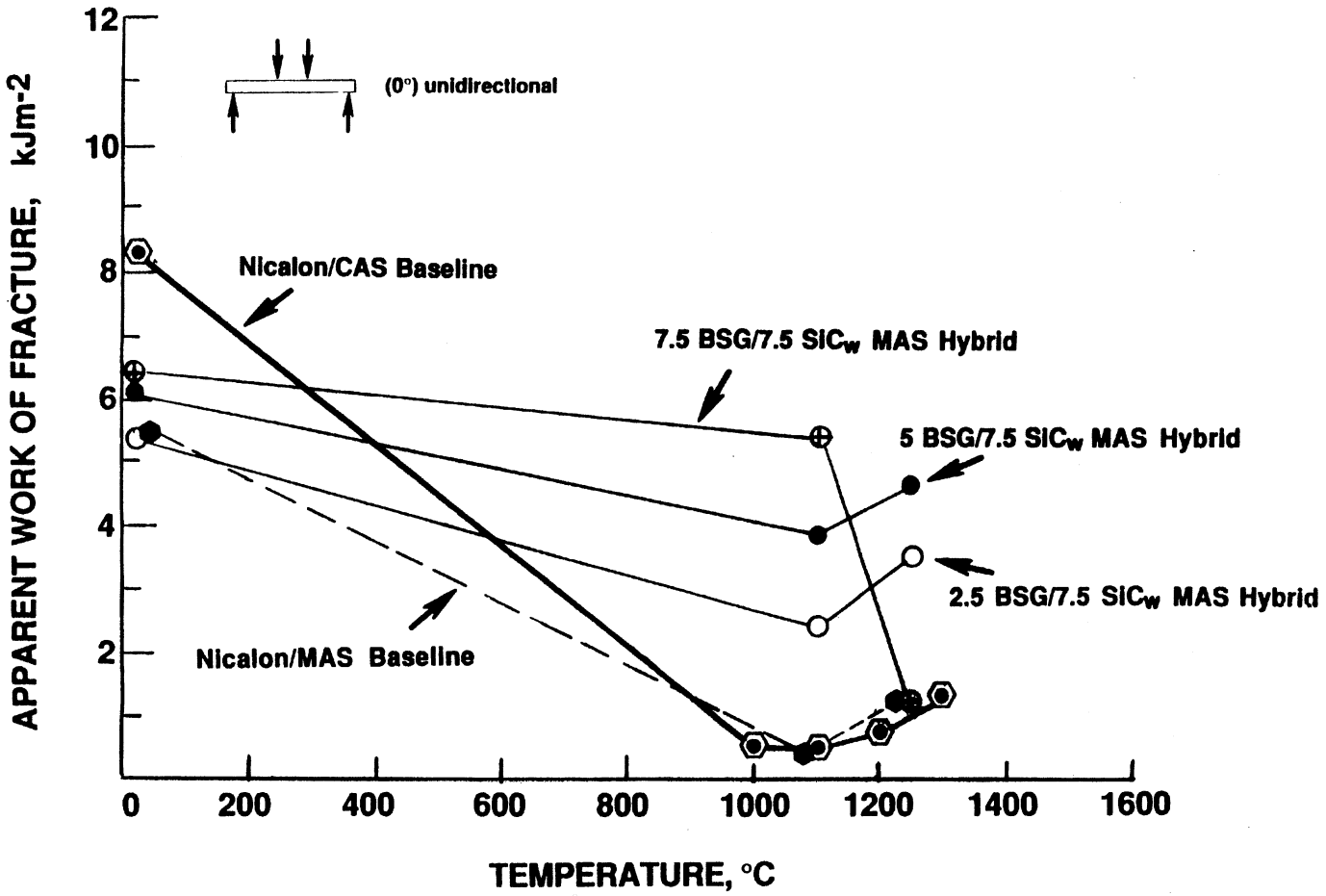

FIGURE 29. WORK OF FRACTURE FOR CAS-, MAS-, AND BSG-HYBRID COMPOSITES

4.2 Thermal Durability Assessment (Task 2)

The objective of Task 2 activities was to investigate and identify the potential critical performance limiting phenomena associated with the high temperature oxidative stability of the composites developed in Task 1. The aim was to downselect to the two (2) most promising CMCs, for which a mechanical properties database could be subsequently obtained in Task 3.

The majority of the testing performed in Task 2 was conducted at Pratt & Whitney (East Hartford, CT). This permitted the testing to shift from flexure to high temperature tension and tensile stress rupture, more fundamental mechanical properties that would lead to a mechanistic understanding of thermal durability issues. This approach also resulted in an interpretation of observed behavior from a user's perspective. This aspect of the program was critical. Material performance was judged with respect to anticipated design requirements, and material's could be judged comparatively with others being developed by the CMC community. It is important to have the potential user involved early in the development of materials such as ceramic composites, which have complex microstructures and which are intended to be used in a complex thermostructural application. This approach can greatly facilitate the development of advanced materials.

4.2.1 Optimized BSG Dopant Level/Downselect Process

Task 1 work described above demonstrated that BSG-doping was the dominant factor in achieving thermal durability-high strength and high failure strain at elevated temperature. No specific benefit of SiC_w matrix toughening was identified in Task 1. Therefore, CMCs with only BSG-doping and no SiC_w additions were studied at the onset of Task 2. The 7.5% BSG dopant level was eliminated since Task 1 work showed that it resulted in significant matrix deformation and refractoriness loss at 1250°C (2300°F). Alternatively, a lower BSG content, 1.25% was examined along with 2.5% and 5% BSG-doped MAS composites. The aim was to determine the optimum BSG level to achieve adequate thermal durability as well as adequate refractoriness.

To determine the optimum BSG-dopant level, cross-ply [0°/90°] composites were tested in fast-fracture tension at 2000°F. Tensile strength and tensile failure strain are plotted as a function of BSG content in Figures 30 and 31, respectively. It is observed that both properties increase substantially as the BSG dopant level is increased from zero to 5%. The 5% BSG level appears optimum, providing for CMCs with the greatest thermal durability. This is illustrated clearly in the 2000°F tensile stress-strain behavior shown in Figure 32. The appearance of the fracture surface is consistent with this. The fibrous nature of the 2000°F fracture for the CMC doped with 5% BSG is shown in Figure 33. Lower BSG levels resulted in picture frame oxidation, with 25% to 50% of the fracture surface being brittle. For comparison, the stress-strain behavior of several CMCs at ~2000°F is provided in Figure 34: conventional MAS and CAS matrix composites versus the 5% BSG-MAS matrix composites.

These results indicated that the optimum BSG dopant level to achieve a high degree of thermal durability without attendant loss of refractoriness is 5% BSG. Recall the Task 1 work illustrated the apparent synergistic effect of employing both BSG-doping and SiC-whisker matrix toughening in the composite. Therefore, two CMCs were downselected for continuing the Task 2 investigation:

(1) Nicalon/5% BSG-doped MAS cordierite

(2) Nicalon/5% BSG-10% SiC_w MAS Hybrid

The remainder of Task 2 entailed a study of tensile, and tensile stress-rupture properties of these CMCs, along with long term unstressed oxidation exposures to comprehensively demonstrate their thermal durability.

4.2.2 Fast Fracture Tensile Behavior

4.2.2.1 Nicalon/5% BSG-MAS Cordierite

Nicalon/5% BSG-doped MAS cordierite CMCs contain only BSG dopants to the matrix, and provide thermal durability by boron modification of the in situ carbon interfacial layer discussed

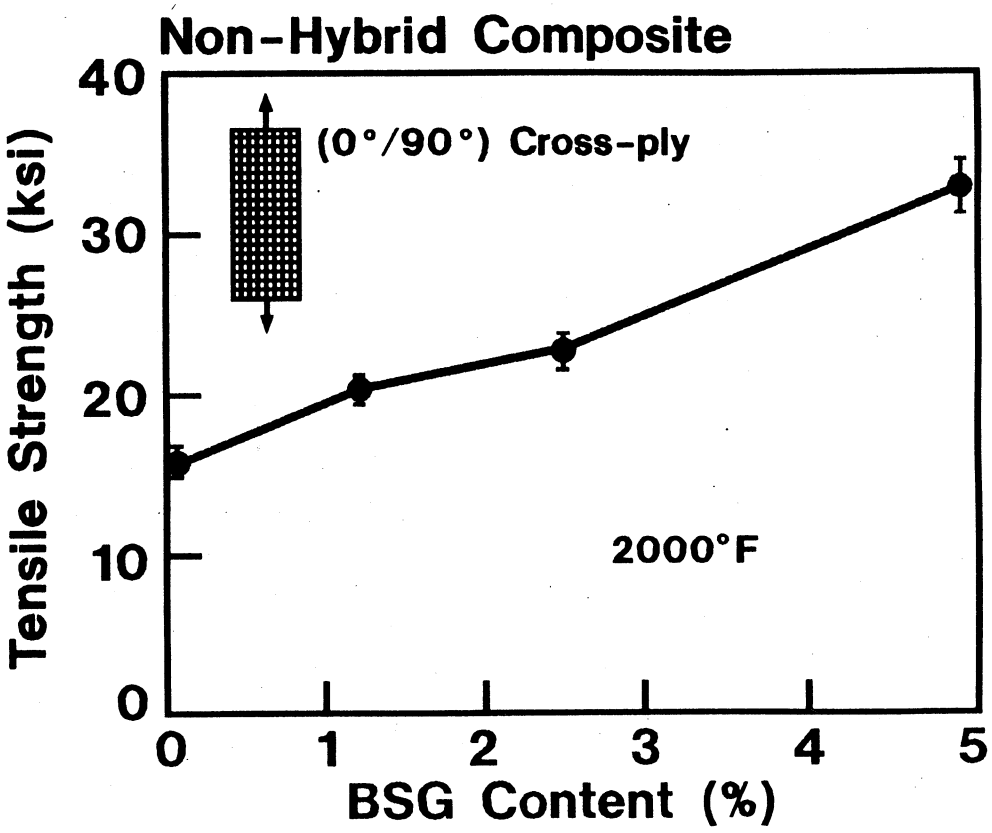

FIGURE 30. TENSILE STRENGTH OF MAS CMCs AT 2000°F

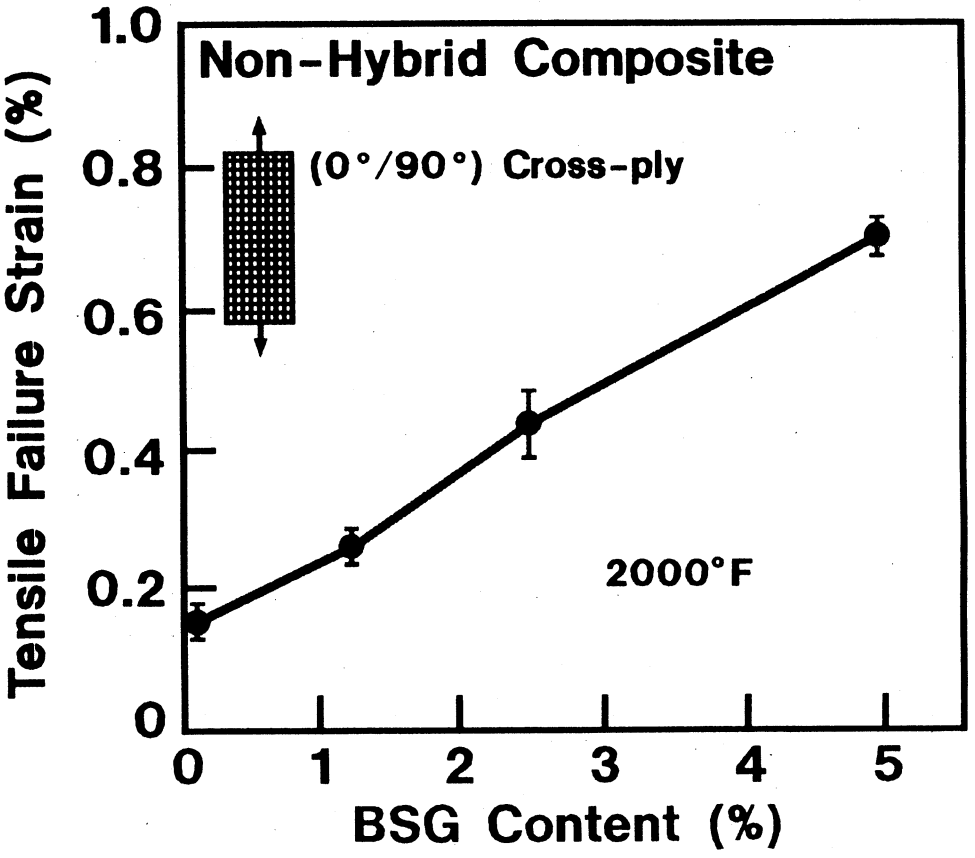

FIGURE 31. TENSILE FAILURE STRAIN OF MAS CMCs AT 2000°F

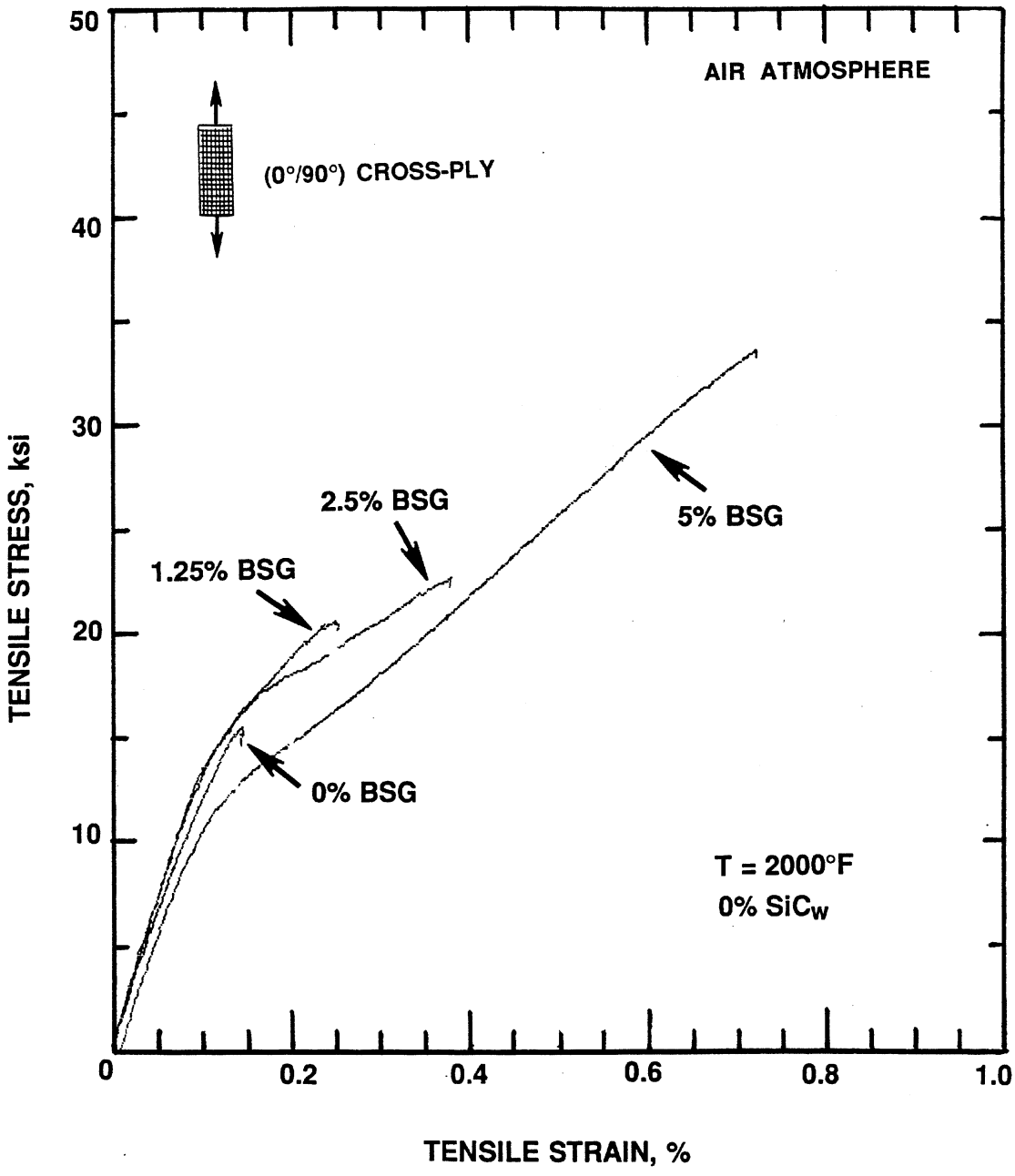

FIGURE 32. TENSILE STRESS-STRAIN BEHAVIOR OF BSG-DOPED MAS CMCs AT 2000°F

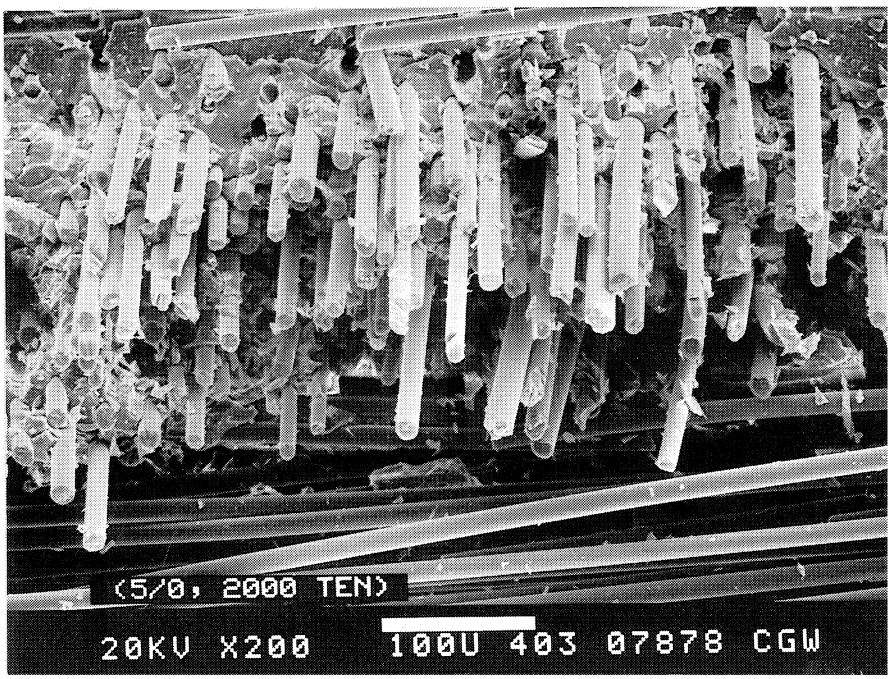

FIGURE 33. TENSILE FRACTURE SURFACE OF 5% BSG-MAS AT 2000°F (LOWER BSG: 25-50% PICTURE FRAME OXIDATION)

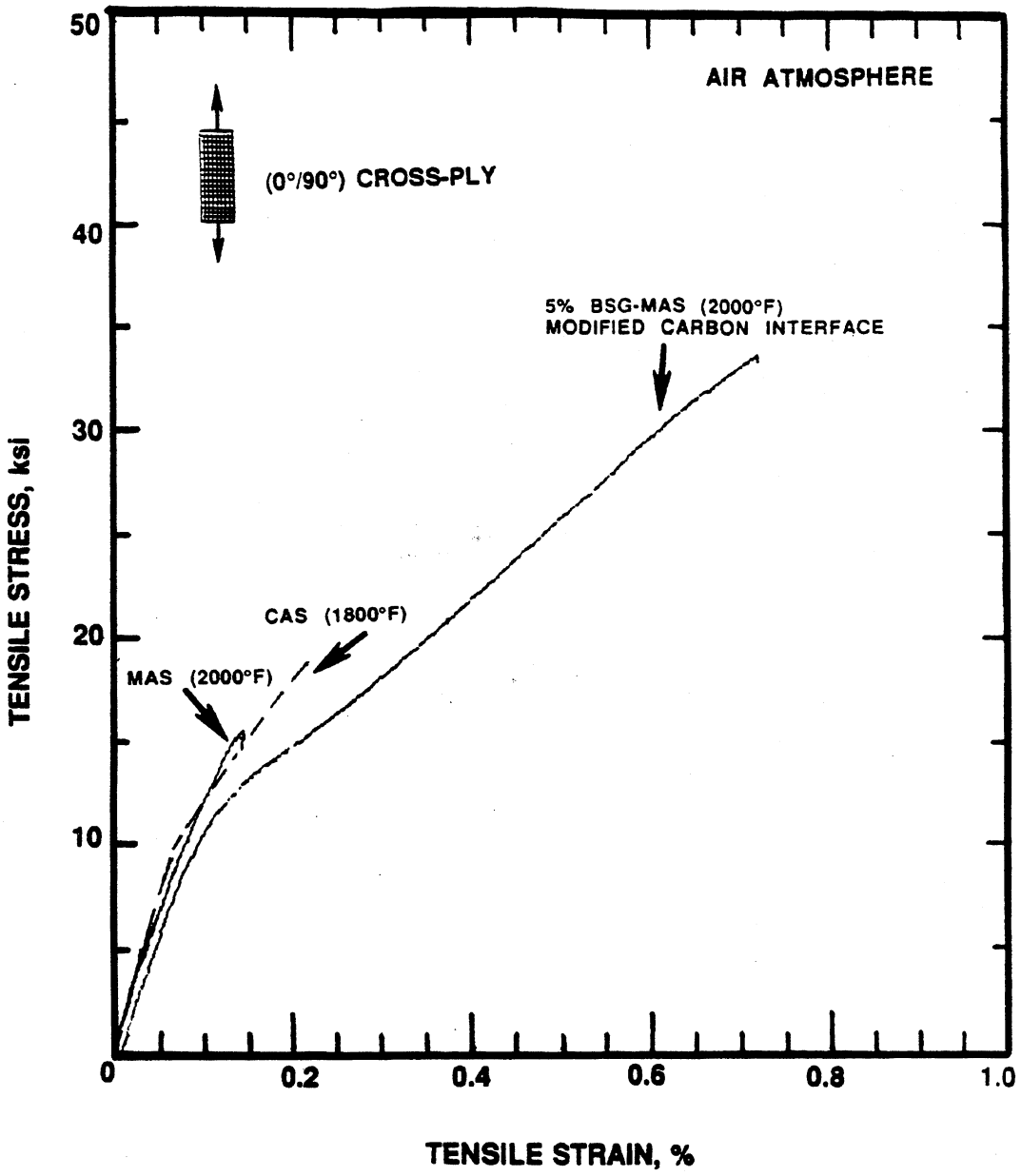

FIGURE 34. TENSILE STRESS-STRAIN BEHAVIOR OF VARIOUS CMCs AT ELEVATED TEMPERATURE

above. Two mechanisms appear operable: (a) the presence of BN and B_2O_3 phases within the in situ carbon interfacial layer, and (b) glass-glazing matrix-side of the in situ carbon interface.

The tensile strength of (0°) unidirectional 5% BSG-doped MAS CMCs at 75° and 2000°F is provided in Figure 35. At room temperature, the CMC exhibits a high elastic limit and a UTS of 65 ksi. At 2000°F, the initial modulus is reduced about 25%, and there is an apparent microcracking event at 15-20 ksi, followed by a linear fiber-dominated stress-strain behavior to the UTS, which is also 65 ksi, as it was at room temperature. The linear portion of the composite stress-strain response at 2000°F has a modulus of ~8.5 Msi. This indicates fiber-dominated behavior, since it is roughly equivalent to $v_f E_f$ (T), and continued microcracking would decrease the compliance of the specimen and result in nonlinear stress-strain. This implies that the knee at 15-20 ksi is a true microcracking event, and not related to deformation at elevated temperature.

Figure 36 presents the family of stress-strain curves for (0°/90°) cross-ply composites from 75° to 2200°F, with all tests in air atmosphere. Note that the proportional limit of the CMC decreases with temperature, but the strain to failure is relatively constant 0.7-0.9% throughout the temperature range. This means that the CMC is thermally durable, and has significant mechanical integrity throughout the temperature range of interest. Additionally, the shape of the stress-strain curves (i.e., linear at high values of stress and strain) indicates that this CMC exhibits minimum deformation and good refractoriness to 2200°F as well.

The relatively temperature-invariant strength and failure strain of 5% BSG-doped MAS cordierite CMCs out to 2200°F is shown in Figures 37 and 38. The fibrous nature of fracture at 1050° and 2200°F is shown in Figure 39. The temperature invariant strength, failure strain, and fibrous fracture morphology are an indication that a significant degree of thermal durability has been achieved in these CMCs.

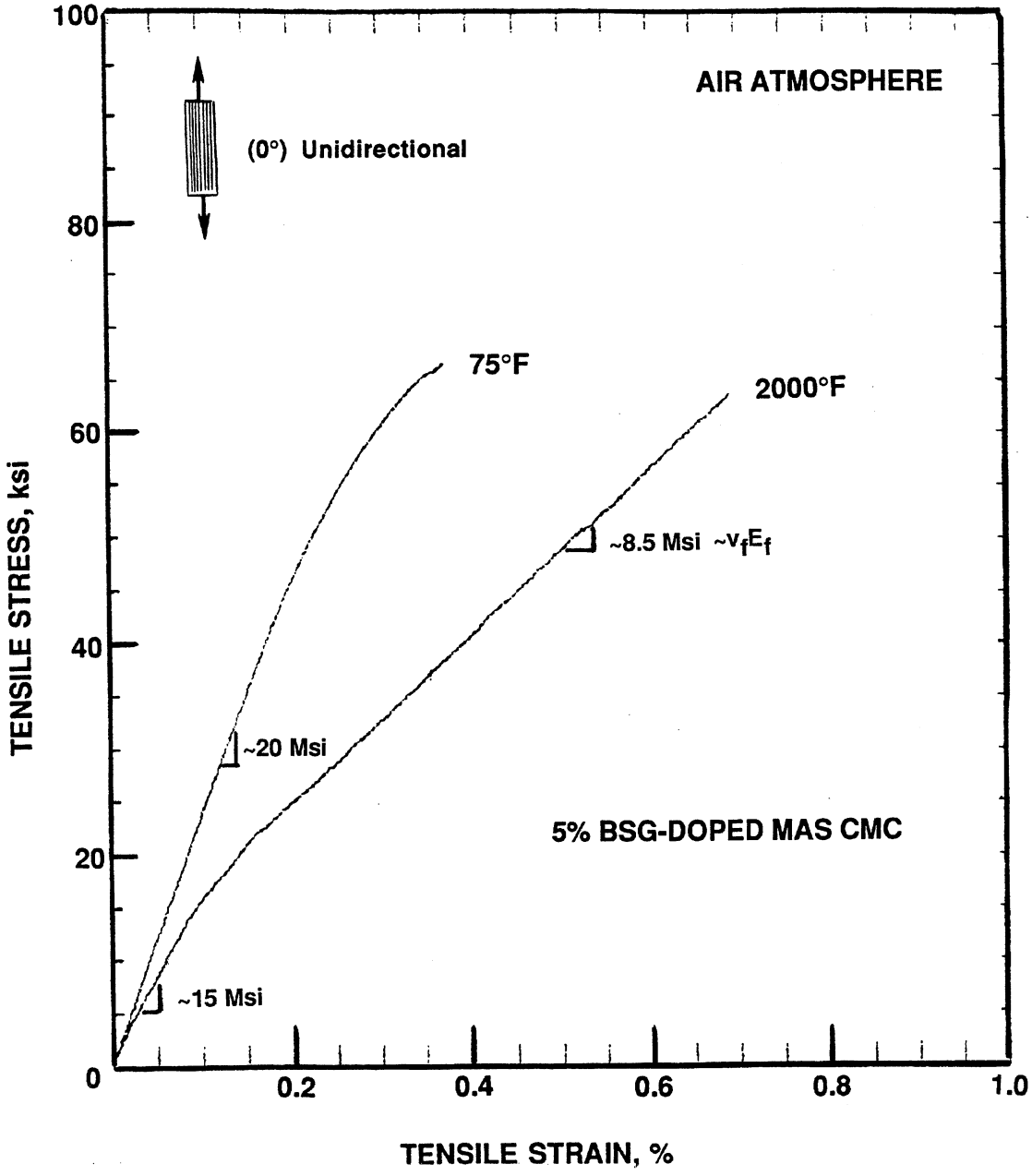

FIGURE 35. TENSILE STRESS-STRAIN BEHAVIOR OF 5% BSG-MAS UNIDIRECTIONAL (0°) LAMINATES

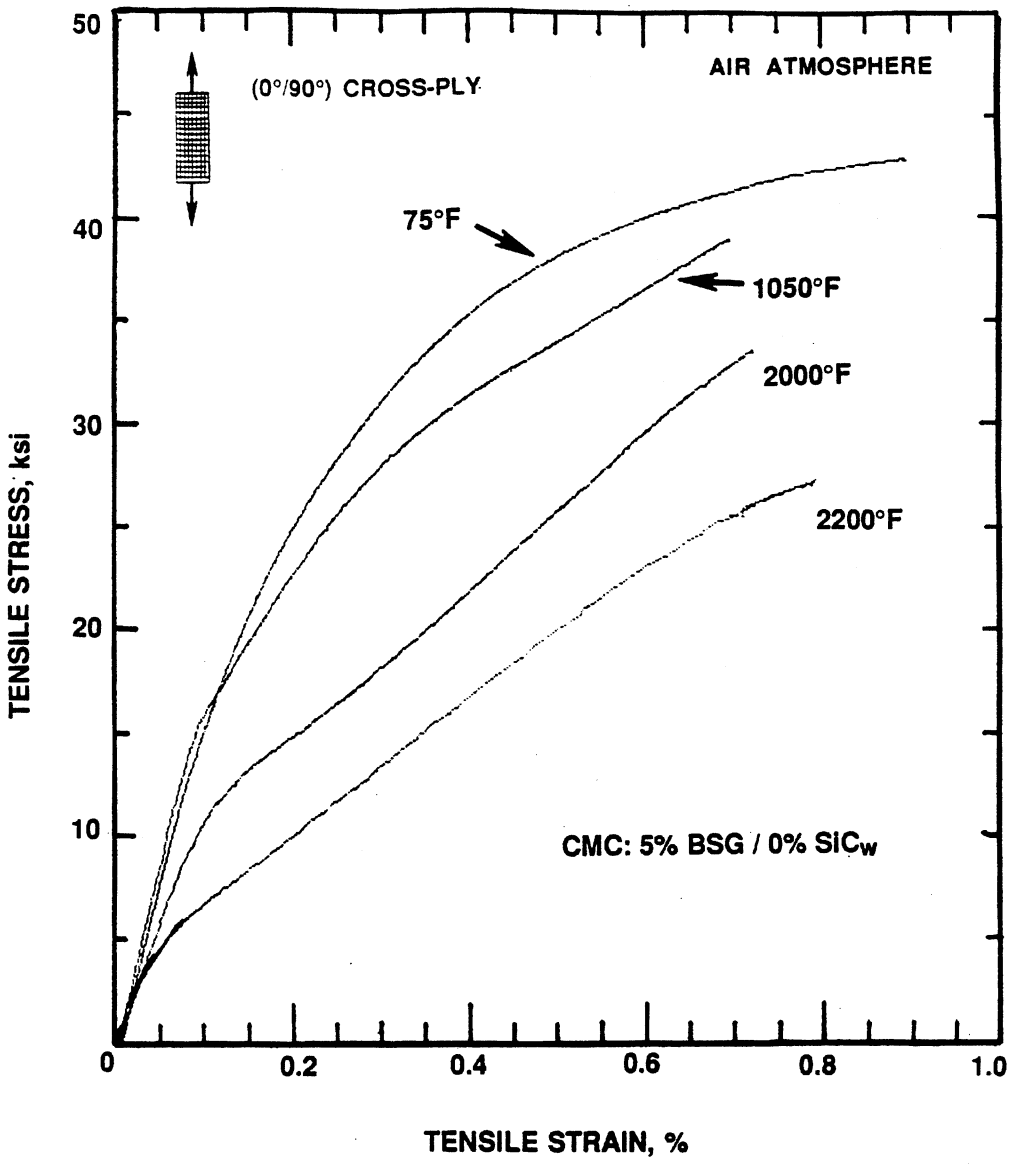

FIGURE 36. TENSILE STRESS-STRAIN BEHAVIOR OF 5% BSG-DOPED MAS CORDIERITE CMCs

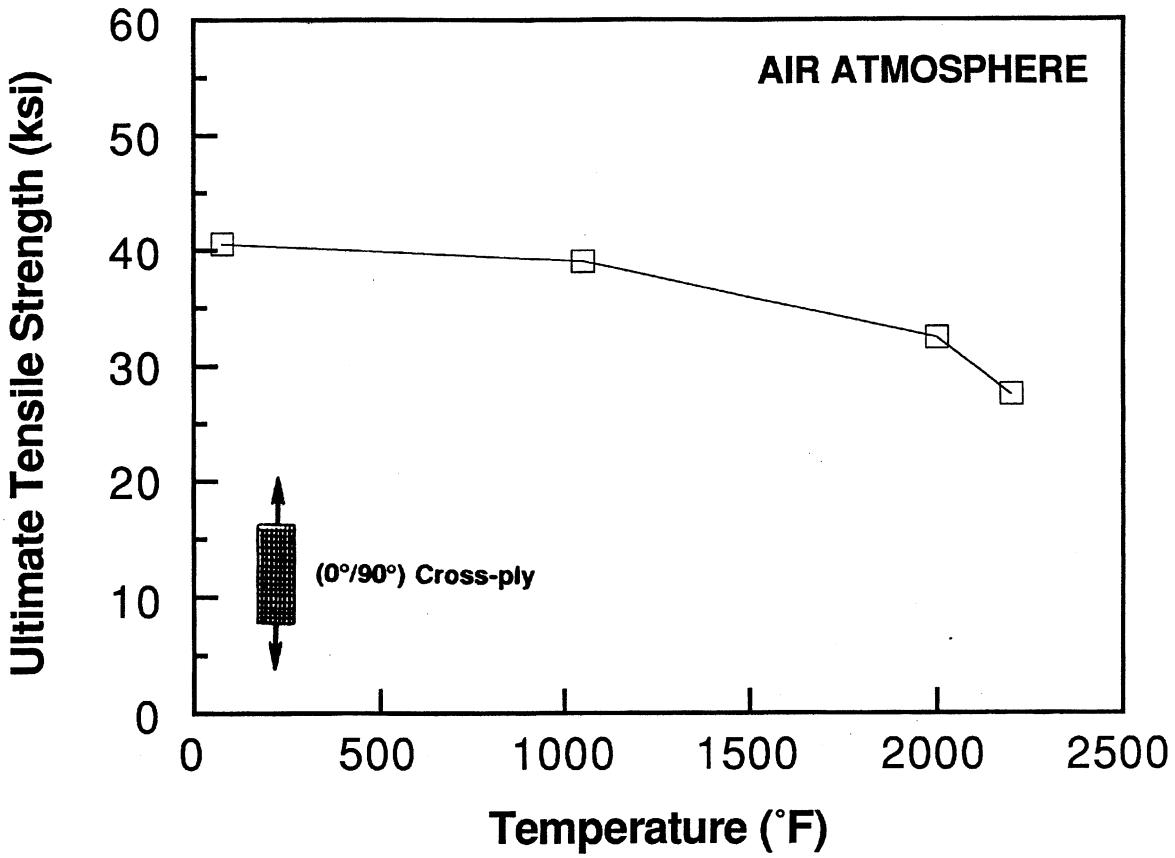

FIGURE 37. TENSILE STRENGTH OF 5% BSG-DOPED MAS CORDIERITE COMPOSITE

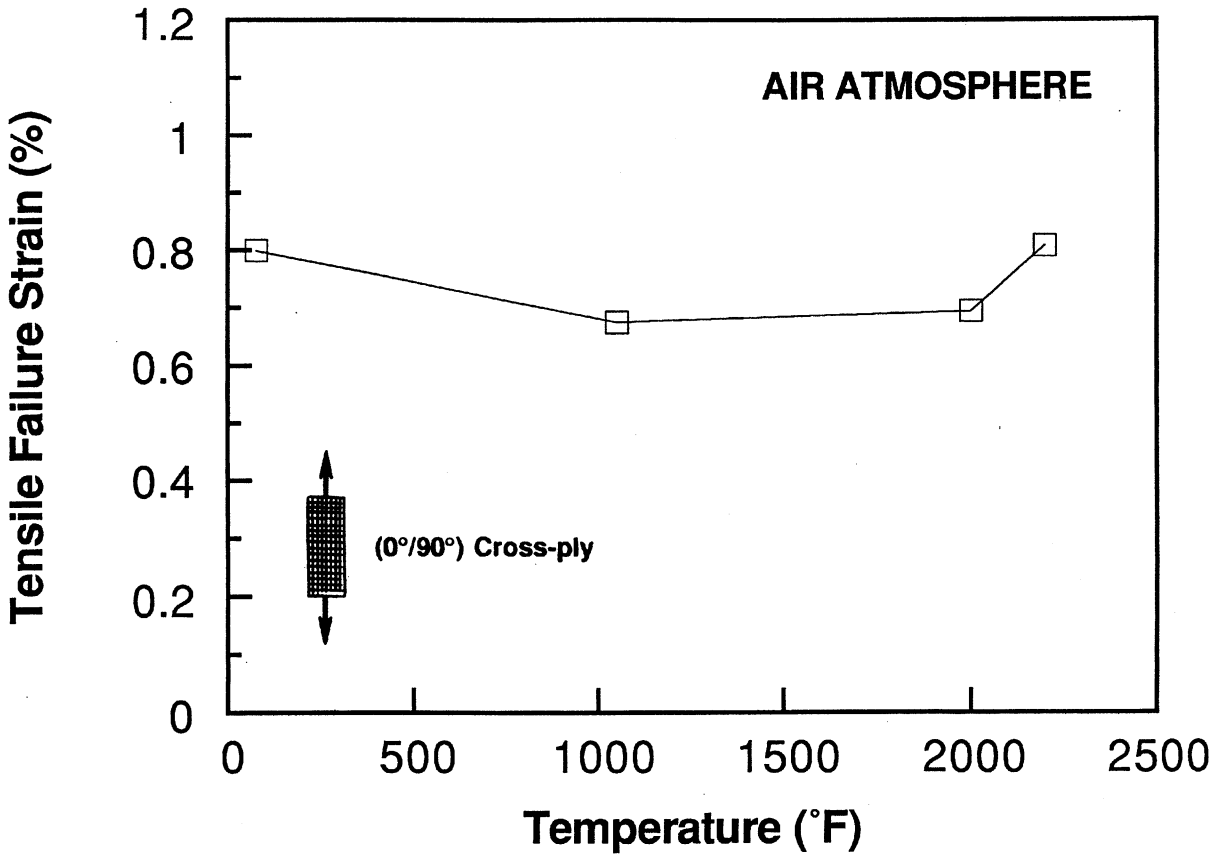

FIGURE 38. TENSILE FAILURE STRAIN OF 5% BSG-DOPED MAS CORDIERITE COMPOSITE

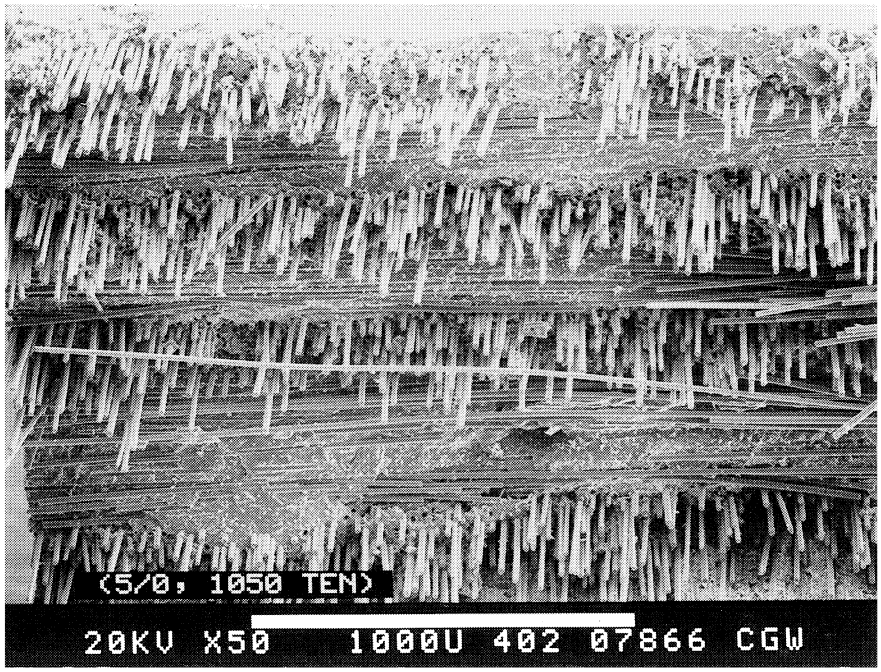

AT 1050°F

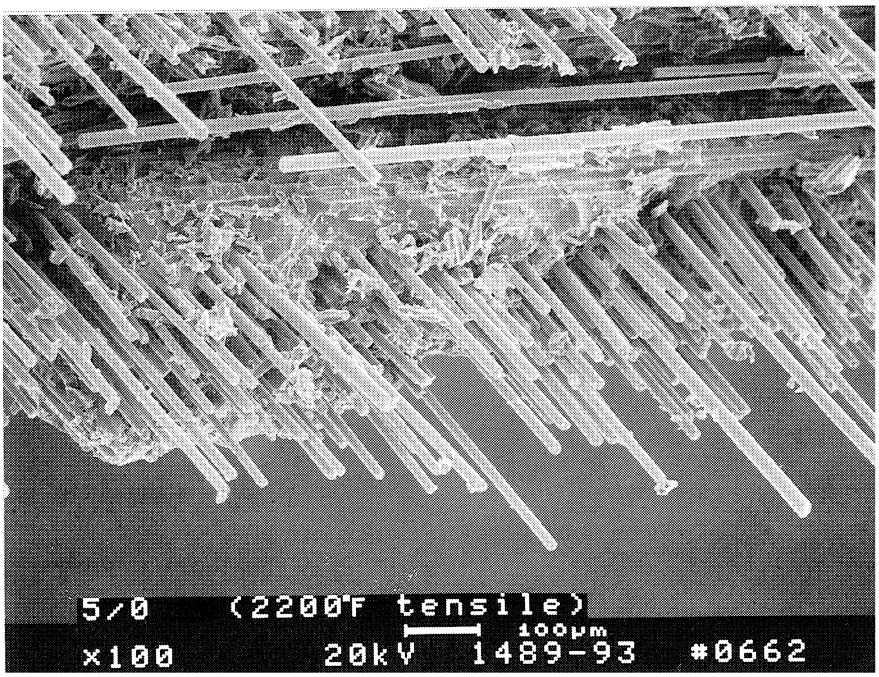

AT 2200°F

FIGURE 39. TENSILE FRACTURE SURFACE OF 5% BSG- MAS

4.2.2.2 Nicalon/5% BSG-doped, 10% SiC_w MAS Hybrid CMCs

As discussed above, the intent of the addition of SiC-whiskers to the MAS matrix of the CMC is to toughen the matrix, thereby delaying microcracks from developing, and raising the composite elastic limit. BSG-doped composites that have whisker-toughened matrices are known as BSG hybrids.

Tensile stress-strain behavior of (0°/90°) cross-ply 5% BSG-10% SiC_w MAS hybrids are shown in Figure 40. Comparison to the nonhybrid version is provided in Figure 41. The strength and failure strain of the hybrid CMCs are plotted as a function of temperature in Figures 42 and 43, respectively. The strength and failure strain are lower for the hybrid, especially at lower temperatures. We speculate that bridging whiskers contact and prematurely fracture reinforcing fibers at the point on the stress strain curve where significant relative motion and fiber pullout occurs. The fracture morphology for the hybrid remains fibrous at 2200°F, as shown in Figure 44. The slightly higher elastic modulus of CMCs with the high modulus matrix addition is shown to hold from 75° to 2200°F, as shown in Figure 45. However, the general trend is the same for both materials, being largely controlled by the behavior of the SiC fiber. The initial elastic modulus decreases ~50% over the 75° to 2200°F temperature range, but remains acceptably high for design purposes, according to Pratt & Whitney ($E \geq 10$ Msi is desired).

4.2.2.3 Summary of Fast-Fracture Tensile Behavior

The mechanical properties of BSG-doped MAS CMCs and their SiC_w matrix-toughened hybrids are tablulated in Table 1. Room temperature behavior is maintained at 1050°F, but there is no apparent influence of BSG-doping; however, properties at 2000°F are greatly improved by BSG-doping. SiC_w addition results in low failure strain at 75° and 1050°F. Otherwise, the conclusions of fast fracture tensile testing are the same as discussed previously in screening flexural testing. The BSG-dopant is responsible for the good high temperature behavior, and there is no apparent refractoriness loss when the BSG level is kept at 5%.

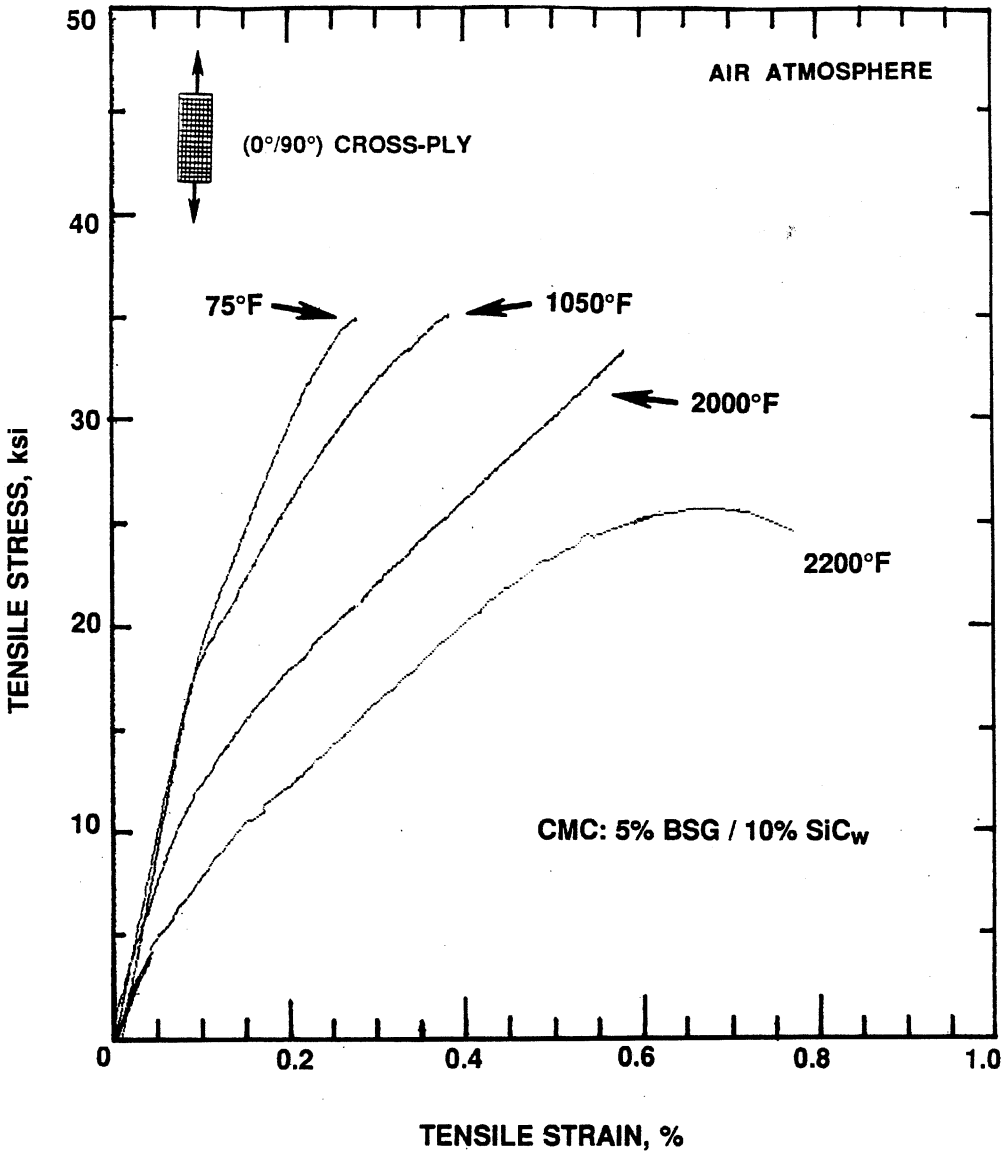

FIGURE 40. TENSILE STRESS-STRAIN BEHAVIOR OF 5% BSG-10% SiC WHISKER HYBRID CMCs

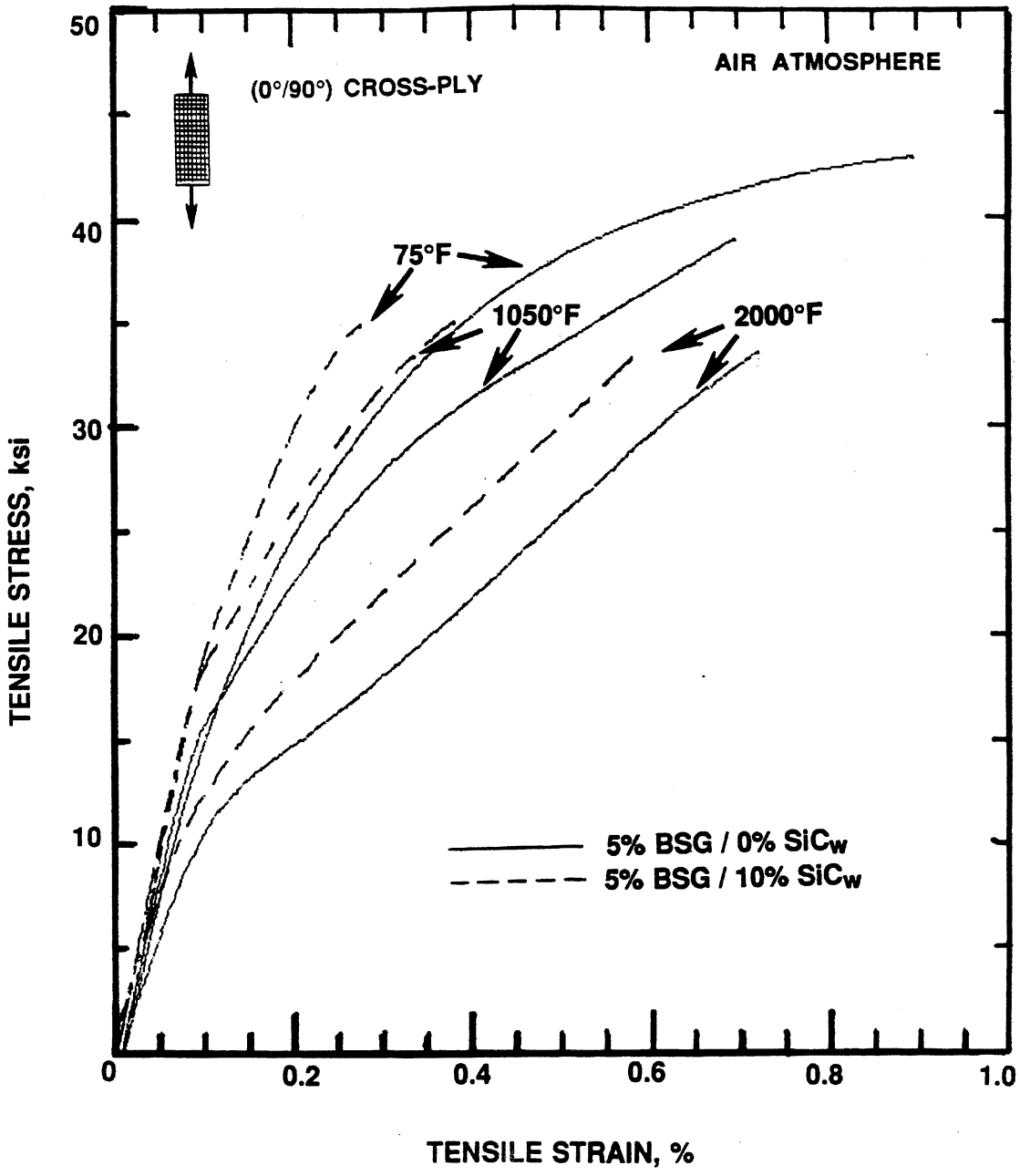

FIGURE 41. TENSILE STRESS-STRAIN BEHAVIOR OF 5% BSG- DOPED MAS CORDIERITE CMCs

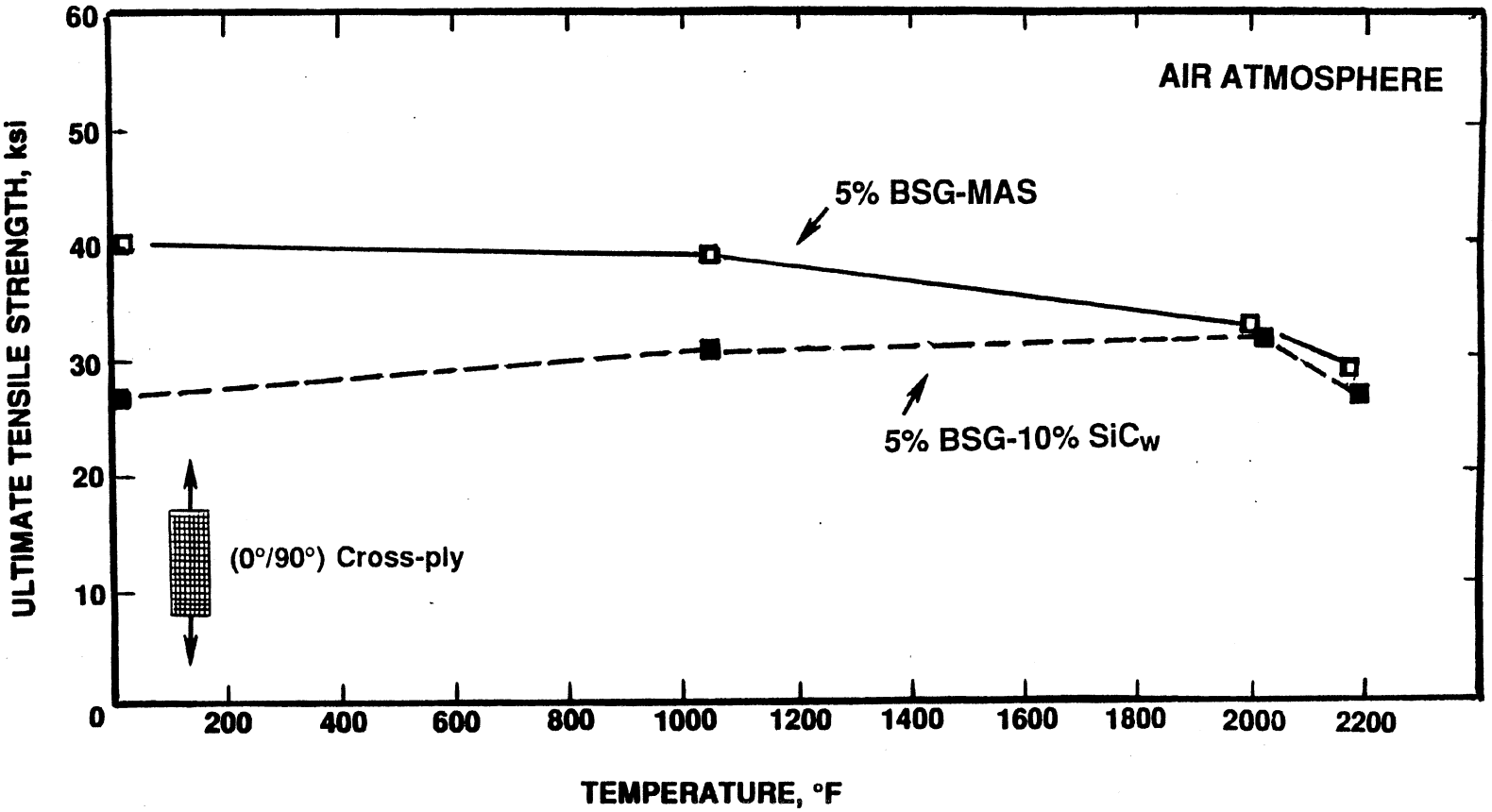

FIGURE 42. TENSILE STRENGTH OF 5% BSG-DOPED MAS HYBRID AND NON-HYBRID CMCs

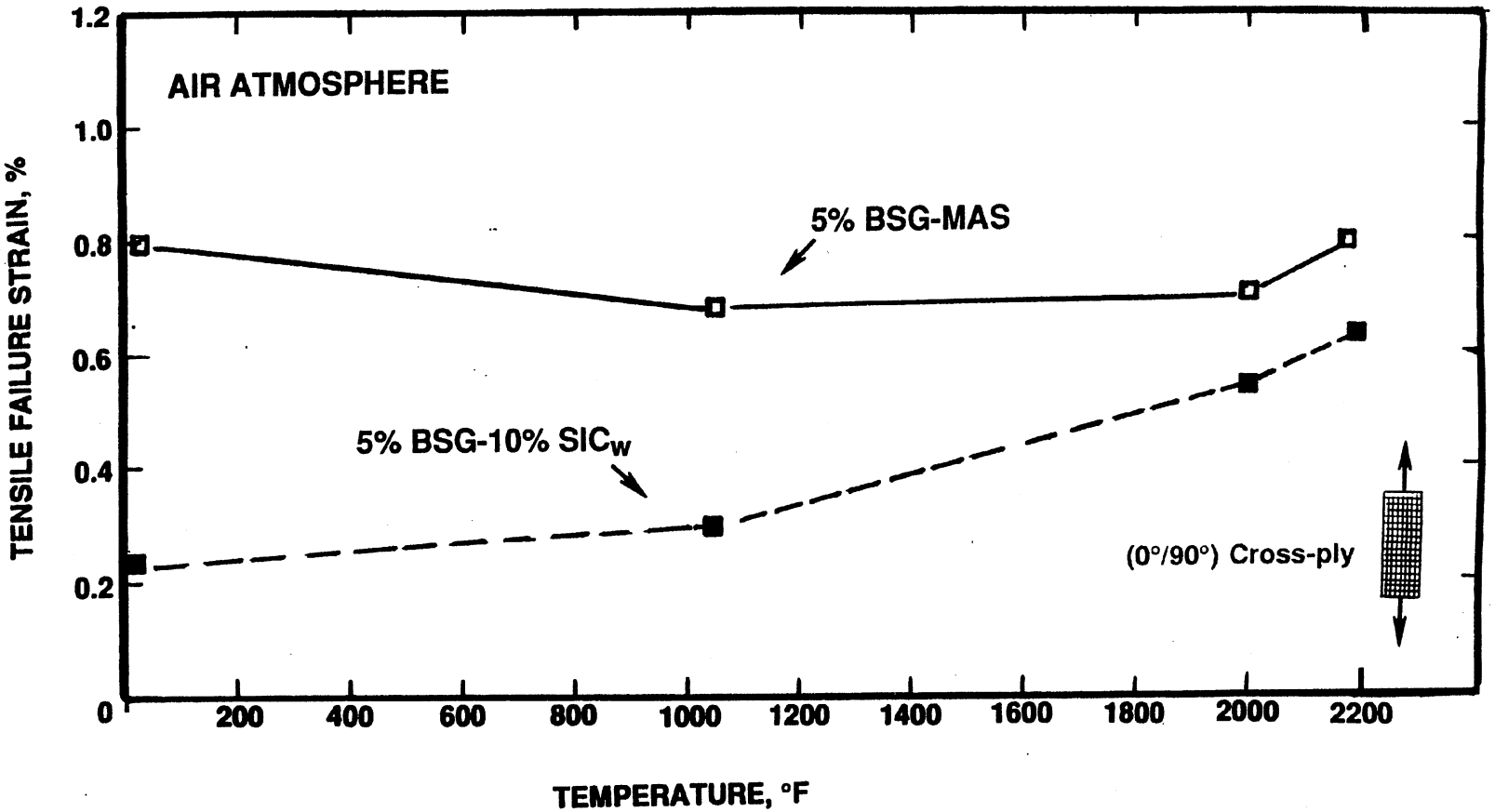

FIGURE 43. TENSILE FAILURE STRAIN OF 5% BSG-DOPED MAS HYBRID AND NON-HYBRID CMCs

Air atmosphere

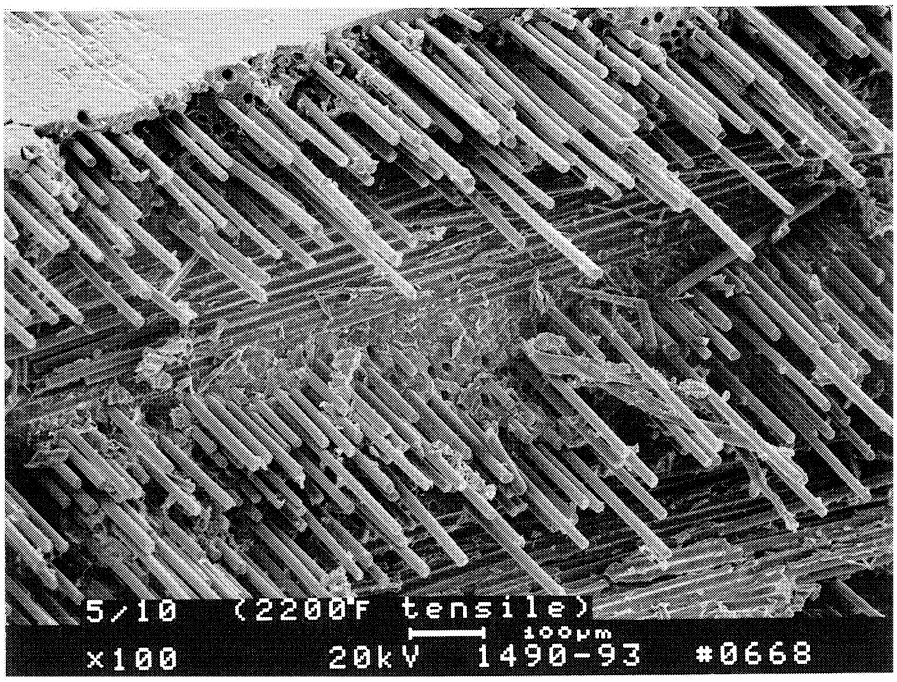

FIGURE 44. TENSILE FRACTURE SURFACE OF 5% BSG-10% SiC_w MAS AT 2200°F

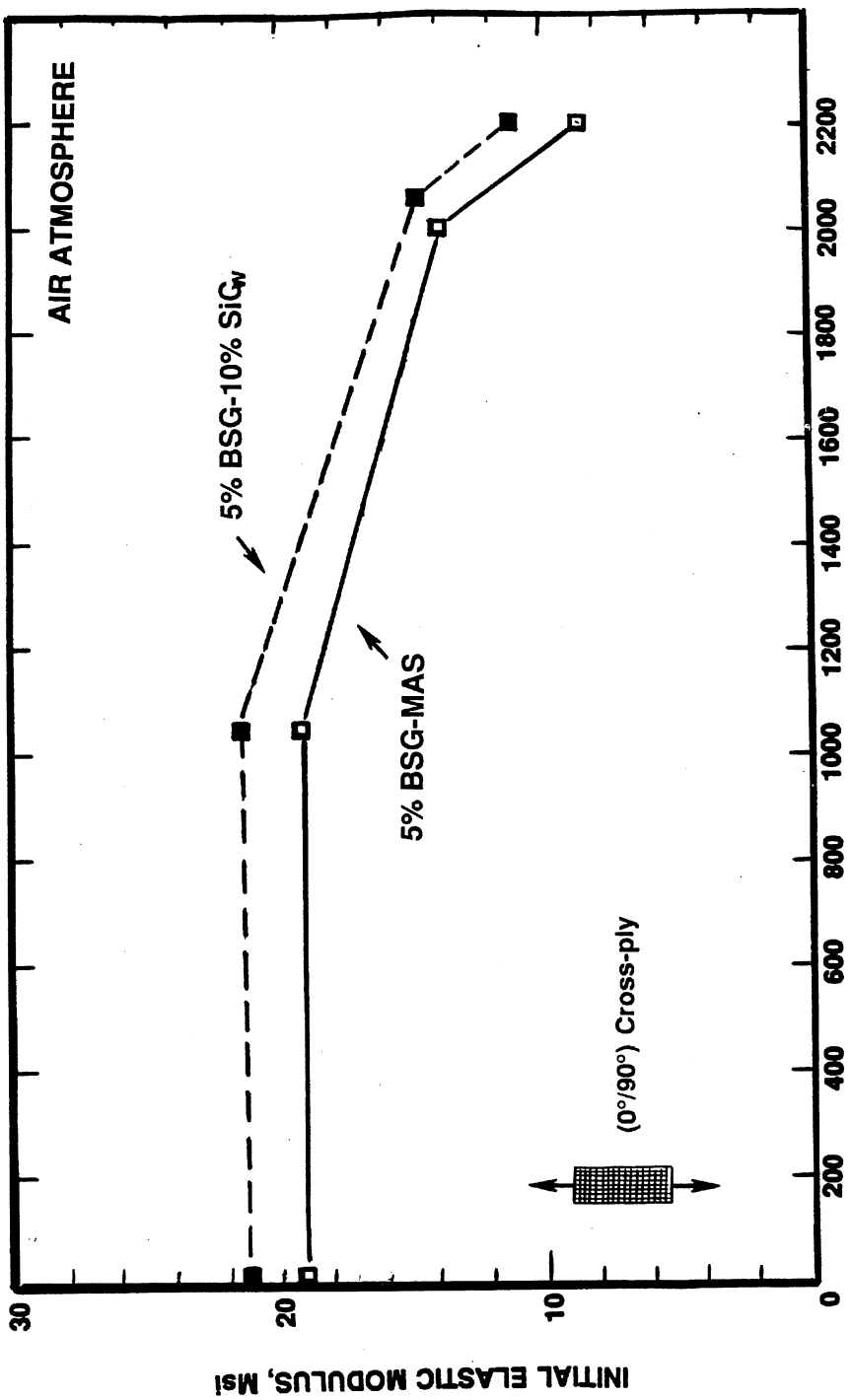

FIGURE 45. TENSILE MODULUS OF 5% BSG-DOPED MAS HYBRID AND NON-HYBRID CMCs

Table 1
TENSILE DATA FOR NICALON 5% BSG-MAS, WITH AND WITHOUT SiC-WHISKER ADDITION

	BSG	5.00%	5.00%
	Wh	0%	10%
RT	UTS	40.6 ±2.3	26.7 ±8.2
	PL	14.5 ±0.3	15.2 ±3.2
	E	19.0 ±0.1	21.2 ±2.7
	ε	0.80 ±0.10	0.23 ±0.05
1050°F	UTS	39.1 ±0.1	30.5 ±4.6
	PL	15.5 ±0.3	18.0 ±0.1
	E	19.2 ±0.8	21.6 ±0.1
	ε	0.68 ±0.02	0.29 ±0.09
2000°F	UTS	32.5 ±1.1	31.5 ±1.8
	PL	9.1 ±0.4	10.0 ±0.4
	E	13.8 ±0.4	14.7 ±0.1
	ε	0.70 ±0.02	0.54 ±0.04
2200°F	UTS	27.6 ±0.1	25.9
	PL	5.6 ±0.2	5.7
	E	8.3 ±0.6	11.0 ±0.5
	ε	0.81 ±.01	0.62 ±.07

All specimens are [(0/90)3]s. Tensile tests are run in duplicate.
± = Ranges

4.2.3 Tensile Stress Rupture

Tensile stress rupture testing is used by Pratt & Whitney as the measure of lifetime at stresses above the elastic limit, and is therefore a prime definitive indicator of thermal durability.

4.2.3.1 Test Methodology

Two tensile stress rupture (TSR) test protocols were employed. In stepped TSR, (0°/90°) cross-plied composites were initially loaded in tension (at 1050° and 2000°F, air atmosphere) at 10 ksi, and incrementally uploaded 2 ksi after each successive 50 hour period of survival. The stepped stress rupture loading continued until eventual sample failure. The final failure stress and total accumulated time under load were recorded. This test protocol is used by Pratt & Whitney to determine the maximum stress where the material exhibits a 50 hour life.

The second test employed to assess life was a conventional TSR test, wherein samples are loaded at a stress level slightly lower than where short term failures were recorded in stepped TSR, run for typically 200 hours, and then rapidly uploaded, at temperature, to failure.

4.2.3.2 TSR Results for BSG-Doped and Hybrid CMCs

Consistent with fast-fracture tensile results, TSR testing on samples with less than 5% BSG doping resulted in early failures at low loads, as shown in tabular summaries of both stepped and conventional TSR tests provided in Tables 2 and 3. This confirms that 5% BSG-doping is optimum, and provides for long life and thermal durability.

TSR testing of BSG-doped MAS composites, both with and without SiC_w addition to the MAS matrix, provided mechanistic insight to the individual roles of BSG-doping and SiC-whisker matrix toughening with respect to the attainment of thermally durable CMCs.

Table 2
STEPPED TSR RESULTS: MAXIMUM STRESS/FAILURE TIME
(max stress for 50 hr lifetime/time to failure)

% BSG/% SiC_w	1050°F	2000°F
0/0	16 ksi/200-260 hr	12 ksi/140-150 hr
1.25/0	16 ksi/200-330 hr	14 ksi/150-260 hr
1.25/10	18 ksi/260-360 hr	18 ksi/270-320 hr
2.5/0	18 ksi/270-400 hr	16-20 ksi/220-340 hr
2.5/10	14-22 ksi/220-380 hr	14-16 ksi/160-240 hr
5/0	18 ksi/240-270 hr	18-20 ksi/290-350 hr
5/10	20-22 ksi/340-390 hr	18 ksi/250-280 hr

Table 3
STRESS FOR 200 HOUR TSR LIFE/RESIDUAL STRENGTH, ksi

% BSG/% SiC_w	1050°F	2000°F
0/0	16 ksi/18-20 ksi	10 ksi/14 ksi
1.25/0	16 ksi/20-26 ksi [a]	- - - - -
1.25/10	18 ksi/20-26 ksi	18 ksi/23 ksi [a]
2.5/0	18 ksi/22-24 ksi	14 ksi/24 ksi
2.5/10	18 ksi/21 ksi	< 12 ksi [b]
5/0	18 ksi/20-22 ksi	16 ksi/24-26 ksi
5/10	20 ksi/22-24 ksi	18 ksi/23-26 ksi [a]

a ignoring one early failure
b all early failures at 12 ksi, 14 ksi

(a) Nonhybrid CMCs Containing Only BSG-doping:

Stepped and conventional stress rupture testing was conducted at 1050° and 2000°F in air atmosphere. Figure 46 presents stepped TSR results for the Nicalon/5% BSG-doped MAS CMC at 2000°F. The stepped TSR data are shown to extend to failure at 20 ksi after nominally 300 hours under load. With the at-temperature fast-fracture stress-strain curve also shown in Figure 46, it is evident that the 5% BSG-doped MAS composite has significant structural life and integrity at 2000°F at stresses well above the material's proportional limit, which was shown earlier to be a microcracking event occurring at the knee in the stress-strain response. Life at stresses greater than the proportional limit is Pratt & Whitney's working definition of thermal durability. The fibrous nature of the fracture morphology for a sample that failed at 20 ksi after 347 hours accumulated time under load at 2000°F is shown in Figure 47. Figure 48 presents the constant stress TSR results for the Nicalon/5% BSG-MAS composite, illustrating a 25 ksi tensile strength (at 2000°F) after a 200 hour runout under a 16 ksi tensile stress. Therefore, 77% of the CMC's strength was retained after the 200 hr/2000°F exposure at a stress level 60% higher than the elastic limit. Such life in a microcracked condition at 2000°F is a clear indication of the high degree of thermal durability attained. Figure 49 illustrates that these promising results extend to 2200°F as well.

The thermal durability for the Nicalon/5% BSG-doped MAS CMC at intermediate temperature, however, is not so promising. Figure 50 presents stepped TSR data for this CMC at 1050°F. Although failure times reached nominally 250 hours and the failure stress was ~20 ksi, both meeting Pratt's generic requirements for thermostructural use, the long term failure occurred at stresses only slightly higher than the at-temperature proportional limit, and only roughly 50% of the fast fracture strength at 1050°F. Additionally, the fracture surfaces of tested TSR samples were not fibrous in appearance. Conventional TSR tests (Figure 51) showed the CMC to have 20 ksi strength after 200 hour runout. While this was significantly better than the performance of baseline Nicalon/MAS composites, it was found in general that BSG dopant up to the 5% level had only nominal influence on the mechanical performance at this intermediate temperature.

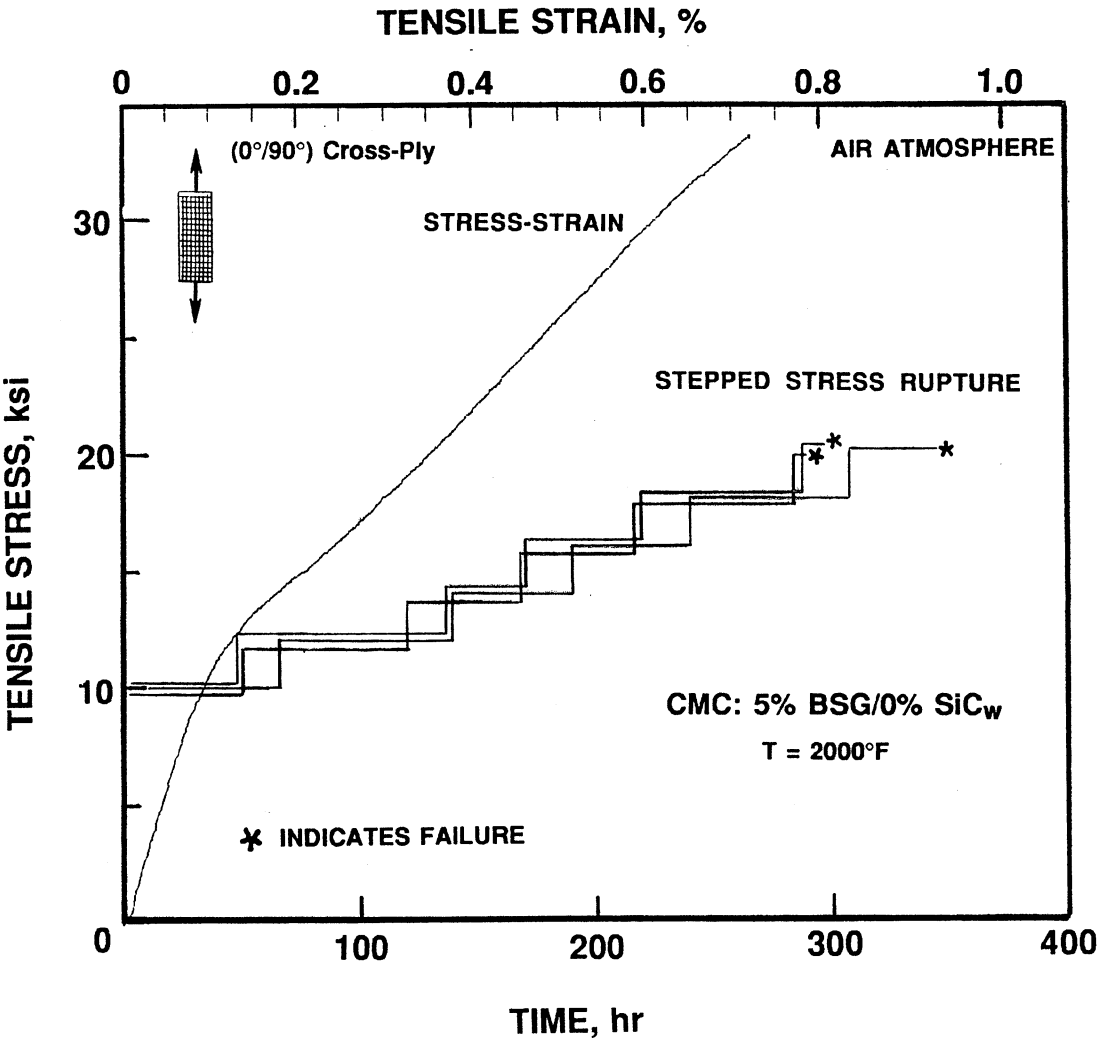

FIGURE 46. STEPPED STRESS RUPTURE RESULTS FOR BSG-DOPED MAS COMPOSITES

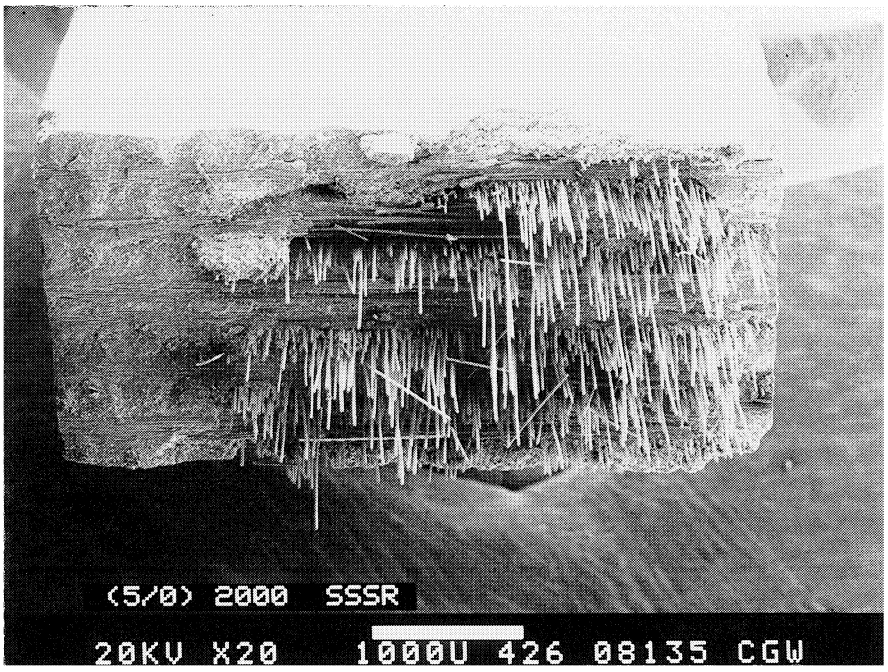

FIGURE 47. STEPPED TSR FRACTURE SURFACE OF 5% BSG-MAS AT 2000 F (failure: 20 ksi/347 hr)

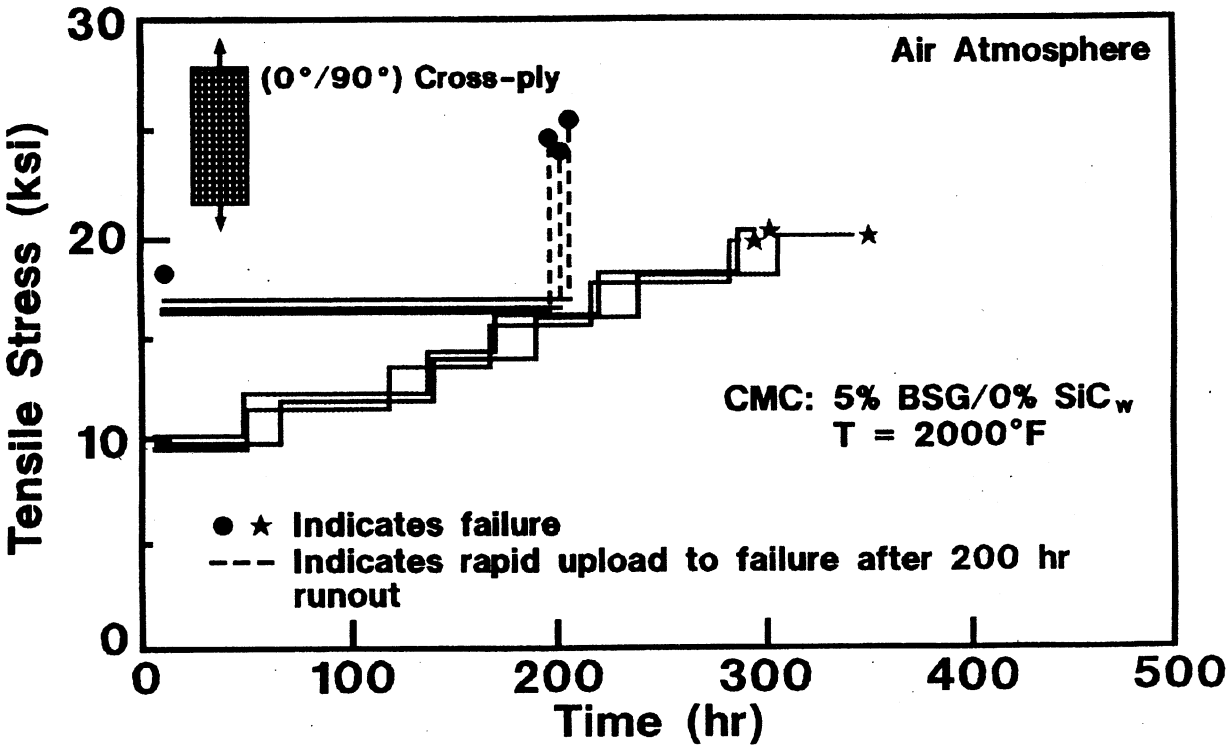

FIGURE 48. TENSILE STRESS RUPTURE RESULTS FOR BSG-DOPED MAS COMPOSITES

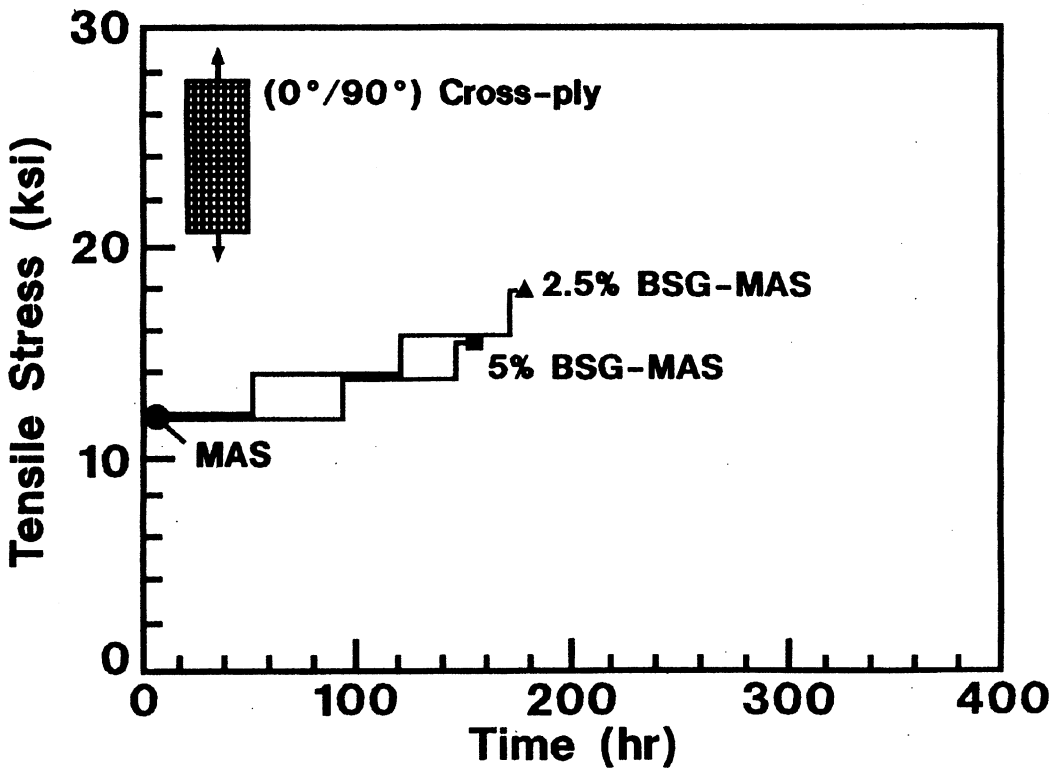

FIGURE 49. **TENSILE STRESS RUPTURE OF BSG-DOPED MAS CMCs AT 2200°F**

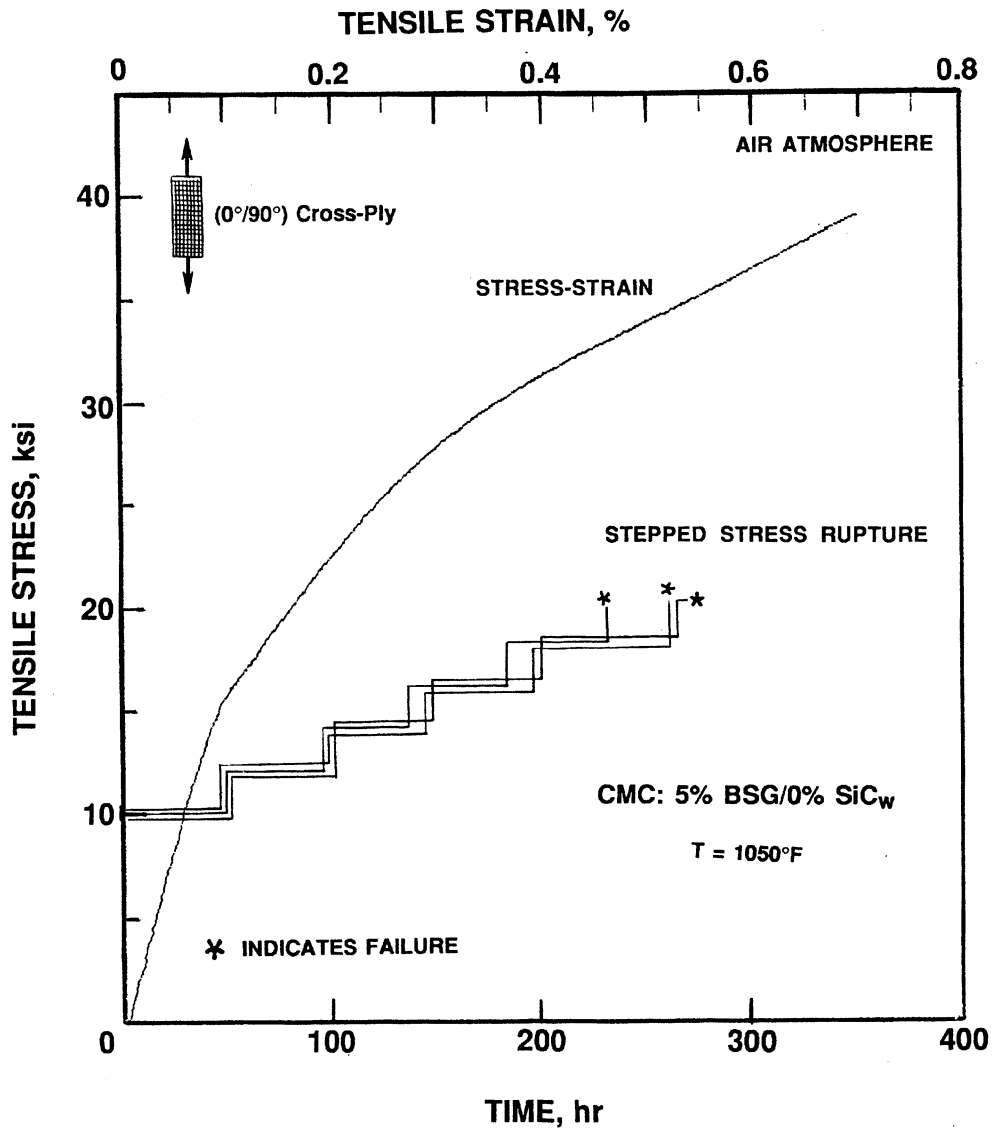

FIGURE 50. STEPPED STRESS RUPTURE RESULTS FOR BSG-DOPED MAS COMPOSITES

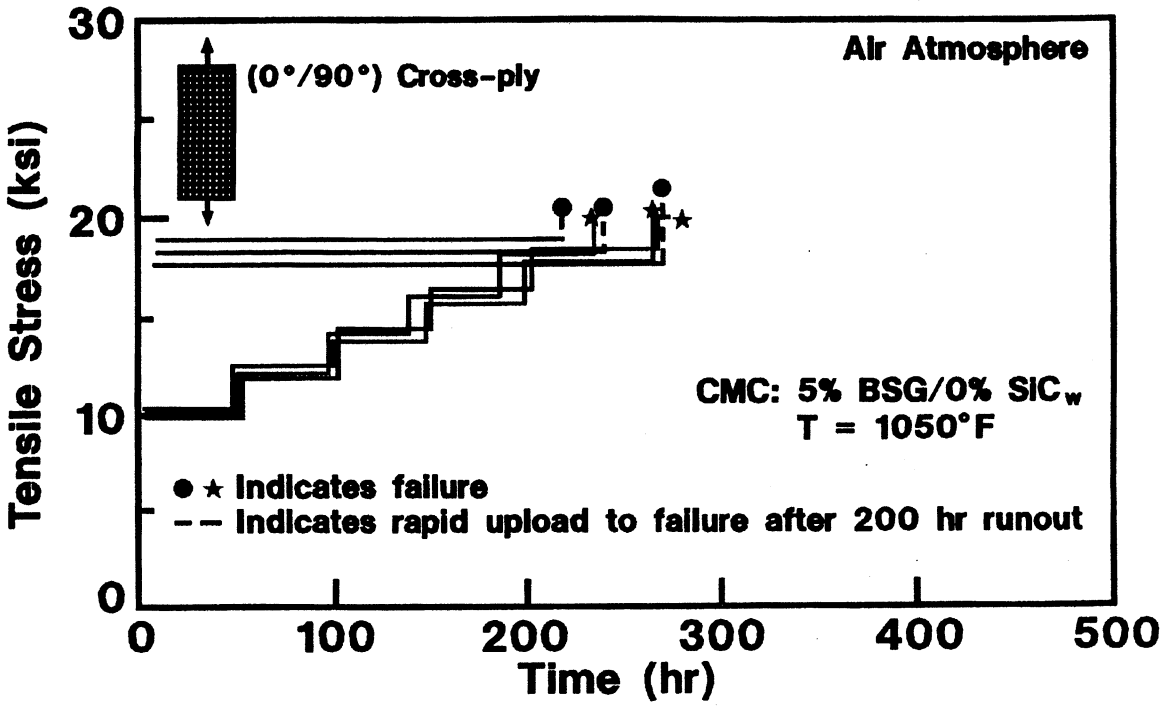

FIGURE 51. TENSILE STRESS RUPTURE RESULTS FOR BSG-DOPED MAS COMPOSITES

These high temperature and intermediate temperature TSR results for the BSG-doped MAS matrix CMCs are entirely consistent with Task 1 screening data based on flexure. BSG-doping provides a mechanism of thermal durability enhancement that is only operable at high temperature.

(b) Hybrid CMCs with SiC_w-Toughened Matrices:

Stepped tensile stress rupture data for the Nicalon/5% BSG, 10% SiC_w hybrid CMC at 1050°F are shown in Figure 52. At this intermediate temperature the addition of SiC-whiskers to the MAS matrix had a pronounced effect (recall that BSG dopants had only minor effect at 1050°F). Figure 52 illustrates that the stress rupture life extends much higher on the fast fracture stress-strain curve. Failure times were as long as 400 hours, and the fracture stress was 22-24 ksi, nominally 70% of the fast fracture strength at 1050°F. Fracture surfaces were mixed fibrous/brittle, as shown in Figure 53. The constant stress TSR test results at 1050°F are provided in Figure 54. 200 hour runout was achieved at an applied stress of 20 ksi, and the residual at-temperature strength upon rapid upload to failure was 24 ksi. Note that these TSR results at 1050°F were the best obtained of all the materials, hybrid and nonhybrid, investigated on this program.

At 2000°F, the TSR results of the 5% BSG, 10% SiC_w hybrid were nominally equivalent to those for the CMC containing a 5% BSG doping alone. This was consistent with Task 1 flexure data which showed no benefit of whisker toughening at high temperatures.

Therefore, the addition of SiC-whisker toughening of the CMC MAS cordierite matrix has the beneficial effect of increasing lifetimes at intermediate temperatures. The stress-strain curves presented in Section 4.2.2 indicated that such CMCs had increased proportional limit. We can therefore conclude that the operable mechanism of enhancing thermal durability in BSG hybrid CMCs is by inhibiting the development of matrix microcracks upon loading.

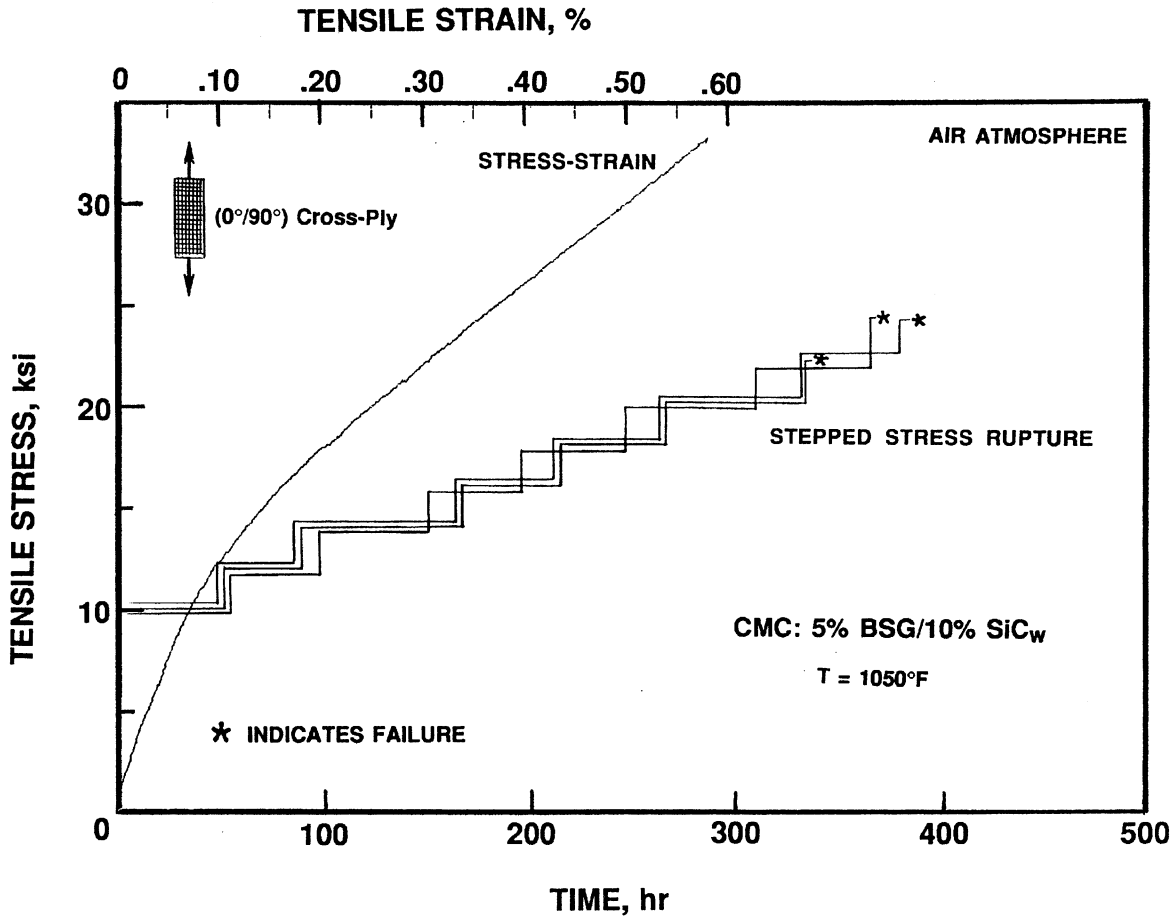

FIGURE 52. STEPPED STRESS RUPTURE RESULTS FOR BSG-DOPED MAS HYBRID COMPOSITES

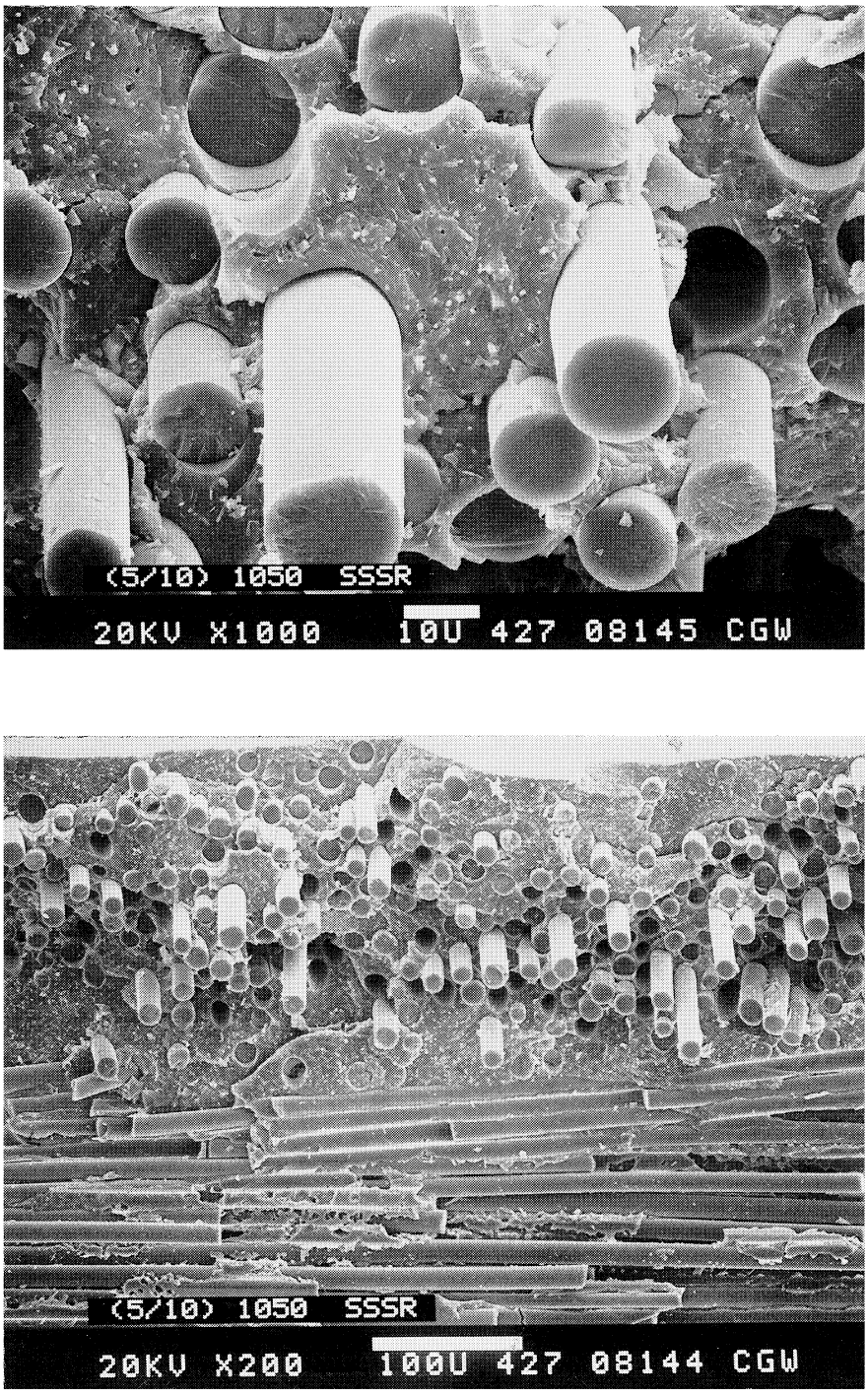

● **Failure: 22 ksi/336 hr**

FIGURE 53. TSR FRACTURE SURFACE 5% BSG-10% SiC_w MAS HYBRID TESTED AT 1050°F

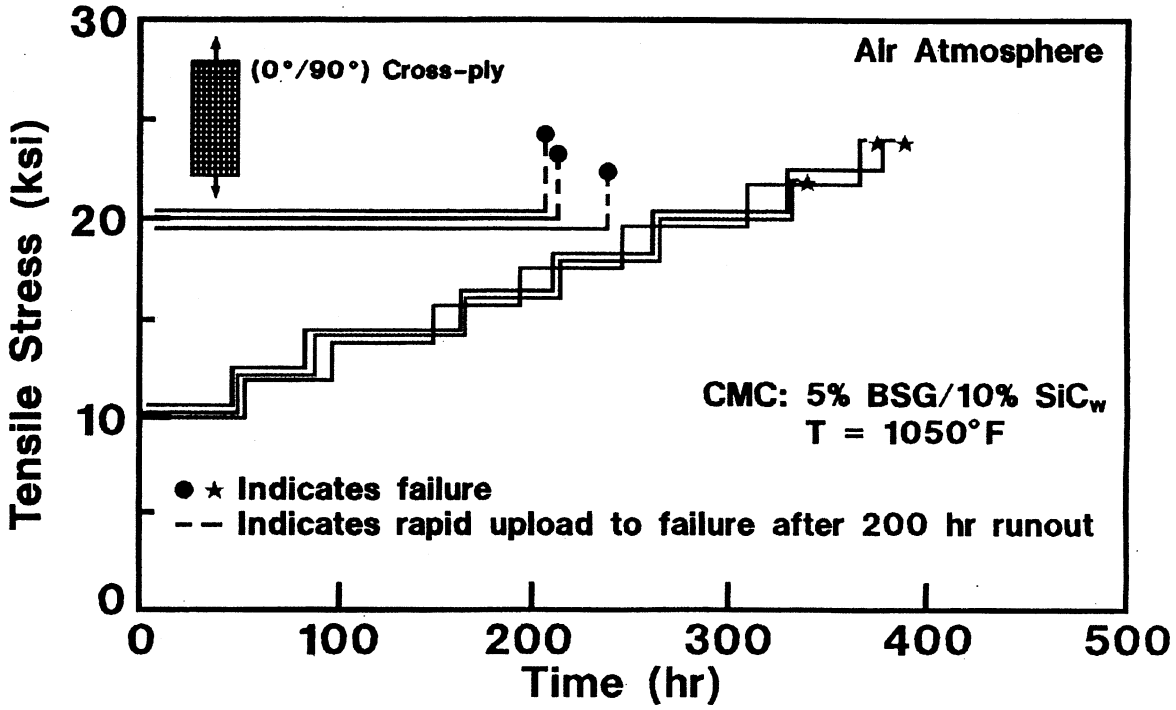

FIGURE 54. TENSILE STRESS RUPTURE RESULTS FOR BSG-DOPED MAS HYBRID COMPOSITES

4.2.3.3 5000 hr Stress-Rupture Testing

The TSR results in the previous section had the focus of thermal durability under microcracked conditions created by loading at high levels of stress. Corning and Pratt & Whitney investigated lower stress thermal durability on a parallel joint IRAD program where the emphasis was on long term thermal stability as well as thermal durability.

Nicalon/2.5% BSG-doped MAS cordierite composites, with and without SiC_w addition to the glass-ceramic matrix, were fabricated in [0°/±45°/90°] laminate construction and subjected to air atmosphere tensile stress rupture tests at Pratt & Whitney.* The applied load was 7 ksi, near the material's elastic limit. The nonhybrid survived the 7 ksi applied stress for 5077.7 hr (7 months) at which point it was rapidly uploaded to failure (at 2000°F); as shown in Figure 55. Its residual strength was 19.5 ksi, greater than 90% of the original fast fracture strength, as indicated by the comparison to the stress-strain response presented with the TSR behavior in Figure 55. Fracture surface examination revealed very fibrous failure of the 45° plies, while the 0° plies were fibrous at the center of the sample cross-section, and brittle near all exposed edges, as shown in Figure 56. A fair degree of toughness and strain tolerance were maintained for the 5000+ hours of thermal exposure. Figure 57 compares the short term stress-strain, stepped tensile stress-rupture (where failure was at ~350 hr), and the 5000 hr TSR test results. It is apparent that the BSG-doped MAS matrix CMC exhibits load rate/history independence over several thousand hours of time.

Similar results were obtained for the 2.5% BSG-doped, 10% SiC-whisker hybrid matrix composite for which more extensive post-exposure microstructural examination was done. Figure 58 presents a TEM replica view of the microstructure of this CMC after the 5000 hr/2000°F TSR exposure. The matrix microstructure appears to have coarsened a bit (compared to Figure 4), but there is no apparent fiber or whisker attack. This is shown more clearly in the TEM thin foil view of the thermally exposed microstructure shown in Figure 59. Note the

---

* Performed prior to our determination that 5% BSG-doping was optimal.

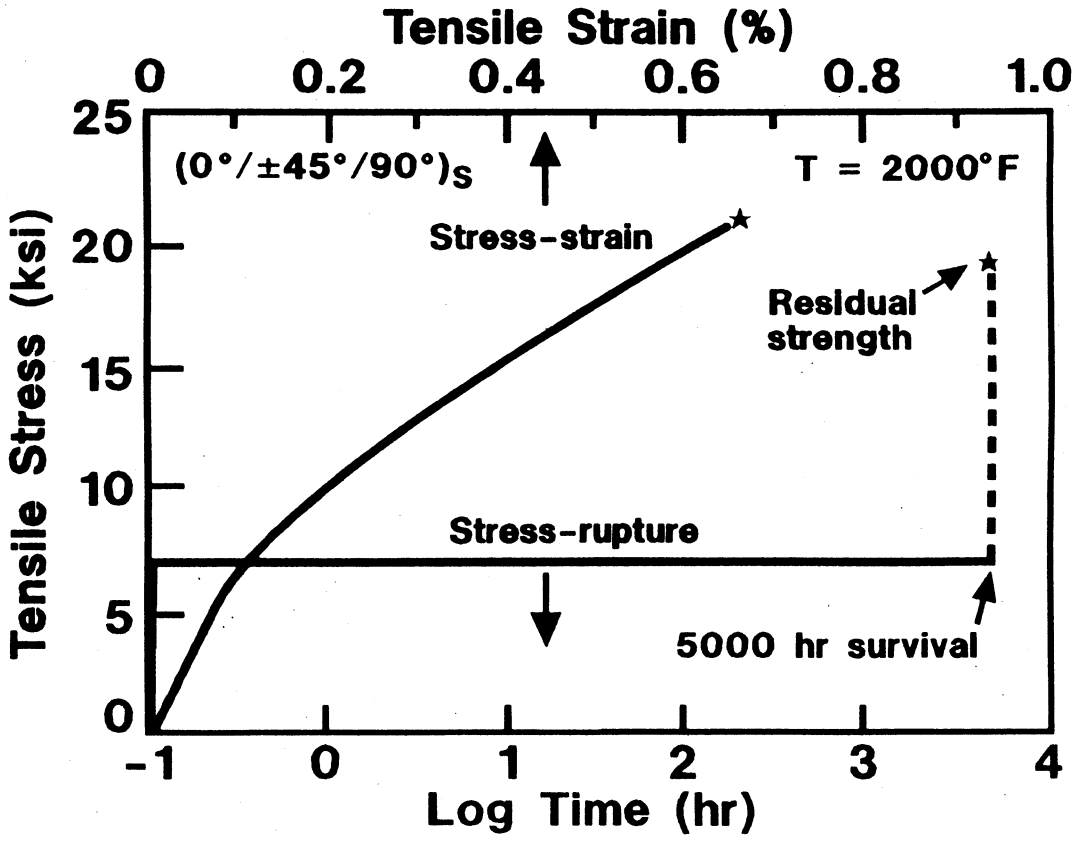

FIGURE 55. 5000 HOUR STRESS-RUPTURE DATA FOR 2.5% BSG-DOPED MAS COMPOSITES

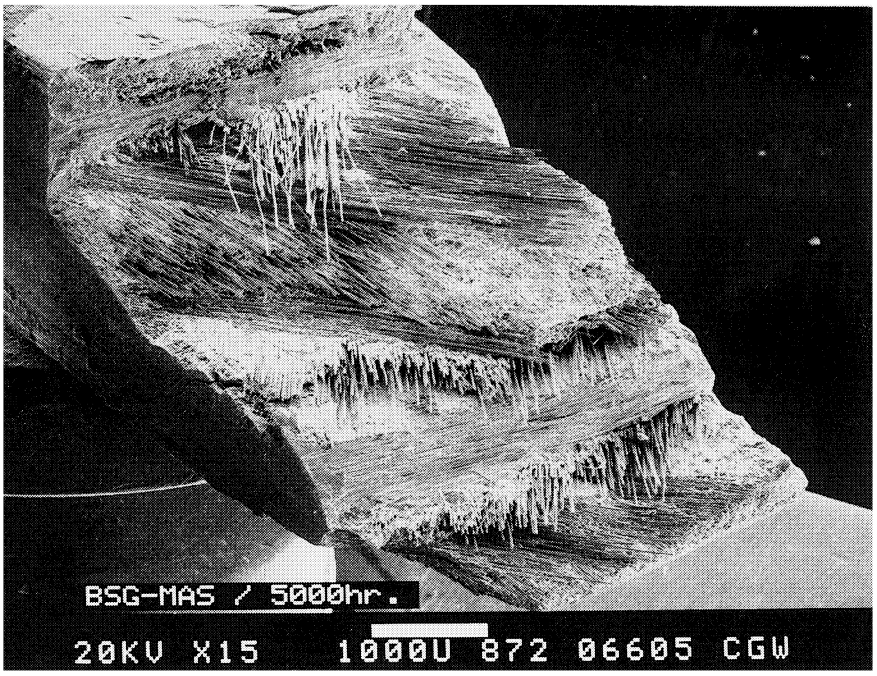

(a) (0°/±45°/90°) TENSILE FRACTURE

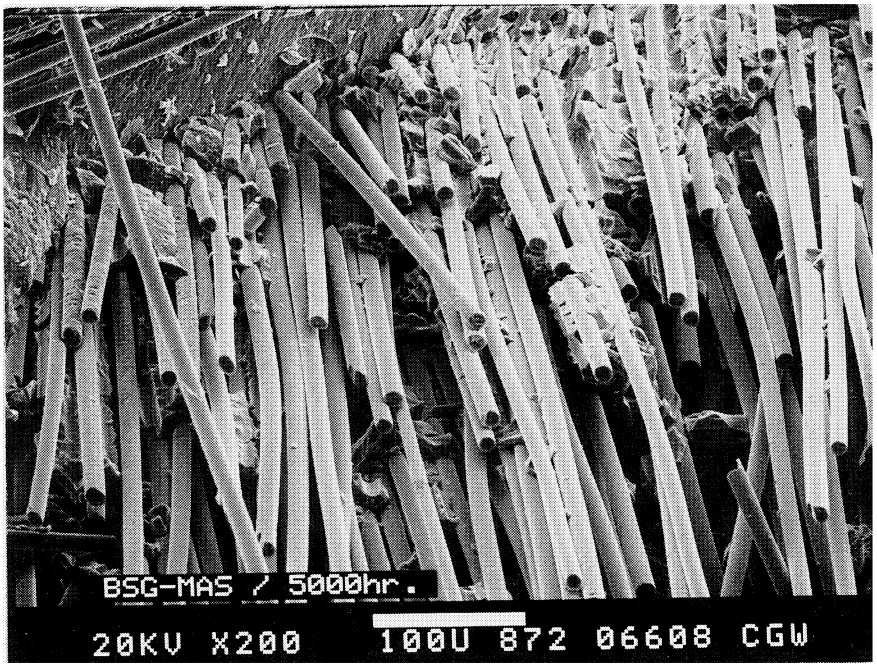

(b) SHEARED-OUT 45° FIBERS

FIGURE 56. **FRACTURE SURFACES OF BSG-MAS COMPOSITE AFTER 2000°F/5000 HR TENSILE STRESS RUPTURE TEST**

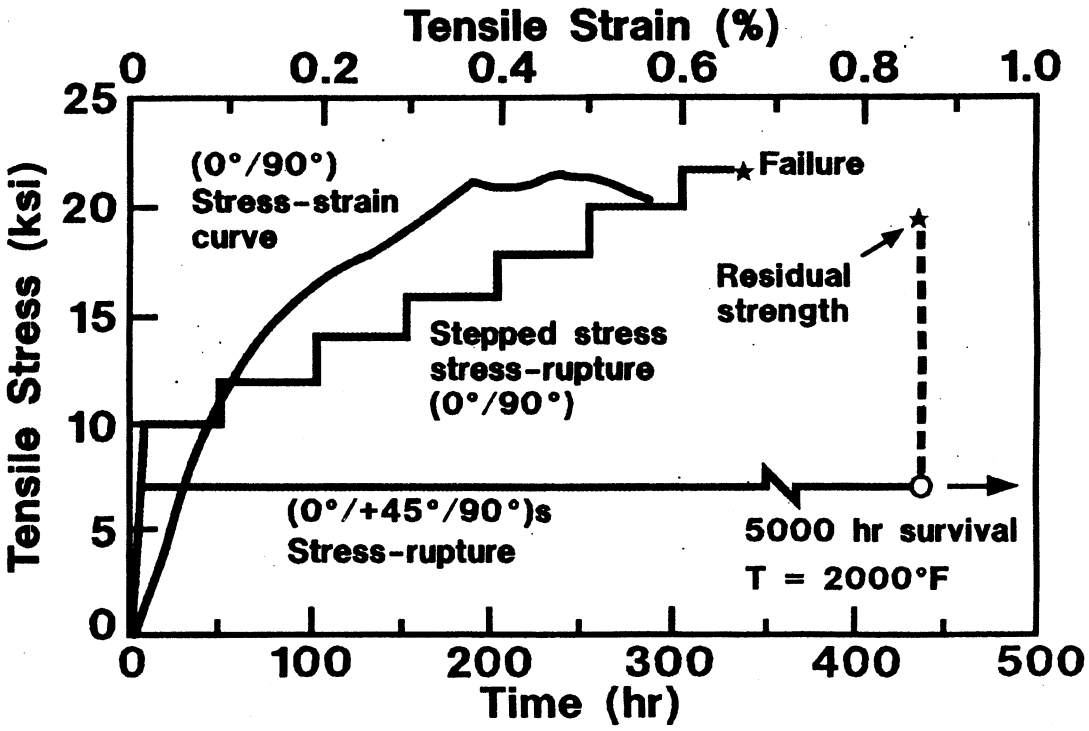

FIGURE 57. STRESS-RUPTURE RESULTS FOR 2.5% BSG-DOPED MAS SHOWING LOAD HISTORY INDEPENDENCE

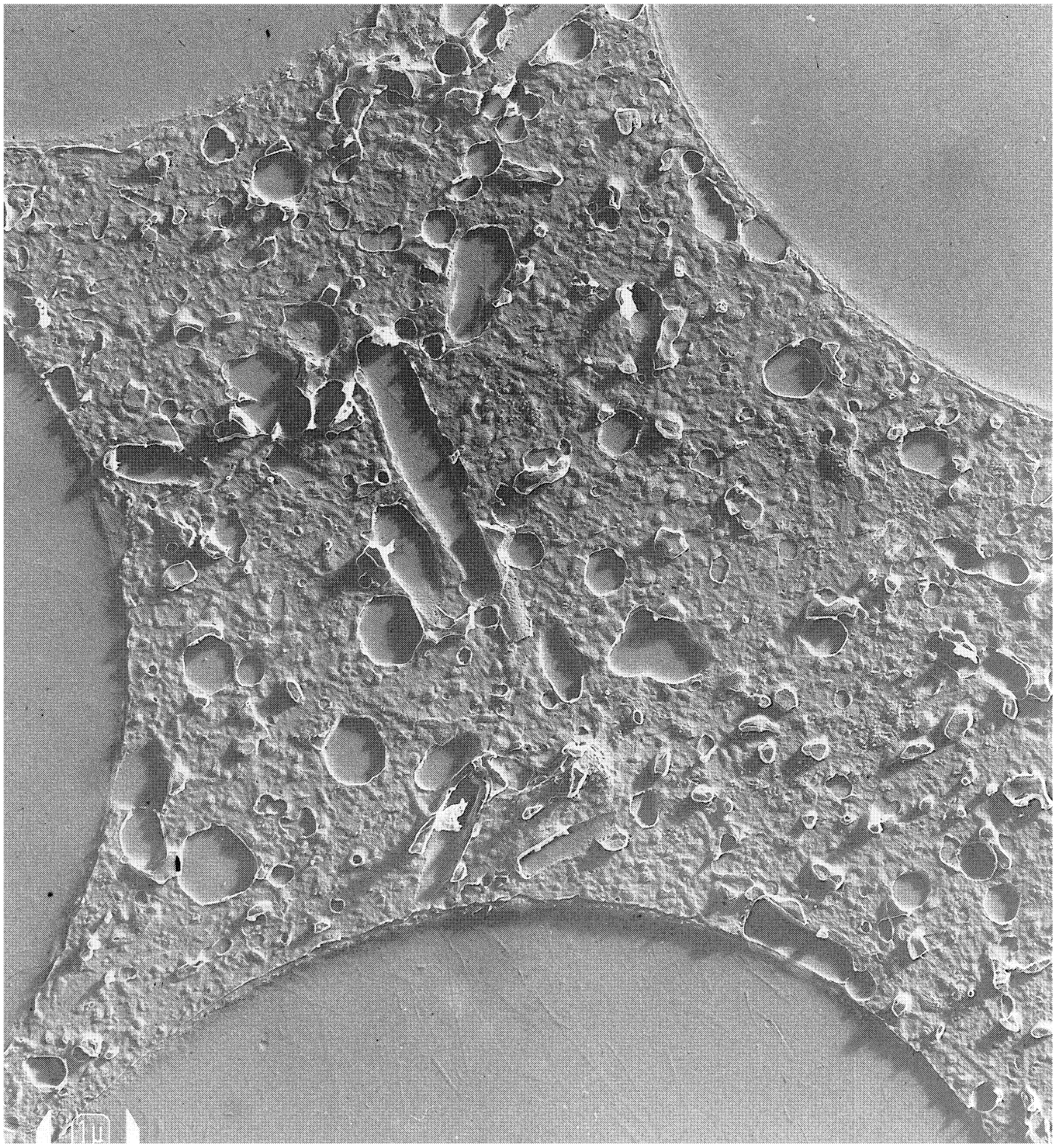

FIGURE 58. TEM REPLICA: 2.5% BSG/10% SiC_w MAS AFTER 5000 HR TENSILE STRESS RUPTURE

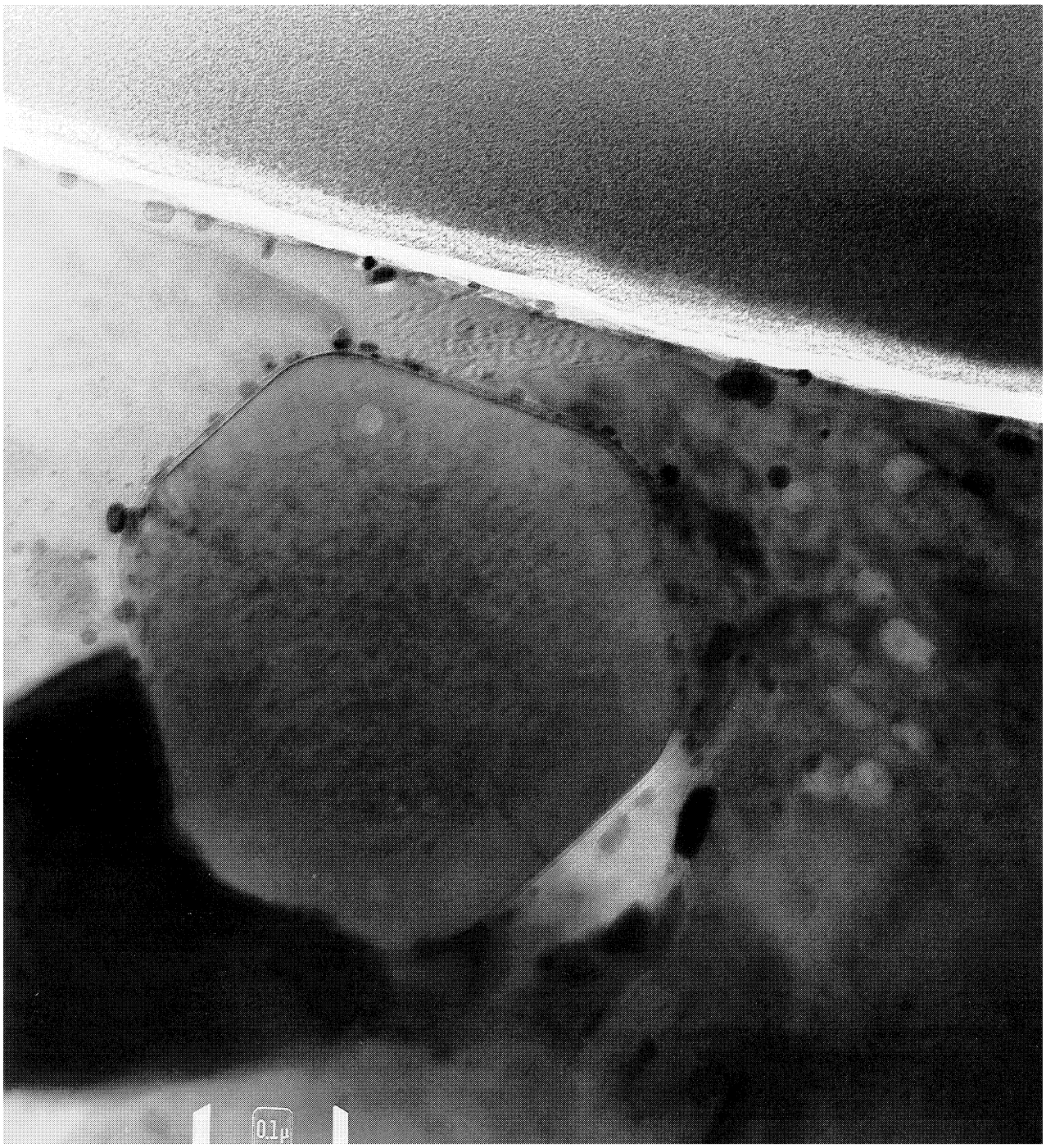

FIGURE 59. **TEM MICROGRAPH OF 2.5% BSG-10% SiC_w MAS HYBRID HAVING SURVIVED 5000 HR TENSILE STRESS RUPTURE TEST AT 2000°F**

integrity of the whisker-matrix boundary and the maintenance of the fiber-matrix interface. The latter is shown more clearly in Figure 60, also a TEM micrograph of a 5000 hr/2000°F TSR sample. Note especially the in situ carbon interface and the matrix-side glass layer, which apparently provides a glaze coating to protect the carbon-rich layer from oxidizing during thermal exposure. The presence of this plugging glaze coating was mentioned previously, and will be discussed in the following section dealing with thermal exposures at intermediate as well as extremely high temperatures.

4.2.3.4 Summary of TSR Testing

Tensile stress rupture testing was found to be a definitive indicator of thermal durability and thermal stability. At intermediate temperature, the presence of SiC whiskers in the microstructure had the affect of increasing lifetimes at high stress, but had no affect at high temperature. Conversely, BSG-doping at the 5% level had no affect at intermediate temperature, but had a pronounced beneficial affect in increasingly thermal durability at 2000°F. The whiskers appear to inhibit matrix microcracking, whereas the BSG glass appears to protect the in situ carbon layer by boron-doping the in situ-carbon layer (B_2O_3 and BN) and providing a matrix-side glaze coating. The simultaneous use of these dopants/additives appears to provide thermal durability over the entire temperature range of interest. Additionally, MAS cordierite microstructures containing these two additives exhibited a high degree of thermal stability in 5000 hour exposures.

4.2.4 Unstressed Isothermal Oxidation

Pratt & Whitney devised a simple, yet environmentally severe test to screen prospective CMC candidates for thermal durability. [0°/90°] cross-ply flexure bars, with as-processed surfaces and machined edges, were exposed for extended times, typically 100 and 500 hr, in air atmosphere at various intermediate and high temperatures. The residual flexure properties were then measured under ambient conditions after the unstressed isothermal oxidation exposure.

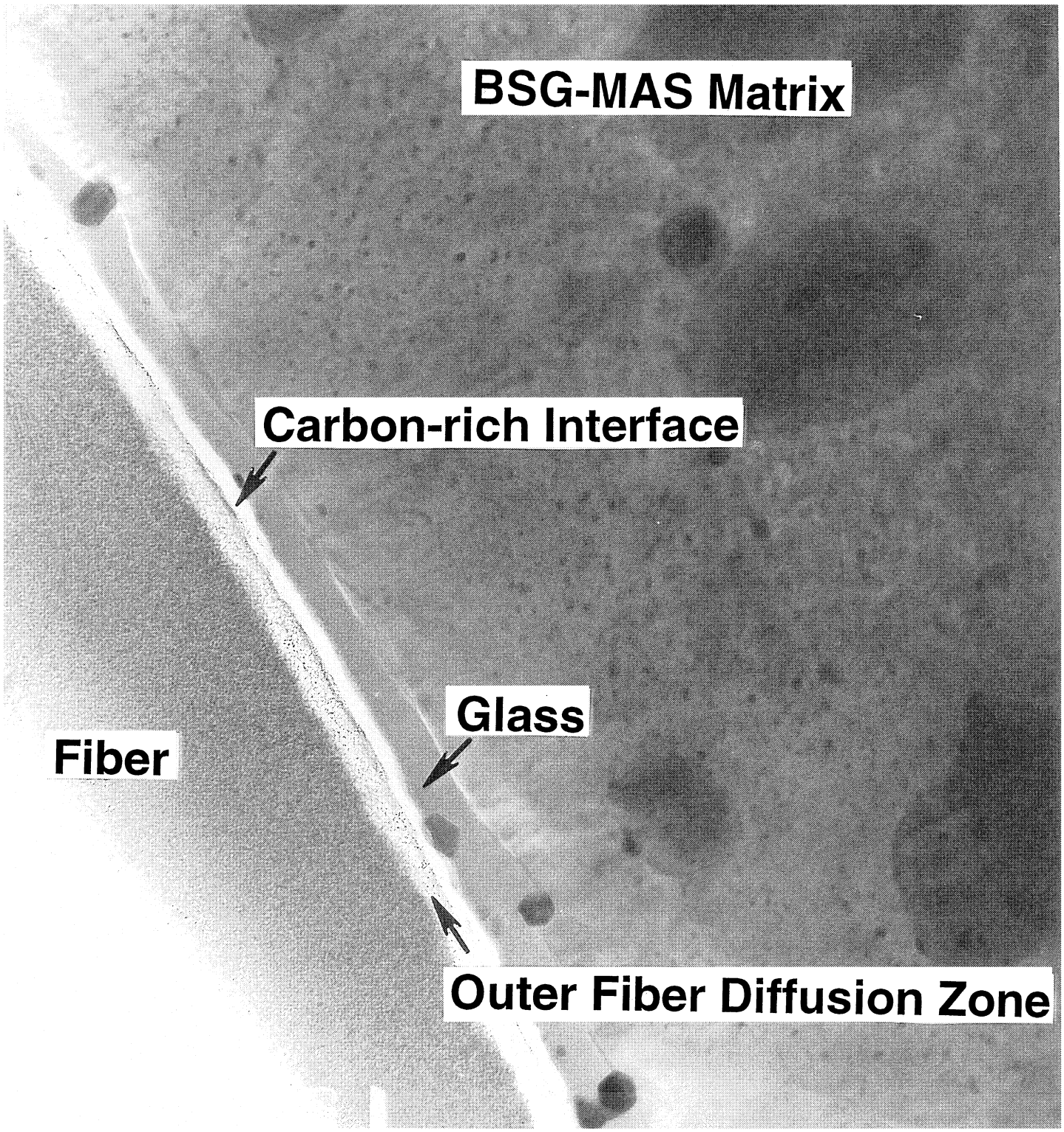

FIGURE 60. **TEM MICROGRAPH OF 2.5% BSG-10% SiC_w MAS HYBRID HAVING SURVIVED 5000 HR TENSILE STRESS RUPTURE TEST AT 2000F SHOWING EXISTENCE OF MATRIX-SIDE GLASS COATING**

The residual flexural properties of Nicalon/5% BSG-doped MAS cordierite CMCs subjected to these various isothermal oxidation exposures are presented in Figures 61 and 62. It is shown that these nonhybrid CMCs experience a significant loss of strength and toughness at 1300°F (700°C). For instance, the 5% BSG-doped CMC experienced a ~70% strength loss and ~40% failure strain reduction after 100 hr isothermal exposure at 1300°F, but tolerated higher exposure temperatures quite well, with residual mechanical properties after 1600° and 2000°F isothermal exposures only marginally affected. The property reduction at 1300°F was accompanied by a change in failure mode from shear, or combined tensile/shear, to tension. Also, the elastic modulus was observed to increase by as much as 20% after the 1300°F exposure, presumably related to the less compliant interface formed upon embrittlement (silica replacing carbon).

This effect has been observed by Pratt & Whitney for a variety of the industry's CMCs, all containing an in situ carbon-rich fiber-matrix interface, and is widely known in the technical community as the intermediate temperature oxidation embrittlement problem.

4.2.4.1 Cause of Embrittlement: Oxidation of Interface

Several aspects of such degradation in properties at intermediate temperatures were considered and investigated further, both with an aim of identifying the underlying cause of the phenomenon of intermediate temperature embrittlement, as well as finding an effective remedy. These are discussed as follows.

(a) Internal Reactivity:

Internal reactivity was eliminated from consideration as the cause of the embrittlement, since intermediate temperature exposure in nitrogen atmosphere did not result in property degradation.

(b) Residual Stress-induced Microcracking:

Similar intermediate temperature embrittlement degradation in extended air atmosphere exposures was observed for a wide variety of matrices having various levels of thermal expansion mismatch with the reinforcing fiber: CAS, MAS, LAS, and BMAS. Therefore, it was concluded that the observed embrittlement was not related to matrix residual stress state and any

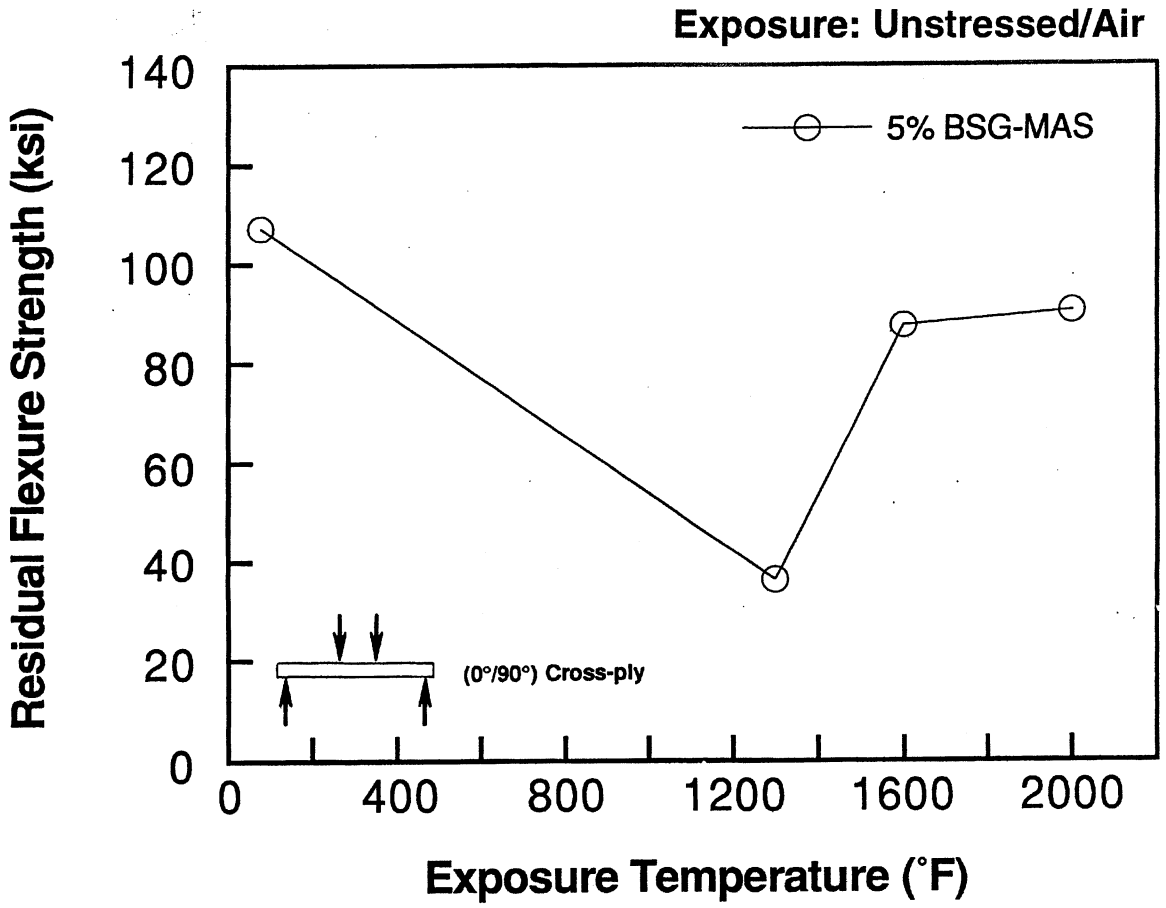

FIGURE 61. 100 HOUR ISOTHERMAL OXIDATION EXPOSURES FOR Nicalon/5% BSG-MAS CMCs

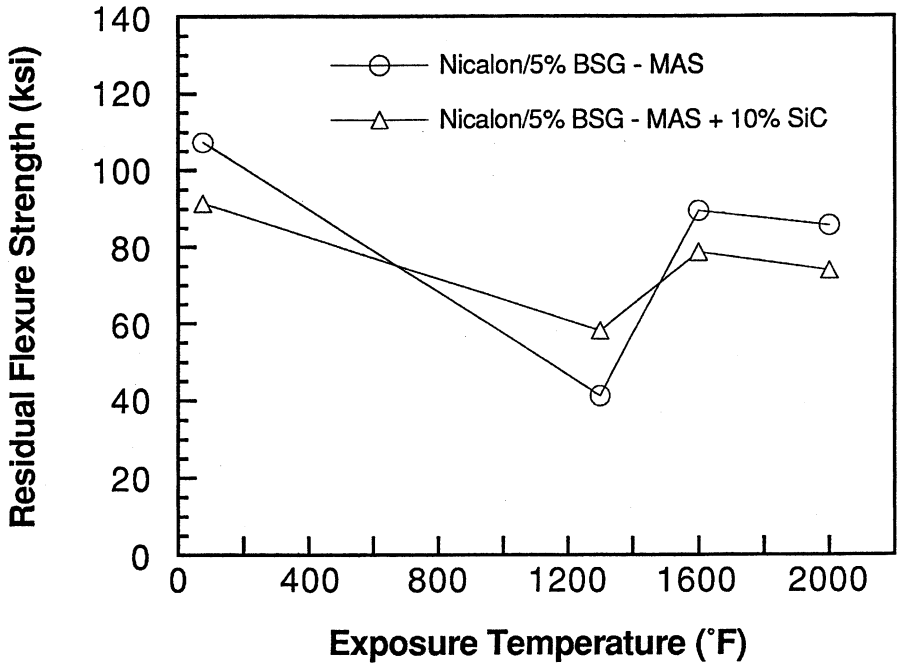

FIGURE 62(a). EFFECT OF 500 HR ISOTHERMAL OXIDATION EXPOSURE ON STRENGTH OF Nicalon/5% BSG-MAS

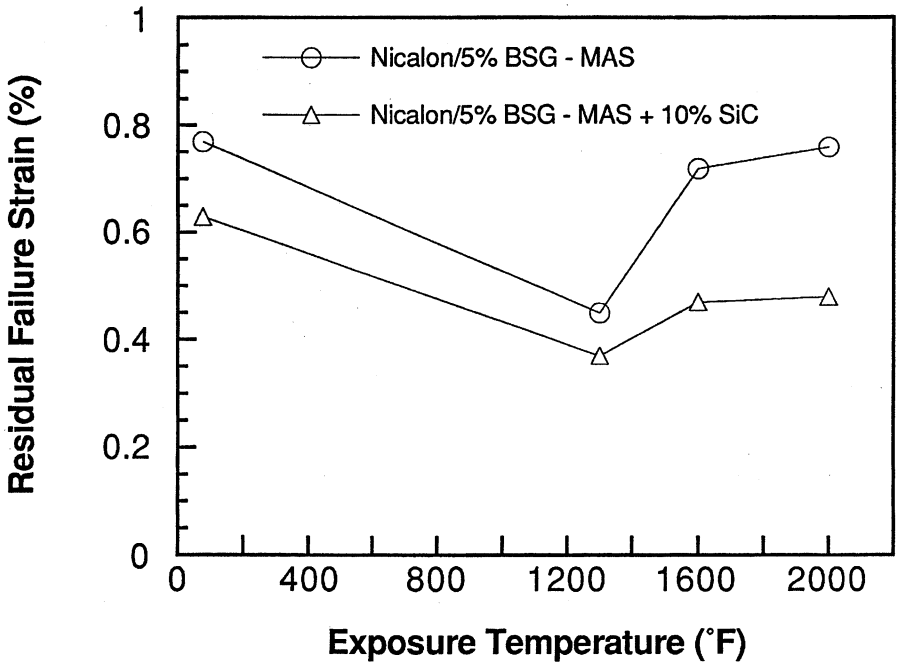

FIGURE 62(b). EFFECT OF 500 HR OXIDATION EXPOSURE ON FAILURE STRAIN OF BSG-MAS MATRIX CMCs

associated microcracking (which would have provided paths for air to reach and oxidize the interface).

(c) Matrix Phase Instability:

As mentioned previously, the MAS matrix of the CMCs investigated on this program is a barium-stuffed cordierite. Barium is somewhat mobile and Ba-MAS destabilization is sometimes observed, but normally only after extended thermal exposure at 2000°F. Celsian, BAS, typically forms in regions of the cordierite microstructure, but its presence has been found to be relatively benign: it is a more refractory phase, and we have found no microcracking associated with such destabilization. Such celsian formation is regarded as a harmless effect, and not the cause of intermediate temperature embrittlement in the CMCs studied on the present program.

(d) Unstable Secondary Phases:

Extensive examination of embrittled CMCs from the present study was conducted. No unstable phases were found in the matrix (such as the NbC transformation to Nb_xO_y effect found in certain LAS matrix CMCs with much higher levels of Nb addition).

These experiments involving possible internal reactivity, residual stresses, and phase instability have confirmed that the observed embrittlement problem is instead related to oxidation of carbon-rich interfacial regions in the microstructure, often referred to as pipeline oxidation.

4.2.4.2 Management of Embrittlement by Flash Oxidation Treatment

It was found that flash oxidation treatment, i.e., short term exposure to oxidizing conditions at very high temperatures, served to almost completely eliminate the intermediate temperature oxidation embrittlement problem in Nicalon/5% BSG-MAS composites. This is illustrated in Figures 63 (a,b), which presents strength and failure strain in three environmentally exposed conditions: (1) as-processed, (2) after 650°C/100 hr exposure (the data in Figure 61), and (3) flash oxidized (three different schedules) prior to 650°C/100 hr intermediate temperature exposure.

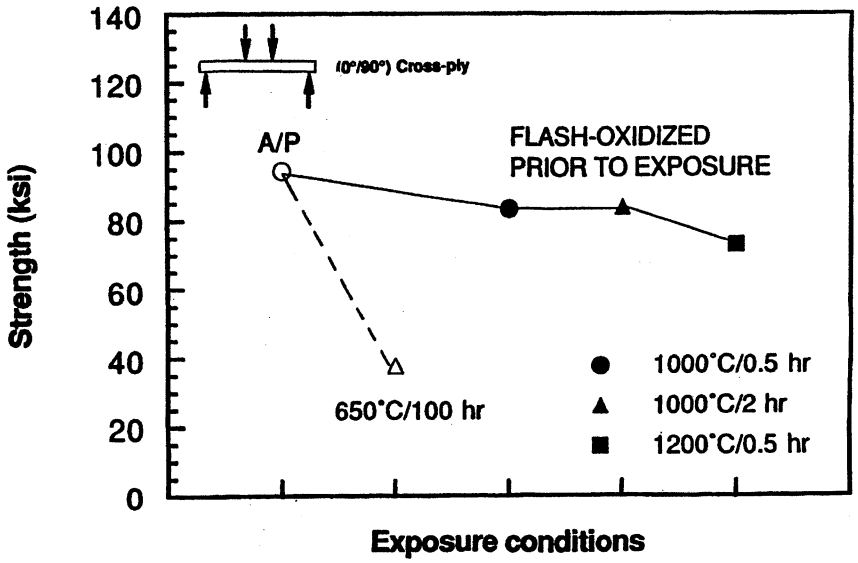

FIGURE 63(a). EFFECT OF FLASH SEALING ON FLEXURAL STRENGTH OF Nicalon/5% BSG-MAS CMCs

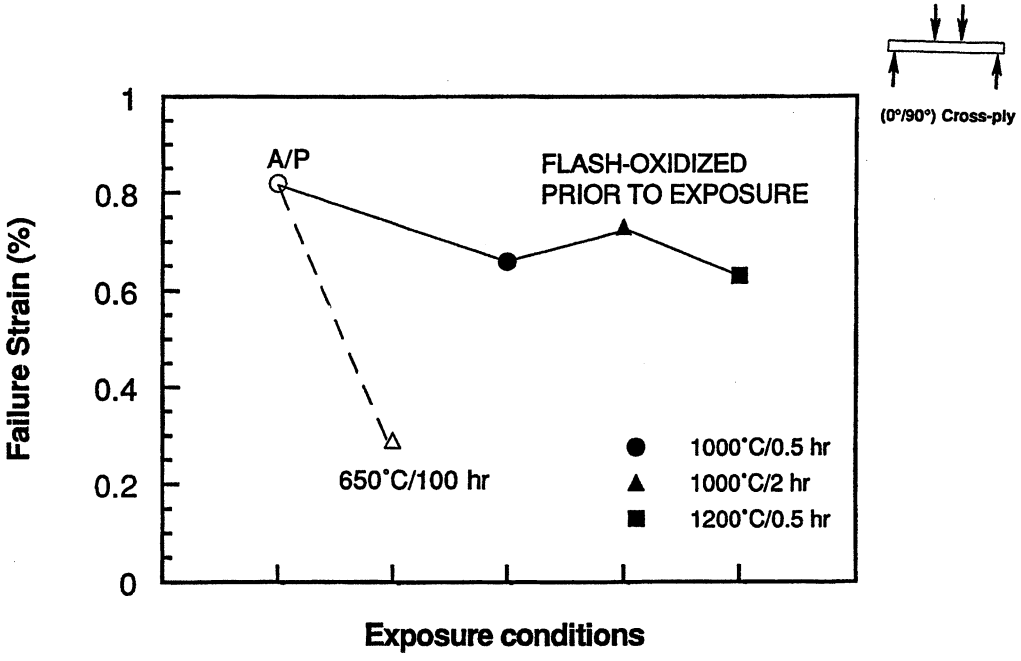

FIGURE 63(b). EFFECT OF FLASH SEALING ON FAILURE STRAIN OF Nicalon/5% BSG-MAS CMCs

The success of flash oxidation surface sealing as the most effective way to minimize intermediate temperature oxidation embrittlement suggests the mechanism to be viscous plugging of the carbon layer by the B_2O_3 present (shown by ESCA/XPS earlier in the program), and by viscous sealing by the BSG glaze coating that TEM thin foil investigation has shown to be matrix-side of the interface (as shown in Figure 60). Presumably, the viscous flow necessary for sealing is not operable at the low/intermediate temperatures in the 600°-700°C range. This idea implies that the degradation mechanism is pipeline oxidation from the machined edges of the bend bar, where the carbon interface is directly exposed to the environment in 90° plies of the laminate.

4.2.4.3 Elimination of Embrittlement by Hybridization

Nicalon/5% BSG-doped, 10% SiC_w hybrid CMCs, containing both BSG-doping and SiC whisker matrix toughening, were also subjected to the unstressed isothermal oxidation exposures at Pratt & Whitney. The results are shown in Figure 64. It is observed that the whisker-toughened hybrid CMC did not experience embrittlement at intermediate temperature. The problem is completely eliminated by the addition of whiskers to the CMC matrix. This correlates with the 1050°F TSR data discussed above (Figure 52, 54). The whisker-containing hybrid exhibited significantly increased lifetime under stress in the intermediate temperature tensile stress rupture tests.

Therefore, the TSR and unstressed oxidation data imply that inhibiting matrix microcracking by toughening the glass-ceramic matrix is a viable way of eliminating embrittlement phenomena. The fact that the hybrid CMC exhibited superior behavior at intermediate temperatures, where viscous plugging of the interfacial BSG phase is not operable, implies that microcracking is associated with the embrittlement of nonhybrid CMCs. Perhaps the tougher SiC_w-containing matrix of the hybrid prevents microcracking during machining of the bend bars, or otherwise inhibits the progression of microcracking that may be occurring during the exposures.

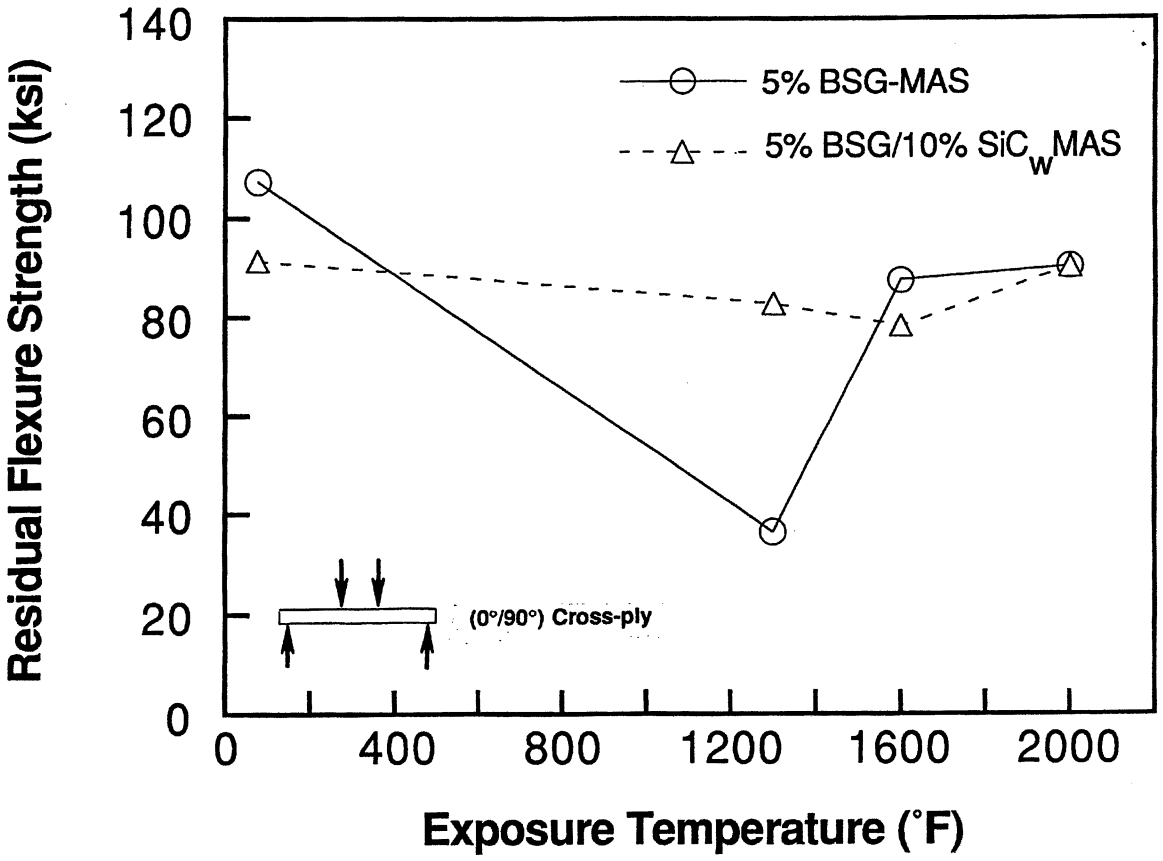

FIGURE 64. 100 HOUR ISOTHERMAL OXIDATION EXPOSURES FOR HYBRID AND NON-HYBRID CMCs

4.2.5 Summary of Task 2 Activities

Thermal durability of the CMCs being developed on this program was successfully assessed by tensile stress-rupture and unstressed isothermal oxidation exposures. This was accomplished in a way that permitted mechanisms of behavior to be inferred.

An optimized 5% BSG doping level was found to result in increased life under stress in high temperature TSR testing. Additionally, intermediate temperature embrittlement was shown to be controlled by a high temperature flash oxidation treatment. Both effects can be explained by the presence of B_2O_3 or BN modification of the carbon-rich interface, or by the presence of a protective borosilicate glass glaze coating matrix-side of the carbon layer. BSG-doping had little or no effect at intermediate temperatures, apparently having a viscosity too high for sealing or plugging.

SiC_w matrix toughening had no effect at high temperature, but was demonstrated to increase lifetimes under stress at intermediate temperatures, and to completely eliminate unstressed intermediate temperature embrittlement. Reduction in the creation of or propagation of microcracks in the glass-ceramic matrix was speculated as the operable mechanism.

4.3 Mechanical Property Assessment (Task 3)

It had been hoped that Task 2 work would permit a downselect to the best single CMC system to pursue in Task 3, which originally had a scope of the generation of a preliminary materials property data base on the downselected CMC. However, both hybrid and nonhybrid CMCs were demonstrated to be beneficial in Task 2 thermal durability studies.

Task 3 was therefore restructured to entail an expanded thermal durability assessment, and measurement of properties such as shear strength and tensile creep that might serve to differentiate hybrid and nonhybrid CMCs. The expanded thermal durability assessment involved notch sensitivity, fatigue, and burner rig testing of 5% BSG-doped MAS CMCs, in both hybrid

and nonhybrid forms. The cyclic mechanical fatigue behavior of these materials is considered by both Pratt & Whitney and the Air Force as the most definitive test of resistance to oxidation embrittlement, and hence thermal durability. Thus, the aim of this further testing, emphasizing long term environmental performance, was to more definitively and comprehensively study their thermal durability.

4.3.1 In-Plane Shear Properties

One of the potential advantages of SiC whisker addition to glass-ceramic matrices of continuous fiber composites was thought to be increased in-plane shear strength. In-plane shear strength, and especially in-plane shear modulus, are matrix-dominated properties for continuous fiber composites, and the employment of a toughened matrix might enhance such off-axis properties, based on the major increase in strength and toughness demonstrated by whisker-only composites.

Accordingly, Pratt & Whitney conducted room and elevated temperature in-plane shear strength measurements on Nicalon/5% BSG-MAS CMCs using the ± 45° tensile coupon. The shear strength results for hybrid and nonhybrid CMCs are presented in Figure 65. It is observed that a 40-50% increase in in-plane shear strength is realized by the whisker-toughened 5% BSG-MAS hybrid throughout the RT-2200°F temperature range. The room temperature shear modulus is shown to increase 34% by SiC_w additions to the CMC matrix. This then provides a possible advantage needed for certain shear critical components.

4.3.2 Tensile Creep Behavior

Tensile creep tests were performed for the Nicalon/5% BSG-MAS CMCs and their SiC whisker toughened hybrids by Pratt & Whitney. Tests were conducted on (0°/90°) cross-ply composites at 2000°F under an applied tensile stress of 15 ksi, in air atmosphere. The results for hybrid and nonhybrid composites are provided in Figure 66. It is observed that the total creep strain after 200 hr was only about 0.5% for the nonhybrid, and only about 0.25% for the hybrid. Note the pronounced lessening of Stage I creep for the hybrid. Both forms of Nicalon reinforced

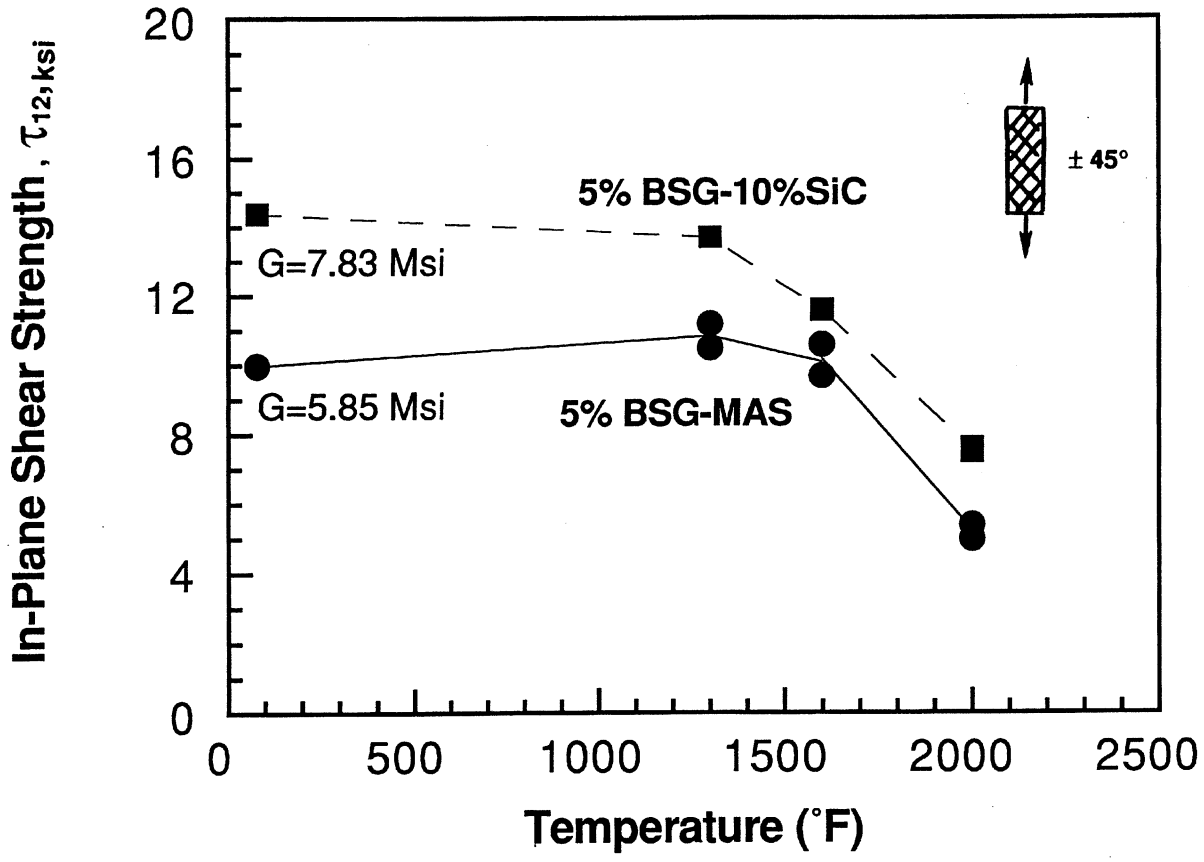

FIGURE 65. IN-PLANE SHEAR STRENGTH OF BSG-DOPED HYBRID AND NON-HYBRID CMCs

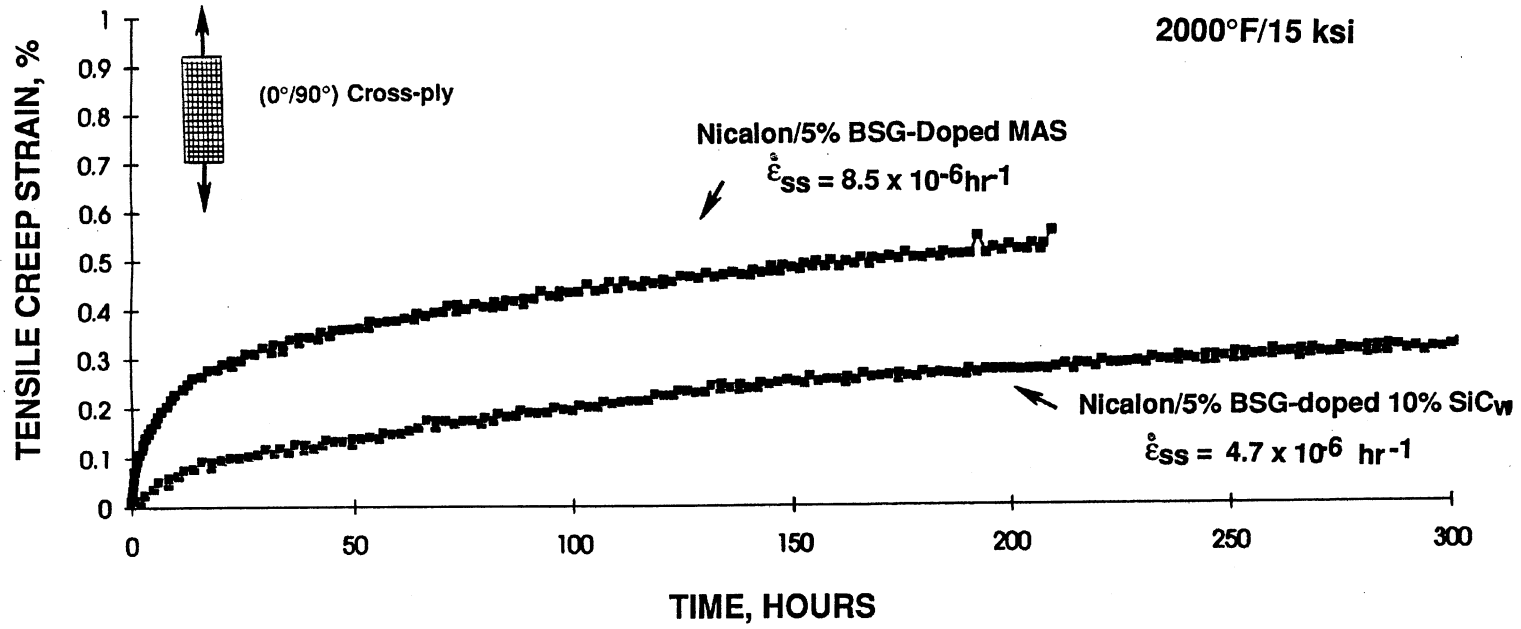

FIGURE 66. TENSILE CREEP BEHAVIOR OF BSG-DOPED MAS CORDIERITE HYBRID AND NON-HYBRID CMCs

composite exhibited very low creep rates, although secondary creep was never attained in the 200-300 hr tests. Both CMCs exhibited creep rates in the 10^{-6} hr^{-1} range, with the hybrid having an exceptionally low steady-state creep rate, 4.7 x 10^{-6} hr^{-1}. This correlates with the excellent stability of SiC whiskers in the cordierite matrix (i.e., no boundary silica is formed at the SiC-cordierite interface).

It is noted with interest that this level of creep resistance is superior to that of nickel base superalloys, the class of materials that CMCs intend to replace. These creep data again confirm the viability of BSG-doped MAS cordierite glass-ceramics as extremely refractory ceramic matrices, and that they produce thermally durable CMCs with sufficiently high usable strength and deformation resistance at elevated temperature for thermostructural applications as envisioned.

4.3.3 Notch Sensitivity

Centerhole tensile testing was conducted (by Pratt & Whitney) at 75°, 1050°, and 2000°F to assess the capability of the BSG-doped MAS matrix composites in a simulated attachment condition. These data provide much information, namely: determination of notch sensitivity for both hybrid and nonhybrid CMC; the effect of broken fibers on the elevated temperature mechanical properties; and a baseline database for cyclic mechanical fatigue behavior.

The samples tested (i.e., both hybrid and nonhybrid) were of 12-ply [0°/90°] cross-ply laminate construction. Straight-sided tensile sample were used, with a width of nominally 0.5-inch. The centerhole had a diameter of 0.1-inch, thereby reducing the load bearing area of the specimen by 20%. Samples were tested in static tension to failure, with the data compared to that from unnotched samples with no centerhole. Calculated stresses for the centerhole samples were based on the load bearing area (i.e., net section strength).

The tensile strength of both unnotched and centerhole samples of both hybrid and nonhybrid CMCs is presented in Figure 67, where the test temperature extended from room temperature to 2000°F, in air atmosphere. The [5/0] notation refers to the Nicalon/ 5% BSG-MAS CMC, and the [5/10] notation refers to the same material hybridized by the addition of 10% SiC whiskers to the MAS cordierite matrix. Open symbols in Figure 67 refer to unnotched specimens, whereas

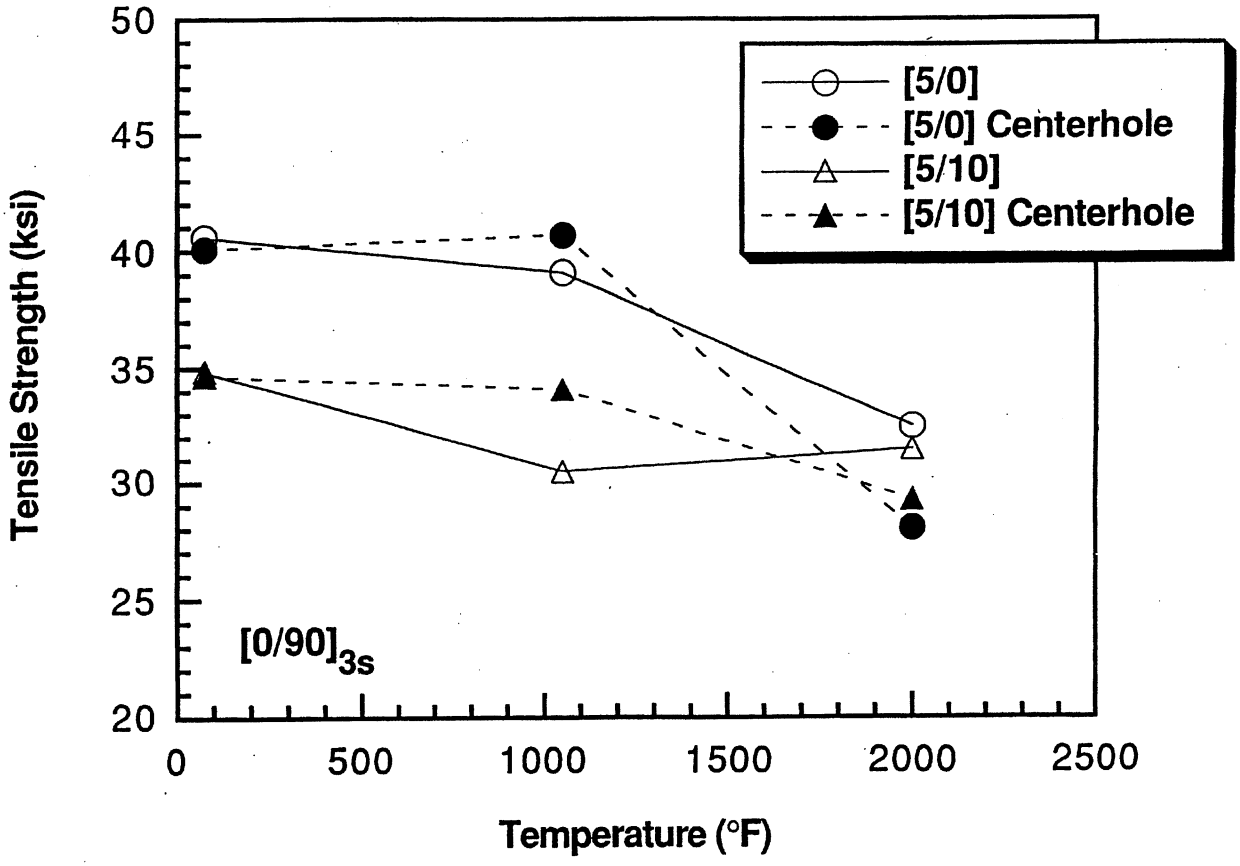

FIGURE 67. EFFECT OF MACHINED CENTERHOLE ON THE UTS OF Nicalon/5% BSG HYBRID AND NON-HYBRID CMCs

closed symbols refer to the behavior of centerhole notched samples. It is observed that at room temperature, both CMCs are notch insensitive; roughly the same UTS was obtained for both notched and unnotched samples. This agrees with data previously obtained for Nicalon/CAS CMCs, where this was attributed to stress redistribution resulting from the extensive matrix microcracking involved in the fracture of ceramic matrix composites, at least those with fully dense glass-ceramic matrices[4]. Interestingly, it is noted that centerhole samples for both hybrid and nonhybrid Nicalon/5% BSG-MAS cordierite CMCs were slightly higher in strength at 1050°F, and lower in strength at 2000°F than their unnotched companion samples. The opposite trend would be expected from the standpoint of oxygen embrittlement, and more such experimental investigation would be required to understand such phenomena.

These data demonstrate that both materials exhibit no notch sensitivity when compared to the smooth (without centerhole) tensile data. This suggests that no knockdown factors would need to be employed in designing for attachment regions of a component fabricated with these CMCs, where tensile limits are the design criteria.

The data revealed that the 5% BSG/10% SiC_w matrix-toughened hybrid CMC does not exhibit a benefit over the nonhybrid 5% BSG-doped MAS matrix composite in fast fracture tensile tests. As was previously demonstrated in unnotched (smooth) tensile data, the strain to failure for the SiC-whisker containing hybrid CMC is significantly lower, the elastic modulus and proportional limit are equivalent when compared to the nonhybrid CMC. This is shown in Figure 68.

4.3.4 High Cycle Fatigue Behavior

Smooth and notched cyclic mechanical fatigue testing was conducted (by Pratt & Whitney) at the same temperatures (75°, 1050°, and 2000°F) as the baseline tensile testing to determine the endurance limit (10^5 cycles), and to generate S-N curves (stress versus cycles). These data provide an assessment of the fatigue capabilities in smooth and notched (attachment) locations for a component fabricated with these CMCs (hybrid and nonhybrid).

The fatigue results for the unnotched nonhybrid (i.e., the basic fatigue data for the Nicalon/BSG-MAS CMC) are presented in Figure 69. The behavior at room temperature shows a classic S-N curve. Evans, et al [5,6], discuss how this is caused by the dominant fatigue
mechanism of interfacial wear. The opening and closing of matrix cracks results in the fiber/matrix interfaces debonding and sliding as the matrix cracks cycle, which is manifest as hysteresis loops. The understanding of the hysteresis behavior is central to the modeling and prediction of fatigue. The mechanism relates to how the interfacial sliding stress changes in

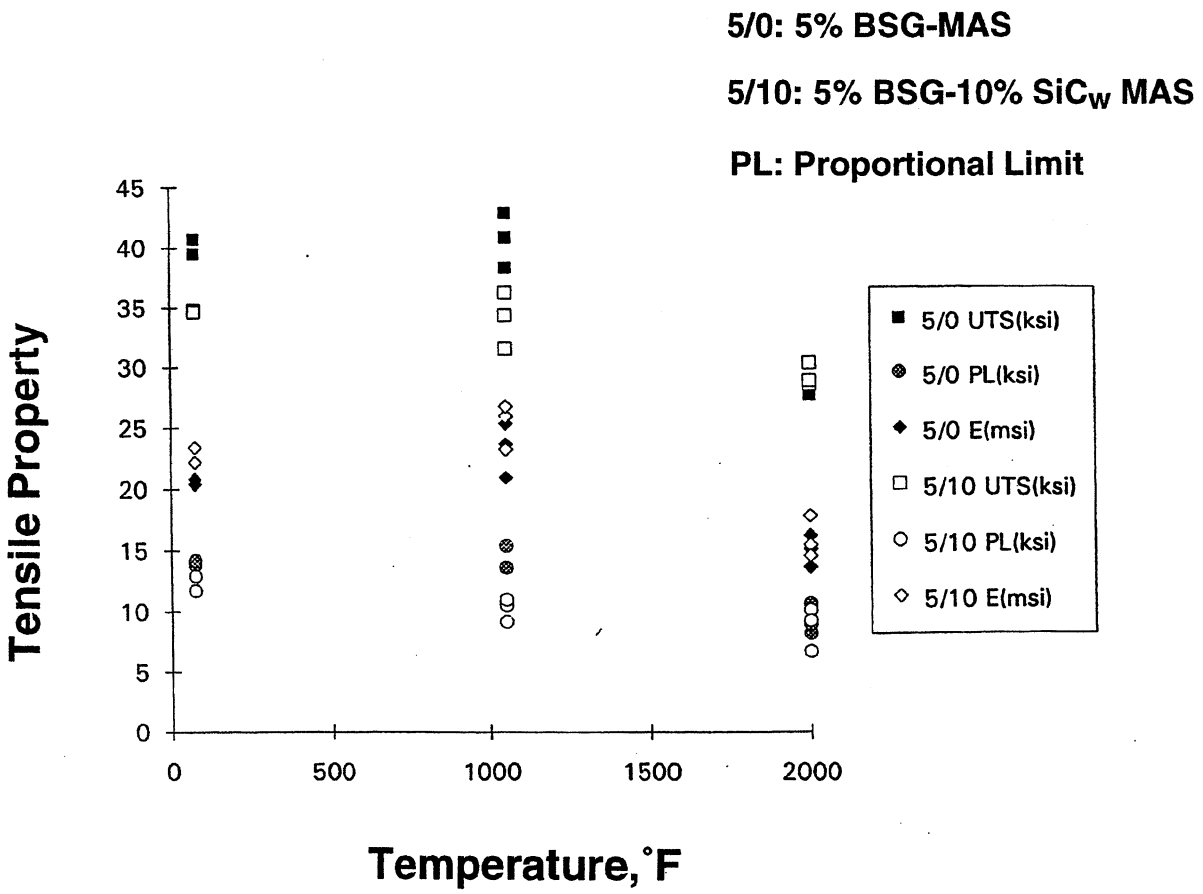

FIGURE 68. **CENTERHOLE TENSION TESTING OF Nicalon/5% BSG-MAS CMCs**

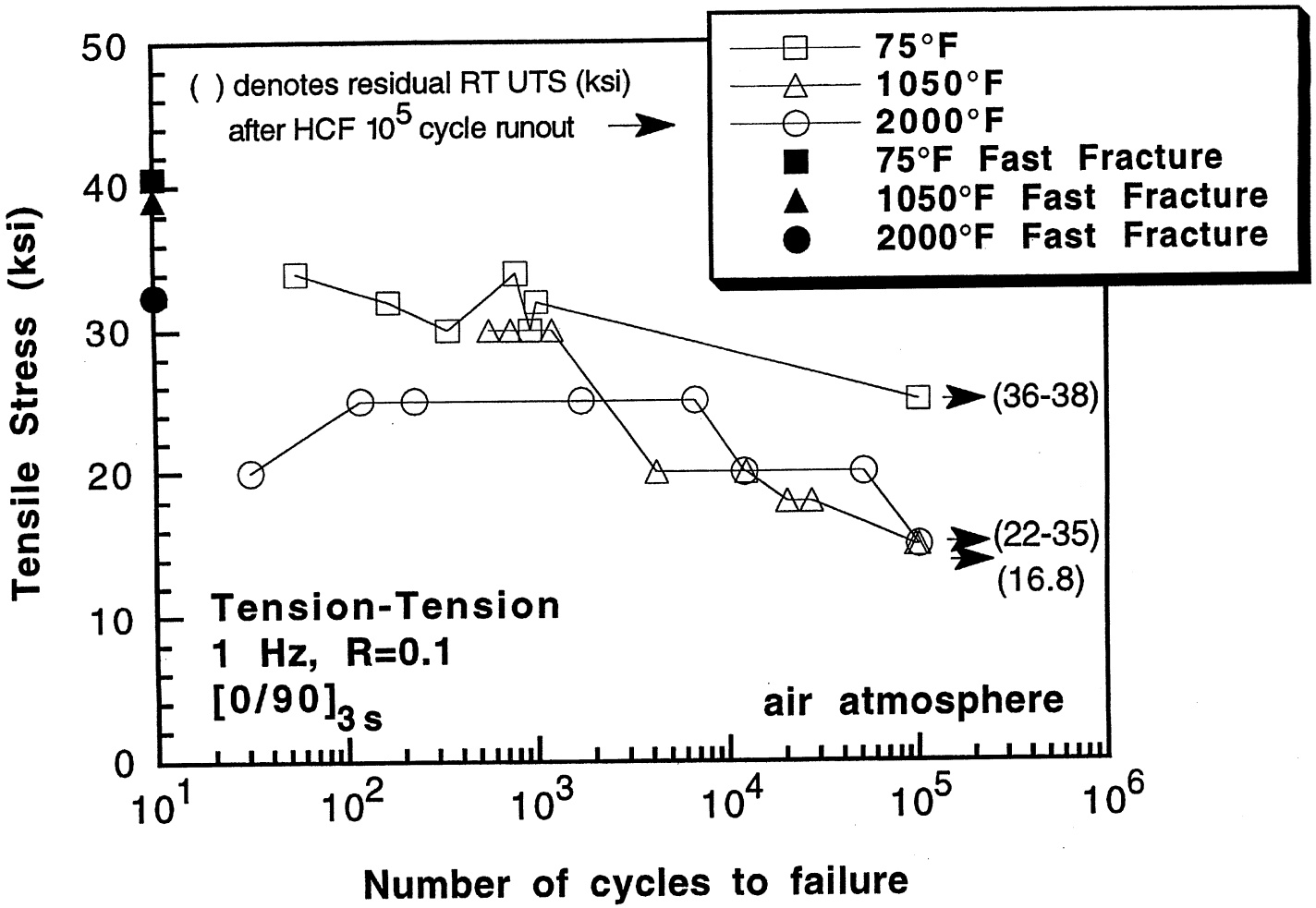

FIGURE 69. CYCLIC MECHANICAL FATIGUE DATA FOR Nicalon/5% BSG-MAS CORDIERITE

response to the cyclic opening and closing of the matrix cracks. The sliding stress diminishes upon cycling. As this occurs, the inelastic strain and the ultimate tensile strength (UTS) are affected, argue Evans, et al. The inelastic strain increases, because the interface sliding distances increase leading to both a reduction in the secant modulus and a permanent strain. Conversely, the UTS decreases, leading to enhanced fiber bundle failure and S-N behavior. Note in Figure 69 that at room temperature, the fatigue threshold is significantly greater than the proportional limit (matrix cracking stress). This is in agreement with the experience of Evans, et al.

Note in Figure 69, that at high temperature, the degradation is significantly greater as the mechanical cycling proceeds. This is consistent with a superimposed mechanism of oxidation embrittlement. Figure 70 presents a Pratt & Whitney analysis of the fatigue data for the Nicalon/5% BSG-MAS CMC at 1050°F, showing both mean data, as well as a 95% confidence interval model developed to describe fatigue statistics for materials. Figure 71 presents the fatigue data for the 5% BSG-10% SiC whisker hybrid matrix CMC. The data show the same trends of degradation as in Figure 69. Contrary to the unstressed isothermal oxidation and tensile stress rupture results discussed above, the SiC_w matrix-toughened hybrid is apparently not a more thermally durable CMC under cyclic loading conditions. The fatigue data for the centerhole notched samples for both CMCs are provided in Figures 72 and 73, respectively.

The fatigue data presented here suggest that there is no benefit to the whisker containing hybrid CMC, since the endurance limits for both materials were nearly the same at all temperatures; being about 60% of the ultimate stress at 75°F, and 50% of the ultimate stress at 1050° and 2000°F. However, the data suggest that there is no notch sensitivity associated with a hole, since the endurance limits were equivalent for both material systems in the notched and smooth conditions.

The fatigue data do tend to suggest, however, that these CMCs can be used above the proportional limit. This is shown in Figures 69-71, where it is demonstrated that 10^5 cycle runout is obtained, at both intermediate as well as at high temperature, at tensile stresses of nominally 15 ksi. This stress level is greater than the proportional limit for either nonhybrid or hybrid CMC (refer to Table 1). This demonstrated long term/high stress life of the BSG-doped CMCs developed on this program clearly shows the high degree of thermal durability achieved by these materials.

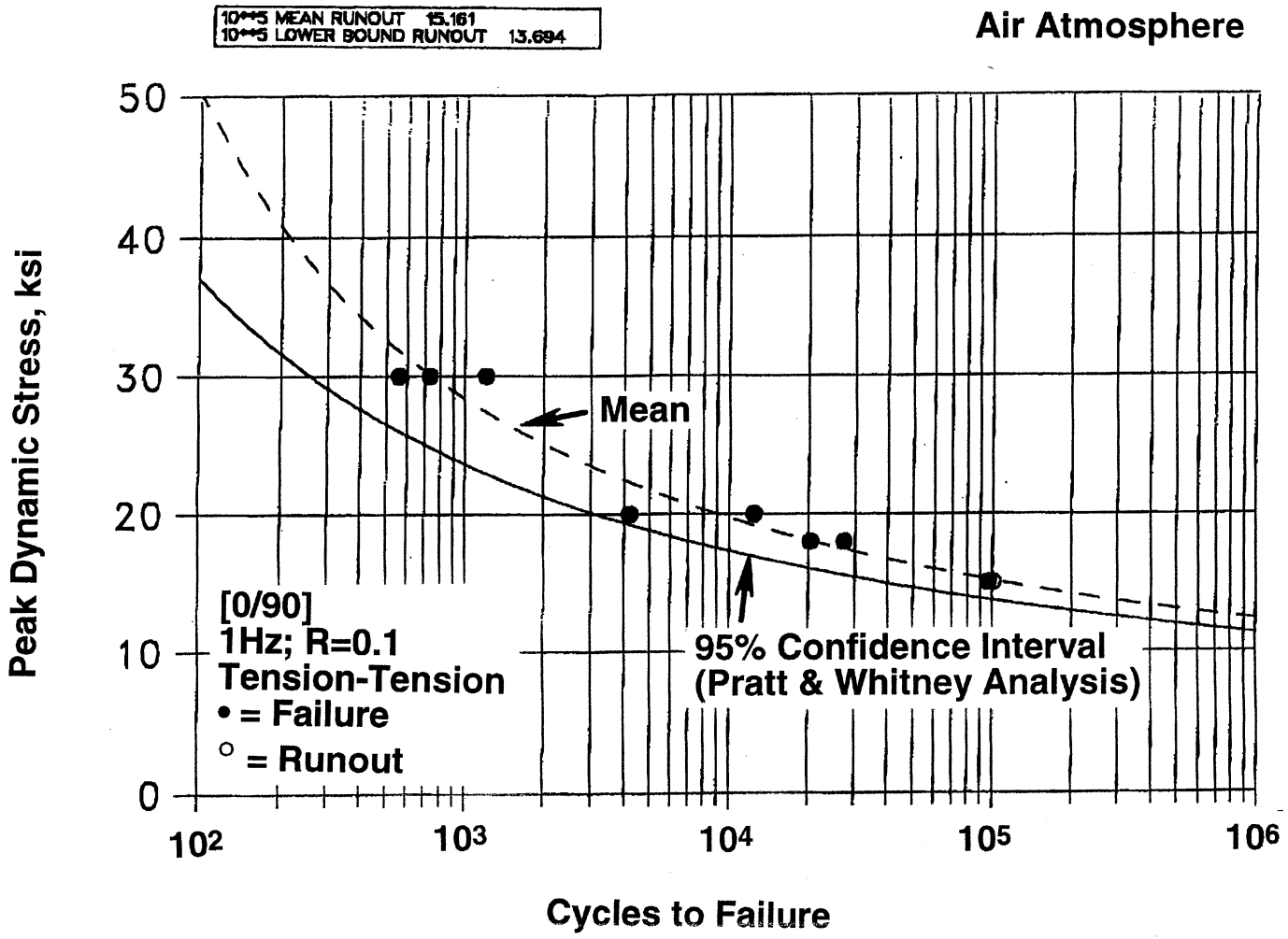

FIGURE 70. STATISTICALLY ANALYZED TENSILE FATIGUE DATA FOR Nicalon/5% BSG-MAS AT 1050°F

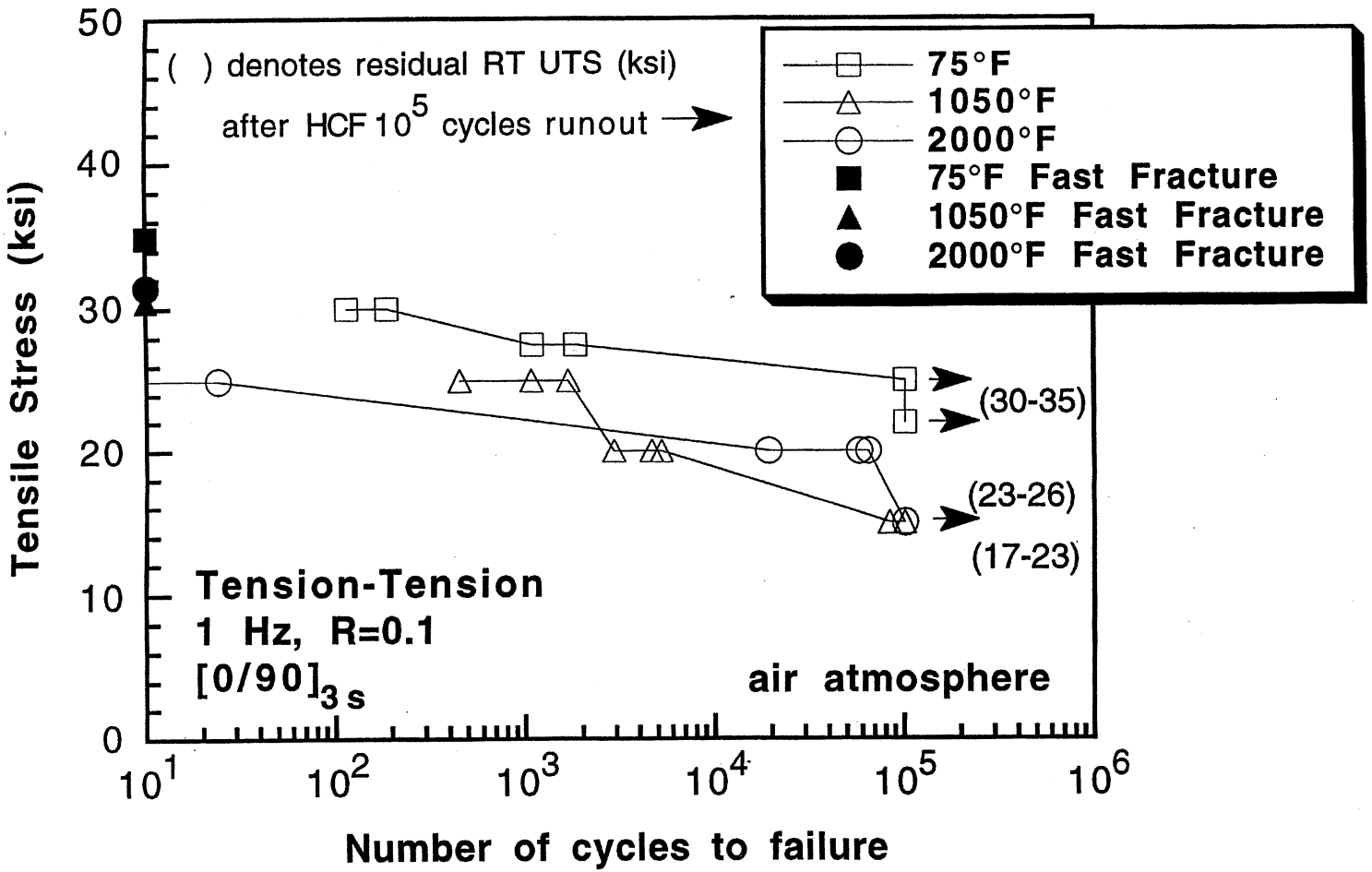

FIGURE 71. CYCLIC MECHANICAL FATIGUE DATA FOR Nicalon/5% BSG/10% SiC_w-MAS HYBRID

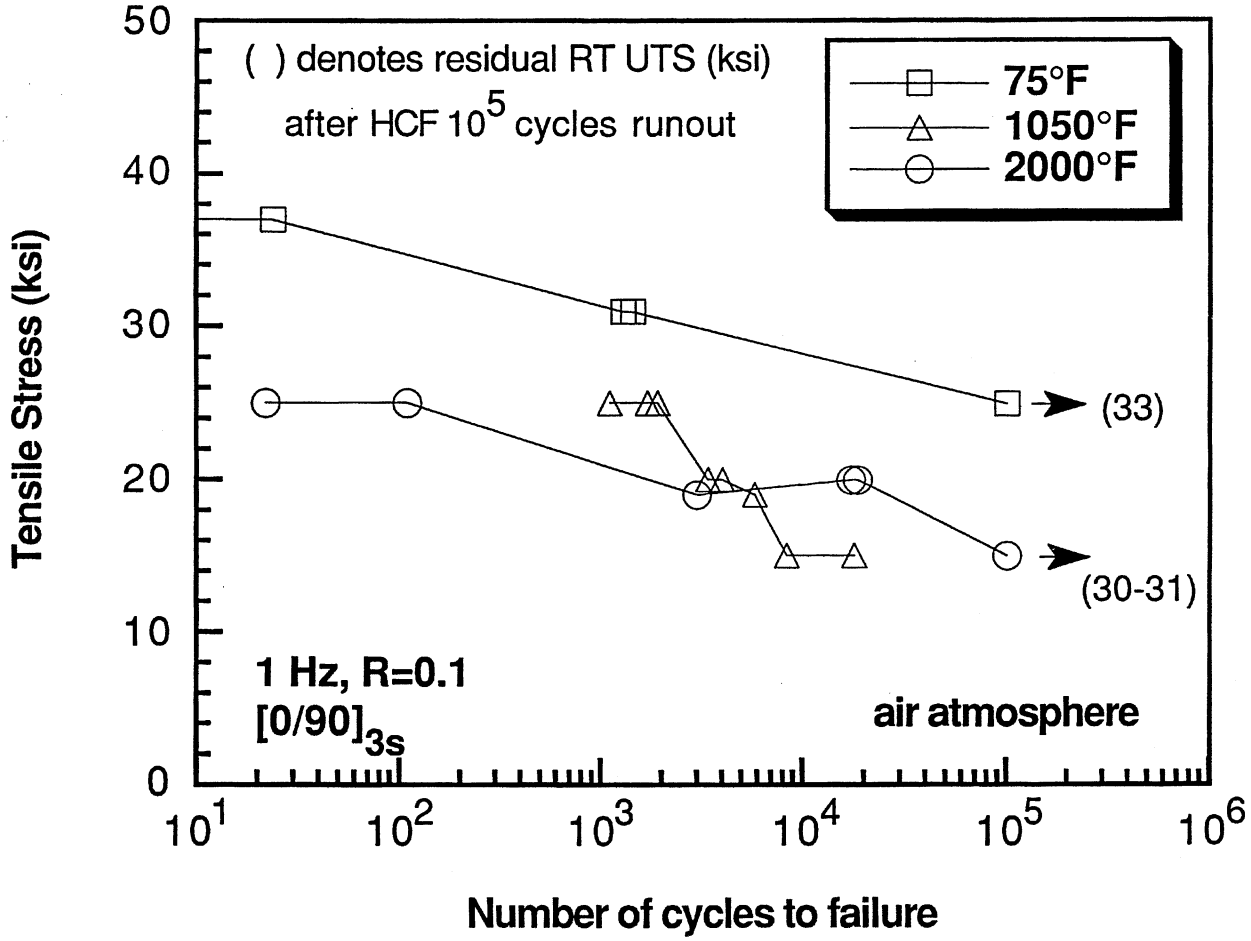

FIGURE 72. CENTERHOLE TENSION-TENSION FATIGUE DATA FOR Nicalon/5% BSG-MAS CORDIERITE

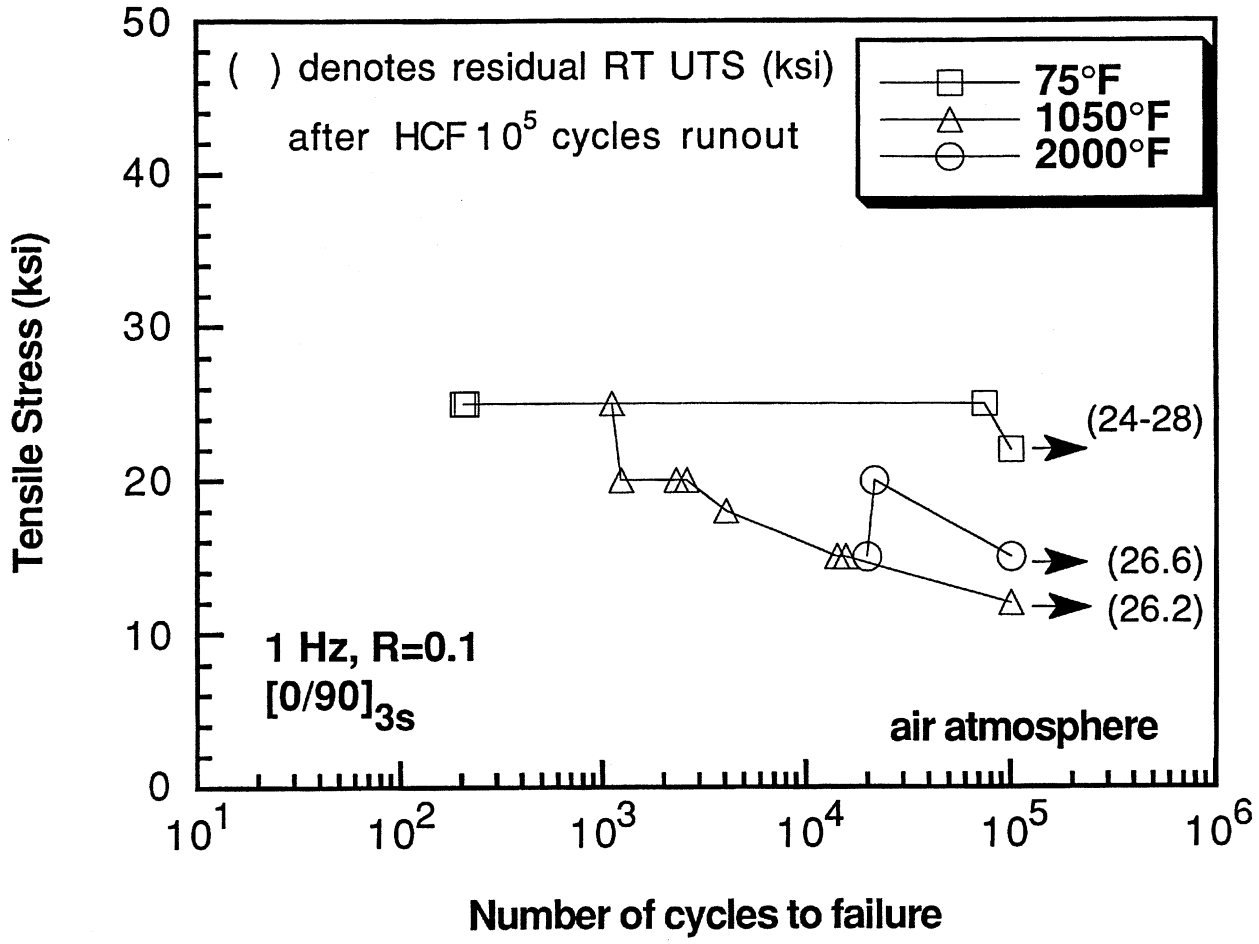

FIGURE 73. CENTERHOLE TENSION-TENSION FATIGUE DATA FOR Nicalon/5% BSG-10% SiC_w-MAS HYBRID

4.3.5 Burner Rig Testing

Burner rig testing is employed by Pratt & Whitney to determine the susceptibility of candidate materials to thermal gradients, thermal transients, and jet fuel chemical attack, which may be present during use in the jet engine environment. The burner rig test involves placing a 4x4x0.1-inch sample in front of a Dil's burner rig. This burner uses Jet A fuel, which is commonly used in Pratt & Whitney commercial engines. The specimen is cycled in and out of the impingement flame, spending 50 seconds in the flame, and 10 seconds cooling. This cycle is repeated 6000 times. Following this exposure, room temperature flexure specimens are machined and tested from various locations in the panel. Past experience with other CMCs has been that specimens taken from the gripping ends of the panel typically exhibit full strength retention; whereas, specimens from the center of exposed panels often exhibit half their initial strength, and low failure strain (brittle behavior).

The Corning 5% BSG-doped MAS CMCs (nonhybrid) tested on this contract successfully completed this burner rig test, showing no mechanical property degradation, as shown in Figure 74. This burner rig exposure test provides much information on the effects of thermal gradients through the panel, thermal transients during the rapid heating cycles, and chemical attack from the Jet A fuel residue on the panel surface. None of these potential degradation mechanisms were evident in the 5% BSG-MAS CMCs tested, although the burner rig exposure does not provide data on the effects of simultaneous mechanical loading, which will be present in the actual engine environment.

The results are not so clear, however, for the matrix-toughened SiC whisker hybrid version of the BSG-doped MAS matrix CMC. Figures 75 and 76 show that the post-burner rig exposure strength, in particular, was low for this CMC, at least in comparison to that shown in Figure 74 for the nonhybrid version of the CMC. However, Pratt & Whitney reports that they are not clear as to whether the hybrid did degrade during the exposure, since a definitive baseline strength for that composition was not established due to plate-to-plate variations in the properties.

4.4 Summary: BSG-Doped MAS CMCs

Oxidation embrittlement consists of the sequential events of matrix microcracking under load, followed by rapid oxidation of carbon-rich fiber-matrix interfacial regions, resulting in increased bonding of the fiber to the matrix and loss of composite strength, toughness, and strain tolerance.

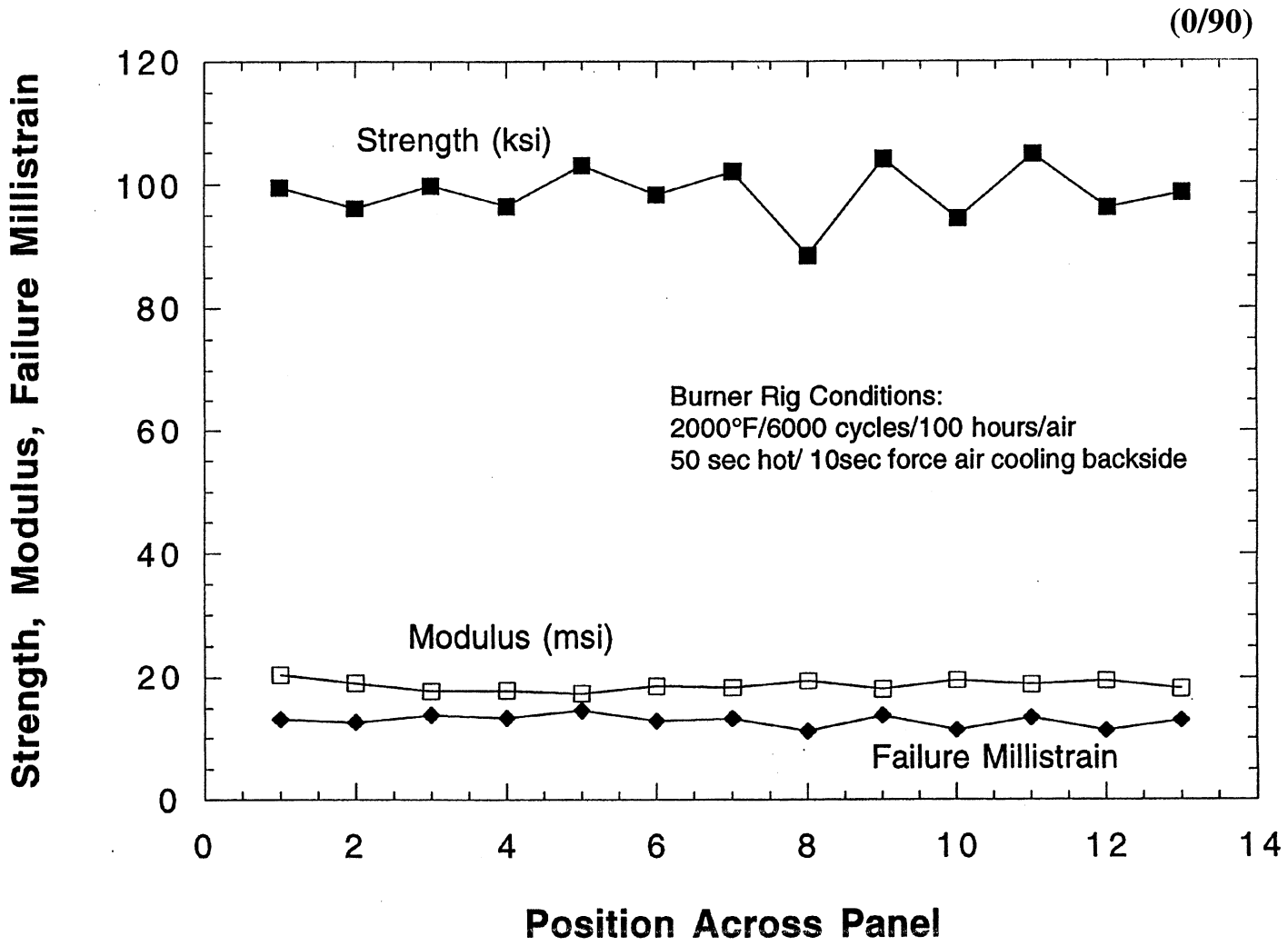

FIGURE 74. RETAINED FLEXURE PROPERTIES FOLLOWING BURNER RIG EXPOSURE FOR 5% BSG-MAS CMC

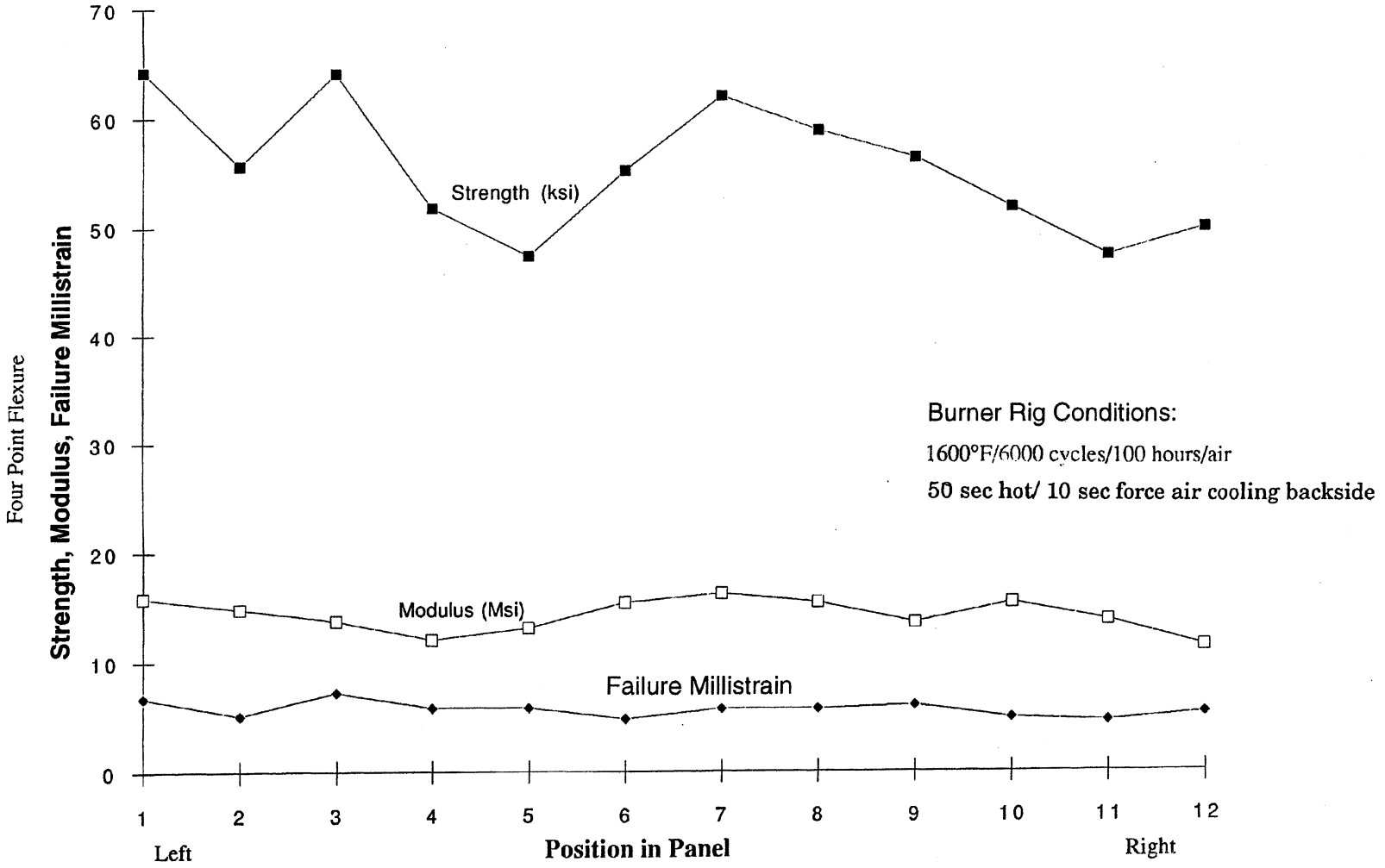

FIGURE 75. RETAINED FLEXURE PROPERTIES FOLLOWING BURNER RIG EXPOSURE FOR 5% BSG-10% SiC_w HYBRID (0/90)

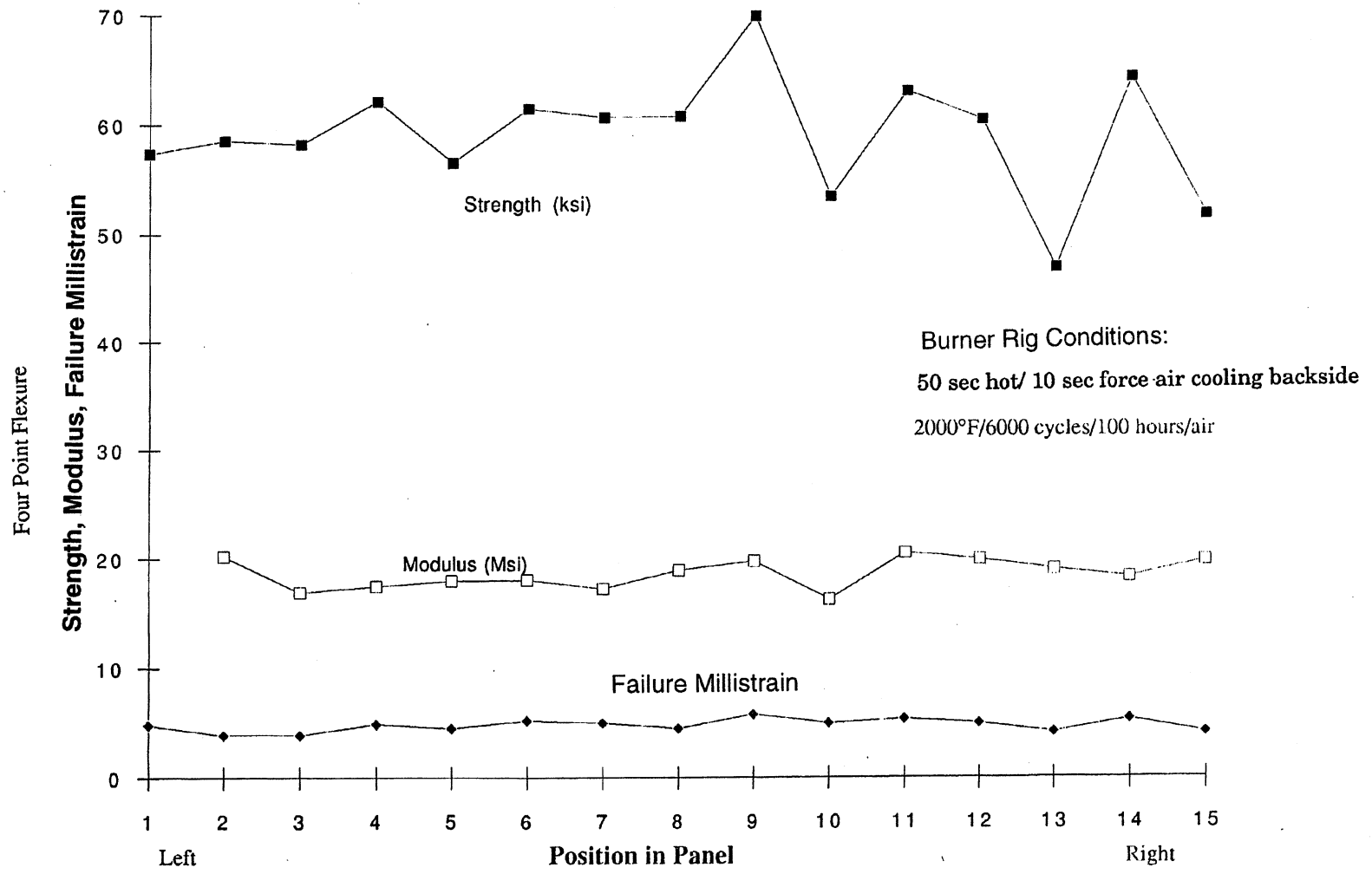

FIGURE 76. RETAINED FLEXURE PROPERTIES FOLLOWING BURNER RIG EXPOSURE FOR 5% BSG-10% SiC_w HYBRID (0/90)

It was demonstrated on this program that the microstructure of an MAS glass-ceramic CMC can be altered by BSG-doping and SiC-whisker additions to manage this problem. This was accomplished both by affecting the way damage accumulates in the matrix in response to mechanical loading, as well as by providing increased levels of interfacial oxidative stability.

The BSG dopant in the MAS cordierite matrix serves as a source of boron, which diffuses to the interface during composite hot consolidation. At the fiber-matrix interface, boron combines with oxygen and nitrogen to form B_2O_3 and BN phases which increase the oxidation resistance of the carbon-rich interface. Additionally, a matrix-side borosilicate glass film further protects the modified carbon interface. These effects of boron provide for increased oxidative stability.

Boron doping also affects the mechanical performance of the composite. A thinner interface develops, but remains mechanically functional as a debond layer in the microstructure. The interfacial shear resistance and debond strength are apparently increased since matrix microcracking is suppressed upon mechanical loading, as evidenced by tensile stress-strain behavior with reduced strain accumulation and increased elastic limit. Thus, BSG-doping reduces matrix microcracking, thereby minimizing the creation of pathways for oxygen ingress to the interface. The physical addition of SiC-whiskers to the MAS matrix strengthens and toughens the matrix, and thus also reduces matrix microcracking in response to externally applied stress.

This ability to alter the manner in which damage accumulates and to increase the oxidative stability of interfacial regions resulted in enhanced thermostructural performance for these CMCs. This was demonstrated in tensile stress rupture testing at intermediate (1050°F) and elevated (2200°F) temperatures in air atmosphere, where it was shown that these CMCs have significant life, hundreds of hours, at stresses well above the material elastic limit. Such TSR behavior is a prime indicator of thermostructural performance.

At room temperature, both BSG-doping and SiC-whisker addition, acting individually, increased the composite elastic limit by inhibiting matrix microcracking. The former had the stronger influence, affecting the interfacial shear resistance, which is related to the interfacial fracture

energy and its control of debonding and frictional sliding at the interface. At intermediate temperatures, 1050°F, SiC-whisker matrix toughening had the strongest influence on mechanical behavior. Increased lifetimes at high stresses in TSR testing, as well as elimination of unstressed oxidation embrittlement, both suggest decreased matrix microcracking for SiC-whisker toughened CMCs. BSG-doping had no influence on mechanical performance at intermediate temperatures.

At high temperature (2000°F), however, SiC-whisker addition had no influence, and BSG doping dominated composite behavior. Protection is provided primarily by a thin borosilicate glass coating matrix-side of the interface, which also explains why flash oxidation treatments eliminated unstressed intermediate temperature oxidation embrittlement as well. The enhanced thermal durability that results from 5% BSG doping far outweighs the associated slight loss of refractoriness. The MAS matrix exhibited excellent thermal stability in extend 5000 hour environmental exposures.

Therefore, there appears to be a synergistic effect of using SiC-whisker and BSG-dopants simultaneously. Reduced microcracking occurs at intermediate temperatures, and a plugging/blunting mechanism is operable at high temperature to protect the functional carbon layer from oxidation. Both additives are needed for enhanced thermal durability over the entire temperature range. Additionally, these CMCs exhibit increased in-plane shear strength, low creep rates, and an absence of notch sensitivity. High cycle fatigue and tensile stress rupture data indicate that they can be used above the composite proportional limit, which constitutes a serviceable definition of the achievement of thermal durability.

The performance of Nicalon/BSG-doped MAS cordierite CMCs, and their SiC-whisker matrix-toughened hybrid variants, has demonstrated the viability of the concept of using physical additives and chemical dopants to modify the composite microstructure to manage the oxidation embrittlement problem in carbon-interface CMCs, providing greatly enhanced thermal durability.

5.0 Mica-Interface CMCs

The second major class of materials investigated on this program incorporates a fully dense, oxidation resistant sheet-silicate (mica) interface to replace carbon and boron nitride. Carbon interfaces, either formed in situ or applied as a fiber coating, are not resistant to oxidation, as discussed in the previous section. BN fiber coatings are an improvement, but also have not been completely free of oxidation embrittlement, and are currently produced by expensive CVD methods.

Sheet silicate (mica) interfaces were investigated on this program. The thrust of this concept is that the weak interfacial bonding necessary in a brittle matrix composite for crack debonding and frictional sliding leading to good fiber pullout and CMC toughness and strain tolerance be achieved by cleavage-dominated fracture of the micaceous glass-ceramic interface. Mica has the advantage of being an oxide, and thus inherently oxidation resistant. It can also be applied as a cost effective (non-CVD) solution coating.

The basic concept is that mica, a fully dense silicate glass-ceramic, is a layered sheet structure that is very strong in the a-b directions parallel to the layering planes, but having a c-direction cleavage strength ranging from weak to strong, being controlled by the ionic charge of the interlayer cation of the structural layers. Several alkali and alkaline earth cations have been successfully synthesized in such fluoromicas. The interest in this micaceous interface for CMCs is that (1) it is weakly bonded parallel to the fiber, (2) it is an oxide, and (3) the desired interfacial shear strength and toughness can be chemically designed into the CMC system early in its overall fabrication. Therefore, this concept offers the potential for engineered interfaces for CMCs that are not only mechanically functional, but that do not suffer from oxidation embrittlement.

5.1 Process Description

A schematic view of the basic sol-gel fiber coating process is provided in Figures 77 and 78 and Table 4. Desized fiber tows are drawn through the sol, which consists of a combination of reactants including metal alkoxides and ammonium fluoride in an acidified solvent system. The wet tow is then drawn through an air dryer at 80°C. The coating is then cured at 300°C to hydrolyze, remove solvent and to increase the inorganic character of the gel coating. This is sometimes followed by a 600°C thermal treatment to remove any remaining water and residual organics, and to complete the gelation process. The gel serves as the binder in the fiber coating process when particulate augmentation is employed.

The baseline process involves the application of two coatings in one pass (coat-dry-cure, repeat), and yields mica coatings of ~200 nm thickness. In general, coating thickness is controlled by solids content, pull rate, and number of passes. The baseline process may also be modified with the addition of crystalline mica flakes to increase the mica content and thickness of the coating. Such mica flakes are 3-5 μm in size in the baseline augmented sol-gel process, and are produced by vibratory milling of melt synthesized mica powder.

At this point in the coating process, the fiber coating is an inorganic gel. The coated tow is then prepregged into fiber mats, which are stacked and subsequently hot-pressed. The prepregging process involves impregnation of coated fiber tow with a slurry consisting of matrix glass particles in a thermoplastic binder. The use of the thermoplastic binder in the prepreg process accomplishes three things: (1) improved handleability of the prepregged fiber tow, (2) shaping of prepregged mats to produce articles of complex curved geometry, and (3) weaving and collimation to produce complex fiber architectures. After layup, the thermoplastic binder is burned out, prior to hot consolidation of the prepregged fiber mat.

It is important to recognize that the hot consolidation step of the process accomplishes three things: (1) consolidation of the glass-ceramic matrix to full density, (2) crystallization of the

Potassium Fluorophlogopite (KFP) – $KMg_3(AlSi_3O_{10})F_2$

Barium Disilicic Mica (BDM) – $BaMg_3(Al_2Si_2O_{10})F_2$

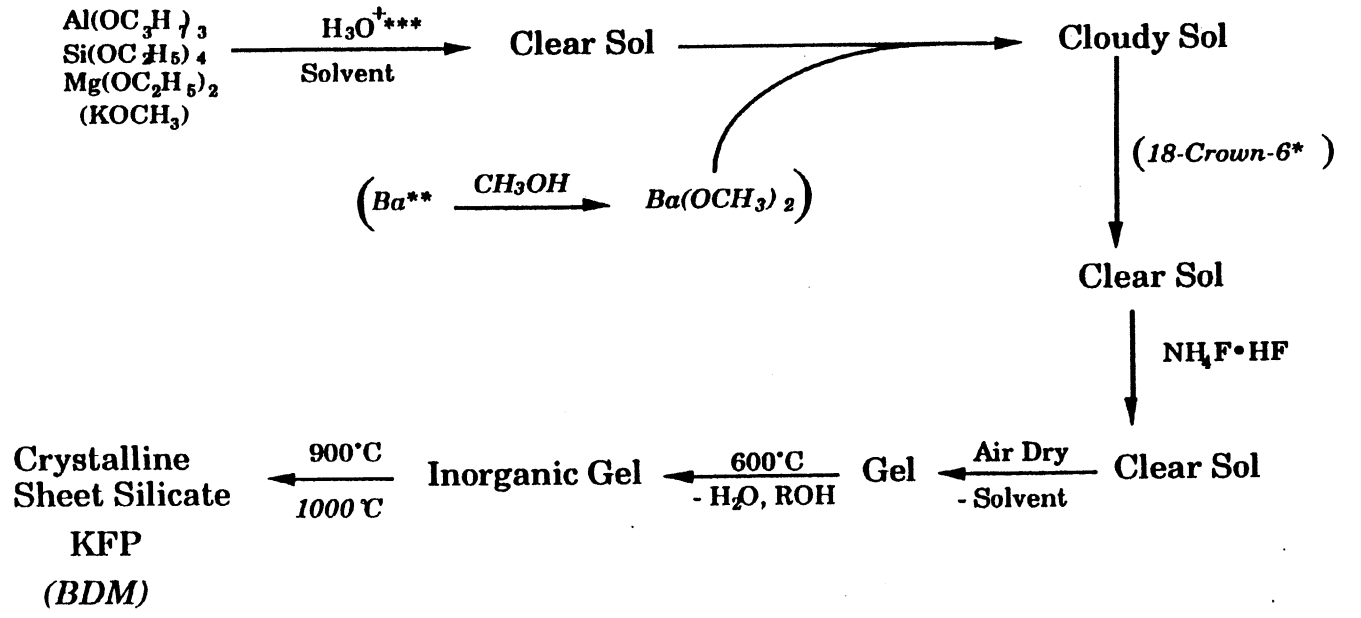

* - 18-Crown-6 is necessary to prevent precipitation of BaF_2 from Sol.
** - Addition of Ba to undissolved alkoxides results in formation of $BaAl_2Si_2O_8$, not BDM.
*** - Crystalline Morphology Varies With Acid Type. i,e, HCl and HNO_3

FIGURE 77. SOL-GEL SYNTHESIS OF SHEET SILICATES

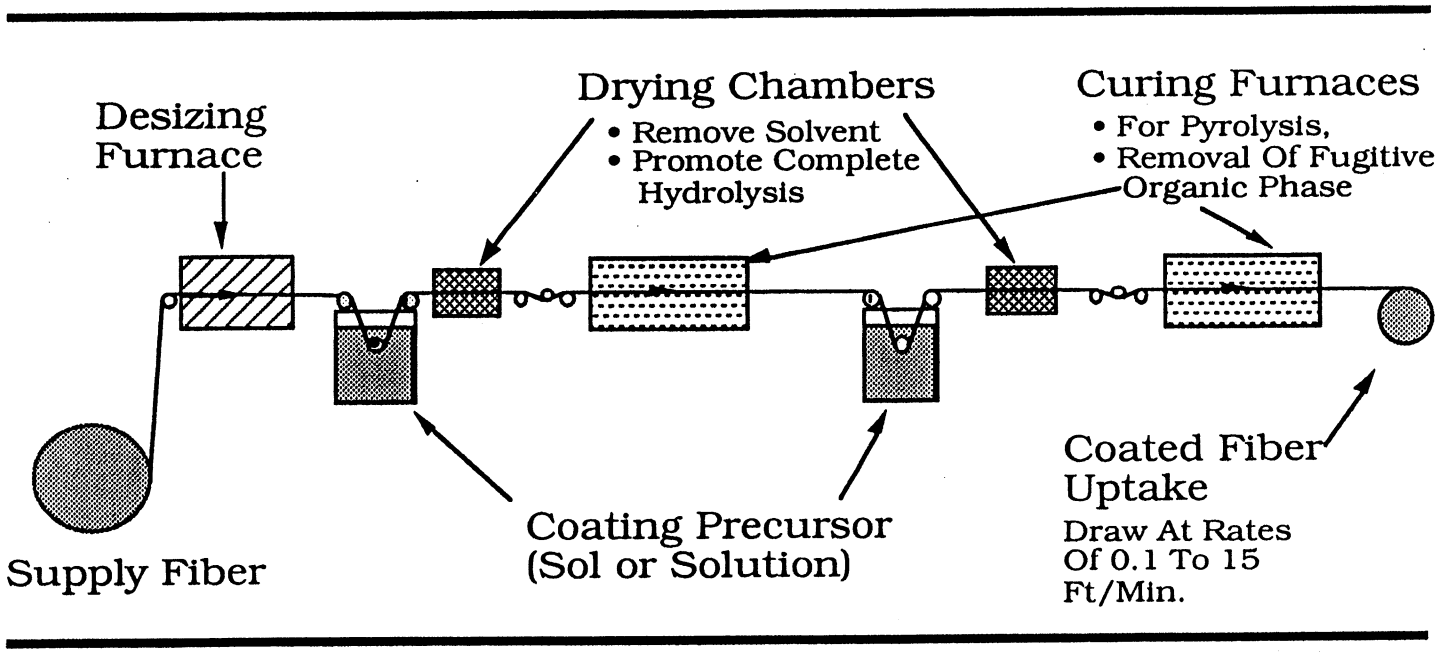

FIGURE 78. SCHEMATIC OF FIBER COATING PROCESS

Table 4
CMC PROCESSING OF SOL-GEL COATED FIBERS

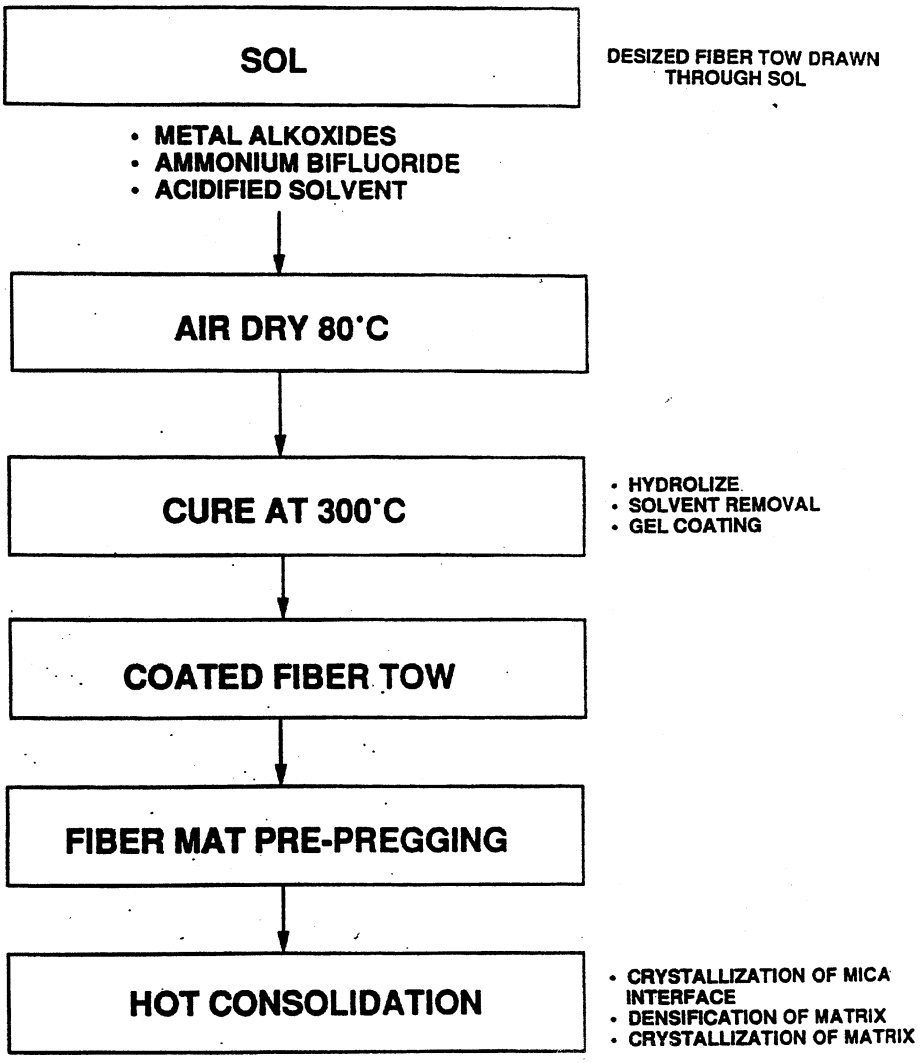

matrix to the desired phase assemblage, and (3) densification and crystallization of the mica fiber coating to the desired phase content and degree of crystallinity.

5.2 Critical Issues

Our previous work on ONR/DARPA Contract N00014-89-C-0164 established the fundamental technology of sheet-silicate interfaces, and defined the critical issues that guide the workscope for these materials on the present program. The overall objective is to create dense, uniform fiber coatings of the optimum phase content, crystallinity, and thickness.

Four critical issues were identified for mica interface CMCs: (1) minimization of mica-matrix reactivity during processing, (2) minimization of in situ carbon layer formation, (3) achievement of 100% mica phase content, and (4) development of sufficient coating thickness to promote crack debonding and provide fully functional mechanical behavior.

Minimizing mica-matrix reactivity is accomplished by selecting compatible mica and matrix constituents. Minimizing carbon layer formation when using Nicalon SiC fibers is accomplished by using low processing temperatures (900-1100°C) and eliminating matrix constituents that promote carbon layer formation (e.g., arsenic).

Achievement of 100% mica phase content and the development of sufficient coating thickness were shown to be the primary areas that need improvement to continue the development of thermally durable mica interface CMCs. The mica coating needs to be thicker and the mica flakes used in the powder augmented sol-gel process need to be smaller than achieved on Contract N00014-89-C-0164. When this is accomplished, the mica interface will be uniform, continuous, and of sufficient thickness to function as the debond layer in a ceramic matrix composite.

Therefore, the overall thrust of this work on sheet-silicate interface CMCs is to achieve a fully micaceous phase at the interface, with minimum in situ carbon formation, that is of sufficient

thickness to promote debonding and fiber pullout mechanisms resulting in good CMC mechanical properties. The following sections review all of Corning's relevant work in this area. Early work on this contract is discussed. Concurrent work on another Air Force program involving these CMCs is summarized. Final work on the present program is then presented, leading to identification of the most promising mica-interface CMCs. This path of investigation involves various combinations of mica composition, mica coating process steps, matrices used, and hot-consolidation process temperatures.

5.3 Initial Process Studies

Initial process studies involved choice of mica composition, fiber coating and prepregging processes to yield optimum mica fiber coatings. Table 5 presents the variety of mica types considered. Potassium fluorophlogopite (KFP) and barium disilicic mica (BDM) were the micas chosen for investigation. This was based on their refractoriness, and included two levels of interlayer bond strength.

The major thrust of early work was to develop process technologies to increase the mica layer thickness (to achieve an interfacial fracture energy low enough to facilitate the debond and pullout process necessary for high CMC strength and toughness). It was thought that a coating thickness of ~1μm would be needed. Initial attempts were made to accomplish this for barium disilicic (BDM) and potassium fluorophlogopite (KFP) sol-gel mica fiber coatings by increasing the solids content of the sol and adding melt synthesized mica particulates to the sol. The sol serves as a binder for the particulate, but high sol content promotes fiber bridging. The particulate (prepared by powdering a melt synthesized mica glass-ceramic) reduces bridging, but high particulate level leads to loss of coating (in the limit, a colloidal particulate coating). Therefore, the optimum combination of sol and particulate was sought.

(a) Thick Particulate Augmented Sol-Gel Mica Coatings:

Although (2s+12P)* sol + particulate mica coatings were >1 μm thick, as desired, interfaces in

---

* An internal designation referring to solids content and amount of particulate augmentation employed.

Table 5
SHEET-SILICATE COMPOSITIONS INVESTIGATED

	COMPOSITION	MINERAL NAME	INTERLAYER CATION CHARGE	MELTING POINT °C	CLEAVAGE STRENGTH
	$Mg_3(Si_4O_{10})F_2$	Fluorotalc	0	-	Weak Interlayer Bond
	$Al_2(Si_4O_{10})F_2$	Fluoropyrophillite	0	-	Weakly Bonded
	$KMg_{2.5}(Si_4O_{10})F_2$	Tetrasilicic Mica	+1	1176	Intermediate Interlayer bond
→	$KMg_3(AlSi_3O_{10})F_2$	Potassium Fluorophlogopite	+1	1387	Intermediate Bonding
	$BaMg_{2.5}(AlSi_3O_{10})F_2$	Barium Trisilicic Mica	+2	1344	Strong Interlayer bond
→	$BaMg_3(Al_2Si_2O_{10})F_2$	Ba-Disilicic Mica	+2	1461	Strongly Bonded

processed MAS matrix CMCs were very nonuniform, indicating deficiencies in our fiber coating and/or prepreg process. This is shown in Figure 79. Additionally, the thick BDM or KFP mica coatings did not consolidate well. For barium-stuffed cordierite matrix CMCs processed at 975°-1150°C, billet density decreased with increased mica content, and was lowest for the highest processing temperature, as shown in Figure 80. Although mechanical properties increased with coating thickness at room temperature, the properties at 1200°C showed decreased strength and increased deformation with increased coating content, shown in Figures 81 and 82. TEM thin foil examination (Figure 83) revealed glass and porosity at the interface, and evidence of an enhanced diffusion zone at the fiber surface in samples exposed for 100 hr at 650°C (Figure 84). SEM examination revealed pitting of the fiber under the mica coating (Figure 85). Mica appeared to be reactive with the fiber, and very sensitive to the air environment, as TEM examination of Nicalon/BaMAS CMCs without mica coatings exhibited no such indication of reactivity at the interface as shown in Figure 86.

Although mica appeared to be reactive in the composite, the results are clouded by the failure of the mica to consolidate, resulting in interfacial paths for accelerated environmental ingress into the microstructure. The porous regions at the interface, and resultant potential for oxidation, precluded a definitive assessment of the inherent reactivity of mica, and its worth as an interfacial debond layer in the composite.

(b) Thinner Sol-Only Mica Fiber Coatings:

Thinner mica fiber coatings without the particulate mica additions, but with increased solids content to increase coating thickness, were distinctly more promising. For instance, sol-only (3S) barium disilicic mica interface Nicalon/MAS cordierite CMCs had less than 1% open porosity, and exhibited reduced environmental influence in comparison to CMCs with the particulate augmented sol-gel coatings. Such CMCs exhibited fairly temperature invariant strength and toughness (failure strain), as shown in Figure 87. This suggests that the inferior performance for the thick (2S+12P) particulate augmented mica fiber coatings were indeed due to the porous nature of the CMC microstructure, and not to thermochemical incompatibility of the mica per se. However, even MAS matrix CMCs employing the more promising (3S) sol-only BDM mica fiber coatings suffered significant degradation in flexural properties after long term unstressed exposures at intermediate (650°C) and elevated (1250°C) thermal exposures in air, as shown in Figure 88.

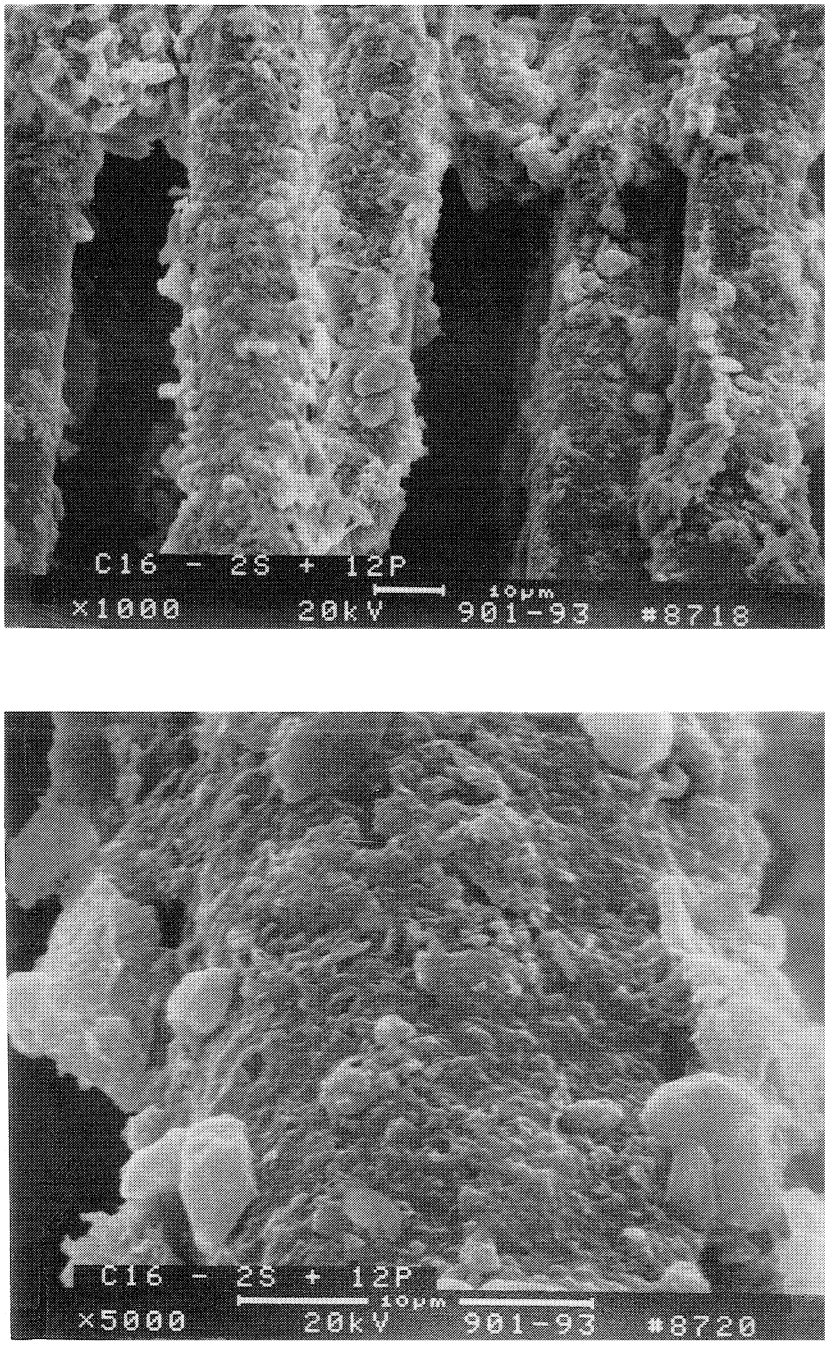

FIGURE 79. **SEMs OF (2S+12p) BDM COATING ON Nicalon FIBER, SHOWING VERY THICK COATING WITH MASSIVE AMOUNT OF PARTICULATE PHASE. SOME CONTACT BRIDGING IS PRESENT**

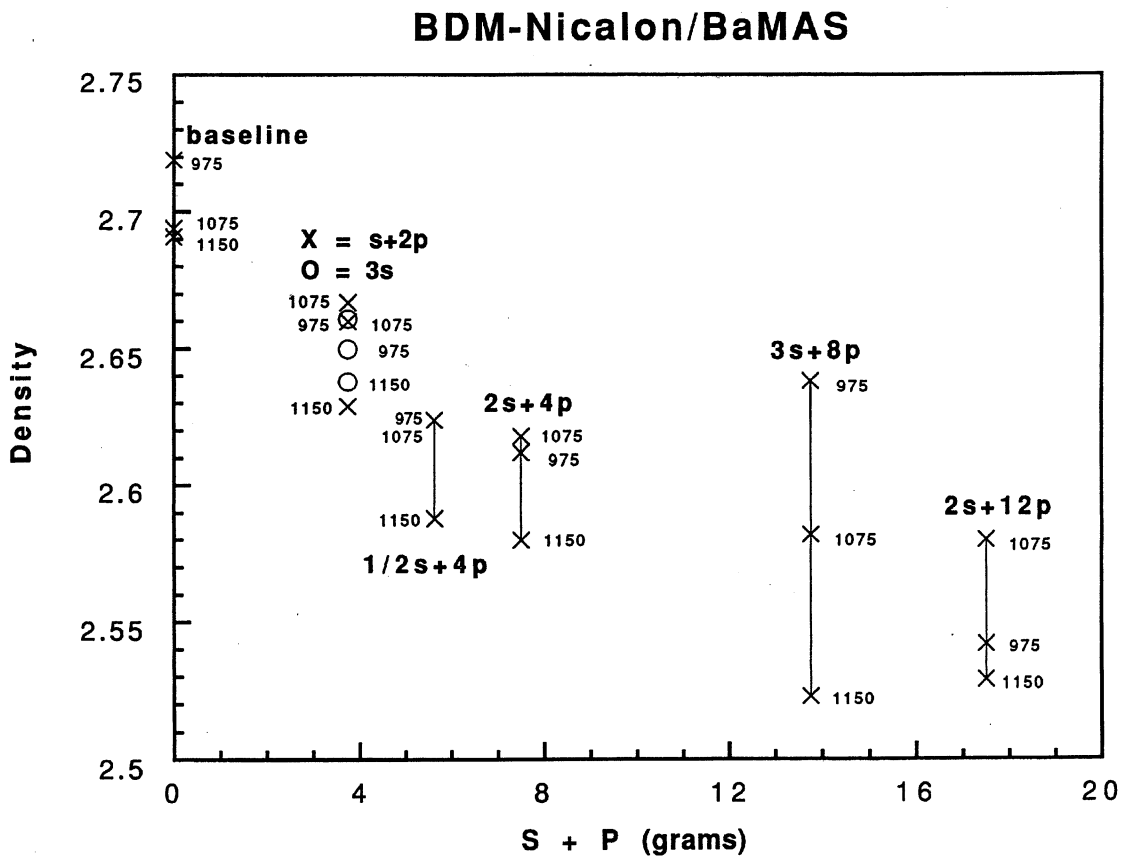

FIGURE 80. CMC DENSITY VS. MICA COATING MASS (THICKNESS)

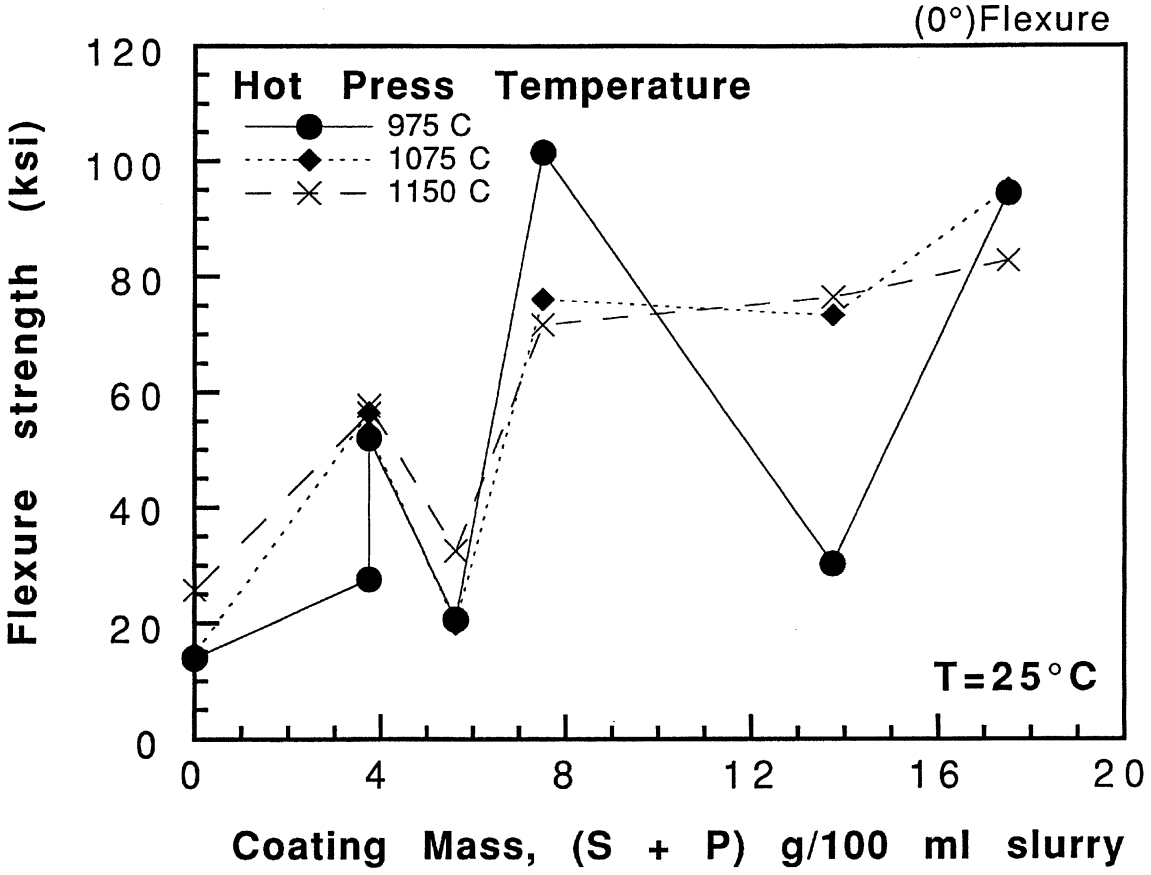

FIGURE 81. **CMC RT STRENGTH VS. MICA COATING MASS (THICKNESS)**

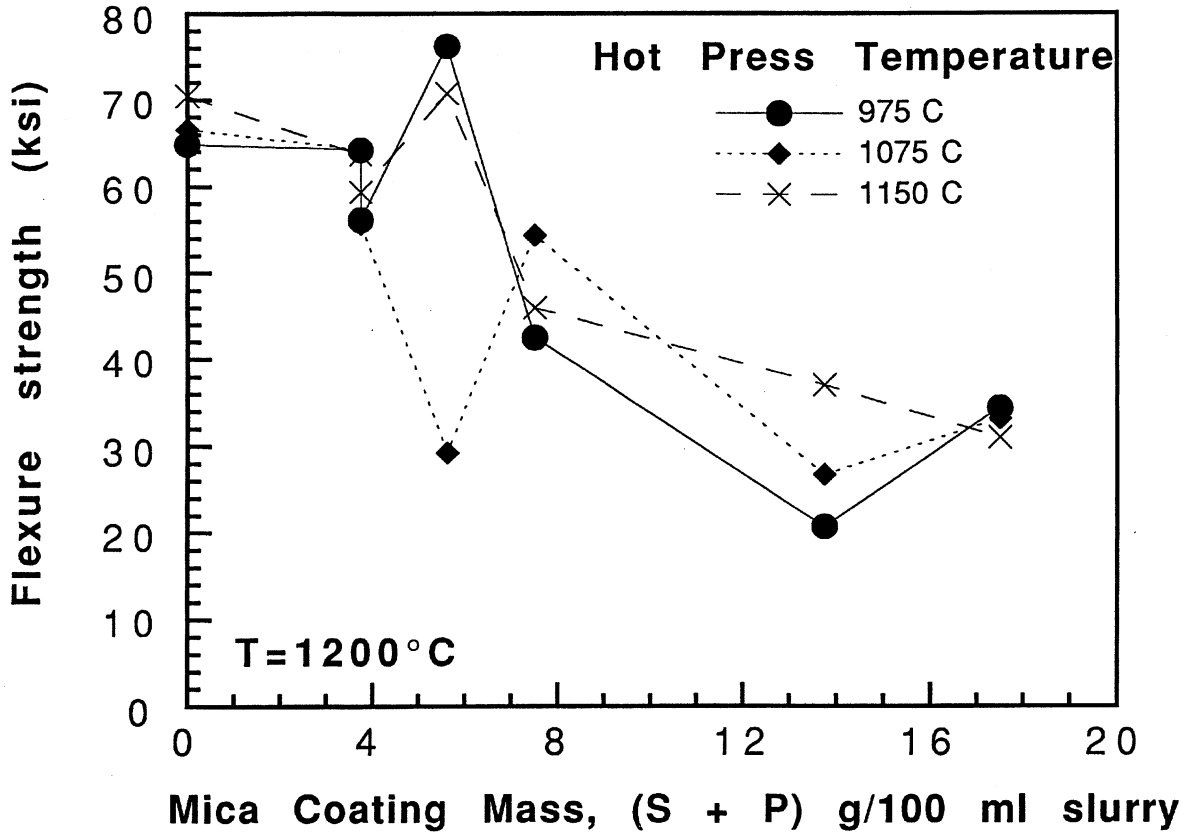

FIGURE 82. FLEXURE STRENGTH OF BDM-Nicalon/BaMAS CMCs AT 1200°C

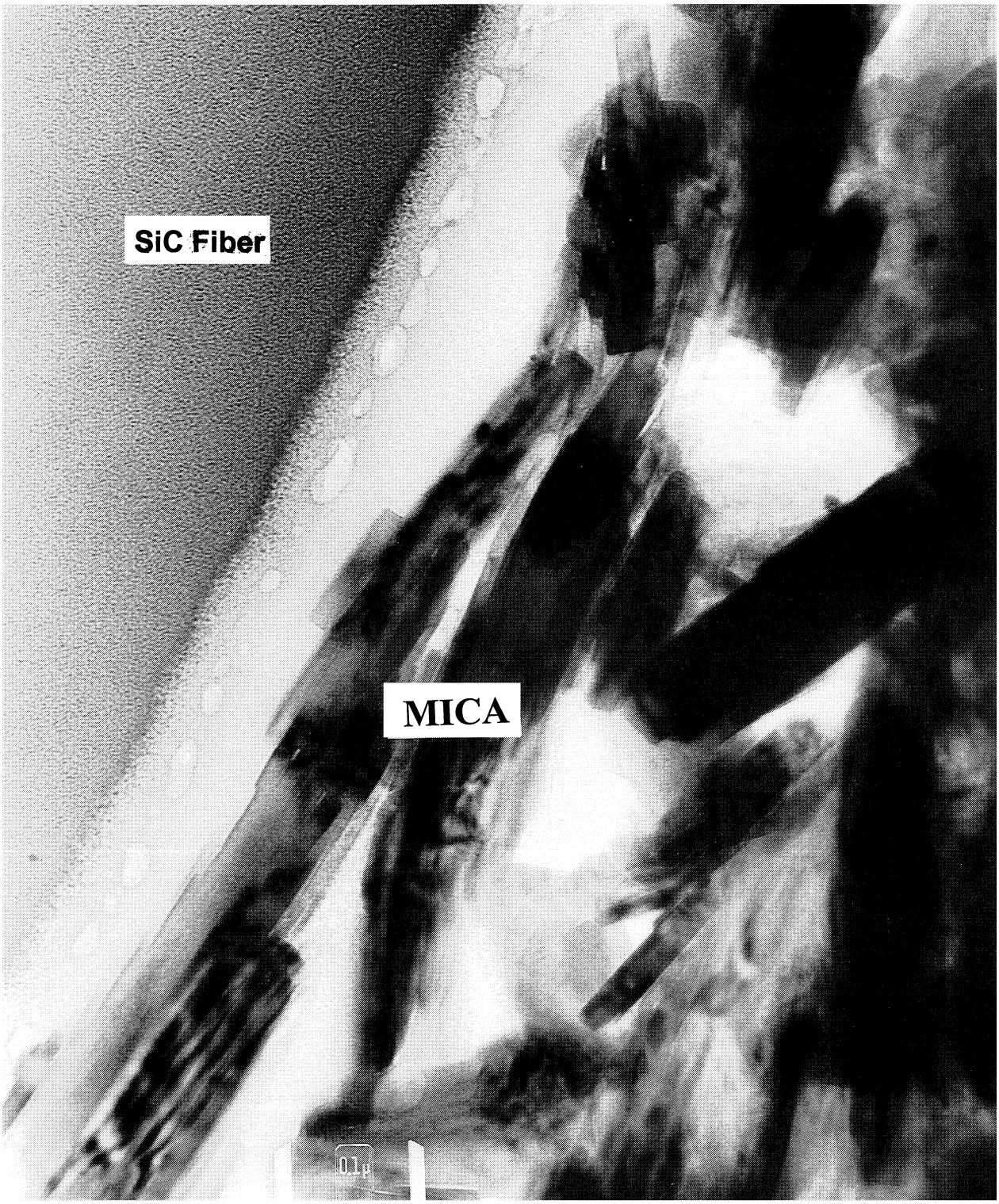

FIGURE 83(a). TEM THIN FOIL MICROGRAPH OF (2S+12P) BDM Nicalon/BaMAS

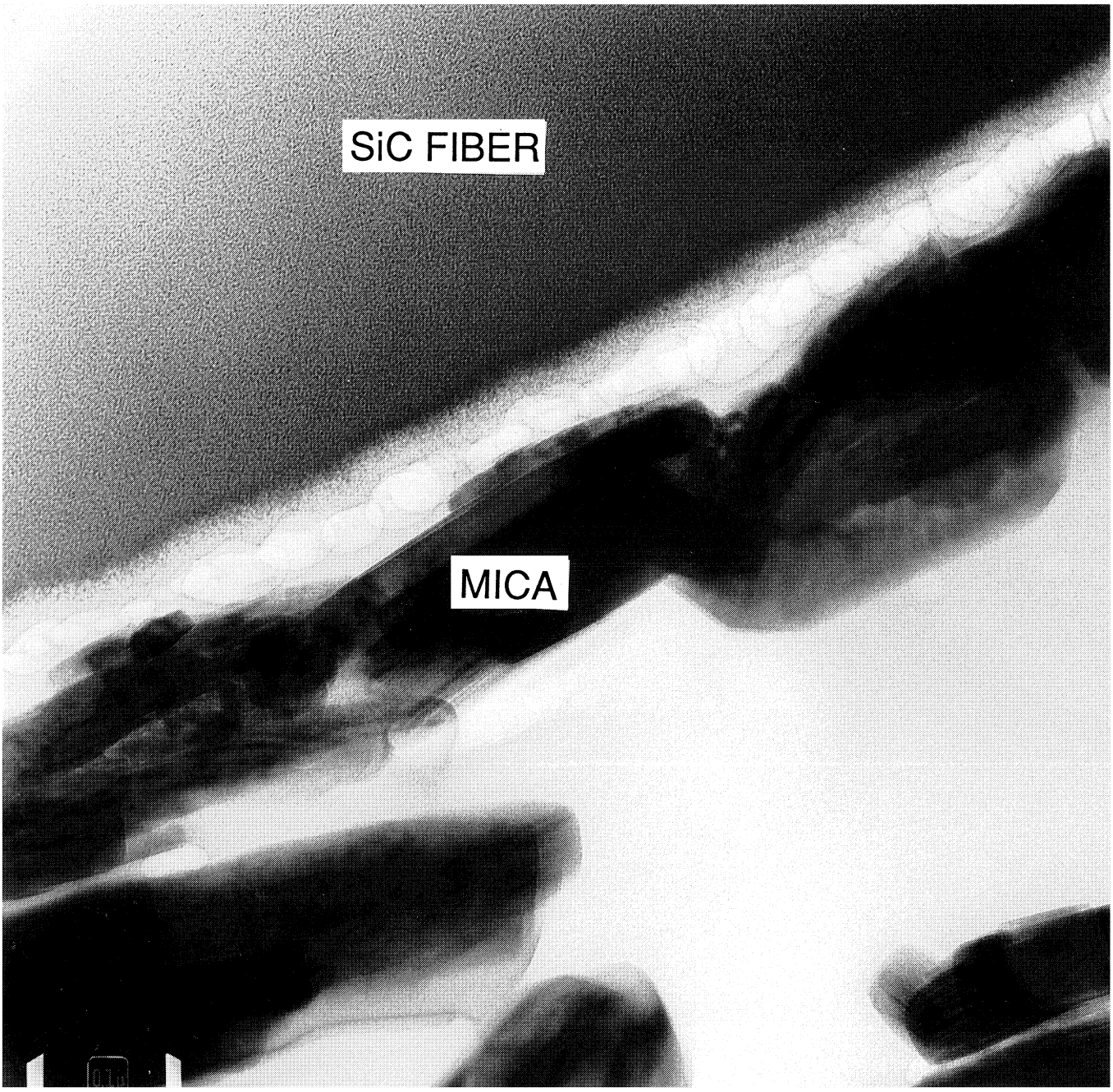

FIGURE 83(b). TEM THIN FOIL MICROGRAPH OF (2S+12P) BDM Nicalon/BaMAS

FIGURE 84. **TEM THIN FOIL MICROGRAPH OF 2S+12P) BDM Nicalon/BaMAS EXPOSED 650°C/100 HR**

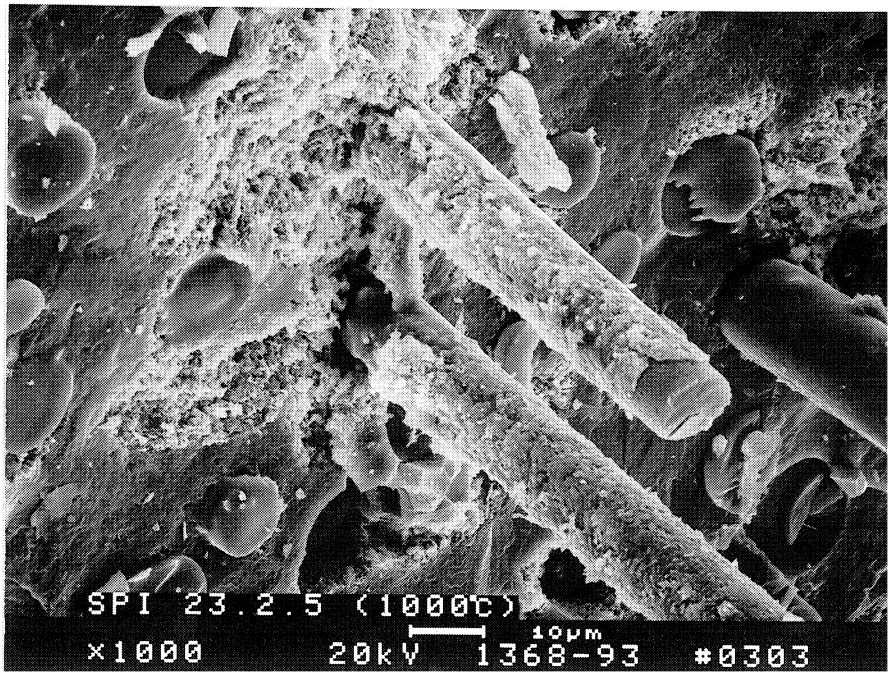

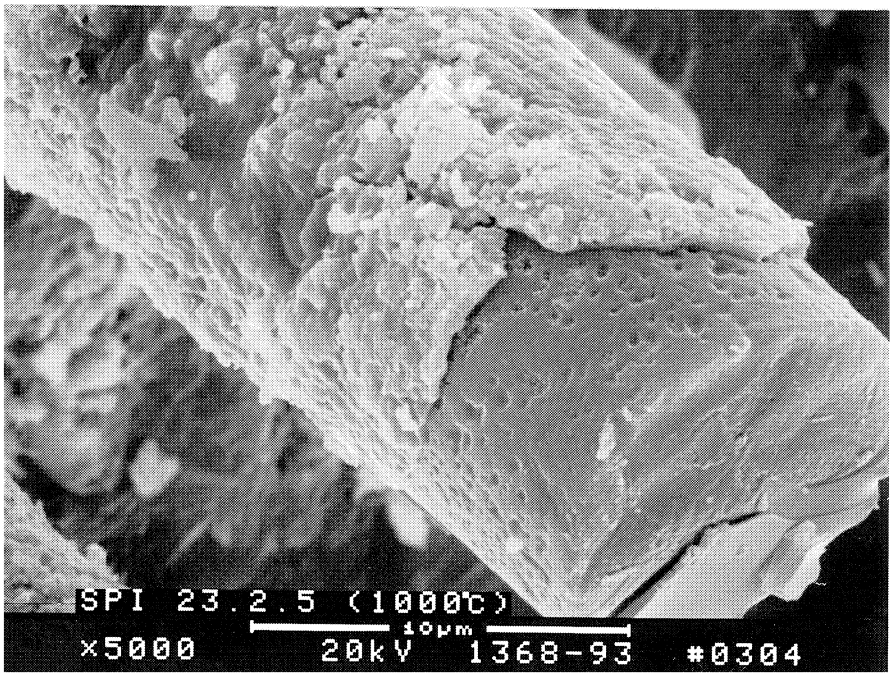

(b) 1000°C

FIGURE 85. SEM VIEWS OF FRACTURE SURFACE OF (2S+12P) BDM COATED Nicalon/BaMAS TESTED AT 1000°C

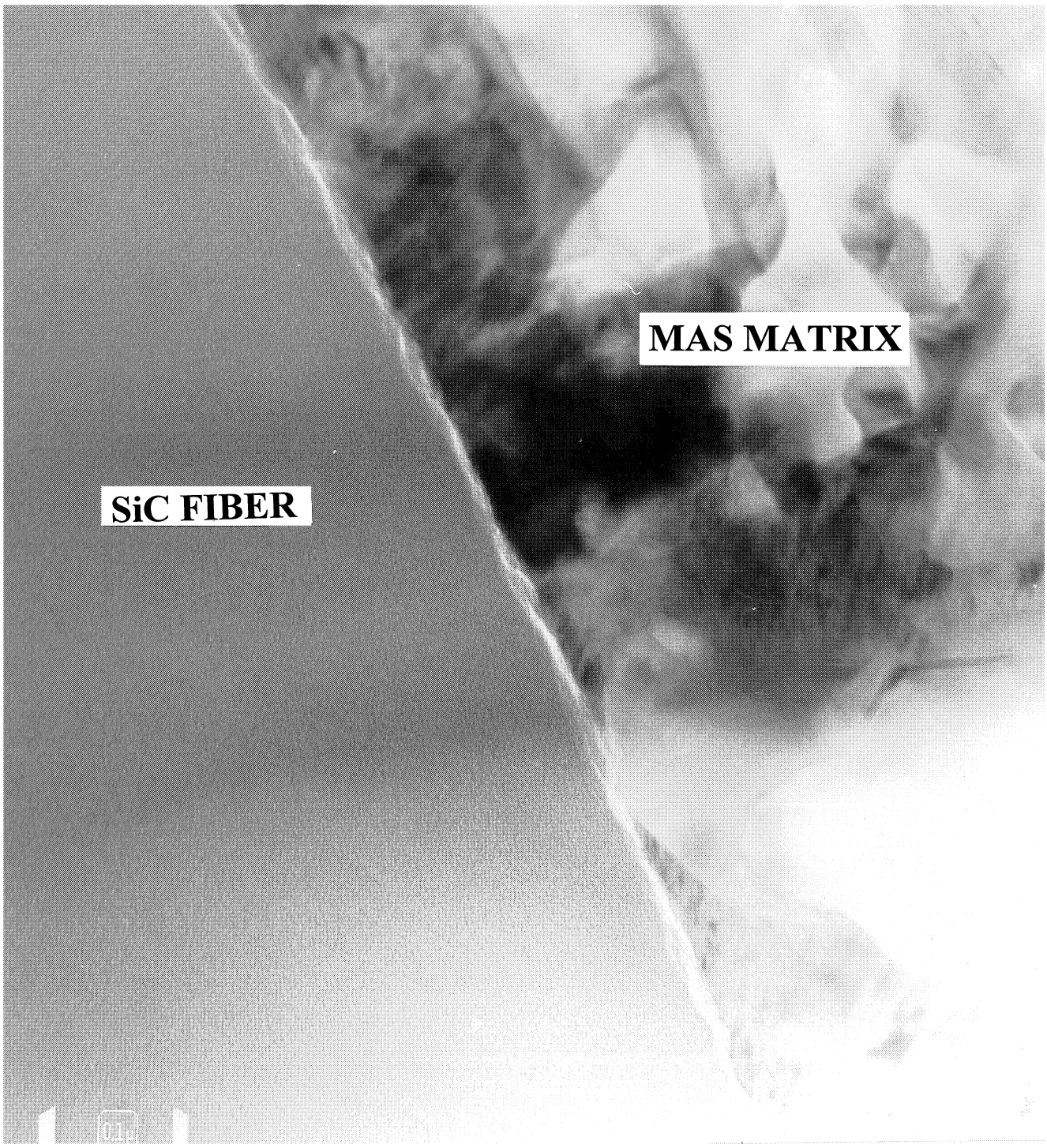

FIGURE 86. TEM THIN FOIL MICROGRAPH OF UNCOATED Nicalon/BaMAS

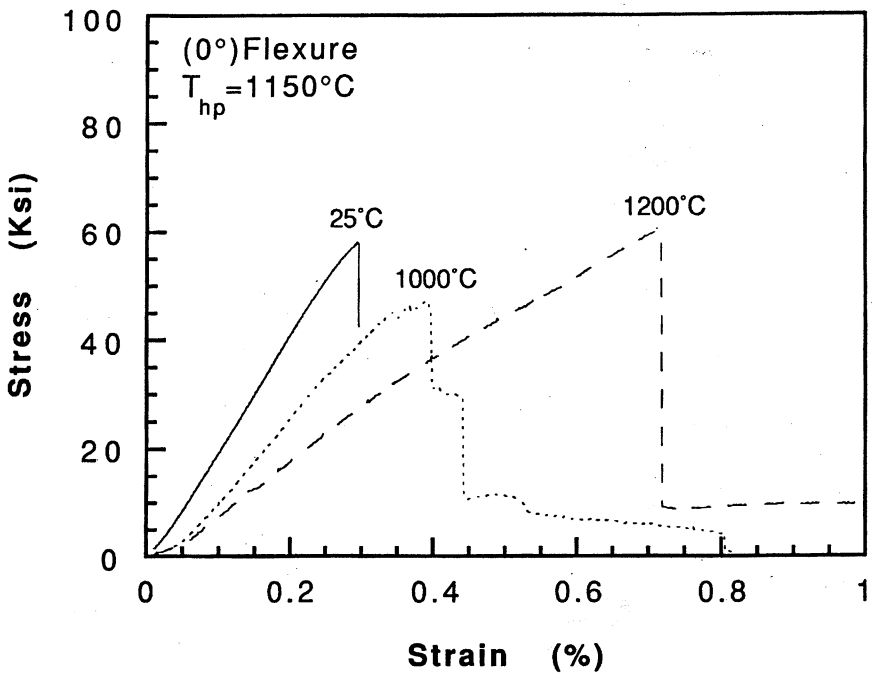

FIGURE 87. STRESS-STRAIN BEHAVIOR OF AS-PROCESSED (3s) BDM-Nicalon/BaMAS CMCs

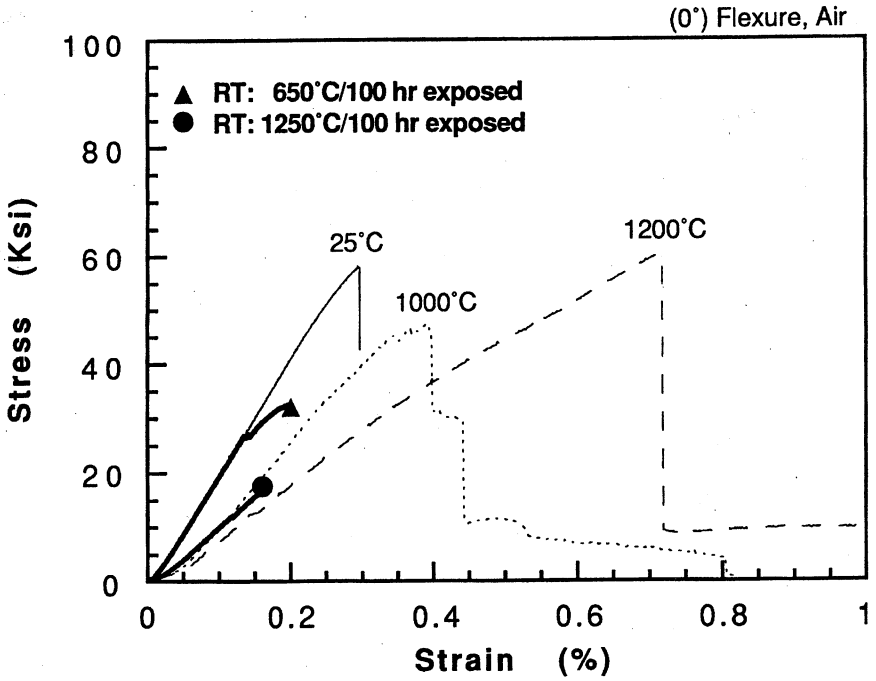

FIGURE 88. STRESS-STRAIN BEHAVIOR OF EXPOSED (3s) BDM-Nicalon/BaMAS CMCs

These results demonstrated that the 3S sol-only mica fiber coatings, with solids content increased from earlier coatings, are the most promising route to increased interfacial thickness in processed CMCs. This technology was introduced to the program as discussed in Section 5.5. First, however, concurrent work on another program developed the importance of using lower temperature processing, and switching to a BSG-doped MAS cordierite matrix, as discussed below.

5.4 Concurrent Work on Pratt & Whitney Ceramic Composite Component Demonstration (C^3D) Subcontract to Air Force Flight Dynamics Directorate Contract F33615-87-C-3222

Using the results of the previous section as a guide, the development of mica interface CMCs was continued on the C^3D Subcontract from Pratt & Whitney under Contract F33615-87-C-3222, where the thrust of the work was the development of dielectric/structural CMCs. In that case, particularly close attention was given to the development of the in situ carbon layer in processed CMCs, and removal of certain elements from the matrix known to promote its development. In the process of doing that, BSG-doped MAS CMC matrices were examined.

The following sections detail (1) the process window studies conducted to avoid in situ carbon layer formation, and (2) the success of BSG-doped MAS matrices. This work was then transitioned to the present program as described in Section 5.5.

5.4.1 In situ Carbon Layer Development

For mica to be an oxidatively stable debond layer in the CMC microstructure, it is critically important to avoid formation of the in situ carbon layer when using commercially available SiC fibers such as Nicalon. The presence of an in situ carbon layer will cause embrittlement effects, and will prevent direct observation of mica layer influence on mechanical properties. The former event would obviate the advantage of having mica at the interface, and the latter inhibits development of an optimum mica composition/process, since individual mica and carbon effects are not isolated.

Consequently, development of the in situ carbon layer as a function of process temperature was examined.* For convenience, uncoated Nicalon/5% BSG-MAS cordierite matrix CMCs (the

* The primary reason for doing this on the C^3D program was to achieve low dielectric properties.

importance of BSG-doped MAS matrices will be explained below) were processed at several temperatures from 975° to 1250°C (specifically, 975°, 1075°, 1150°, and 1250°C). Uncoated fibers were used, since the main objective was to determine, by measurement of mechanical and electrical properties, the process window boundaries for avoiding formation of the in situ carbon layer when using CG-Nicalon fibers with MAS cordierite based glass-ceramic matrices.

The room temperature stress-strain behavior of these [0°/90°] cross-ply CMCs is shown in Figure 89, and the room temperature flexure strength is plotted as a function of process temperature in Figure 90. It is seen that there is a direct relation between mechanical performance and process temperature. Processing at ≤1075°C resulted in composites that were distinctly lower in strength and failure strain than CMCs processed at ≥1150°C. We speculate that the in situ carbon layer is not fully developed for process temperatures ≤1075°C; however, there appears to be an incipient carbon layer in those low temperature processed CMCs, since they are not completely brittle.

The appearance of the fracture surfaces, or rather the progression of the fracture process, for these CMCs corroborates this conjecture about the in situ carbon layer forming more completely as the process temperature is increased. The two CMCs processed at ≤1075°C exhibited fibrous initial tensile fractures followed by extensive multiple shear propagation nearer the neutral axis of the flexure beam. The latter failure mode is normally associated with the existence of a fully developed and mechanically functional carbon layer.

Room temperature X-band (8-12 GHz) dielectric constant data measured at Pratt & Whitney tends to confirm the speculation about the development of the in situ carbon layer as determined by process temperature. The dielectric constant is plotted vs. process temperature in Figure 91, where it is shown that the dielectric constant increases monotonically with process temperature, consistent with the development of an in situ carbon layer. The direct relation of mechanical and electrical performance of CMCs processed at different temperatures is shown in Figure 92.

Figure 93 presents the high temperature strength and failure strain for the CMCs processed in this overall set of experiments. It is interesting that the properties at elevated temperature are independent of process temperature. Our interpretation of this is as follows. As discussed above, the good strength and failure strain at RT for the CMCs processed at 1150° and 1250°C is because a functional in situ carbon layer formed, and the poor RT properties for CMCs processed at 975° and 1075°C are because the in situ carbon layer only partially developed. At high temperature, the behavior of the CMCs processed at 975° and 1075°C does not change from RT levels, since there is nothing in the composite microstructure that is changing with temperature;

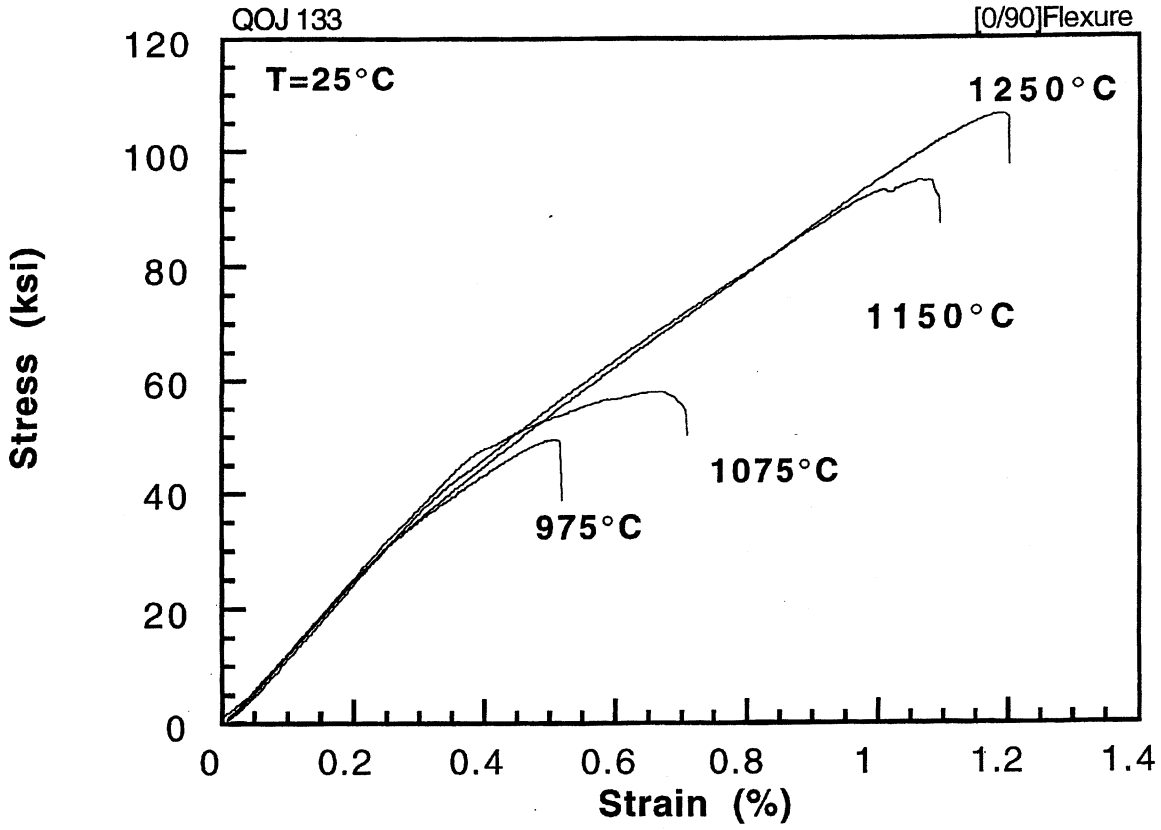

FIGURE 89. STRESS-STRAIN BEHAVIOR OF UNCOATED Nicalon/5% BSG-MAS PROCESSED AT VARIOUS TEMPERATURES

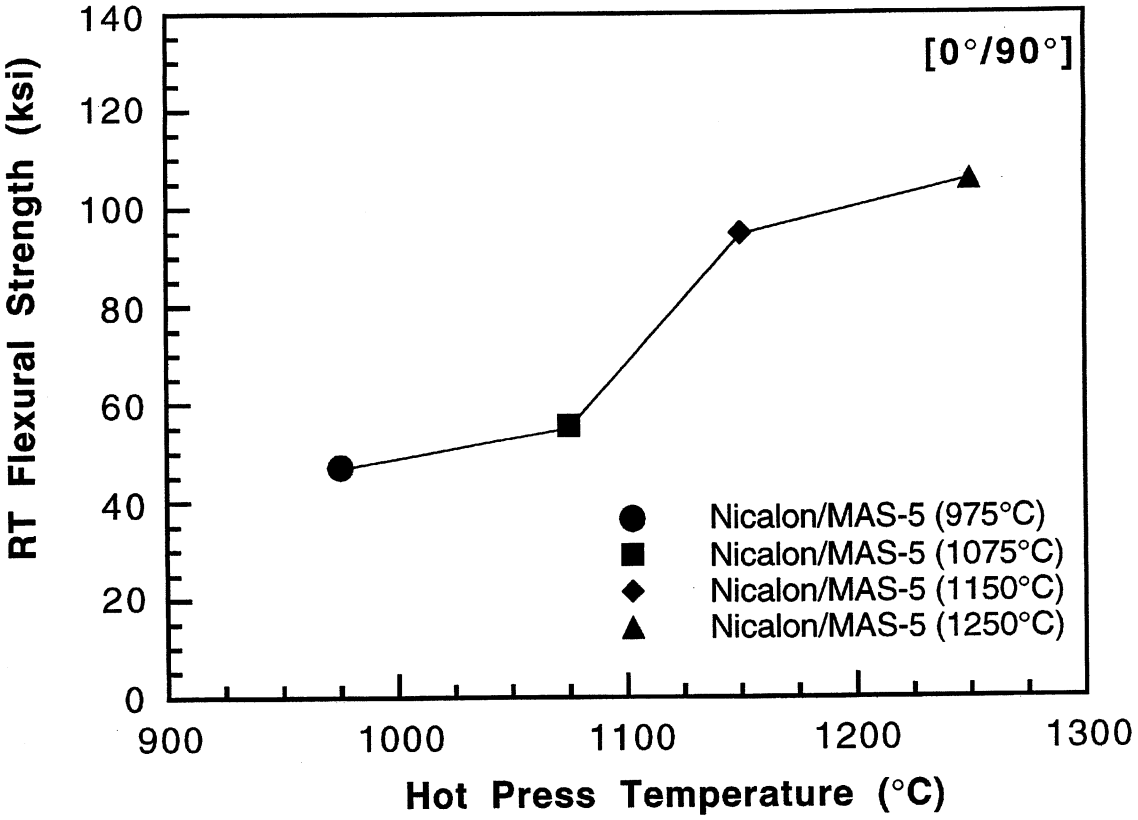

FIGURE 90. FLEXURAL STRENGTH VS. HOT PRESS TEMPERATURE FOR 975-1250°C HOT PRESSED Nicalon/5% BSG-MAS

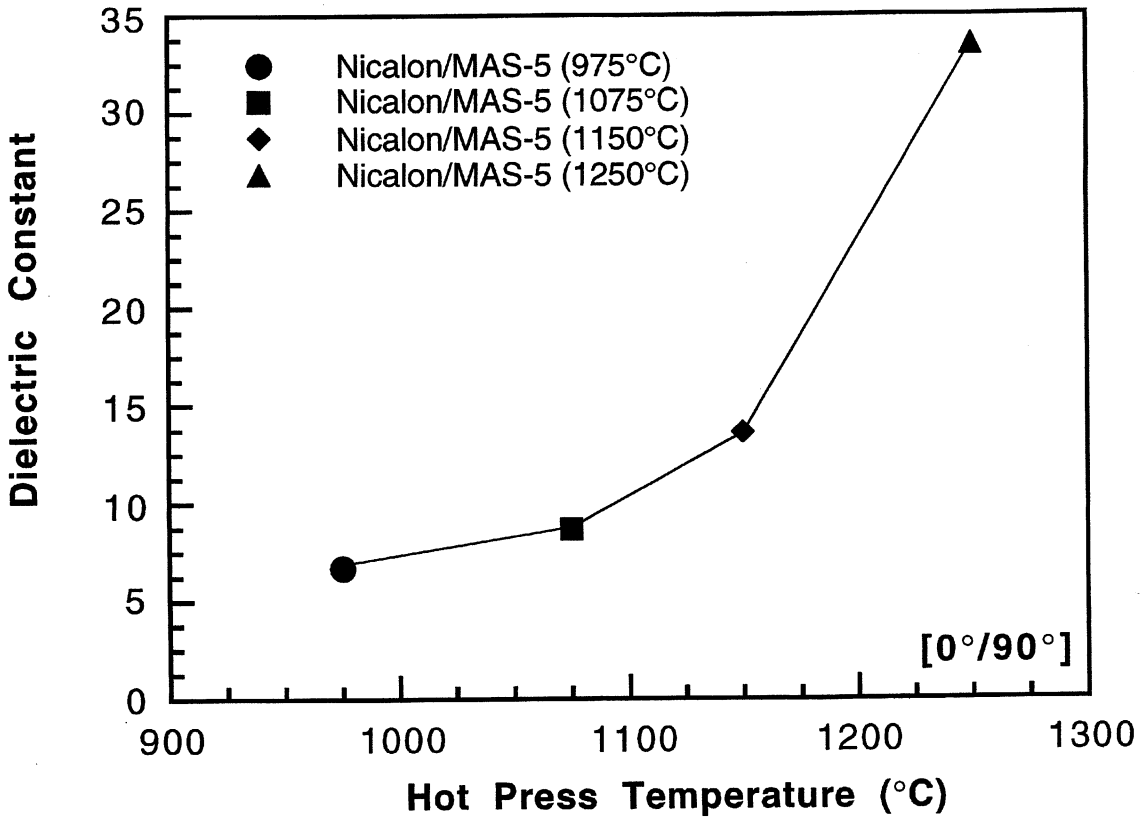

FIGURE 91. DIELECTRIC CONSTANT VS. HOT PRESS TEMPERATURE FOR 975-1250°C HOT PRESSED Nicalon/5% BSG-MAS

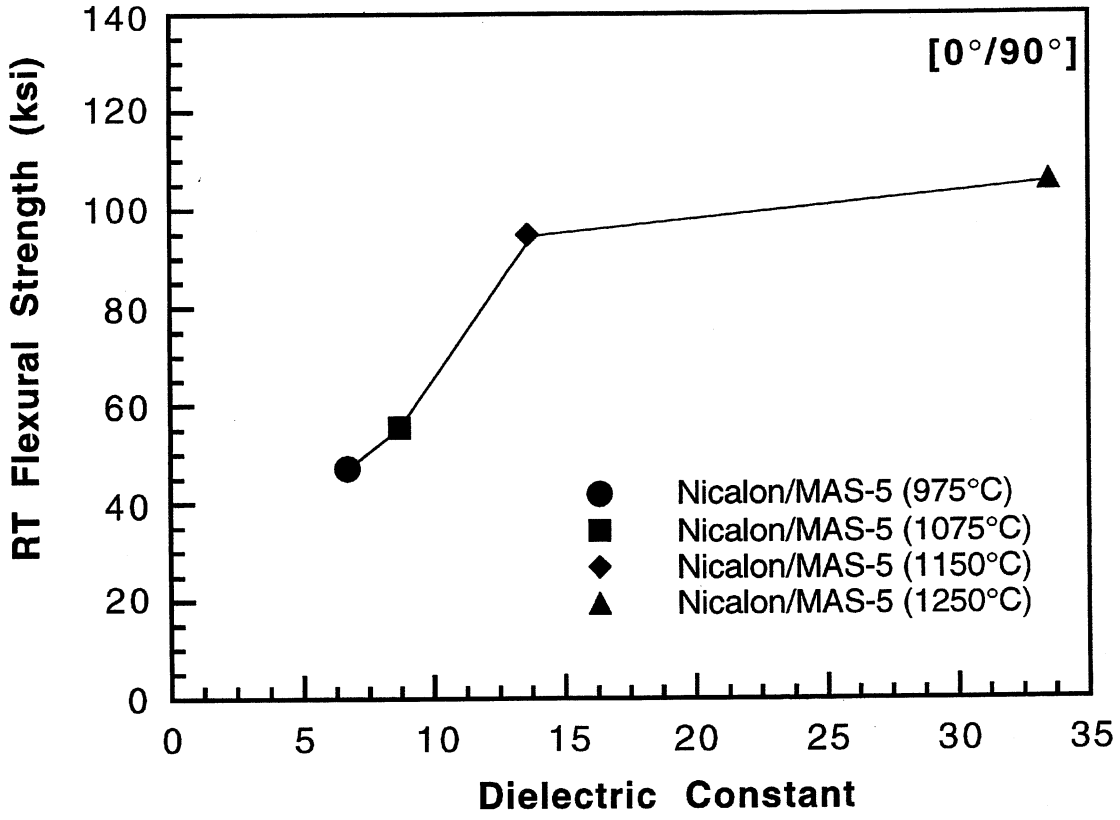

FIGURE 92. FLEXURAL STRENGTH VS. DIELECTRIC CONSTANT FOR 975-1250°C HOT PRESSED Nicalon/5% BSG-MAS

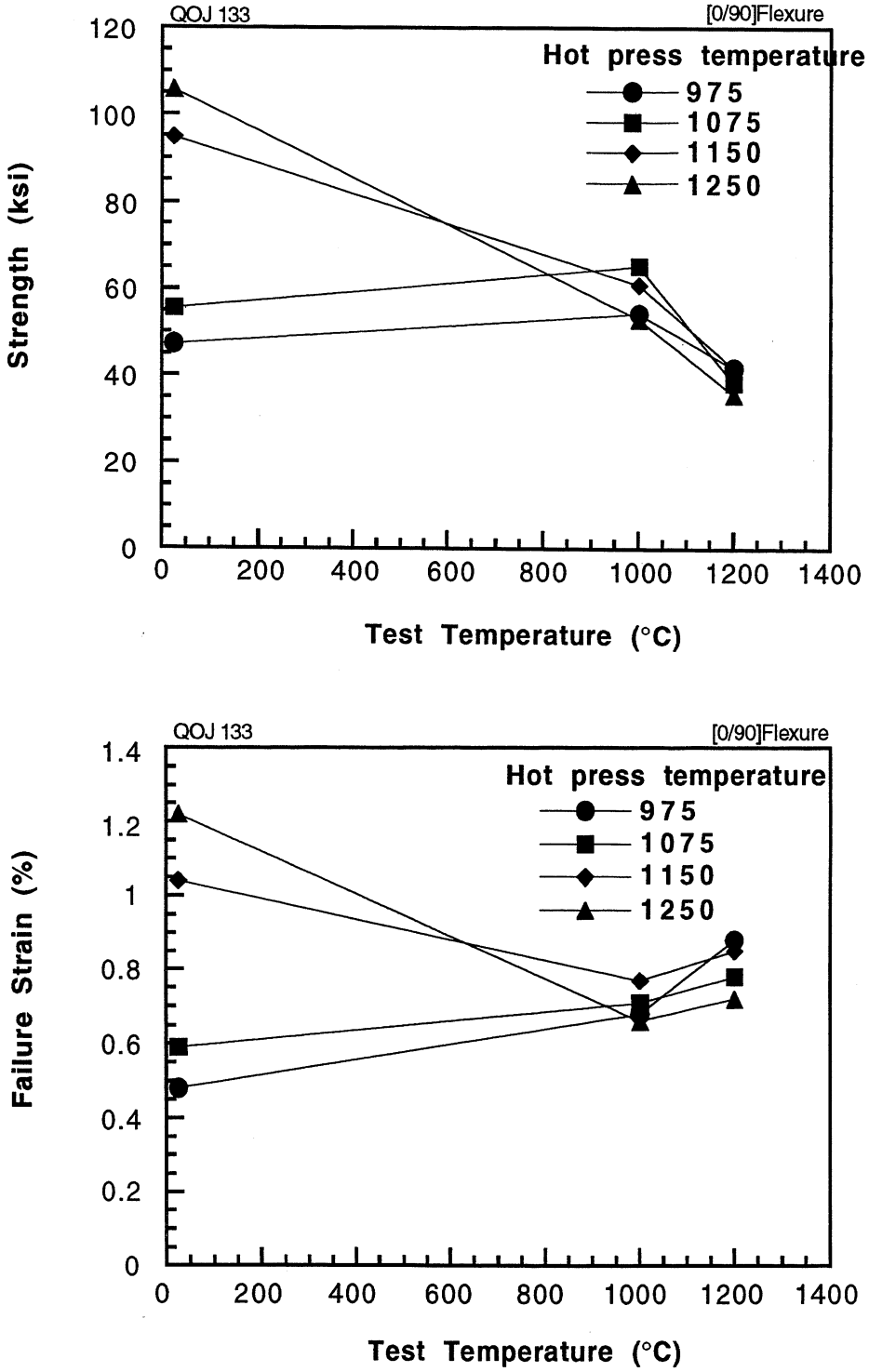

FIGURE 93. MECHANICAL PROPERTIES OF UNCOATED CG Nicalon/5% BSG-MAS PROCESSED AT VARIOUS TEMPERATURES

there is no well-developed in situ carbon layer to begin with.* The properties remain relatively low, as they were at RT.

For the CMCs processed at 1150° and 1250°C that exhibit good RT properties (since a fully developed carbon layer is present), the high temperature properties show a significant degradation. This degradation is due to oxidation embrittlement, removal of the carbon layer by oxidation at high temperature. Note that there still is embrittlement with these CMCs since the interface is predominately carbon, but the degraded properties are still rather good (as shown in Figure 93), since the carbon layer is boron-modified, and BSG-glazed (the matrix is BSG-doped MAS).

It is perhaps not too suprising that the high temperature properties are the same for all process conditions. All CMCs at high temperature will have the same partially developed in situ carbon layer. The low temperature-processed ones have it since it never developed completely during processing; the high temperature-processed ones have it since it was there originally, but was partially removed by oxidation embrittlement.

Direct microstructural evidence of the development of the in situ carbon layer as a function of process temperature is provided in the TEM micrographs shown in Figure 94. As the process temperature is increased from 975° to 1250°C, it is observed that the character of the interface and fiber near-surface regions changes significantly. The light phase in the interface would normally be associated with a developed carbon layer, but no electron diffraction was performed to confirm that. The major microstructural feature at the interface associated with the progression of process temperatures from 975° to 1250°C is the increased evidence of a diffusion zone near the fiber surface. This is shown in Figures 94(a-d), and is thought to be the diffusion of free carbon to the fiber-matrix interface during CMC processing. This free carbon (i.e., the in situ carbon interface) is responsible for the mechanical and electrical behavior of the CMCs.

---

* Dielectric data (e.g., Table 6) and mechanical property data we have observed for a variety of CMC systems indicates that formation of the in situ carbon layer occurs mainly during hot consolidation, and not during subsequent thermal exposure; the microstructure of the CMC is locked-in during processing; it is not formed during exposure, but an existing one can be removed by exposure, by oxidation embrittlement.

Table 6
DIELECTRIC PROPERTIES OF UNCOATED CG NICALON/ 5% BSG-MAS AS A FUNCTION OF HOT PRESS TEMPERATURE

CMC Designation	Hot Press Temperature	As-received	As-received	Post 100hr/ 1800°F	Post 100hr/ 1800°F
		ε'	ε"	ε'	ε"
QOJ 133.1	975°C	6.7	1.2-1.9	6.9-7.3	2.4-3.5
QOJ 133.2	1075°C	8.2-9.1	6.5-9.3	9.0-10.1	8.7-12.2
QOJ 133.3	1150°C	11.9-15.2	17.3-23.9	12.9-16.0	18.4-25.3
QOJ 133.4	1250°C	24.6-42.3	30-35	24.1-40	40-58

[0/90] cross-ply laminates Measured at Pratt and Whitney

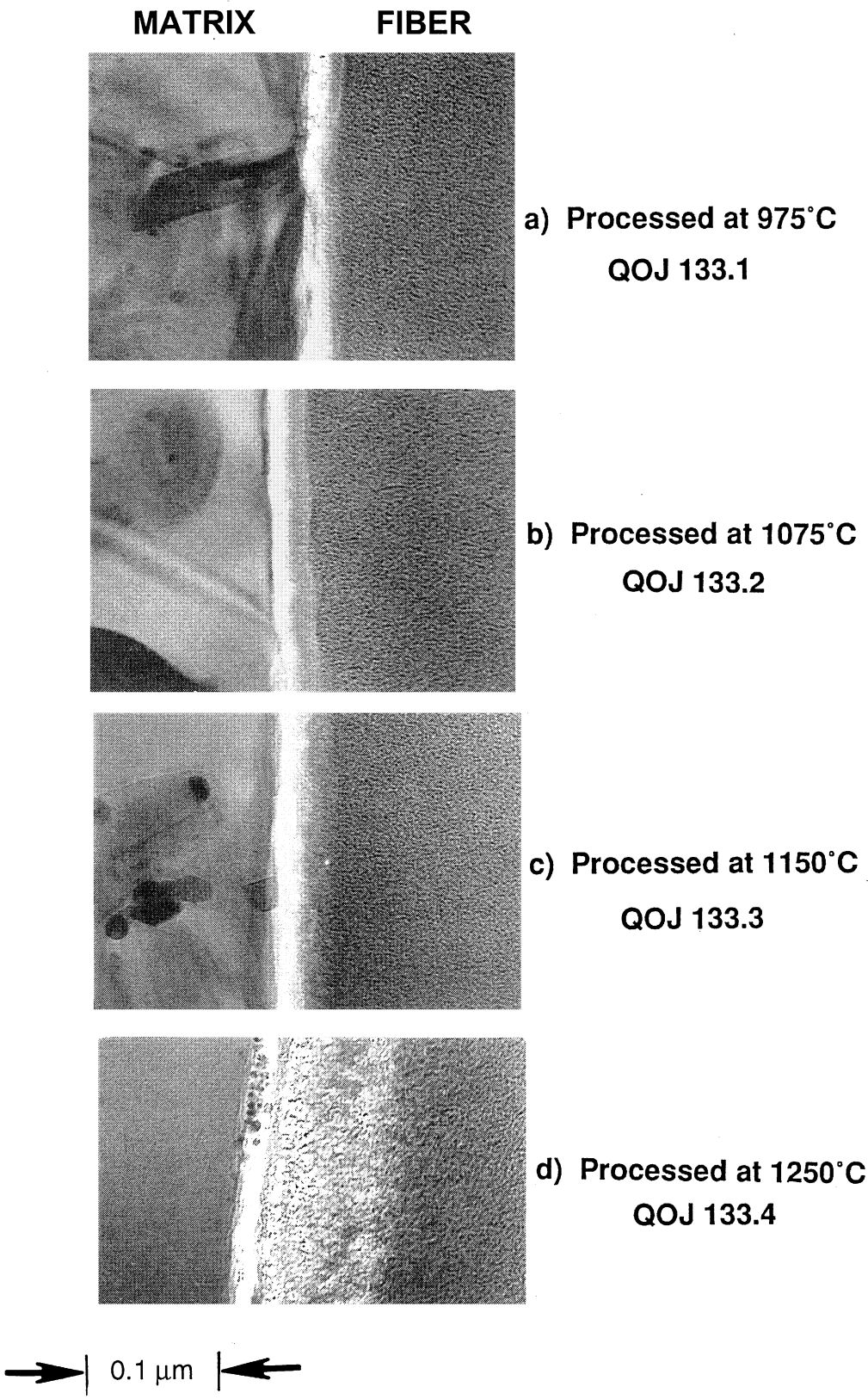

FIGURE 94. **TEM THINFOIL MICROGRAPHS OF INTERFACIAL REGION IN UNCOATED Niclaon/5% BSG-MAS AS A FUNCTION OF PROCESS TEMPERATURE**

Having therefore shown that formation of the in situ carbon layer can be avoided by low temperature processing, it is important to also investigate the character of the glass-ceramic matrix that has been processed at such low temperatures. It is of particular interest to determine if the matrix has fully consolidated, and whether it is highly crystalline. The former aspect is important for avoiding environmental ingress through a porous matrix; the latter is important from a refractoriness or upper use temperature standpoint.

Accordingly, density and XRD measurements were made on the CMCs from this study. Table 7 illustrates that even at such low process temperatures, the composites are consolidated to full density. The slightly higher density for the lowest process temperature, 975°C, is typical crystallization behavior for cordierite glass-ceramics. The glass is more dense than the crystalline form (expanded cage structure); the implication here is that for 975°C processing, a slight glassy phase is probably present in the matrix microstructure. However, it is only present in a small volume fraction, and not expected to adversely affect refractoriness. This is confirmed by XRD results, presented in Figure 95, which show that identical cordierite X-ray patterns are exhibited by CMCs processed from 975° to 1250°C. This means that highly refractory CMCs can be achieved through low temperature processing, without the necessity of post-processing heat treatment to crystallize the glass-ceramic matrix (i.e., no ceram cycles). This fact is also confirmed by the stress-strain behavior shown in Figure 89. CMCs processed at all temperatures from 975°-1250°C had the same elastic modulus. Ultimate strength and failure strain are solely determined by the character of the in situ carbon layer.

These experiments have demonstrated that processing ≤1075°C does not produce a significant in situ carbon layer. As discussed above, the ability to accomplish that is essential to utilizing mica interface technology to produce oxidation embrittlement resistant CMCs.

5.4.2 Improved BSG-doped MAS Cordierite Matrices

The combination of mica interfaces with BSG-doped MAS cordierite matrices was first investigated in Corning in-house research several years ago. Early vintage materials of this type exhibited promising mechanical properties at high temperature (1100°-1200°C), but also had significant degradation at intermediate temperatures (650°C). Processing of those CMCs was at >1100°C, and therefore, an undesirable in situ carbon layer was present. Additionally, the barium disilicic (BDM) mica used was of low solids content, and thus the sol-gel fiber coating was too thin to be effective. Also, the BSG-dopant content of the matrix was only 2.5%, too low

Table 7
DENSITY OF UNCOATED CG NICALON/5% BSG-MAS CMCs VS. PROCESS TEMPERATURE

Process Temperature (°C)	CMC Density ($g \cdot cm^{-3}$)
975°	2.660
1075°	2.616
1150°	2.617
1250°	2.611

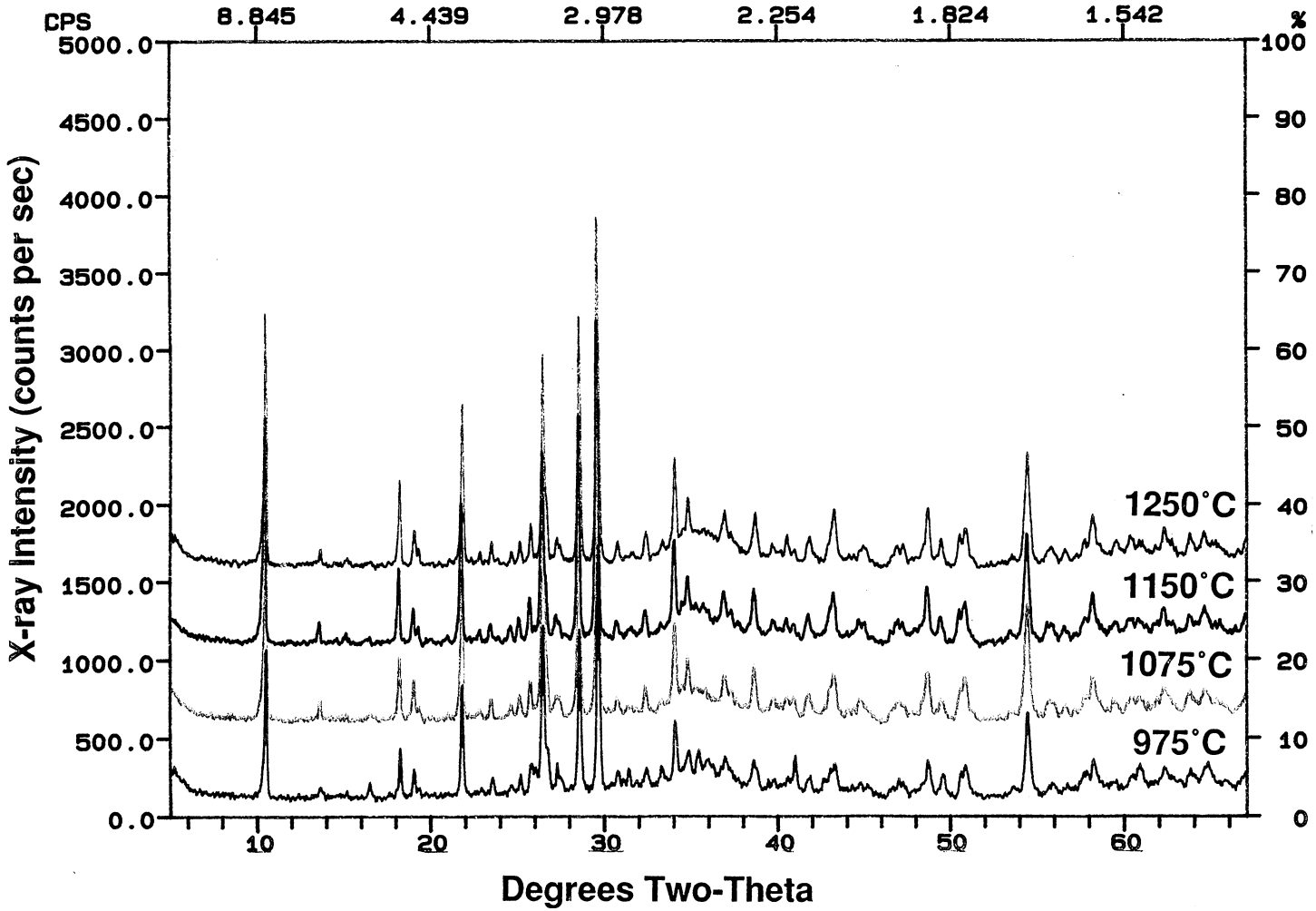

FIGURE 95. XRD FOR Nicalon/5% BSG-MAS PROCESSED AT VARIOUS TEMPERATURES

to be effective in limiting carbon layer formation and boron-modifying the carbon that did form at the composite fiber-matrix interface.

In Corning's C^3D subcontract under Contract F33615-87-C-3222, various improvements in mica coating and processing technology were implemented, especially (a) higher solids content sol-gel mica fiber coatings (that were developed earlier in this program), (b) low temperature (975°C) processing to avoid carbon layer formation, and (c) higher BSG content, to 5-6% BSG-dopant level in the Ba-MAS cordierite matrix, to further inhibit carbon layer formation. (It was shown earlier in this program that BSG dopants tended to reduce the thickness of the in situ carbon layer.) Additionally, matrix compositions were examined where arsenic fining agents were removed, since it had previously been shown that As tended to promote carbon layer development.[7] The removal of Nb nucleation additives from the matrix was also investigated, to eliminate potentially unstable secondary phases (i.e., NbC).

Initial experiments focused on 975°C low temperature processing of a variety of [0°/90°] cross-ply CMCs, employing both BDM barium disilicic and KFP potassium phlogopite mica interfaces, made of high solids content sols with little or no particulate mica addition (following the results discussed above). It was found that K-MAS matrix CMCs gave similar poor results in comparison to the Ba-MAS matrix CMCs investigated on the subject program. It was also found that BSG-doped MAS matrices were apparently more thermochemically compatible with mica, since distinctly better mechanical properties were obtained. The benefit of the mica interface was directly shown for BSG-doped MAS matrix composites through use of appropriate uncoated control samples. The screening results for the mica coated BSG-containing MAS cordierite matrix composites are shown in Figures 96 and 97. Note that unlike the CMCs produced earlier on this contract, these CMCs were of [0°/90°] laminate orientation, and so their high strengths are even more significant in comparison to results for previous unidirectional non-BSG-doped MAS cordierite matrices. Therefore, the strengths and failure strains shown in Figures 96 and 97 for these mica interface CMCs were judged fairly promising. Only limited fiber pullout was exhibited by these CMCs, as shown in Figure 98. However, no degradation was observed in 100 hr/1000°C extended thermal exposures that were of particular interest on the C^3D program, as shown in Figures 99-101.

The CMC that was judged most promising was a (3S) BDM mica coated CG-Nicalon/6% BSG-MAS cordierite, the matrix free of Nb and As compounds that might have deleterious effects on either the mechanical or the electrical performance of the CMC. This downselect was made after careful consideration of mechanical as well as electrical property data (in as-processed, high

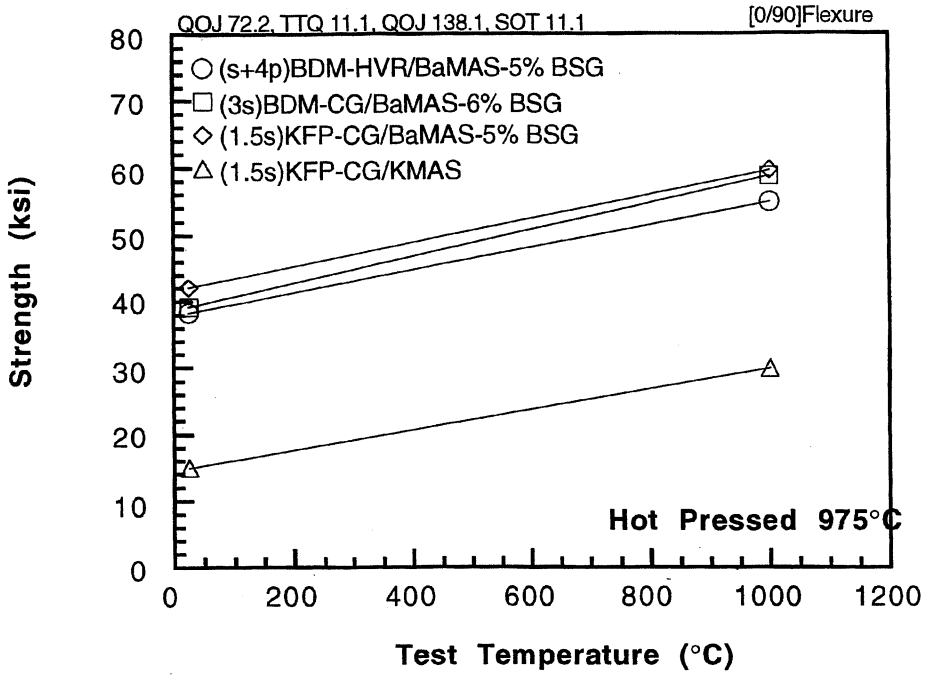

FIGURE 96. FLEXURAL STRENGTH VS. TEST TEMPERATURE FOR VARIOUS MICA-COATED Nicalon CMCs

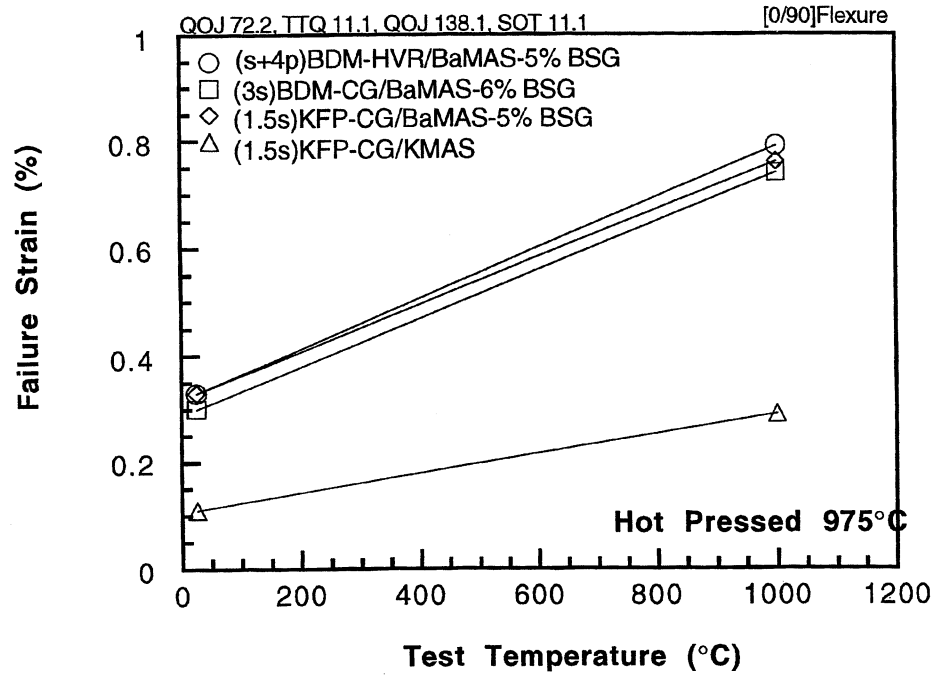

FIGURE 97. FAILURE STRAIN VS. TEST TEMPERATURE FOR VARIOUS MICA-COATED Nicalon CMCs

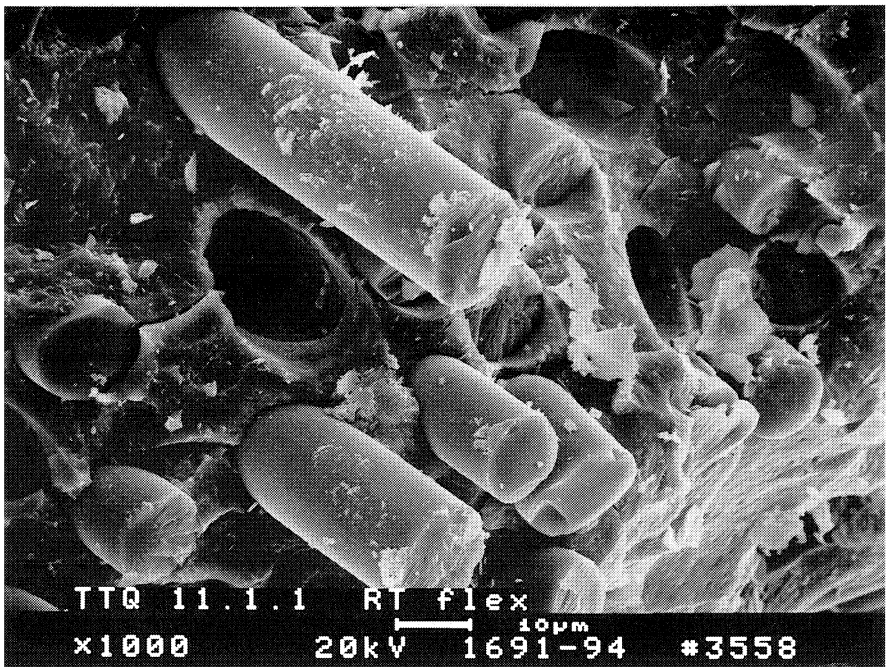

(a) TESTED AT ROOM TEMPERATURE

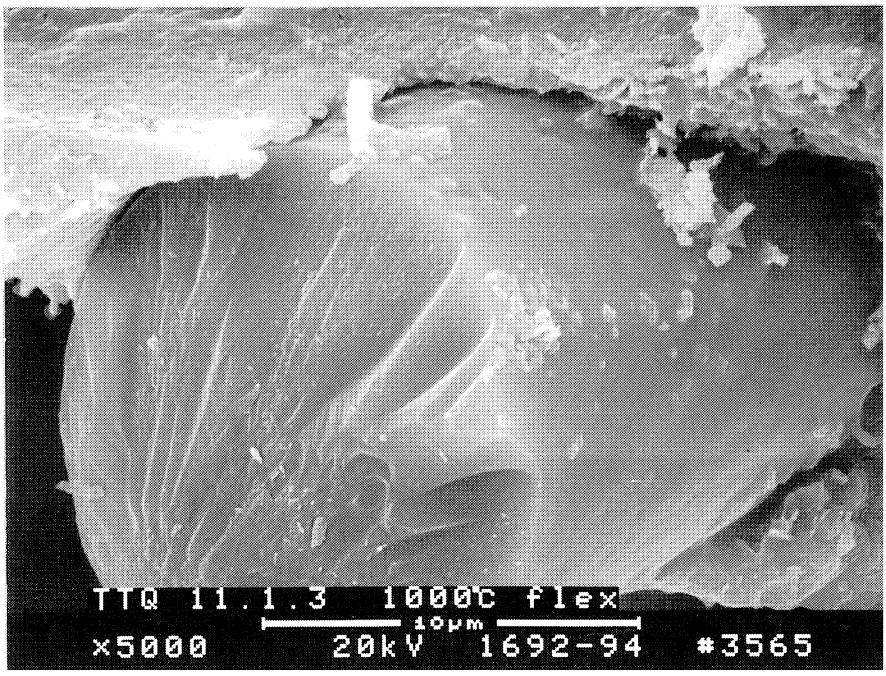

(b) TESTED AT 1000°C

FIGURE 98. SEM VIEWS OF FRACTURE SURFACES OF (3s) BDM MICA-CG Nicalon/6% BSG-MAS

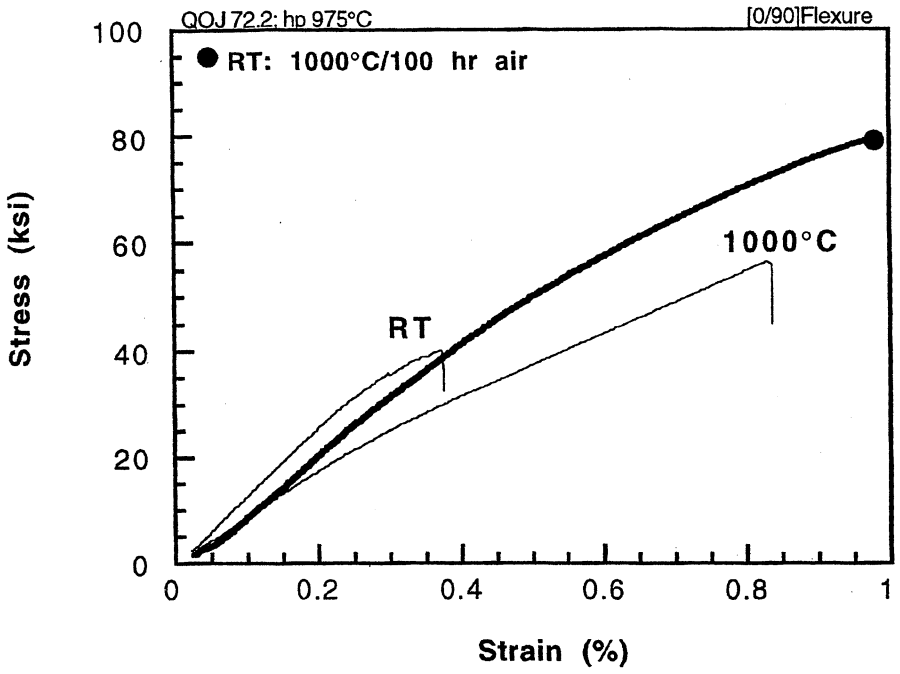

FIGURE 99. STRESS-STRAIN BEHAVIOR OF (S+4P) BDM MICA-HVR Nicalon/5% BSG-MAS

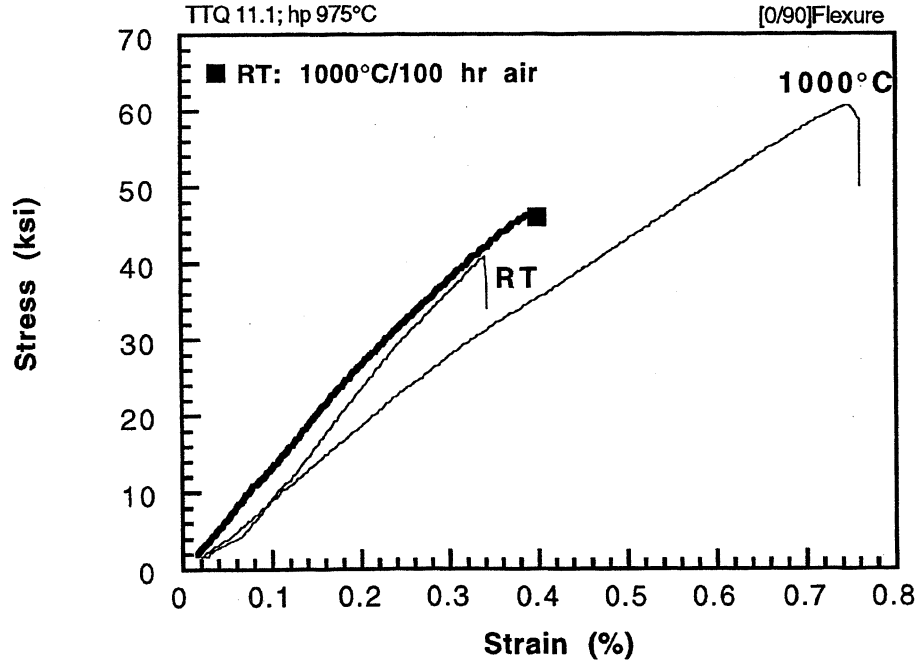

FIGURE 100. STRESS-STRAIN BEHAVIOR OF (3s) BDM MICA-CG Nicalon/6% BSG-MAS

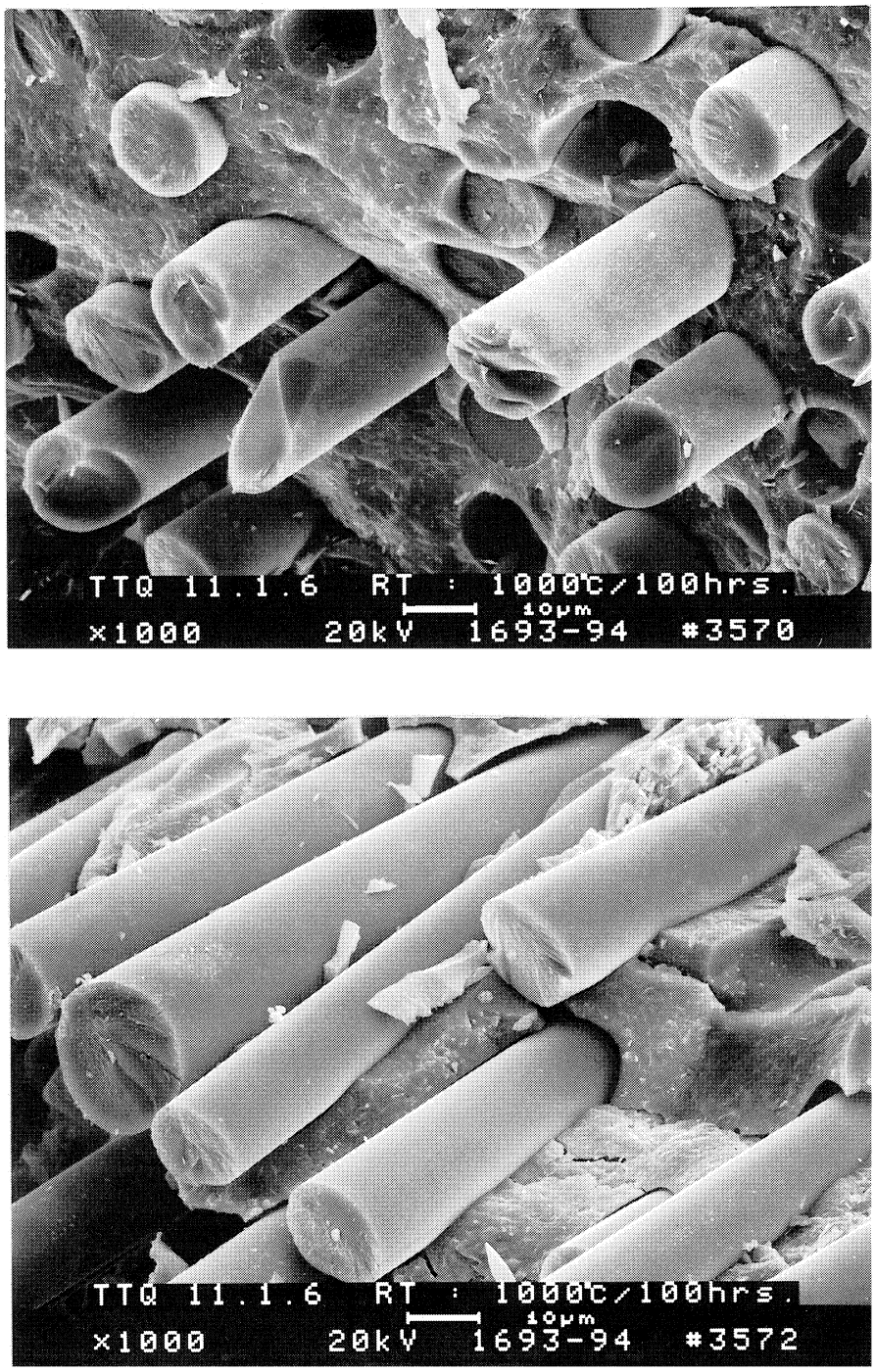

FIGURE 101. SEM VIEWS OF FRACTURE SURFACES OF (3s) BDM MICA-CG Nicalon/6% BSG-MAS AFTER 100 HOUR EXPOSURE AT 1000°C

temperature, and environmentally exposed conditions). The microstructure of interfacial regions of that CMC is shown in the TEM thin foil micrograph shown in Figure 102. It is observed that, unlike previous mica interfaces produced earlier on this contract, the interfacial mica is highly crystalline and free of bubble porosity. This is apparently a consequence of increased thermochemical compatibility with BSG-containing matrices. Also note in Figure 102 the absence of any in situ carbon layers; this is a direct consequence of the low temperature processing employed. Strengths and failure strains of this downselected CMC are provided in Figures 103 and 104. These promising properties are a result of the high quality mica interface achieved.

5.5 Mica-Interface Nicalon/BSG-doped MAS CMCs

Having demonstrated under the C^3D effort that low temperature processing of mica interface CMCs employing BSG-doped MAS cordierite glass-ceramic matrices exhibited promising mechanical properties, variants of those CMCs were investigated on the present program. In particular, it was of interest to more comprehensively investigate intermediate temperature oxidation effects for improved mica interface CMCs, since the presence of mica, and the absence of in situ carbon, could be the solution to the intermediate temperature oxidation embrittlement problem that plagues all CMCs with carbon-rich interfaces.

Additionally, other commercially available SiC fibers were investigated to determine the possible effect of lower oxygen content, since previous mica work showed reactivity at the mica interface that appeared sensitive to oxidative environments. Along that same line, potassium phlogopite mica was included, along with the downselected barium disilicic system. This was done, since early non-optimized KFP mica systems did not appear to degrade in extended thermal exposure tests as much as the BDM mica containing CMCs did.

Accordingly, a series of [0°/90°] cross-ply CMCs were produced, with processing at 975°C, with both (3S) BDM and (2S) KFP mica interfaces (the highest sol-only solids contents thus far found achievable). Three fibers were employed: (1) CG-Nicalon, containing ~11% oxygen, the downselected fiber from the C^3D program, (2) low oxygen (1-2%) Hi-Nicalon, and (3) the more handleable (and possibly interchangeable) Tyranno LOX-M fiber, containing ~13% oxygen, similar to CG-Nicalon. The test protocol involved (1) room temperature, intermediate temperature, and elevated flexure testing of as-processed CMCs and (2) 100 hr thermal exposures at those same intermediate and elevated temperatures, followed by measurement of the residual room temperature flexural stress-strain behavior.

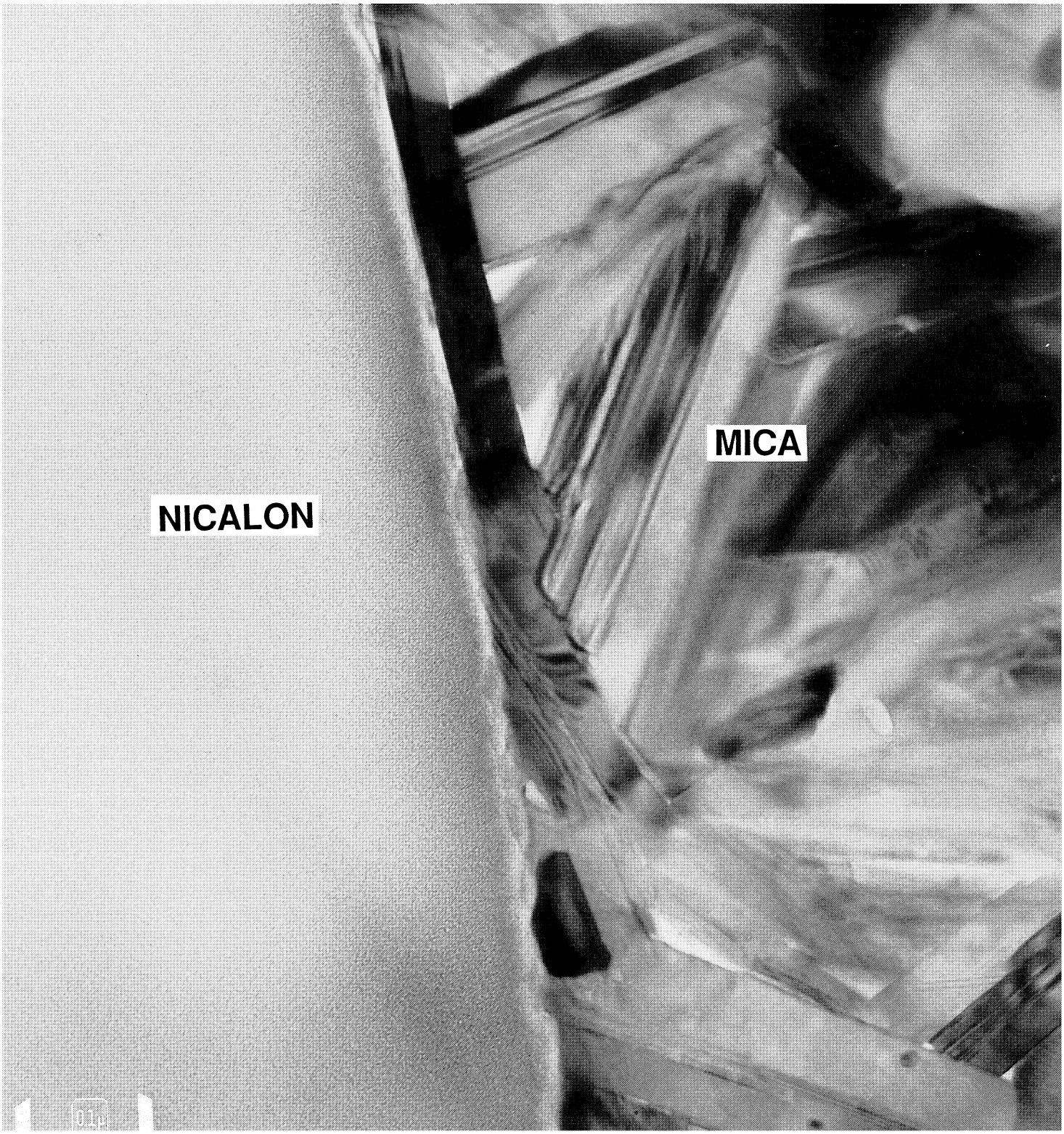

FIGURE 102. TEM THINFOIL OF MICA-Nicalon/6% BSG-MAS CMC (TTQ 11.1)

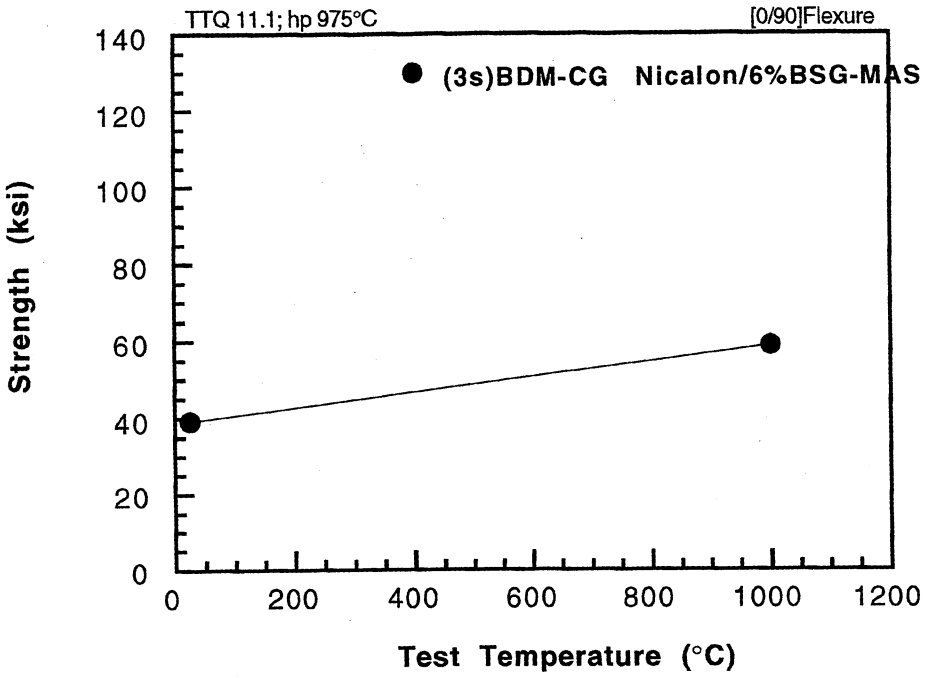

FIGURE 103. FLEXURAL STRENGTH VS. TEST TEMPERATURE FOR FINAL DOWNSELECTED DIELECTRIC CMC

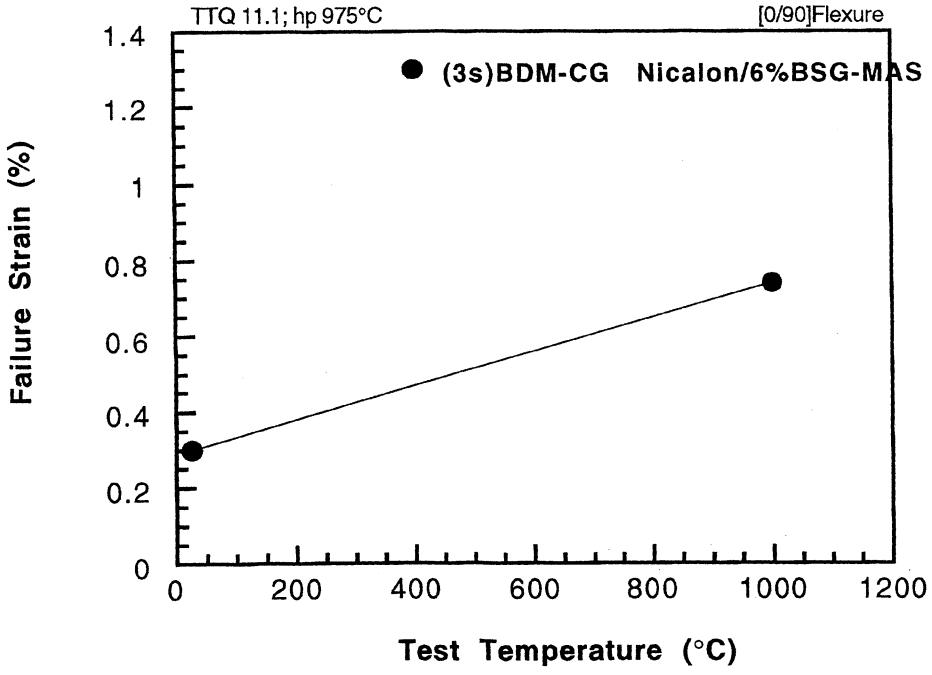

FIGURE 104. FAILURE STRAIN VS. TEST TEMPERATURE FOR FINAL DOWNSELECTED DIELECTRIC CMC

We attempted to answer three questions in this study:

1) Does a mica interface offer a viable solution to the intermediate temperature embrittlement problem?

2) Which mica, BDM or KFP, is more promising?

3) Which fiber system, with a mica interface, would be the choice in a downselect to the most promising single CMC for future investigation?

5.5.1 Uncoated Baseline CMCs

Three uncoated baseline composites were made, one for each of the three reinforcing fibers used in the study. All were fully dense (as were all the coated fiber CMCs produced). The flexural stress-strain behavior of these uncoated baseline CMCs is presented in Figure 105. All are similar in one primary way: the ultimate strength and failure strain increased substantially with test temperature, progressing from low strength and brittle at 25°C to high strength and failure strain above 1000°C. This appears to be a characteristic of low temperature processed CMCs, as has been observed in other CMCs produced at Corning. It is thought to be a real affect of temperature, and not simply caused by the development of the in situ carbon layer as the temperature is increased. Support for this view is shown in Figure 106, where the stress-strain behavior of uncoated CG-Nicalon/6% BSG-MAS (also processed at 975°C) is plotted in three conditions: (1) as-processed material at room temperature, (2) as-processed material at 1100°C, and (3) the residual room temperature behavior after thermal cycling to 1100°C and back to room temperature. It appears that the improved mechanical properties at high temperature are not due to the development of an in situ carbon layer (otherwise, the properties of the thermally cycled sample would have been higher).

Considering other aspects of the uncoated baseline CMCs shown in Figure 105, it is noted that the Tyranno LOX-M CMC has the most temperature invariant behavior, especially in terms of its elastic modulus. The highest elastic moduli were obtained for the Hi-Nicalon reinforced CMC. It had the highest elastic modulus at 1200°C, and exhibited no permanent deformation. The CG-Nicalon CMC had the most elastic modulus loss with temperature, and exhibited slight deformation at 1200°C. These observations with respect to refractoriness are consistent with the relative oxygen contents for these three reinforcing fibers.

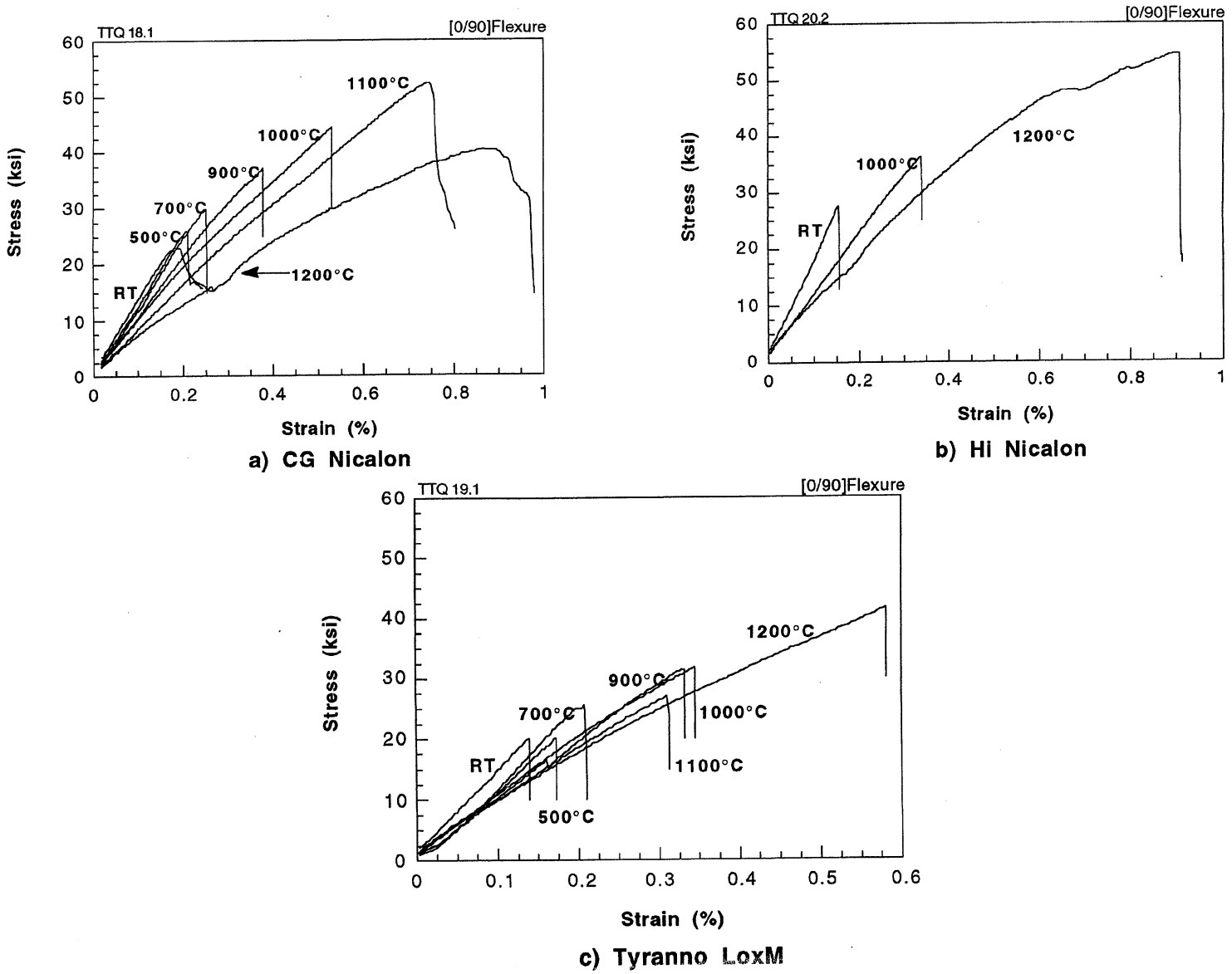

FIGURE 105. STRESS-STRAIN BEHAVIOR OF UNCOATED BASELINE/6% BSG-DOPED MAS CORDIERITE CMCs

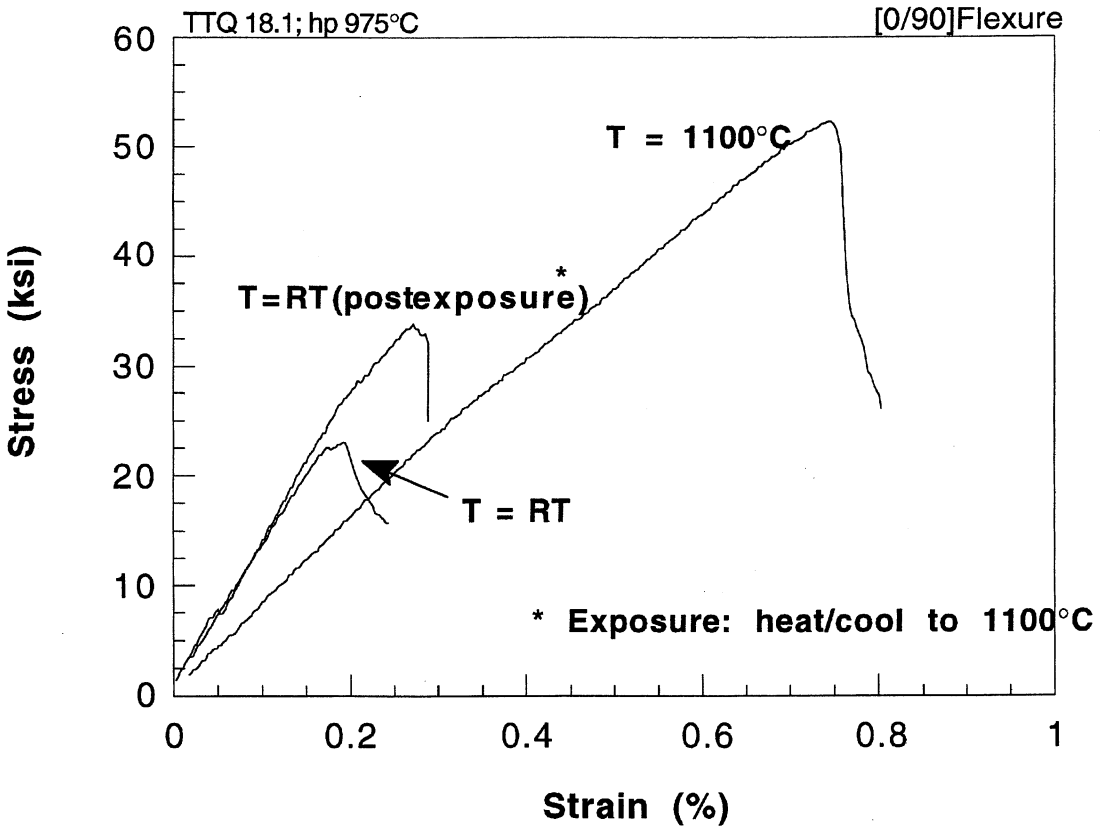

FIGURE 106. STRESS-STRAIN BEHAVIOR OF UNCOATED CG Nicalon/6% BSG-MAS AS A FUNCTION OF TEST TEMPERATURE

5.5.2 Mica Coated CMCs: As-Processed Behavior

Barium Disilicic Mica: The flexural strength and failure strain of as-processed (3S) BDM mica-coated SiC fiber/6% BSG-MAS cordierite CMCs is provided in Figure 107, where comparison is made to the baseline uncoated CG-Nicalon reinforced CMC. It is observed that all CMCs exhibited similar behavior, i.e., they were low strength and brittle, except the one reinforced with CG-Nicalon. That CMC was the only one that exhibited high strength and toughness, and was particularly good at low and intermediate temperatures. Consistent with this, the fracture of the BDM-coated CG-Nicalon CMC was distinctly fibrous at 25°C, and progressed to splintery at 500°C to woody at higher temperatures. In contrast, the BDM-coated Hi-Nicalon and Tyranno LOX-M CMCs all exhibited fairly brittle failures.

Figure 108 presents the stress-strain behavior of these CMCs at all test temperatures. When these curves are compared to those of uncoated baseline CMCs for the three fibers, very similar behavior is observed. The predominant effect is one of increased strength and toughness as the test temperature is increased. With the possible exception of the CG-Nicalon sample, either the mica is not thick enough at the interface, or its presence has little to do with the performance of the CMCs.

For all three reinforcing fibers, permanent deformation of the flexure bars was experienced at lower temperatures (~100°C lower) than exhibited by the respective unreinforced baseline samples. The BDM mica-coated Hi-Nicalon and LOX-M Tyranno CMCs experienced only slight permanent deformation at 1200°C, in contrast to the significant deformation experienced by the BDM mica-coated CG-Nicalon CMC. However, since they were also brittle at room temperature, the quality of the mica coating (i.e., uniformity, continuity, thickness) on those CMCs is questionable. Analytical electron microscopy was not conducted for these CMCs. It is recognized that without such investigation, only limited conclusions can be made regarding the performance of the CMCs tested.

Potassium Phlogopite Mica: The behavior of the potassium phlopogite (KFP) mica interface CMCs was similar, with generally the same property trends observed, as shown in Figures 109 and 110. Note that the only KFP mica-coated CMC to possess high strength and toughness at room and intermediate temperatures was the KFP mica coated CG-Nicalon/BSG-doped KMAS composite. This was a special matrix that combined the BSG dopant with a potassium stuffed cordierite matrix (all other matrices were barium-stuffed cordierite). This matrix was thought to be more refractory with KFP mica, and will be discussed below.

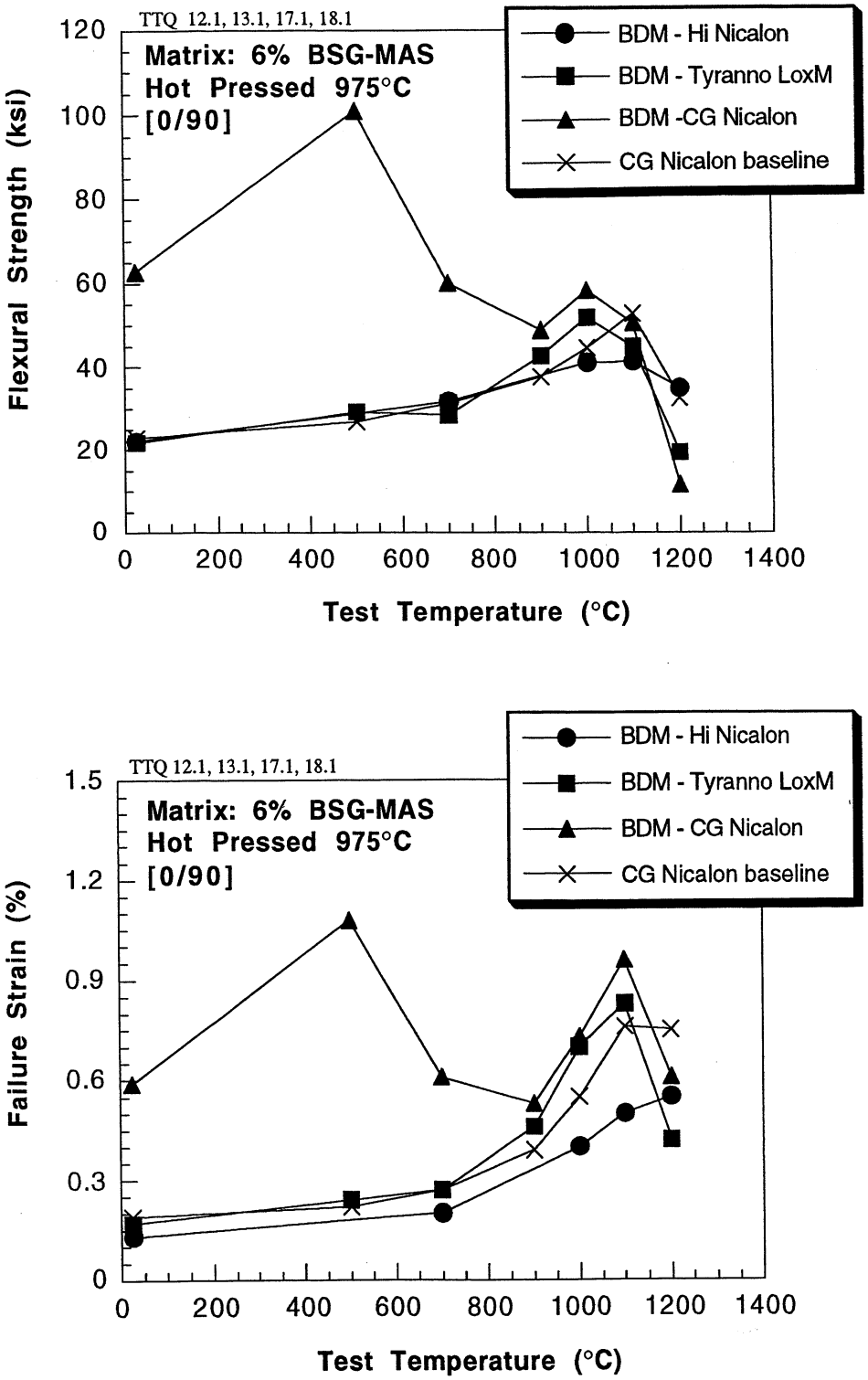

FIGURE 107. FLEXURAL STRENGTH AND FAILURE STRAIN FOR AS PROCESSED FAST FRACTURE TESTED BDM MICA COATED SiC FIBER CMCs

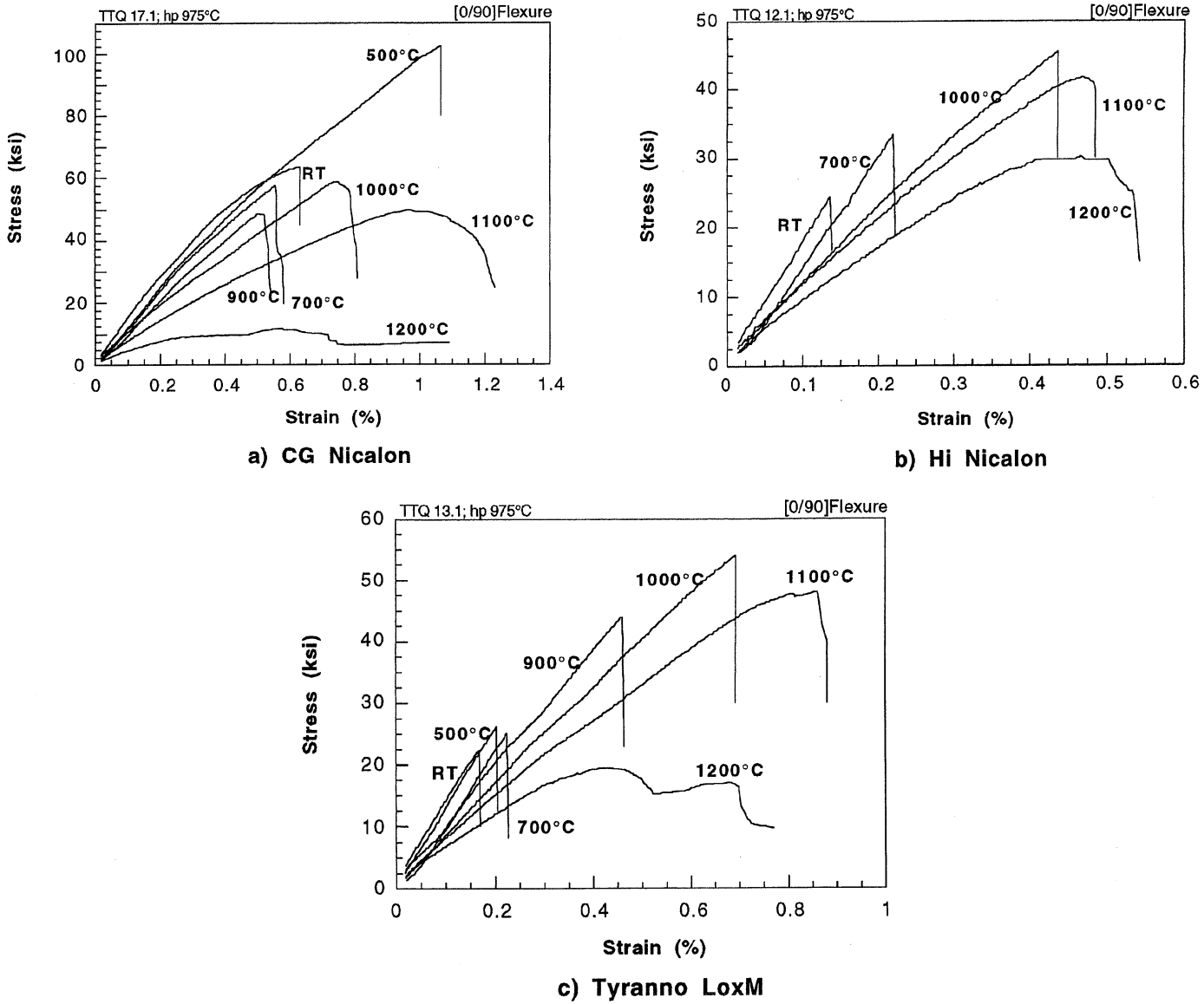

FIGURE 108. STRESS-STRAIN BEHAVIOR OF (3s) BDM MICA COATED SiC FIBER/6% BSG-MAS MATRIX CMCs

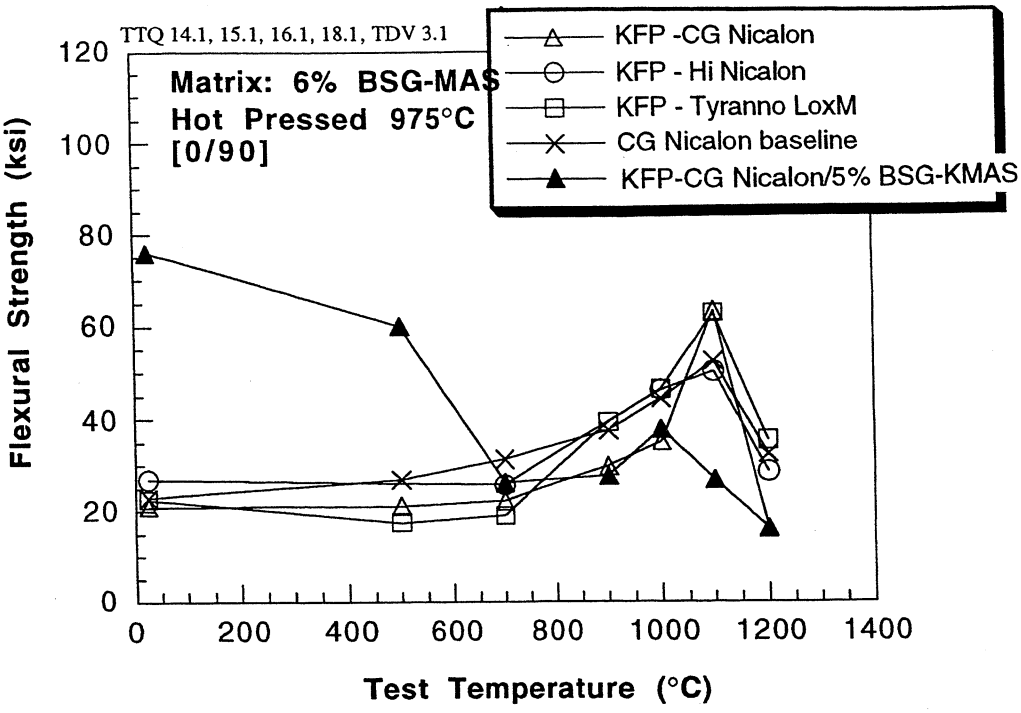

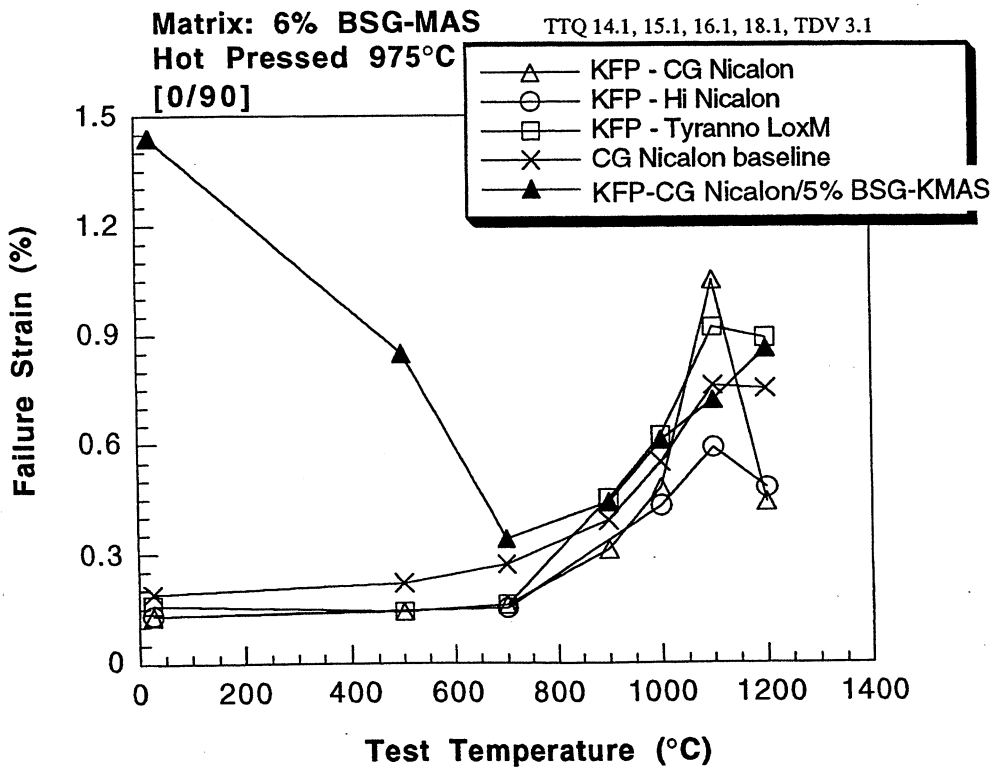

FIGURE 109. FLEXURAL STRENGTH AND FAILURE STRAIN FOR AS PROCESSED, FAST FRACTURE TESTED, KFP MICA COATED SiC FIBER CMCs

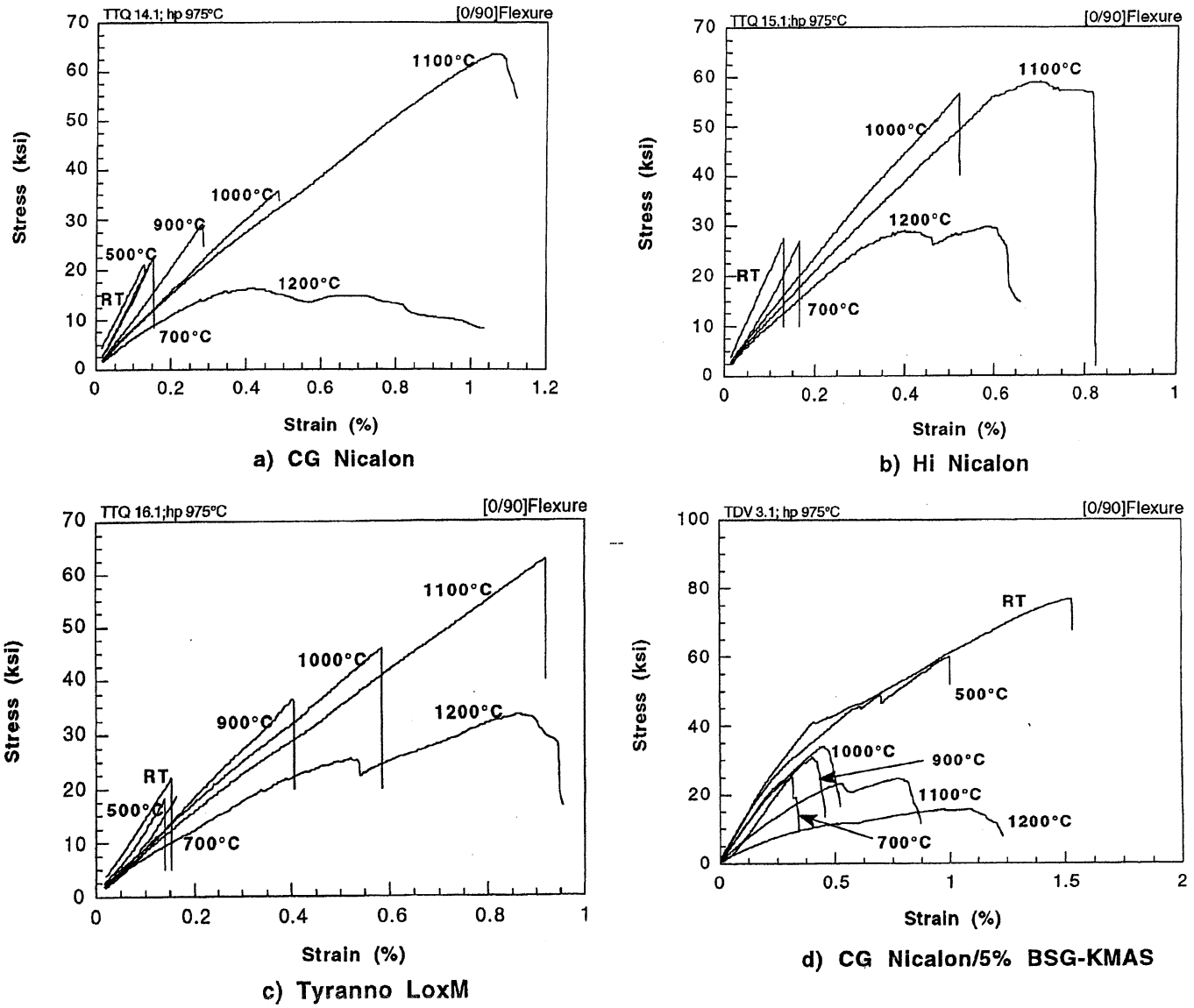

FIGURE 110. STRESS STRAIN BEHAVIOR OF (2s) KFP MICA COATED SiC FIBER/6% BSG-MAS MATRIX CMCs

5.5.3 Thermally Exposed CMCs: Mica Interface and Uncoated

In this study [0°/90°] cross-ply CMCs were thermally exposed (in air), since interface pipeline embrittlement effects have been most readily observed in such CMCs with in situ carbon phases most directly exposed to the oxidative environment (short path length from a machined sample edge along interface of 90° plies). All samples were exposed unstressed.

Uncoated Baseline CMCs: After 100 hr exposure, uncoated baseline samples (which are low strength and brittle to begin with since they were processed at low temperature and have no in situ carbon layer) start to exhibit visual effects of oxidation at 1100°C, where glassy bubbles are typically observed on 90° plies on the machined sample edge. This indicates that the fibers are oxidizing and producing a gaseous reaction product. The accepted oxidation reaction for SiC is:

$$SiC + 3/2\ O_2 = SiO_2(s) + CO(g)$$

The effect is not related to the formation of the in situ carbon layer for Nicalon SiC fibers, since we have demonstrated that the same effects of bubbles present on the edges of 90° plies occurs in exactly the same manner for CMCs with a carbon layer as it does for CMCs without a carbon layer (i.e., for the CMCs processed at 975°-1250°C described in Section 5.4.1 above).

For extended thermal exposures at higher temperatures, 1200°C, significant distress is present: glassy/crystalline scale product on all sample surfaces, with significant evidence of a gaseous reaction product (bubbles).

Barium Disilicic Mica-Interface CMCs: The residual flexural strength and failure strain of various (3S) BDM mica-coated SiC fiber CMCs are provided in Figure 111. It is observed that the same CMC that looked promising in fast fracture tests is somewhat promising after extended exposure at intermediate temperatures, the BDM coated CG-Nicalon CMC. All other CMCs exhibited poor mechanical properties after thermal exposure; however, since their as-processed properties were not good, their poor performance after thermal exposure can not necessarily be the result of oxidation.

Note the one CMC that did not suffer intermediate temperature embrittlement had the poorest properties after high temperature (>900°C) thermal exposure. Thus, the mica interface concept appears to have the potential of solving the intermediate temperature embrittlement problem, but

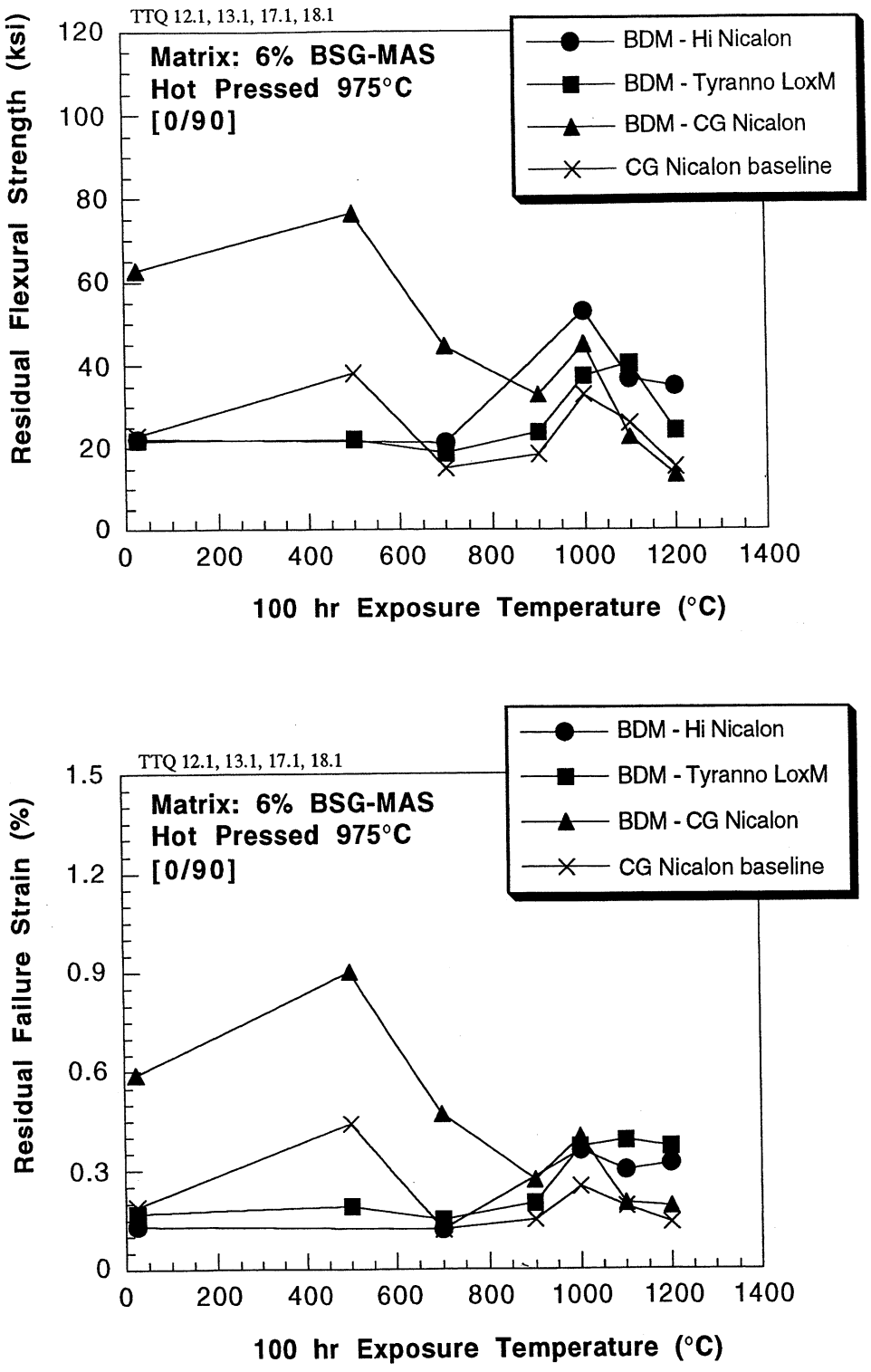

FIGURE 111. Residual Flexural Strength and Failure Strain After Thermal Exposure for BDM Mica Coated SiC Fiber CMCs.

seems to result in reduced performance at temperatures >900°C. The physical appearance of the thermally exposed samples corroborate this. Significant scale/bubble formation was noted for all 100 hr thermally exposed BDM coated fiber composites (i.e., for all three fibers) at 100°C lower than observed for the respective uncoated baseline CMCs (i.e., after 100 hr/1000°C exposure).

Figure 112 presents the flexural stress-strain behavior of as-processed and thermally exposed samples of the best performing CMC: (3S) BDM mica-coated CG-Nicalon/6% BSG-doped MAS cordierite. Note in Figure 112(a) that the stress-strain response for samples thermally exposed in the intermediate temperature range (500°-700°C) were even better than in the as-processed condition. Figure 112(b) shows the decrease in performance in samples thermally exposed at 900°C and 1100°C.

Potassium Phlogopite Mica Interface CMCs: The residual strength and failure strain of thermally exposed samples containing the KFP mica interface are provided in Figure 113. In this case, note that the low oxygen content Hi-Nicalon CMC was somewhat promising under conditions of extended unstressed exposures at 900°C and above. This might be the result of its low oxygen content. Note also that the best performing CMC overall was the KFP mica coated CG-Nicalon reinforced BSG-doped K-MAS cordierite matrix. This CMC had a potassium stuffed cordierite matrix as mentioned above. This particular CMC appears to have good thermal durability over the entire temperature range, from intermediate to very high temperatures, as shown in Figure 113.

There is a plausible reason for the improved thermal durability exhibited by the CMC that combined a KFP mica interface with a K-MAS cordierite matrix. Recall from earlier work that the extensively investigated particulate augmented BDM mica fiber coatings resulted in glassy interfacial regions with significant bubble porosity. KFP mica systems were not as extensively studied, but there appeared to be less evidence of a glass phase at the interface in CMCs that combined a KFP mica interface and a K-MAS matrix. A KFP mica coated Nicalon/K-MAS CMC, one of the more promising CMCs from that earlier study, was subsequently subjected to unstressed extended thermal exposure at various temperatures. The results were compared to previous BDM-mica coated CMCs, and demonstrated that the KFP mica/K-MAS matrix composite suffered only minimal degradation of properties after extended thermal exposure (even though the matrix contained no BSG doping, and the process temperature was 1075°C, slightly higher than is presently considered optimal).

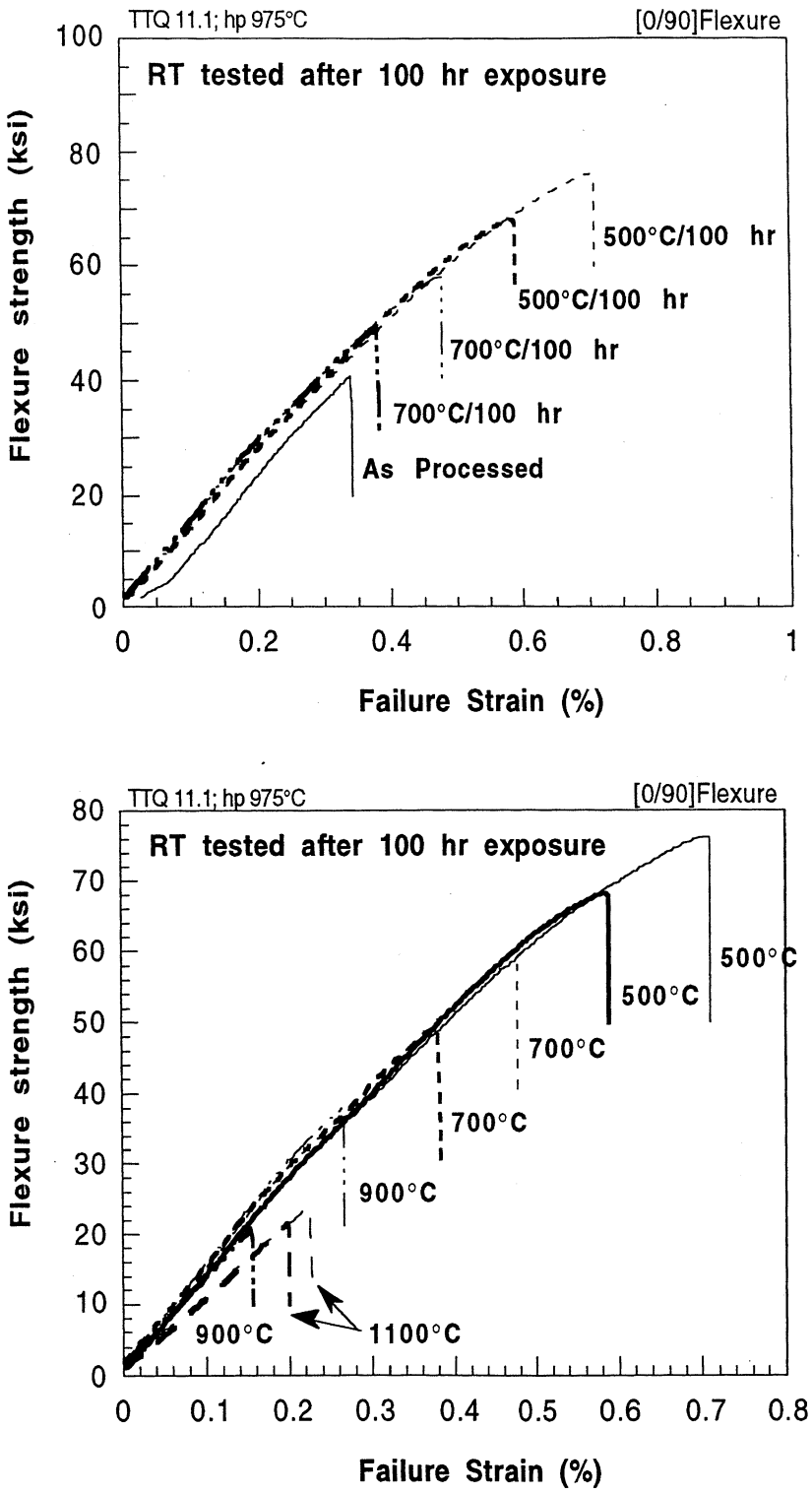

FIGURE 112. STRESS-STRAIN BEHAVIOR FOR (3s) BDM MICA COATED CG Nicalon/6% BSG-MAS CMCs AFTER LONG TERM THERMAL EXPOSURE

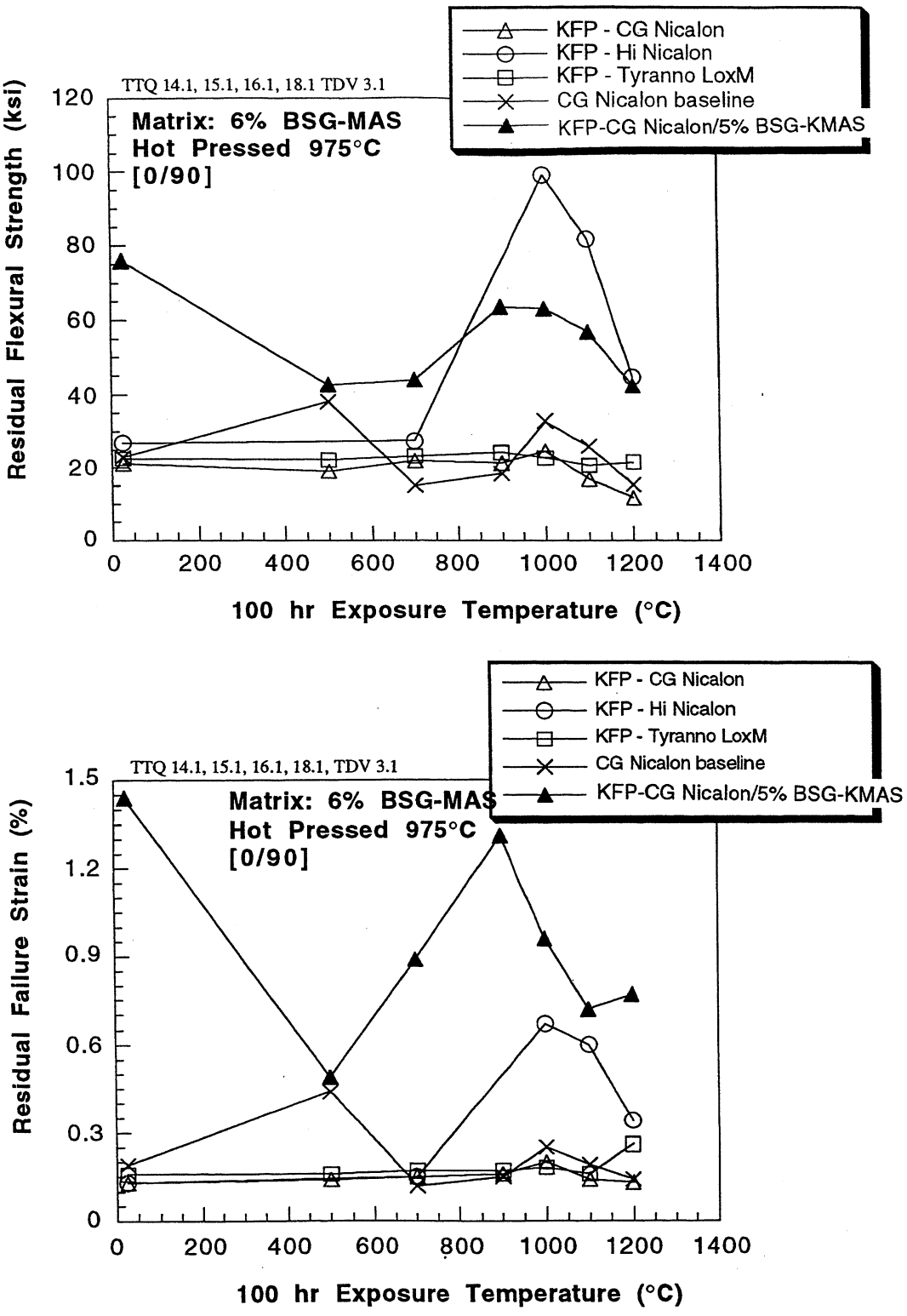

FIGURE 113. RESIDUAL FLEXURAL STRENGTH AND FAILURE STRAIN AFTER THERMAL EXPOSURE FOR KFP MICA COATED SiC FIBER CMCs

Therefore, the results presented in Figure 113 for the more optimal BSG-doped K-MAS matrix CMC that was processed at only 975°C are consistent with the previous data. In the present case, the KFP mica/BSG-doped K-MAS combination gave less permanent deformation and less evidence of reactive gas evolution as well. To summarize, the presence of bubbles on the edges of 90° plies indicates gas evolution and a glassy reaction product or surface scale. The temperature where this is first noticed on 100 hr exposed samples (CG-Nicalon fiber) is:

Uncoated BSG-doped Ba-MAS matrix CMC: 1100°C

BDM mica/BSG-doped Ba-MAS matrix CMC: 1000°C

KFP mica/BSG-doped Ba-MAS matrix CMC: 1100°C

KFP-mica/BSG-doped K-MAS matrix CMC: 1200°C

The reactivity of KFP mica systems is less than for the BDM mica systems, especially when a K-MAS or BSG-doped K-MAS matrix is present. We speculate that this is because the probable reaction product for a KFP/BSG-doped K-MAS couple would be a refractory and very viscous potassium borosilicate glass, instead of the fluid barium borosilicate glass that might have formed for a BDM mica/BSG-doped Ba-MAS couple. This reaction requires oxygen/silica, which is present as the SiC fiber oxidizes, or in the case of the particulate augmented sol-gel fiber coatings, through environmental ingress made possible by the porous nature of the particulate mica containing coating. Another factor contributing to the stability of the system is the inherent stability of the K-MAS glass-ceramic matrix itself, in comparison to the Ba-MAS matrix (Ba more mobile than K).

We did not pursue any of the KFP mica fiber coatings at the time of the earlier study on this program, since the BDM barium disilicic mica system appeared more readily crystallized in TEM studies. The present results would perhaps indicate it prudent to re-look the KFP mica fiber coating, in view of its improved thermochemical compatibility and thermal durability when used with potassium stuffed cordierite matrices.

5.6 Summary Of Results: Mica Interface CMCs

Processing at low temperature, 975°C, resulted in fully dense, fully crystalline BSG-doped cordierite CMCs, with no evidence of the in situ carbon layer detected in thin foil TEM

examination. Mica sol-gel fiber coatings were found necessary for high mechanical strength and toughness; mechanical properties for such low temperature processed CMCs were significantly better than their uncoated control CMCs. The best mica coatings contained no precrystallized particulate mica components. Rather, high solids content sol-only mica coatings were more durable and mechanically functional. Even so, the mica fiber coatings were found, in general, to be nonuniform and noncontinuous. However, the effect of this on mechanical properties and inter- or intra-panel variability was not investigated.

Only when using BSG-doped MAS cordierite matrices were fiber-mica interfaces distinct and free of bubble porosity, indicating good thermochemical compatibility. The two most promising mica interface CMCs developed were:

(3S) BDM-coated CG-Nicalon/6% BSG-doped Ba-MAS (1)

(2S) KFP-coated CG-Nicalon/5% BSG-doped K-MAS (2)

CG-Nicalon was the most successful fiber used with mica; Ti-containing Tyranno LOX-M and low oxygen Hi-Nicalon did not yield particularly promising mica interface composites, although no interfacial microscopy was performed to investigate possible causes. The result for low oxygen SiC fiber was particularly unexpected, given that mica has been shown to be thermochemically compatible with pure SiC.

The strength, failure strain, and stress-strain behavior of the BDM mica/Ba-MAS matrix CMC (#1 above) indicate significant loss of refractoriness at 1200°C. It is suspected that mica is still somewhat reactive, and that a fluid barium borosilicate glass at the interface might be responsible for this (not investigated by AEM). An all-potassium system, KFP mica coupled with a K-stuffed MAS matrix, might form more refractory reaction products (a higher viscosity glass), and therefore, a variety of KFP mica-coated CG-Nicalon composites were also investigated. The (2S) KFP mica-CG-Nicalon/5% BSG-K-MAS CMC system was the most promising, although it also exhibited refractoriness limitation at temperatures greater than 1100°C.

TEM studies of mica interface CMCs readily found BDM mica at the interface, but finding large grains of crystalline KFP in the microstructure was more difficult. With the above comments regarding the increased glass associated with mica in mind, it is possible that one of the mechanisms operable with mica interface CMCs is a glaze coating at the interface that protects the fiber but deforms at elevated temperatures.

The most important aspect of these studies, however, was the unstressed oxidation exposures at intermediate temperatures. The two aforementioned CMC systems (#1 and #2 above) were the most promising, as shown in Figure 114, which presents the residual RT strength and failure strain after various 100 hr exposures at both intermediate and high temperatures. Perhaps the most promising is the all-potassium KFP mica-coated CG-Nicalon/5% BSG-doped K-MAS cordierite CMC. That CMC experienced only slight degradation in performance after both intermediate and high temperature thermal exposures. This demonstrates that the mica interface concept is a potentially viable solution to the intermediate temperature embrittlement problem.

In summary, when mica was present in sufficient thickness to benefit room temperature properties, the high temperature properties diminished, especially the amount of permanent deformation experienced in flexure tests. In a similar manner, the presence of mica in the microstructure usually resulted in more glass at the interface, and increased evidence of gaseous reaction products (although that was minimized with the CMC system employing KFP mica and a BSG-KMAS cordierite matrix).

The keys to achieving the promising mechanical properties of these CMCs are: (1) the use of mica as a debond layer, (2) the use of thermochemically compatible BSG-doped Ba- or K-MAS matrices, and (3) the use of low temperature processing (975°C) to preclude in situ carbon layer development with commercially available Nicalon fibers. Such CMCs experienced no, or only minimal, intermediate temperature oxidation embrittlement effects in long term oxidative exposures.

Mica interface CMCs have been demonstrated on this program to be a potential solution to the intermediate temperature embrittlement problem, but at the expense of some refractoriness. They show promise, but are at a very early stage of development.

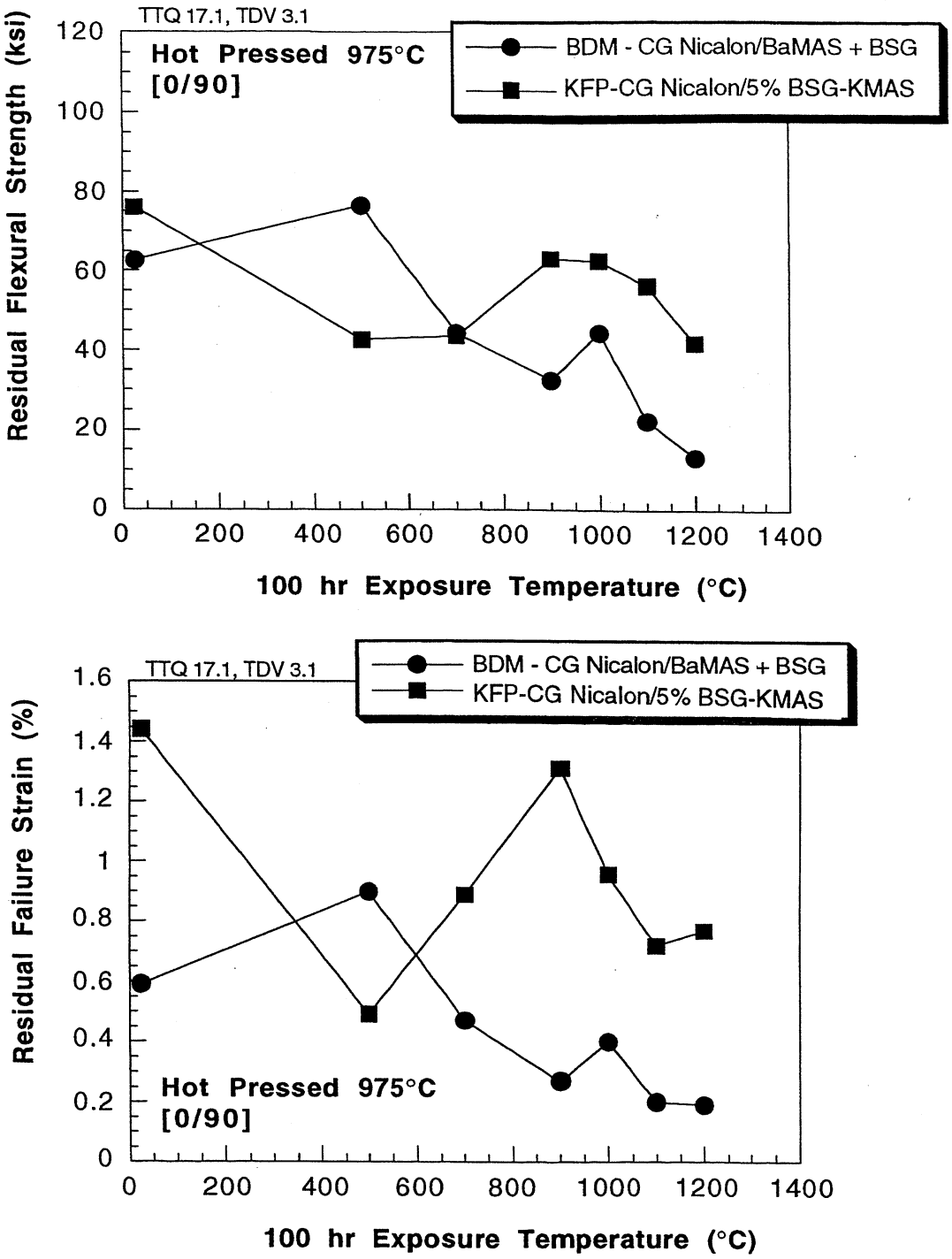

FIGURE 114. LONG TERM UNSTRESSED OXIDATION FLEXURAL STRENGTH AND FAILURE STRAIN FOR THE TWO MOST PROMISING MICA INTERFACE CMCs

6.0 Conclusions

The objective of this program was to develop thermally durable CMCs with enhanced structural properties. Two approaches were investigated: (1) mica-interface CMCs and (2) BSG-doped MAS CMCs, with and without SiC-whisker matrix toughening.

The former material, with mica interface, has the potential to be a fundamental solution to the oxidation embrittlement problem, but remains embryonic in maturity. Process conditions (low temperature) were developed to eliminate carbon-layer formation, and mica layers were produced that were of sufficient thickness to be the functional debond layer in the composite. When these two conditions were achieved, mica-interface CMCs were demonstrated to be free of oxidation embrittlement at intermediate temperatures. However, the sol-gel mica coatings were nonuniform in thickness, and showed evidence of environmental reactivity at high temperatures. These two areas require much attention for mica interface CMCs to be candidate materials for more advanced thermal durability testing and evaluation.

The second material investigated on this program, BSG-doped MAS cordierite CMCs with SiC-whisker toughened matrices, is much more mature and has demonstrated enhanced thermal durability. The functional approach is to manage the problem of oxidation of interfacial carbon by (a) boron-doping the matrix, providing a plugging/blunting protective borosilicate glass film matrix-side of the carbon interface, and (b) reducing microcrack generation in the matrix during mechanical loading. The latter is accomplished by (a) boron diffusion to the interface to create thinner, more tightly bonded interfacial regions affecting shear and sliding resistance, and (b) by SiC-whisker matrix toughening to increase the fracture energy of the glass-ceramic matrix. This ability to alter the manner in which damage accumulates and to increase the oxidative stability of the modified in situ-carbon interface resulted in enhanced thermostructural performance. Tensile stress-rupture and high cycle fatigue data showed significant life, hundreds of hours, at stresses above the elastic limit, which is the most widely accepted indicator of the achievement of thermal durability. Additionally, the intermediate temperature oxidation embrittlement problem was eliminated in these CMCs. Mechanistically, SiC-whisker addition to increase matrix toughness and reduce microcracking was the dominant determinant of mechanical performance at intermediate temperatures, whereas BSG doping to create the boron-modified interface and the BSG protectant interfacial film (Figure 115) was dominant at elevated temperatures.

The performance of Nicalon/BSG-doped SiC_w-toughened MAS cordierite CMCs has demonstrated the validity of the concept of using physical additives and chemical dopants to

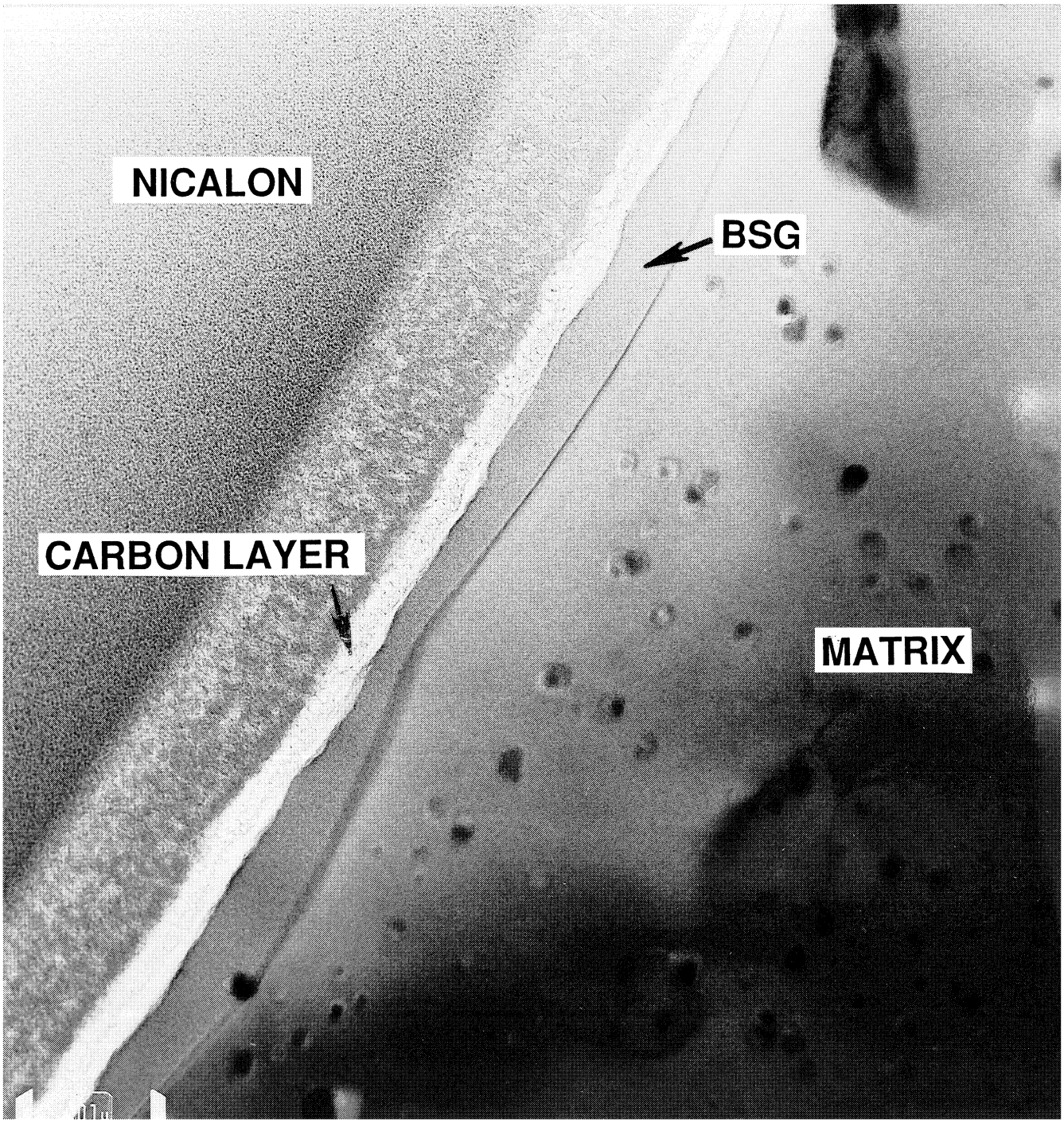

FIGURE 115. TEM THIN FOIL OF INTERFACIAL REGION OF NICALON/5% BSG-DOPED MAS CMC

modify the composite microstructure to effectively manage the oxidation embrittlement problem in carbon-interface CMCs. It is important to recognize that the enhanced thermal durability achieved was done so by modifying the way damage accumulates in the matrix, and by protecting the interface from oxidation. The improved thermal durability of these CMCs was achieved without the use of either fiber coatings or external surface coatings, and therefore in a very cost-effective and affordable manner. The thermal durability demonstrated by both hybrid and nonhybrid versions of the BSG-doped cordierite CMC illustrates the flexibility of the glass-ceramic matrix approach to oxidatively stable and embrittlement resistant CMCs.

The properties obtained by the Nicalon/BSG-MAS CMCs developed on this program meet Pratt & Whitney's generic requirements for a thermostructural material: 15 ksi usable strength at 2200°F, with a failure strain >0.5%. This generic requirement was communicated to Corning early in the time frame of this program. Whereas these CMCs are not presently mature enough for early incorporation into Pratt & Whitney engines, and they do not have quite the level of performance as do competing BN-interface BAS celsian glass-ceramic CMCs, they are sufficiently promising to be considered for inclusion in component development programs, and are a promising low-cost approach for a thermally durable CMC.

The contributions of this program to CMC technology were many. CMCs with vastly enhanced thermal durability were developed. Critical issues of performance deficiencies were uncovered and highlighted by involvement of Pratt & Whitney to generate materials properties and to provide a working definition of thermal durability. Mechanisms of behavior were adequately identified. And finally, concepts of physical and chemical doping were demonstrated that can be used to selectively alter the performance of glass-ceramic matrix CMCs. Thus, promising approaches to the attainment of thermally durable CMCs were identified.

REFERENCES

1. J. Aveston, G.A. Cooper, and A. Kelly, "Single and Multiple Fracture", pp. 15-26 in The Properties of Fibre Composites, National Physical Laboratory Conference, Surrey, England; IPC Science and Technology Press, Ltd. (1971).
2. K.P. Gadkaree and K. Chyung, "Silicon Carbide Whisker Reinforced Glass and Glass-Ceramic Composites", Am. Ceram. Soc. Bull. 65 (2) 370-76 (1986).
3. K.P. Gadkaree. "Whisker Reinforcement of Glass-Ceramics", J. Mat. Sci. 26 4845-54 (1991).
4. C.M. Cady, T.J. Mackin, and A.G. Evans, J. Amer. Ceram. Soc. 78 77-82 (1995).
5. A.G. Evans and F.W. Zok, J. Mat. Sci. 29 3857-3896 (1994).
6. A.G. Evans, F.W. Zok, and R.M. McMeeking, Acta Met. Mater., 43 859-875 (1995).
7. R.F. Cooper and K. Chyung, J. Mat. Sci. 22 3148-3160 (1987)